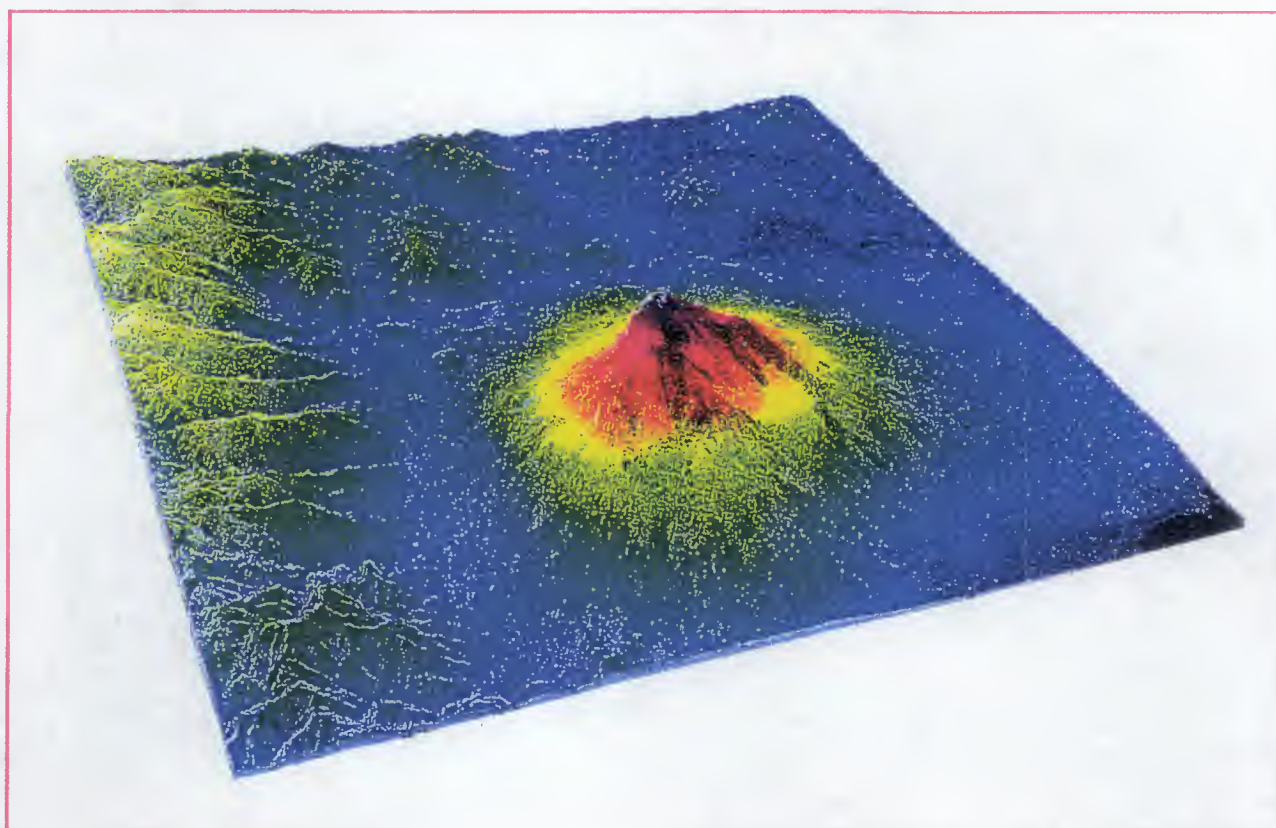




# **ERS Tandem Mission**

**SAR Interferometry  
Early Results from  
ERS-2 Commissioning Phase**



THE UNIVERSITY OF CHICAGO  
DEPARTMENT OF CHEMISTRY  
1155 EAST 58TH STREET  
CHICAGO, ILLINOIS 60637

# The ERS Tandem Mission

## Early INSAR Results

### from ERS-2 Commissioning Phase

#### Purpose

This note reports on an activity undertaken during the Commissioning Phase of ERS-2 and prior to the formal approval of the full ERS Tandem Mission.

The scope of this activity was to demonstrate the potential of the ERS Tandem Mission through the generation of first results from the technique of SAR Interferometry (INSAR). The activity was carried out by providing a strictly limited amount of ERS SAR data during ERS-2 Commissioning Phase to a small number of groups working on specific test sites which covered the main application domains of:-

- Digital Elevation Models; DEM's (for Mapping / Cartography)
- Land Surface Motion (for Earthquakes / Volcanos)
- Ice Surface Motion (for Glaciology)
- Land Surface Change/Classification (for Forestry / Agriculture)

#### Tandem Aims & Objectives

The successful launch of ERS-2 in April 1995, together with the continued excellent in-orbit performance of ERS-1, presented a world-first occasion to fly two spaceborne SAR payloads in Tandem. This has considerably excited both the scientific community and value-added industry.

The ERS Tandem mission started on the 16th August 95 for a period of 9 months up to end-May 1996. The two satellites are both in 35 day repeat orbits (for global coverage) but with ERS-2 following approximately 30 minutes behind ERS-1 in the same orbital plane such that there is a 1-day interval between ERS-1 & ERS-2 observing the same area of ground. This makes a series of new and improved observations of geophysical phenomenon possible by the INSAR technique.

In order to push forward the scientific and application benefits arising from Tandem Operations, the European Space Agency has released a related Announcement of Opportunity (AO) to the scientific/academic community early in 1996.

#### Tandem SAR Interferometry

The main driver for the Tandem Mission has been that of SAR Interferometry with a 1-day repeat interval between ERS-1 and ERS-2 which is particularly well suited to the exploitation of the technique.

Through experience with ERS-1, the INSAR technique, even prior to the ERS Tandem mission, has become well established as a method of producing detailed and accurate Digital Elevation Models (DEM's) of the Earth's surface. In addition, an extension of the basic technique, known as Differential INSAR, allows the detection of very small (centimetre-scale) movement of land surface, as demonstrated with ERS-1 repeat data for the Landers earthquake in California of 1992.

Today, approximately 65% of the global land surface has been surveyed by a variety of techniques, but there exist major gaps over such areas as S. America, Africa, Australia, Antartica and S.E. Asia. Self-consistent DEM's are essential input for many

geoscience applications (eg. geomorphology, hydrology, ice mass-balance studies) and are increasingly used in a growing number of commercial projects (eg. mobile telecommunication networks, civil engineering activities). Furthermore, a globally self-consistent and complete DEM would be of prime importance for the geo-correction of payload data from both present and future spaceborne Earth-Observing missions. The main objective of the Tandem Mission has been, therefore, to ensure acquisition of a unique and valuable data set of SAR Interferometric pairs suitable for future DEM exploitation.

Each year there are about 10 sizeable earthquakes globally (ie about 3 occurring on land). These events cause thousands of deaths and considerable costs in terms of property damage and lost revenue (eg. the recent Kobe 'quake in Japan incurred over 5 kilo-fatalities and damage estimates exceeding \$100 billion). The geoscience community has a pressing need of a global data set of densely sampled preseismic observations to study earthquakes. SAR Interferometry has the potential to provide that data set and one of the specific aims of the Tandem Mission has been to evaluate the Differential INSAR technique for geo-hazard risk assessment arising from earthquakes, volcanic eruptions, landslides, glacial surges, etc.

### **SAR Acquisition & Orbit Maintenance Status**

The geolocation of all ERS Tandem INSAR pairs acquired up until May 1996 and suitable for DEM generation is given in the first figure of Annex A. It is evident that almost all of the global land surface (including Antarctica) is currently covered.

The Flight Dynamics group at ESA's is closely monitoring and manoeuvring the orbits of both ERS satellites to deliver the stringent cross-track separations required for DEM generation. For the total period up until May 1996, about 79 % of all Tandem INSAR pairs are suitable for DEM's, 20 % of potential use for Differential INSAR (ie land motion detection) and just 1 % unsuitable for INSAR.

### **Early Tandem INSAR Results**

#### **ERS-1 / ERS-2 Doppler Offset**

There is an offset of about 280 Hz between the peak Azimuth power spectra of Single Look Complex SAR image products between ERS-1 & ERS-2. This offset has a small variation with latitude and corresponds to a relative pointing misalignment between the two SAR antennae of both platforms of about 70 mdeg. The offset can be taken into account during the processing up to an Interferogramme with the consequent loss of spatial resolution in azimuth of about 20 % (ie degradation from 4 m to 5 m in azimuth). The doppler offset is not considered to be a significant issue.

#### **Tandem Phase Coherence**

The expected overall improvement of interferogram quality (phase coherence) from the 1-day Tandem-configuration with respect to the 35-day & 3-day single satellite repeat cycles is confirmed. This is difficult to easily quantify due to the strong dependence of coherence on specific terrain conditions. Values of coherence as high as 0.7/0.8 have been observed for some areas, however, occurrences of extremely low coherence have been seen for snow-covered regions (possibly due to summer melting).

#### **Atmospheric Artefacts**

Localised artefacts in the Interferogramme continue to be observed in ERS Tandem data indicating that the timescale for these phenomenae is less than one day (as expected). These problems could, on principle, be eliminated **provided** there is available a sufficient sequence of Tandem acquisition pairs (absolute minimum of 3).

Applications results achieved with data provided during the ERS-2 Commissioning Phase are given in Annexes B to N in the form of short reports received from individual participants. A summary of the main points for each of the application domains is given below. All groups report a benefit associated with the addition of ERS-2 SAR data to that of ERS-1 alone.

#### **Digital Elevation Models (DEM's)**

DEM's have been generated for the areas of Gaeta (Italy), Etna (Italy), Maastricht (Netherlands) and Bern (Switzerland). These Tandem DEM's have not yet been subject to an exhaustive quantitative assessment of height accuracy.

Based on results achieved with ERS-1, the improved coherence from Tandem should result in DEM rms height errors of less than 10m across the complete 100 x 100 km image, and less than 2m for local regions within the image, under favourable conditions.

A Differential Interferogramme has been generated for Bern (Switzerland) which measures directly the residual height errors between the surface topography recoverable from ERS Tandem and a precision DEM. The results show good agreement (ie almost flat height residuals, after removal of systematic phase trends).

It is still an open question as to whether surface topography can be recovered over the tropical rain-forest canopy. Encouraging results have been obtained in the form of an Interferogramme for a site reported to be forest close to the Ivory Coast (African equatorial region), but the exact nature of the surface conditions is to be determined.

#### **Land Surface Motion**

Differential Interferogrammes of surface motion have been generated for the volcano Etna (Italy). These surface displacement images correspond to re-inflation on the scale of centimetres of the volcanic dome following the deflation observed during the eruption of 1992/3. Interpretation of these results with geophysicists is in progress.

#### **Glacial Motion**

Maps of ice motion velocity vectors have been derived from ERS Tandem interferogrammes mid-latitude glaciers in Canada. Topography was removed by use of an interferogramme from an airborne INSAR survey. The resulting ice motion vectors have been compared with in-situ data and show excellent agreement (within 2cm/day) even for peak flow rates of close to 40 cm/day. Fine scale velocity structure is observed in the ERS Tandem data which is repeatable for Tandem acquisition pairs separated by 19 days, therefore suggesting real ice-motion effects as the origin. It is thought that the technique will work best during winter when the potential of daytime melting (and consequent loss of coherence) is minimised.

#### **Land Surface Change / Classification**

This is an area of on-going research. Results with the ERS Tandem data substantiate the possibility of land surface cover discrimination when coherence is combined with the radiometry. Further work is required with Winter Tandem acquisitions where experience with ERS-1 indicates that coherence over the Northern forests is high enough to allow meaningful investigation.

Further work to quantitatively substantiate these first findings is currently in progress.

## Conclusions

The following conclusions can be drawn from the remarks contained in the annexed reports.

The ERS Tandem mission holds the prospect of many significant results with SAR Interferometry which are difficult to obtain using a single satellite in a repeat cycle. This is particularly so in the applications of DEM generation (with a 35-day repeat cycle) and the measurement of the motion of fast Ice-Flows.

Both the ERS-1 & ERS-2 orbits have been maintained successfully such that the stringent conditions necessary for INSAR have been met by almost all of the Tandem acquisitions.

Atmospheric artefacts are clearly problematic in specific cases, but localised effects could, in principle, be eliminated with repeated Tandem acquisition pairs of the same area. In addition, some rapidly changing land surface areas (eg snow-covered during summer) appear not to retain sufficient phase coherence for useful results, even at 1-day interval between acquisitions.

Such problematic effects could be substantially reduced **provided** there exist a sufficient number of Tandem acquisition pairs. This is considered a pre-requisite for producing with confidence DEM's over areas where little a-priori knowledge exists about the surface topography. Therefore, it is widely recognised that continuation of ERS Tandem acquisitions over poorly known specific sites is of significant benefit in order to fully realise the potential of the INSAR technique.

Further scientific work is required to consolidate these early results and to systematically investigate further specific applications of the ERS Tandem SAR data which were not possible to address within the very limited scope and timescales of this exercise. The results of the Announcement of Opportunity for ERS Tandem are, therefore, expected to significantly advance these issues.

The ERS Tandem INSAR global acquisitions represent a world-first unique and valuable data set with important exploitation potential for the years to come.

# Annex A

## Geographical area

Planet Earth

## Research institute

ESRIN

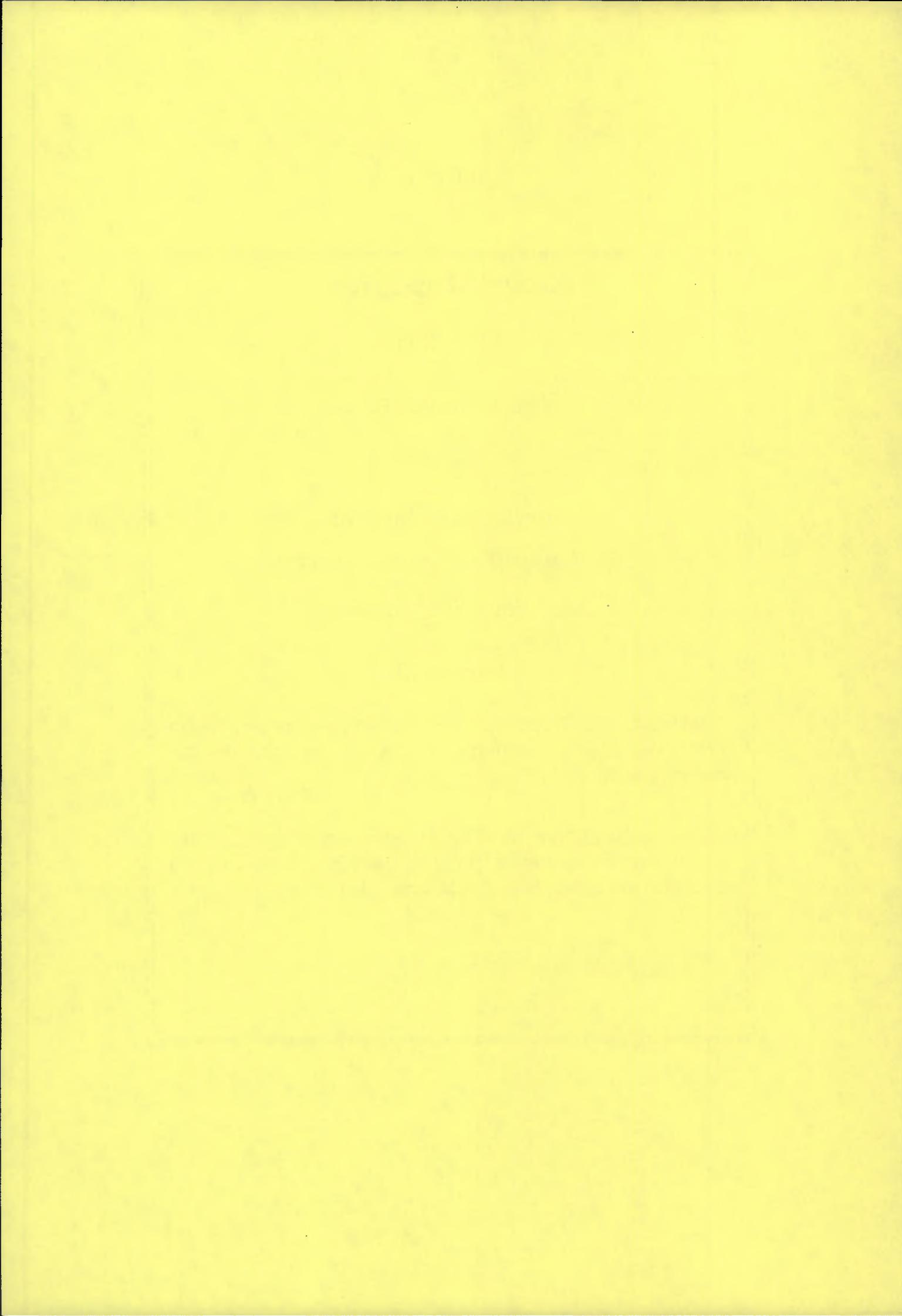
## Application domain

ERS Tandem INSAR Acquisition status  
&  
Orbit Maintenance Performance

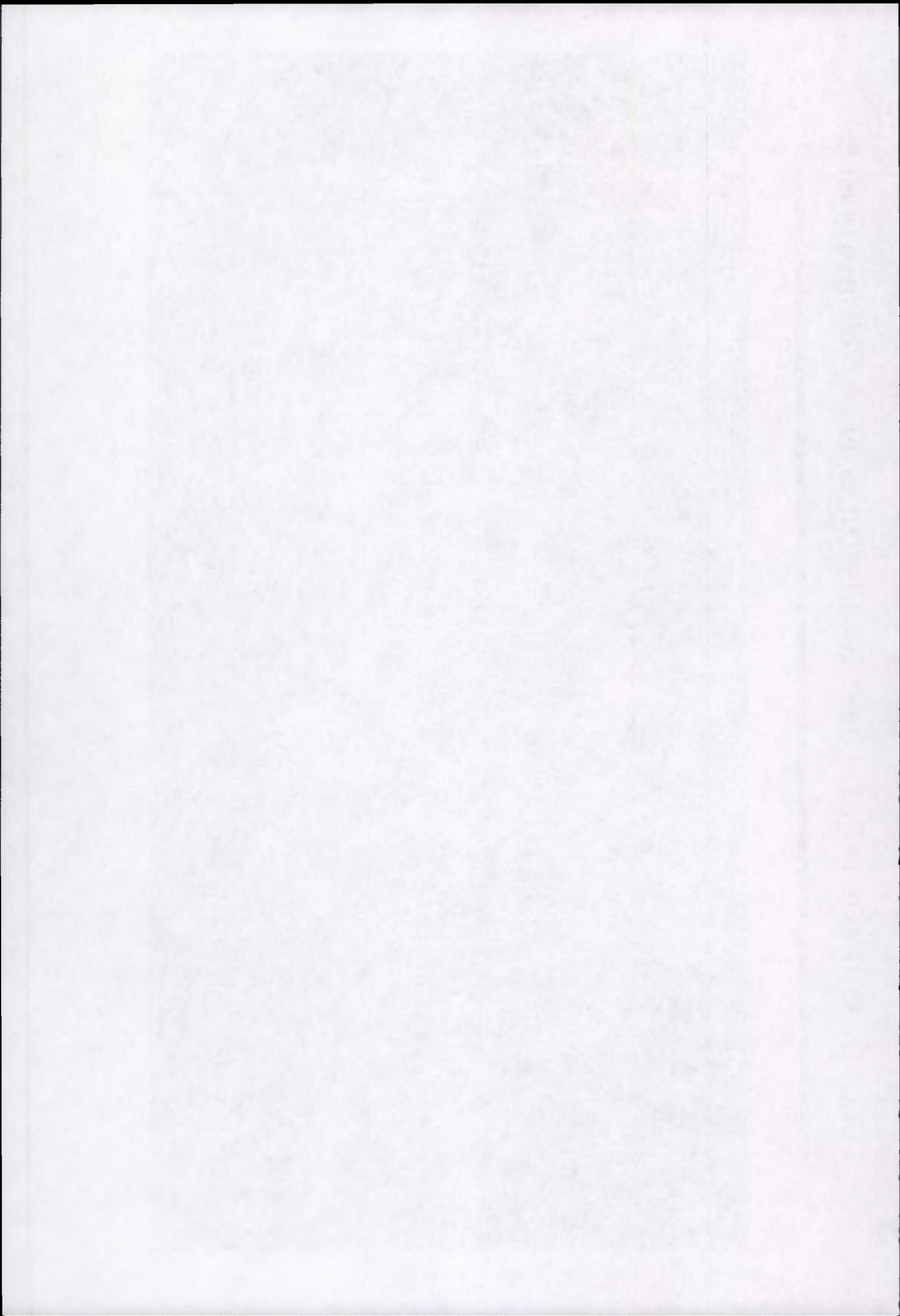
## First results

Geolocation of all Tandem INSAR acquisition pairs suitable for DEM generation (ie satisfying the appropriate orbit baseline separation criteria).

Overall statistics, for all ERS Tandem acquisitions, of the INSAR Baseline separation,  $B_{\text{perp}}$  (values of  $B_{\text{perp}}$  between 50 m and 300 m are optimum for DEM generation).







**TANDEM ORBIT MAINTENANCE PERFORMANCE (01 May 95 - 01 May 96)**

$ B_{\text{perp}}  < 50 \text{ m}$	:	21380 frames, 26%
$50 \text{ m} <  B_{\text{perp}}  < 300 \text{ m}$	:	74528 frames, 72%
$300 \text{ m} <  B_{\text{perp}}  < 600 \text{ m}$	:	6221 frames, 7%
$600 \text{ m} <  B_{\text{perp}} $	:	1028 frames, 1%

THE UNIVERSITY OF CHICAGO  
DIVISION OF THE PHYSICAL SCIENCES  
DEPARTMENT OF CHEMISTRY  
5708 S. UNIVERSITY AVENUE  
CHICAGO, ILLINOIS 60637

RECEIVED

# **Annex B**

## **Geographical area**

Gaeta, Italy

## **Research institute**

POLIMI, Italy

## **Application domain**

Digital Elevation Models (DEM)

## **First results**

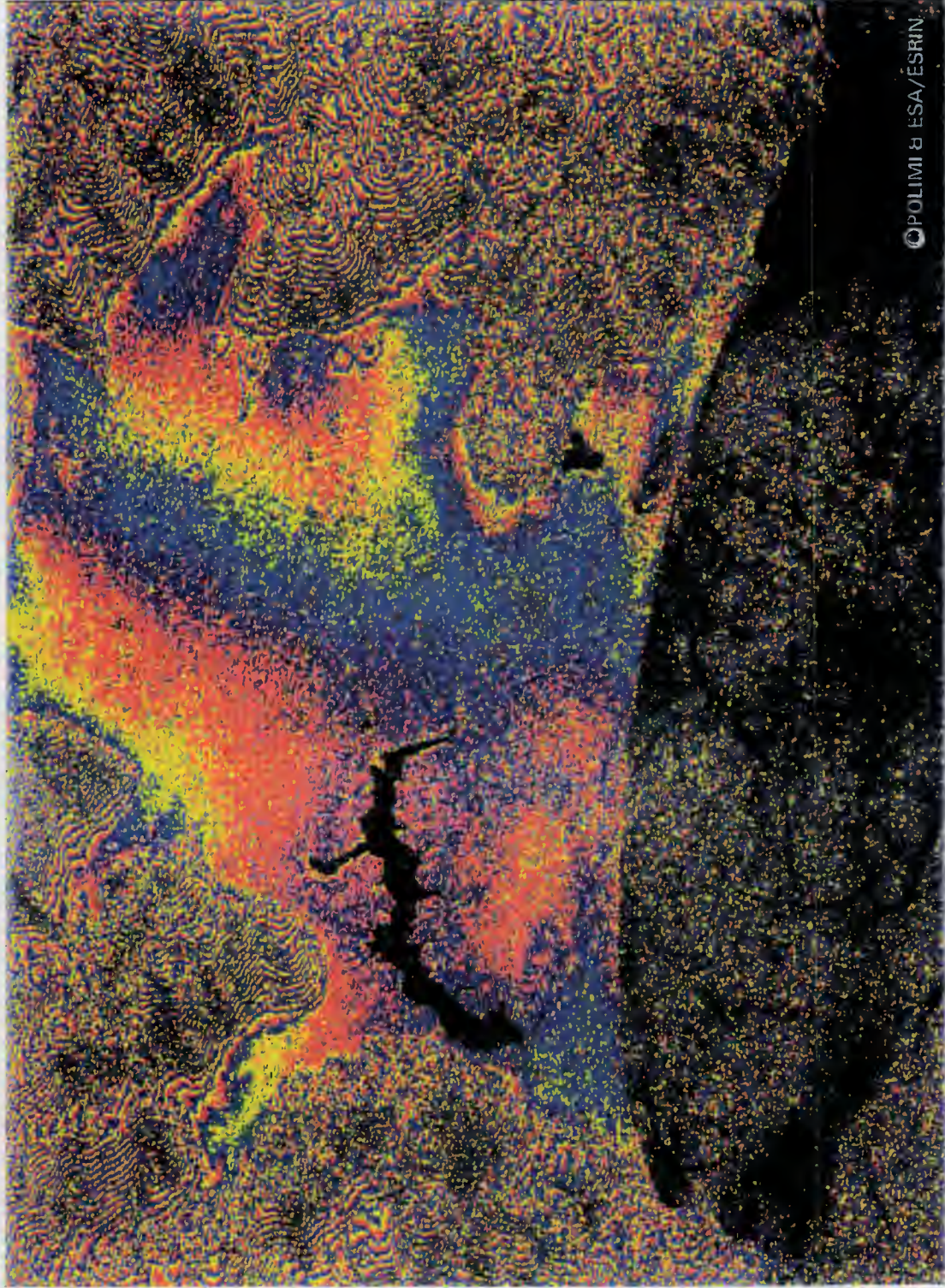
First ERS Tandem Interferogramme (01 + 02 May 1995).

Corresponding coherence image (high coherence, white ; low coherence, black) & analysis of coherence distribution for selected areas within the image. Mountain slopes exhibit very good phase stability over 1-day (coherence 0.7).

Corresponding DEM showing flat valley region surrounded by hilly peaks.

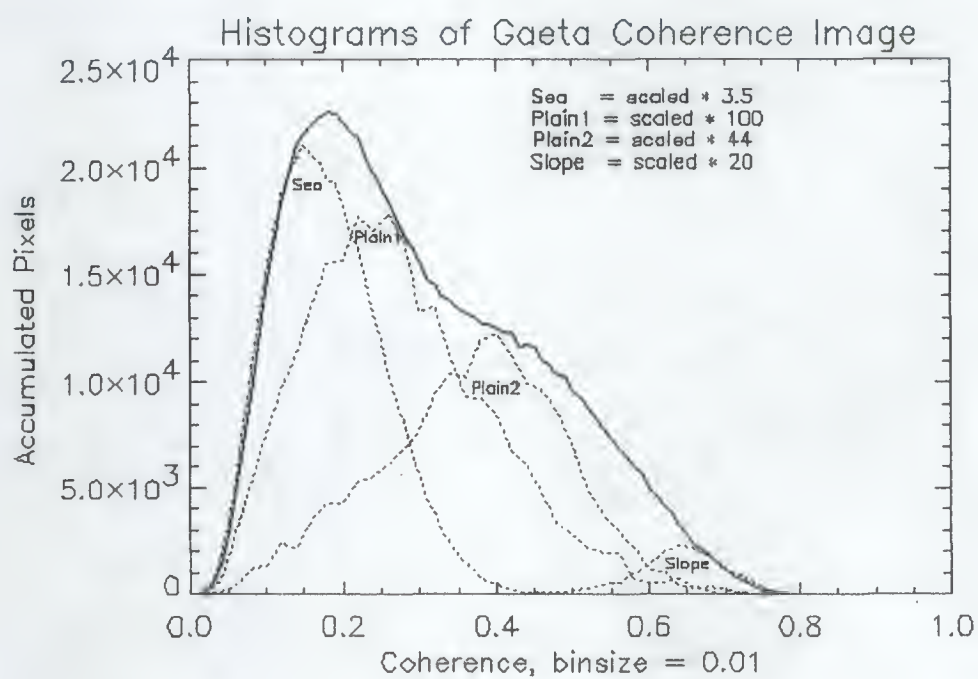
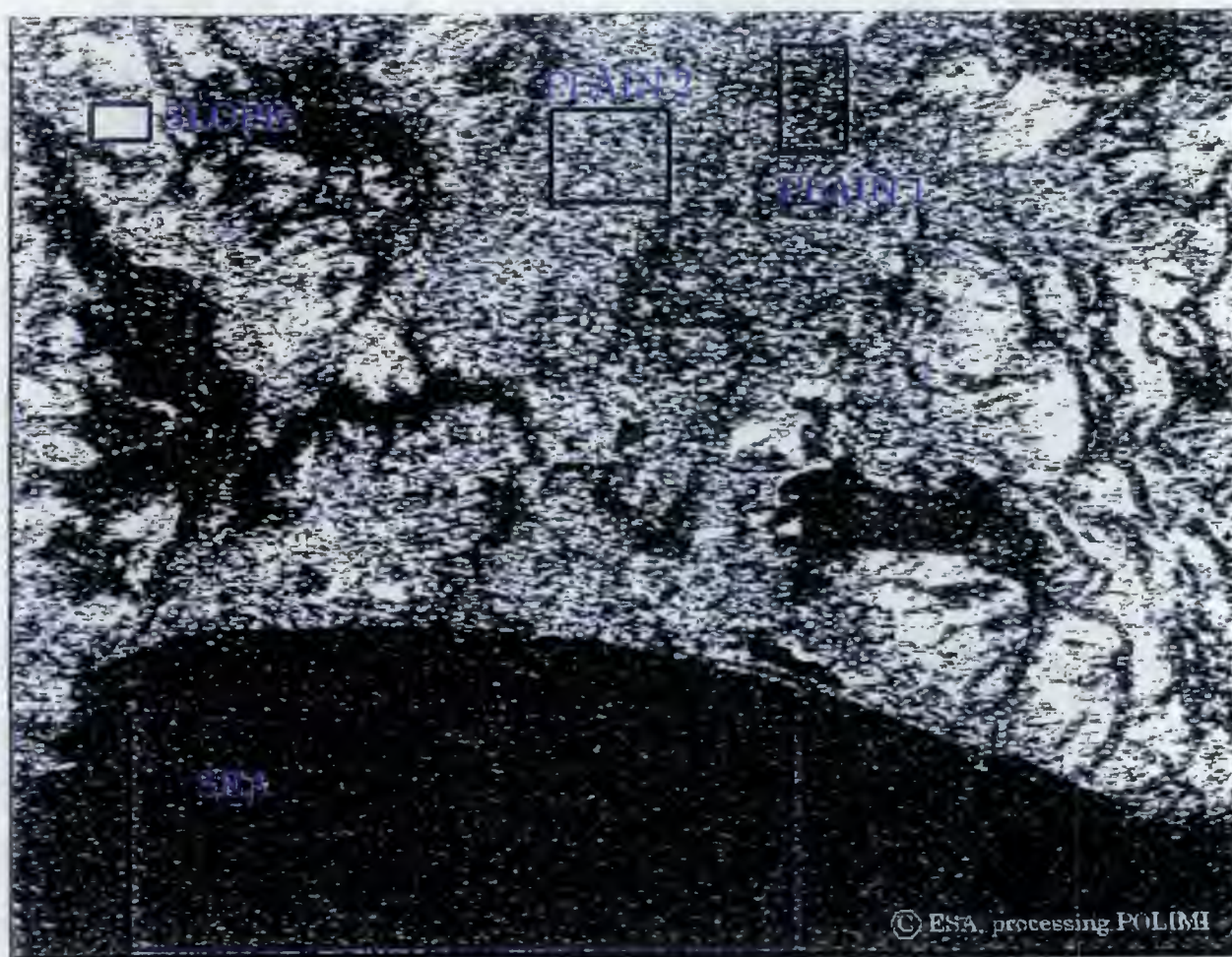


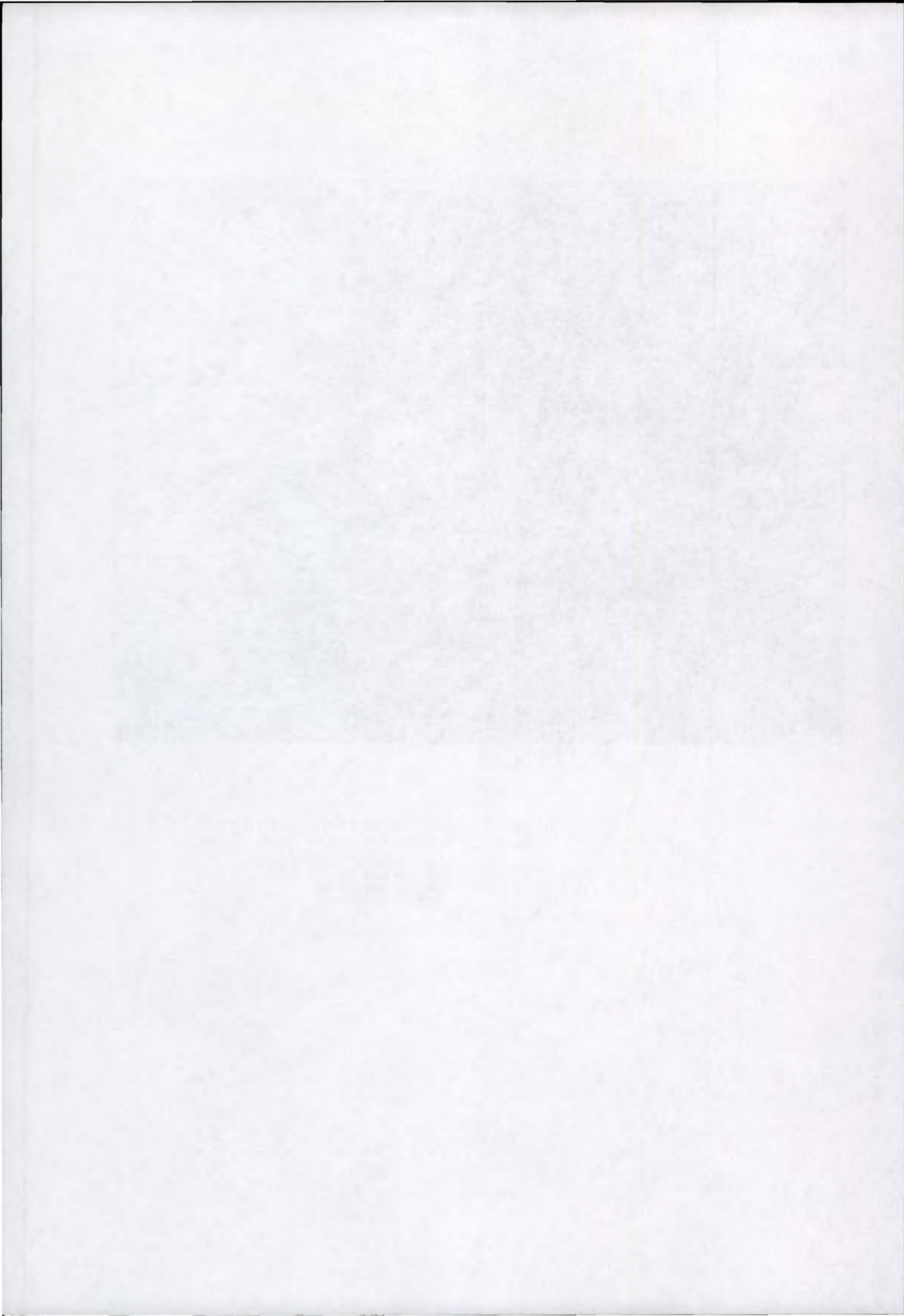
FIRST TANDEM INTERFEROGRAMME (Gaeta, Italy 01+02 May 95)



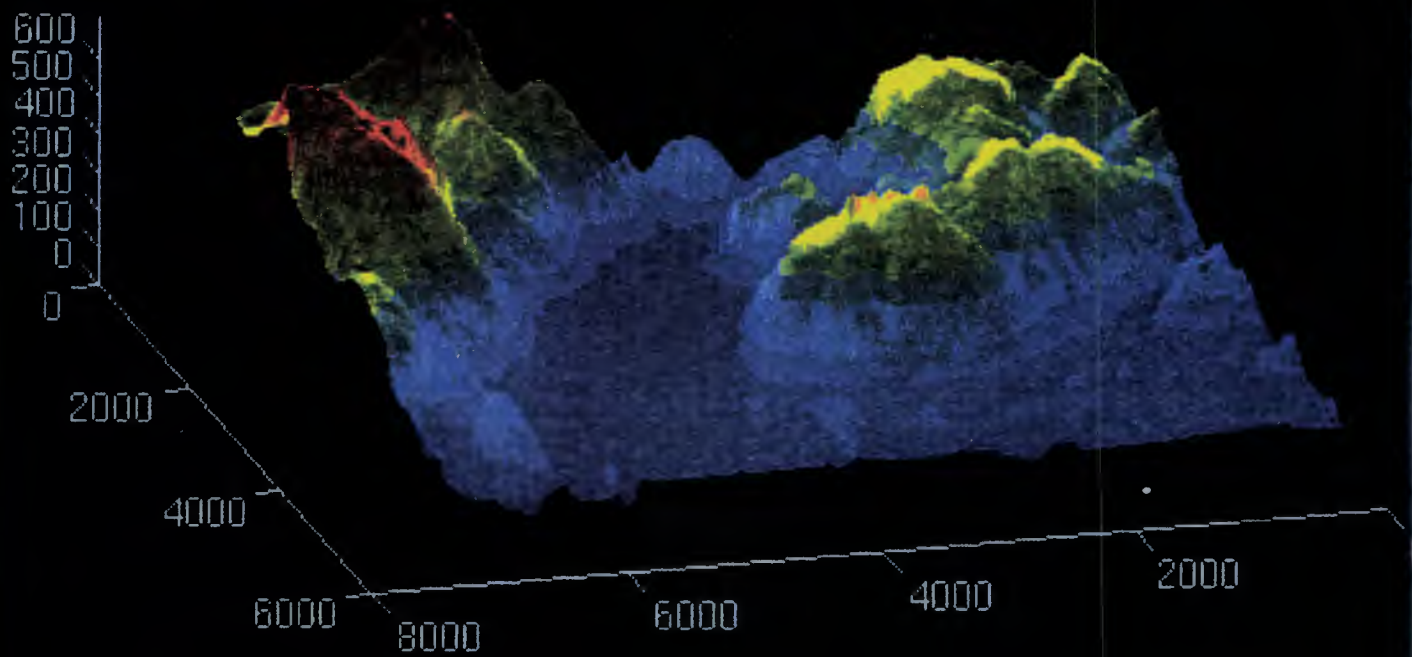
©POLIMI & ESA/ESRIN

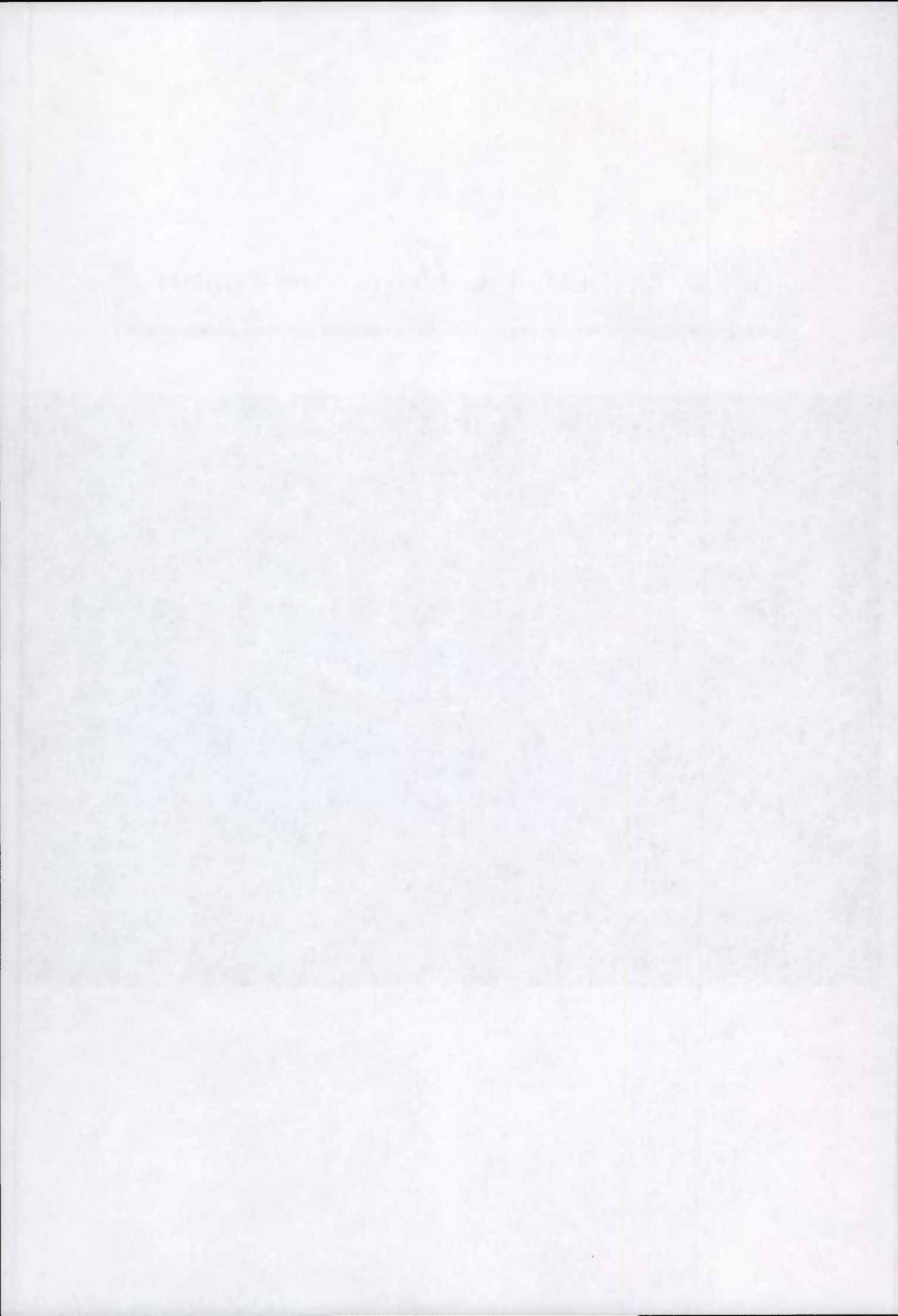


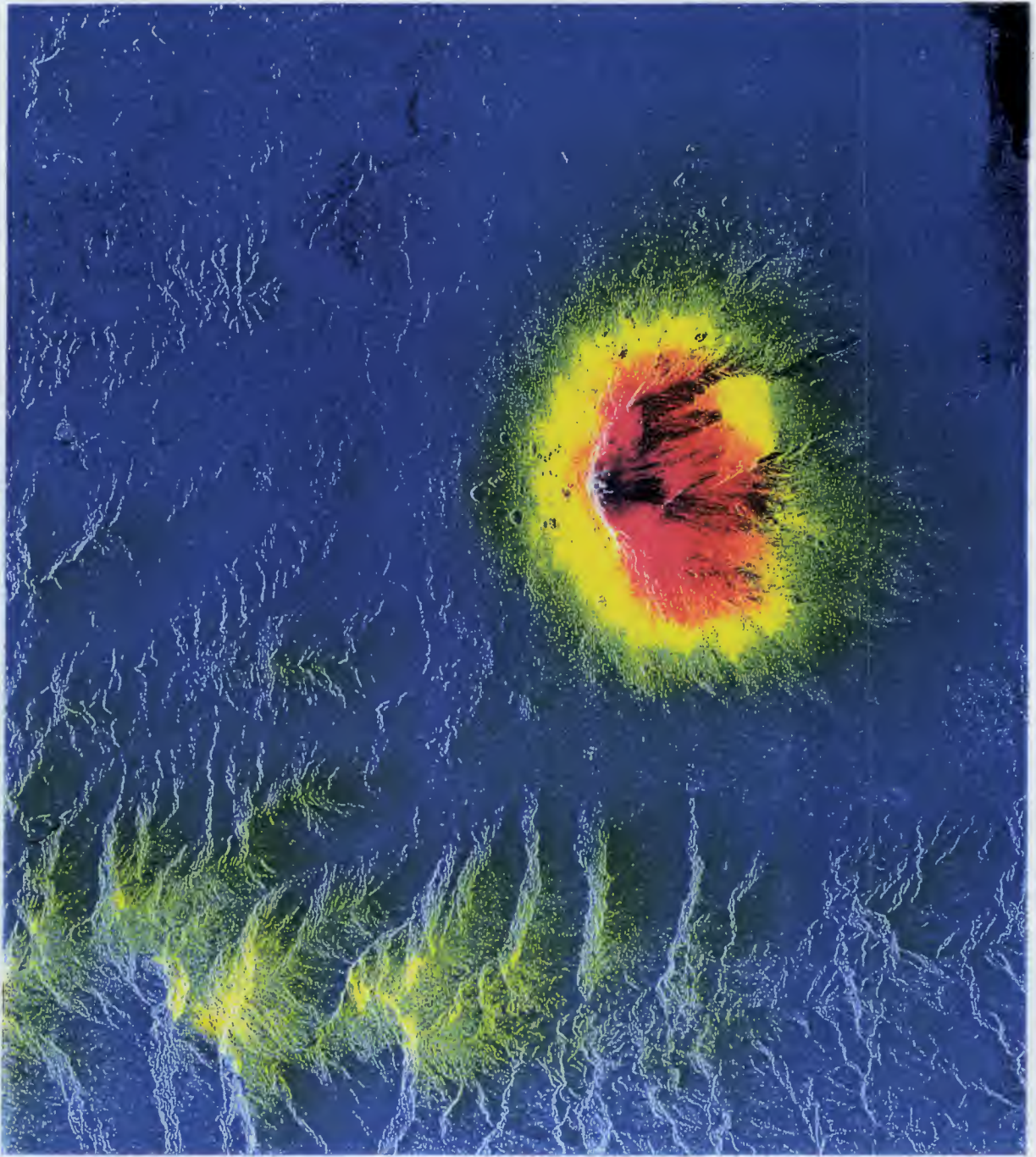


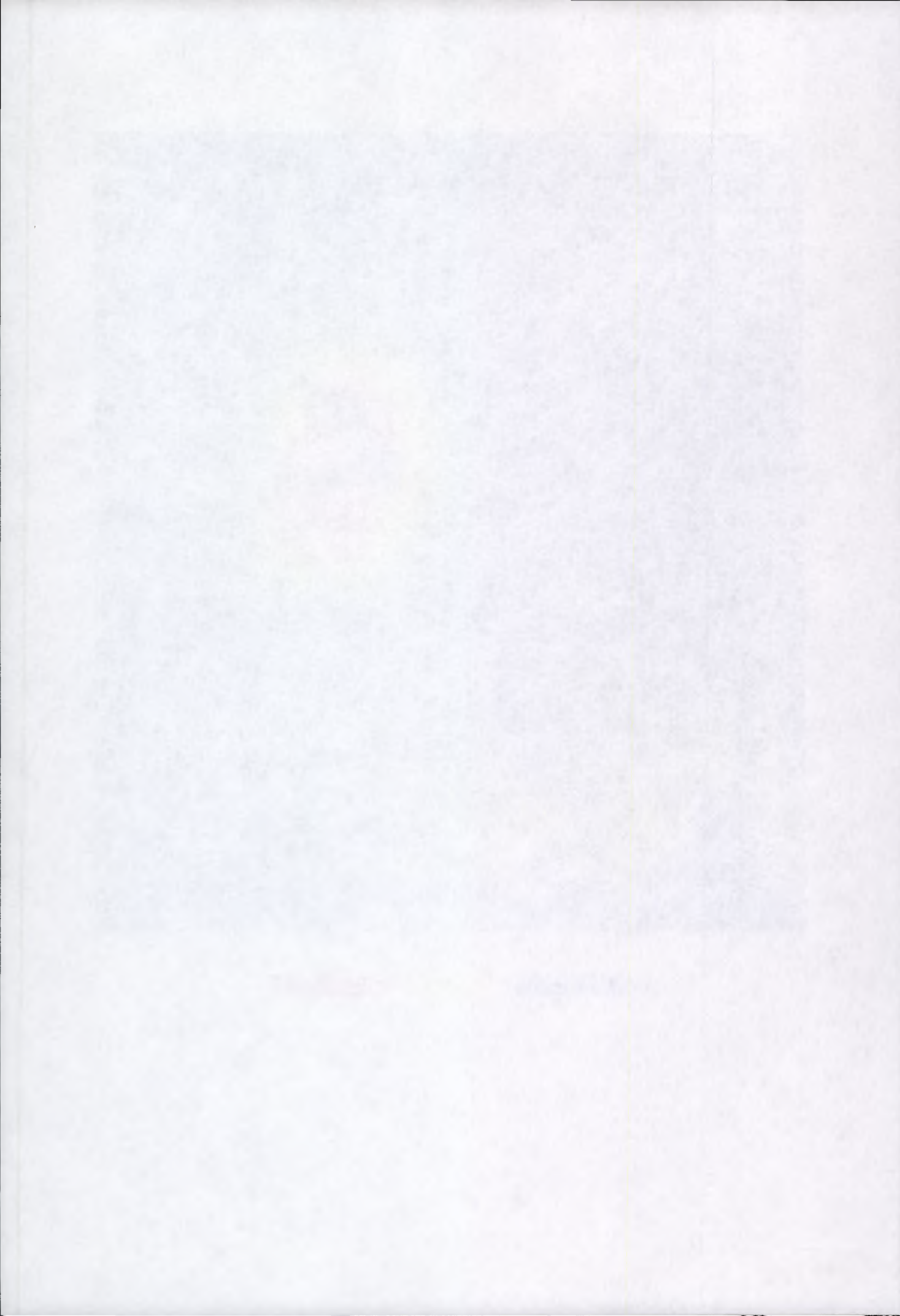


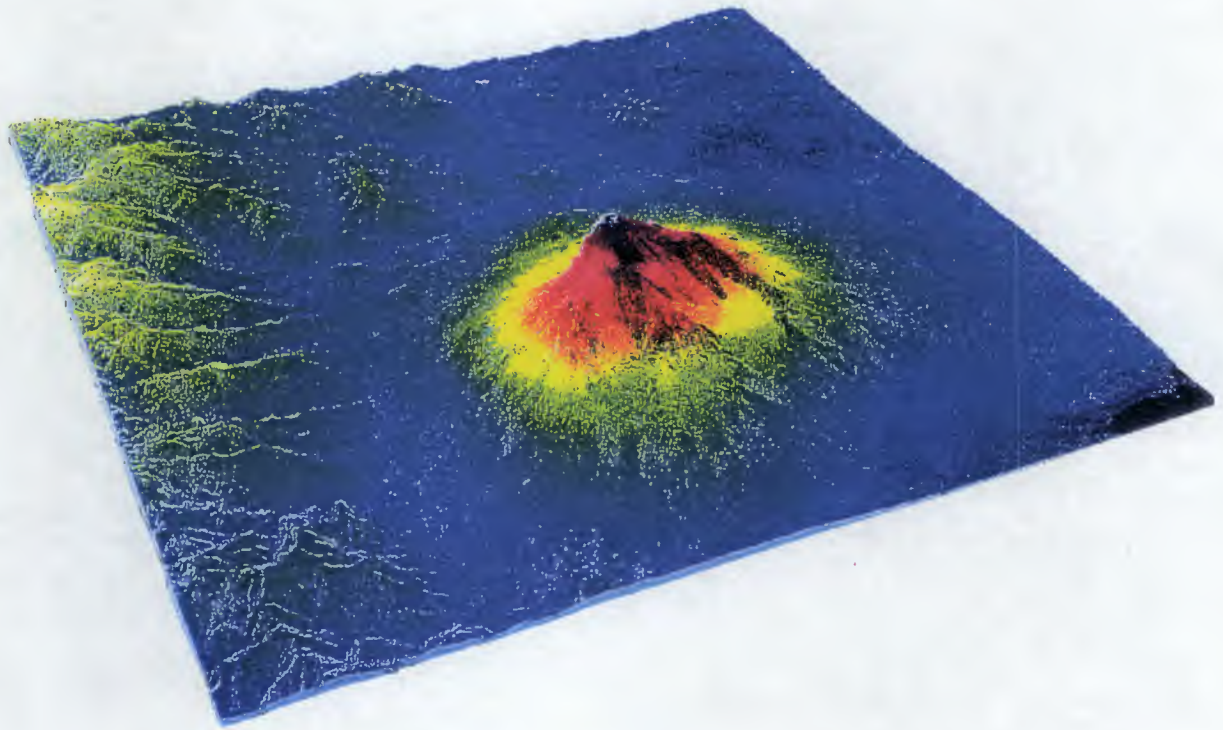
## GAETA TANDEM Digital Elevation Model (DEM)













# Annex C

## **Geographical area**

Etna, Italy

## **Research institute**

Institute for Navigational Studies, Stuttgart, Germany

## **Application domain**

Digital Elevation Models (DEM)

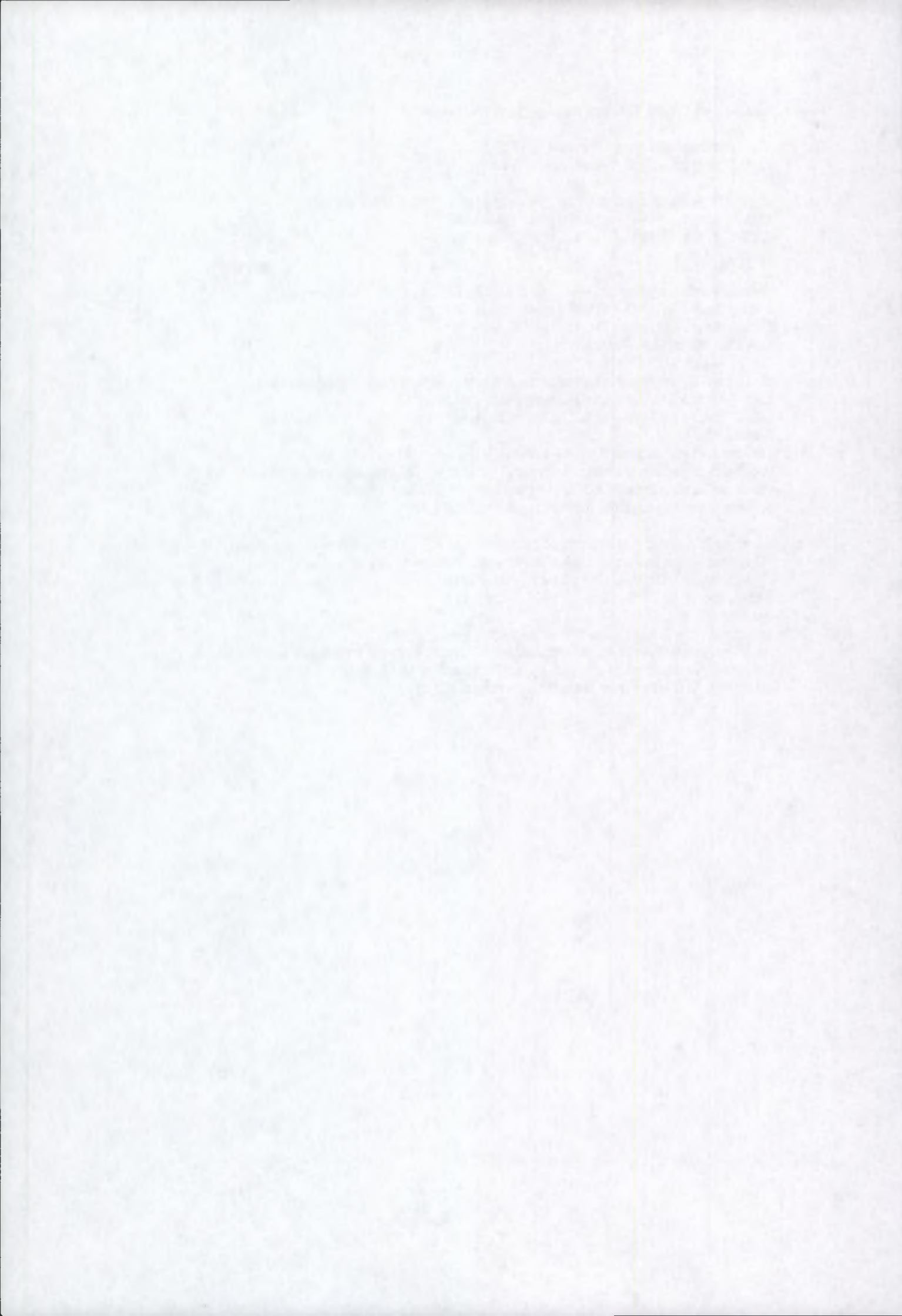
## **First results**

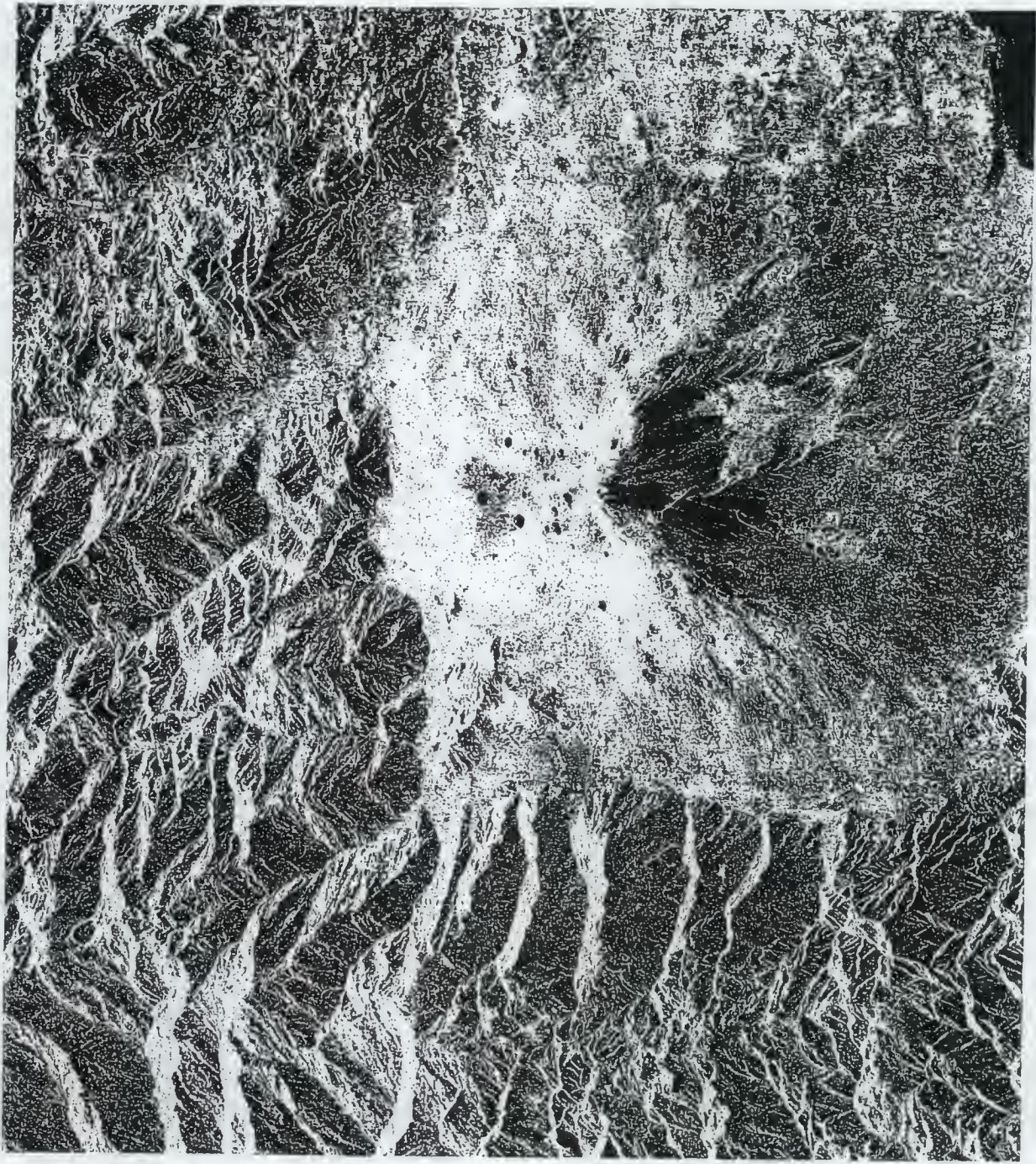
ERS Tandem Interferogramme, Coherence image & corresponding DEM with the ERS-2 SAR Intensity image overlaid. On the basis of previous results with ERS-1 repeat INSAR, the improved coherence obtained with the Tandem 1-day interval is expected to result in height errors of less than 10m rms across the image, and less than 2m rms for local areas (on the scale of 2x2 km) within the image.



## Results achieved with ERS-Tandem Data of the ETNA area:

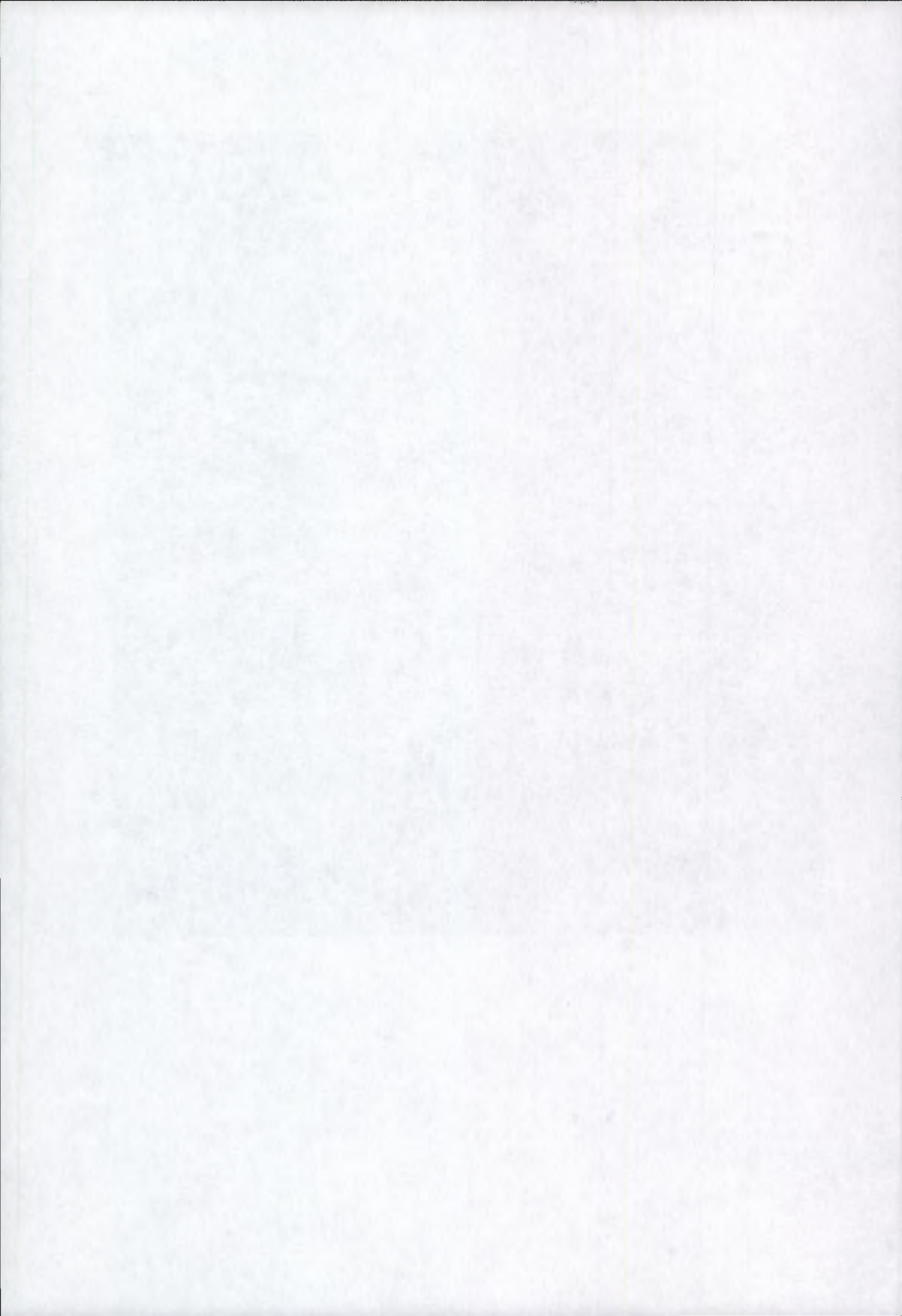
- Fig. 1: shows the Intensity image acquired by ERS-1  
date: 5.09.1995 Orbit: 21660 Frame. 747
- Fig.2: shows the coherence image of the following ERS-1 / ERS-2 Tandem pair  
ERS-1: date: 5.09.1995 Orbit: 21660 Frame. 747  
ERS-2: date: 6.09.1995 Orbit: 1987 Frame. 747  
Baseline: 105 m
- Fig.3: shows the relative phase image of the following ERS-1 / ERS-2 Tandem pair  
ERS-1: date: 5.09.1995 Orbit: 21660 Frame. 747  
ERS-2: date: 6.09.1995 Orbit: 1987 Frame. 747  
Baseline: 105 m 2 Pi-Elevation: 83 m
- Fig.4: shows an IHS image combination of the following ERS-1 / ERS-2 Tandem pair  
ERS-1: date: 5.09.1995 Orbit: 21660 Frame. 747  
ERS-2: date: 6.09.1995 Orbit: 1987 Frame. 747  
Baseline: 83 m  
I = Intensity is taken from the ERS-1 intensity image  
H= Hue is taken from the height information calculated from the unwrapped relative phase  
the colour bar correspond to height values between 0 m and 3300 m.  
S= Saturation is taken from the coherence image (Fig 2)
- Fig.5: shows an IHS image combination of the following ERS-1 / ERS-2 Tandem pair converted to a  
3D-image, where the height component is used as elevation in z-direction  
ERS-1: date: 5.09.1995 Orbit: 21660 Frame. 747  
ERS-2: date: 6.09.1995 Orbit: 1987 Frame. 747  
Baseline: 83 m  
I = Intensity is taken from the ERS-1 intensity image  
H= Hue is taken from the height information calculated from the unwrapped relative phase  
the colour bar correspond to height values between 0 m and 3300 m.  
S= Saturation is taken from the coherence image (Fig 2)

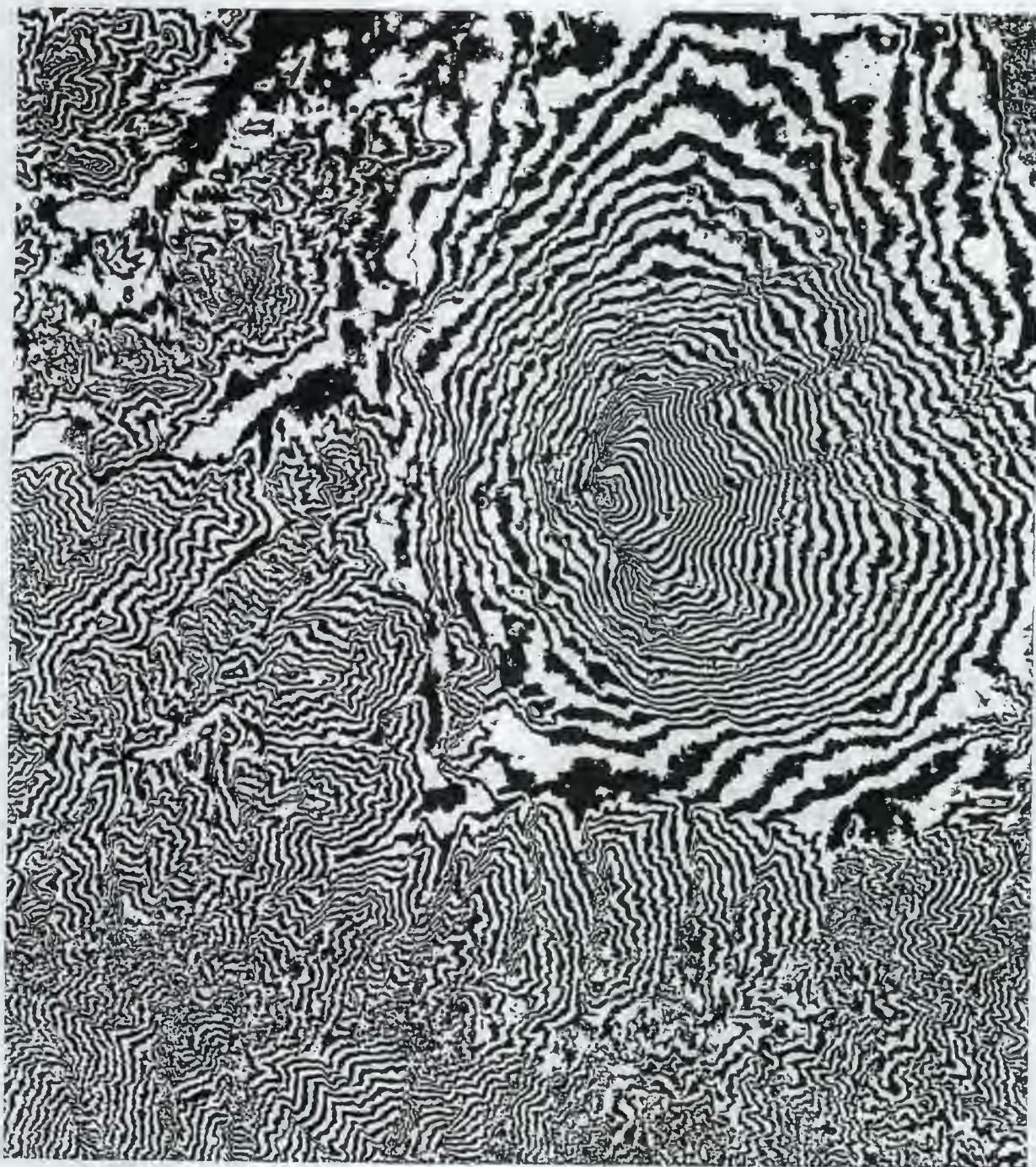


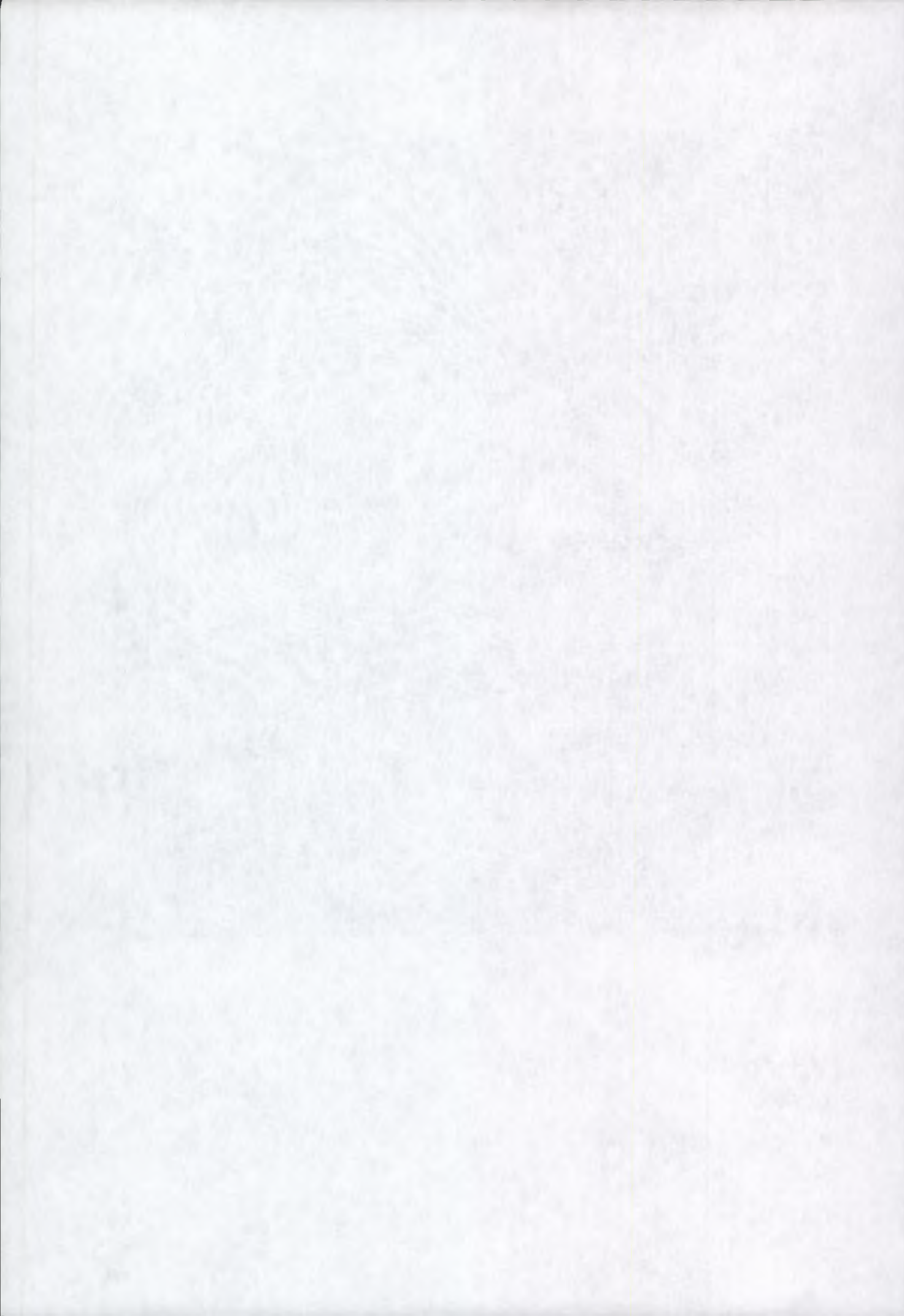








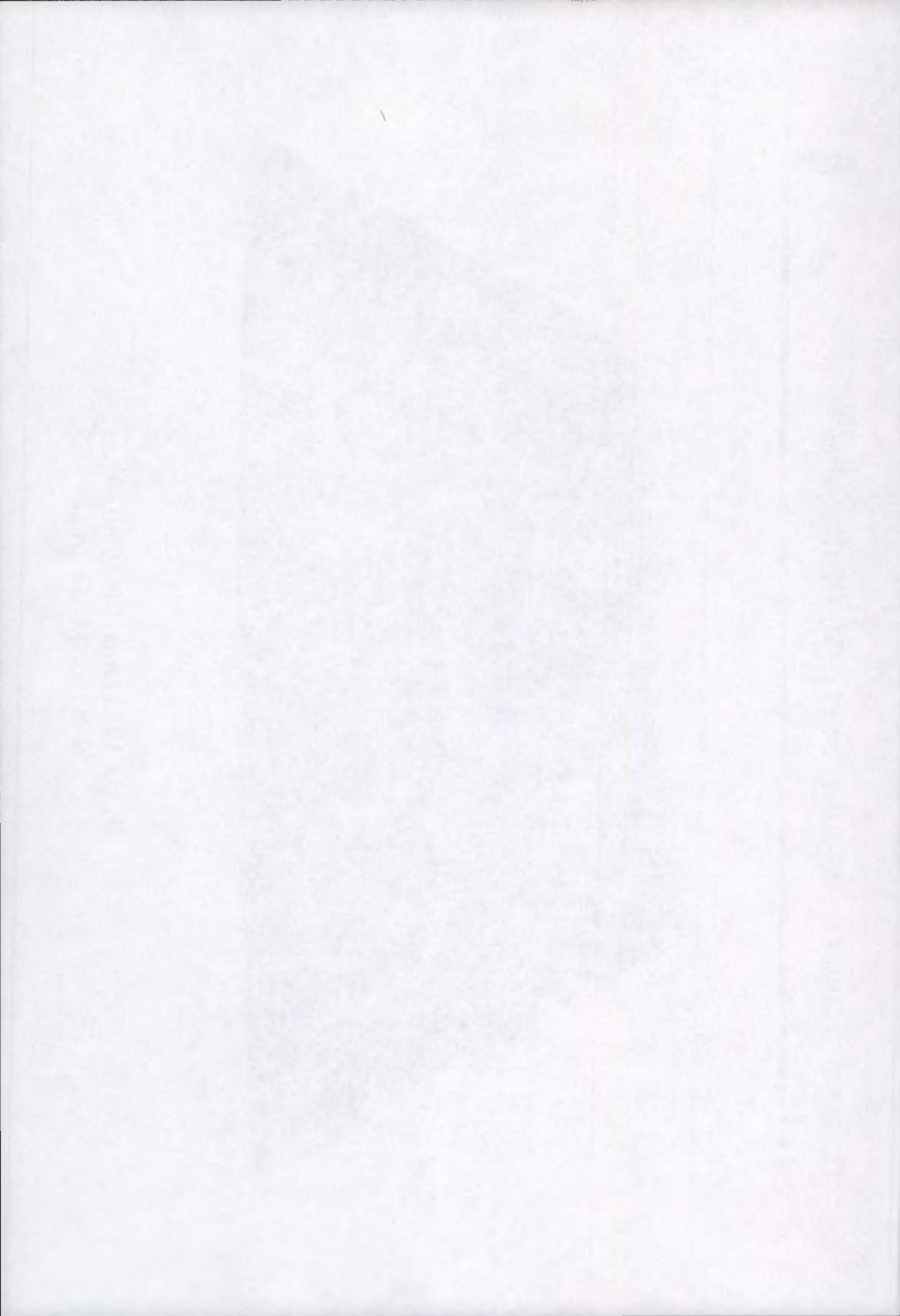




**TANDEM DEM + ERS-2 INTENSITY IMAGE (Etna, Italy)**



$H_{err} < 10$  m (rms) for 100x100 km  
< 2 m (rms) local areas



# Annex D

## Geographical area

Bern, Switzerland

## Research institute

Dornier, Germany

## Application domain

Digital Elevation Models (DEM)

## First results

ERS-1 orbit 20322, 04-06-95, time 10:22:09

ERS-2 orbit 649, 05-06-95, time 10:22:12.

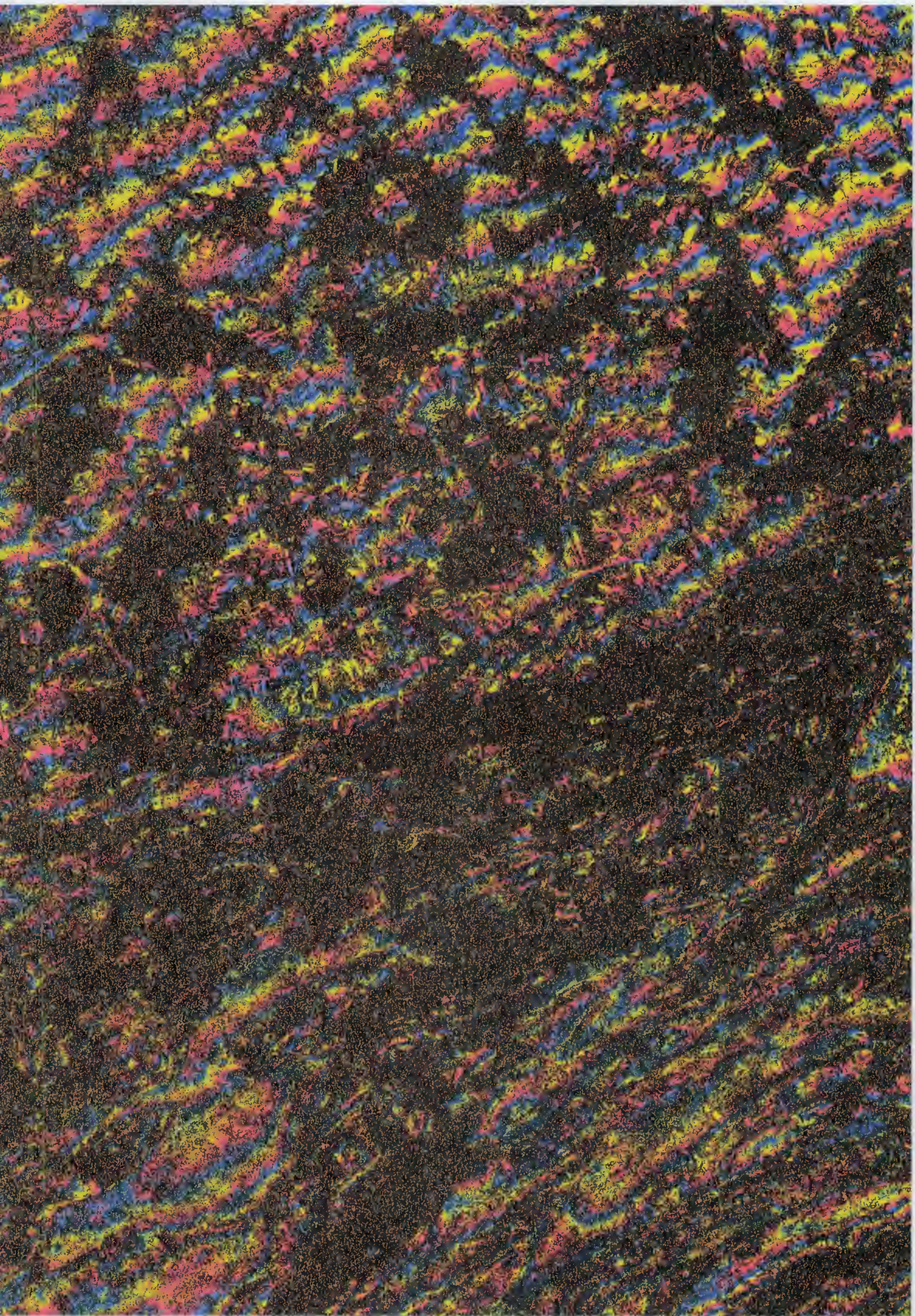
Two sequences of 3 images, each sequence for Quadrant 3 & 4 of the 100x100 km acquisition. For each sequence :-

- ERS-2 Single Look Complex Intensity Image.
- ERS Tandem Flat Earth removed Interferogramme.
- ERS Tandem coherence image; colour code : blue corresponds to low coherence (0), red/yellow corresponds to high coherence (1). Forested regions appear blue.

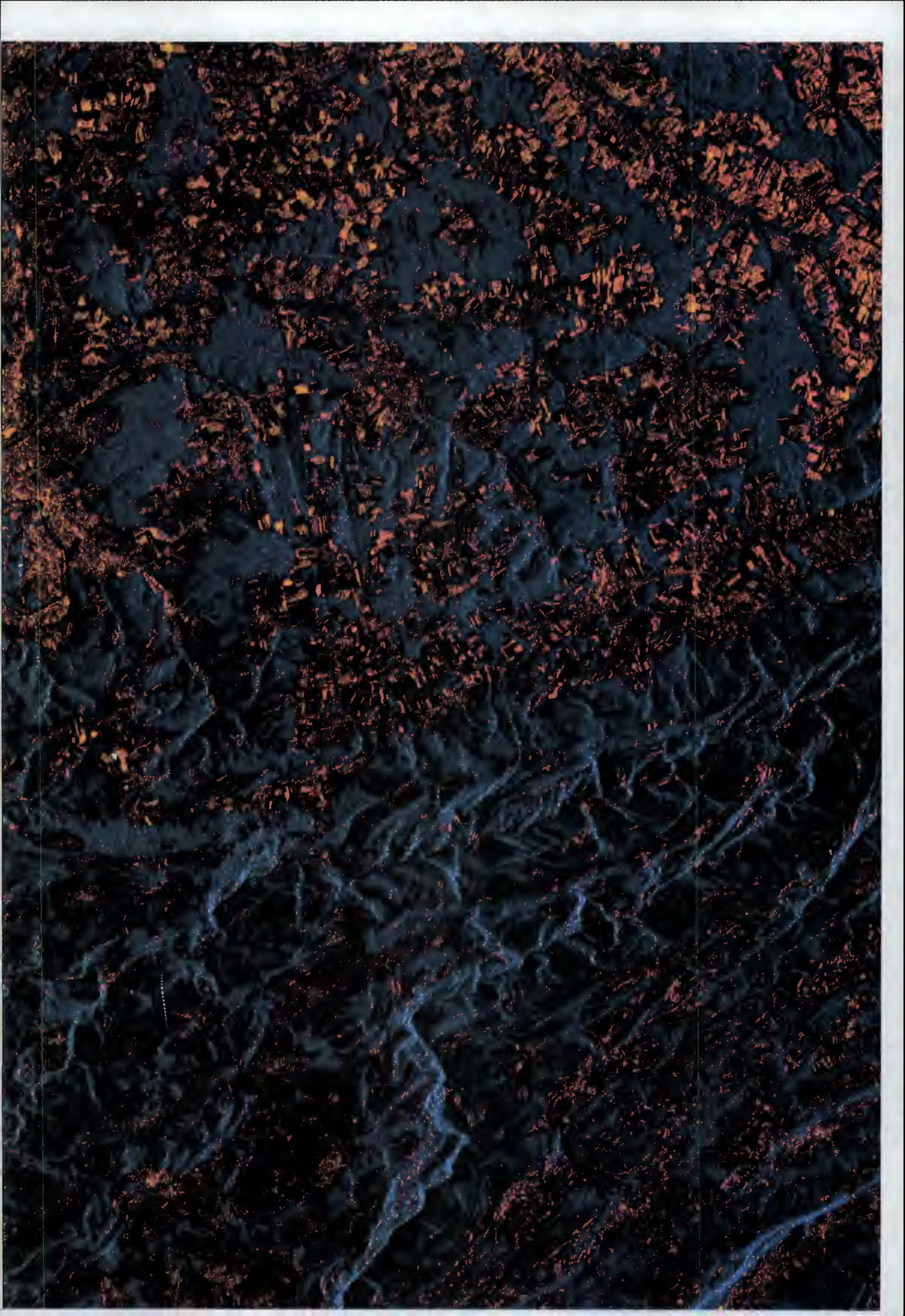


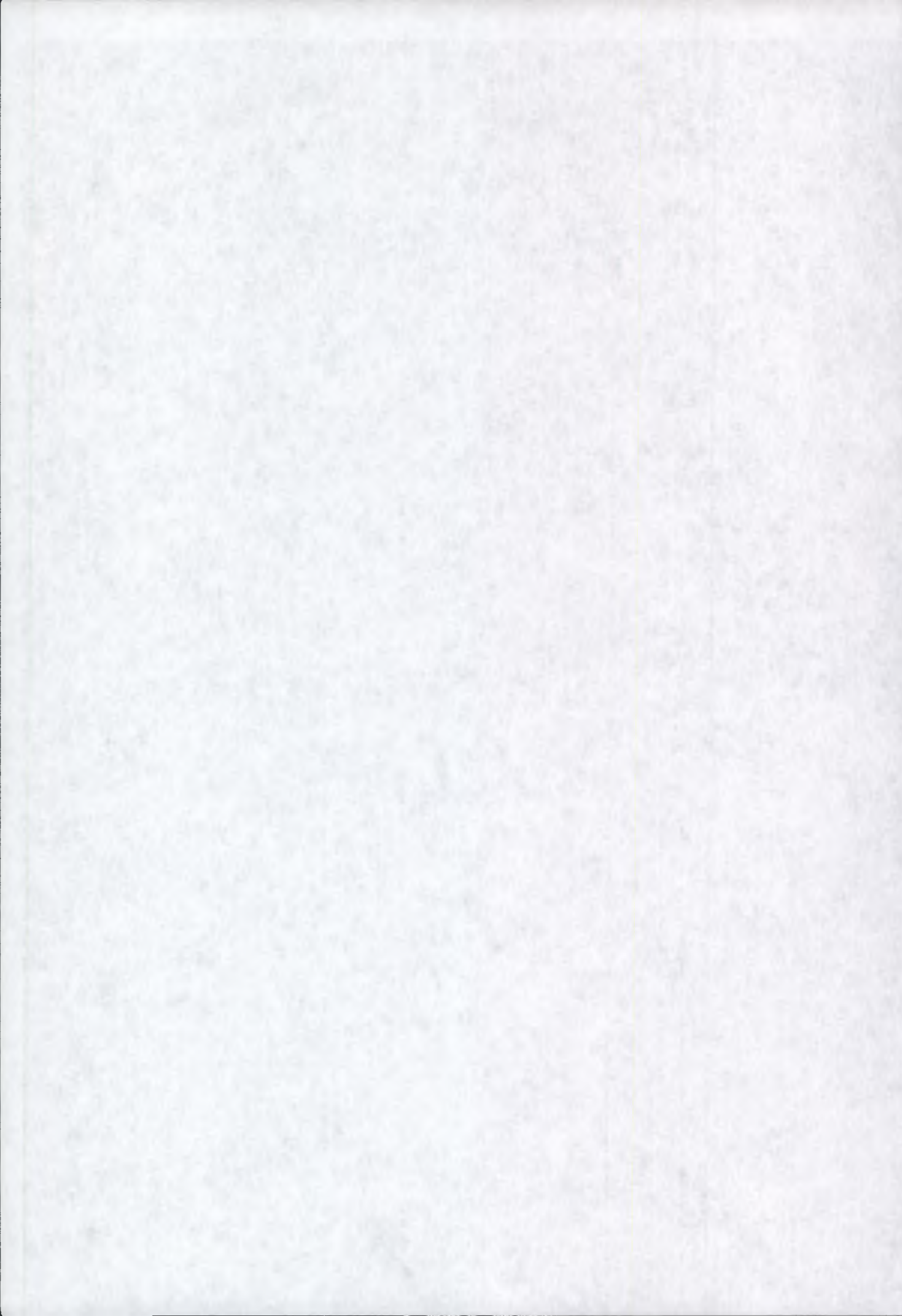




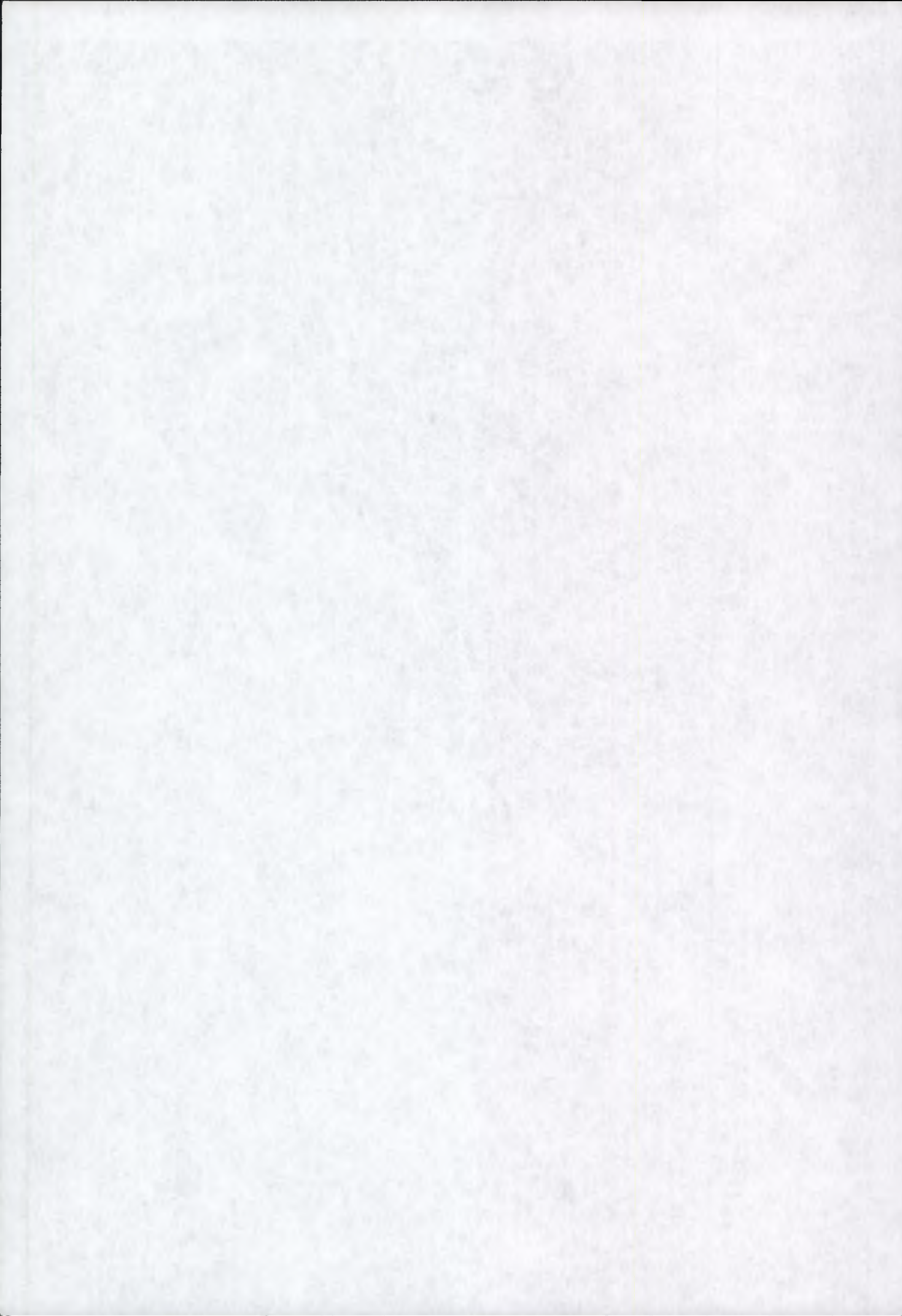


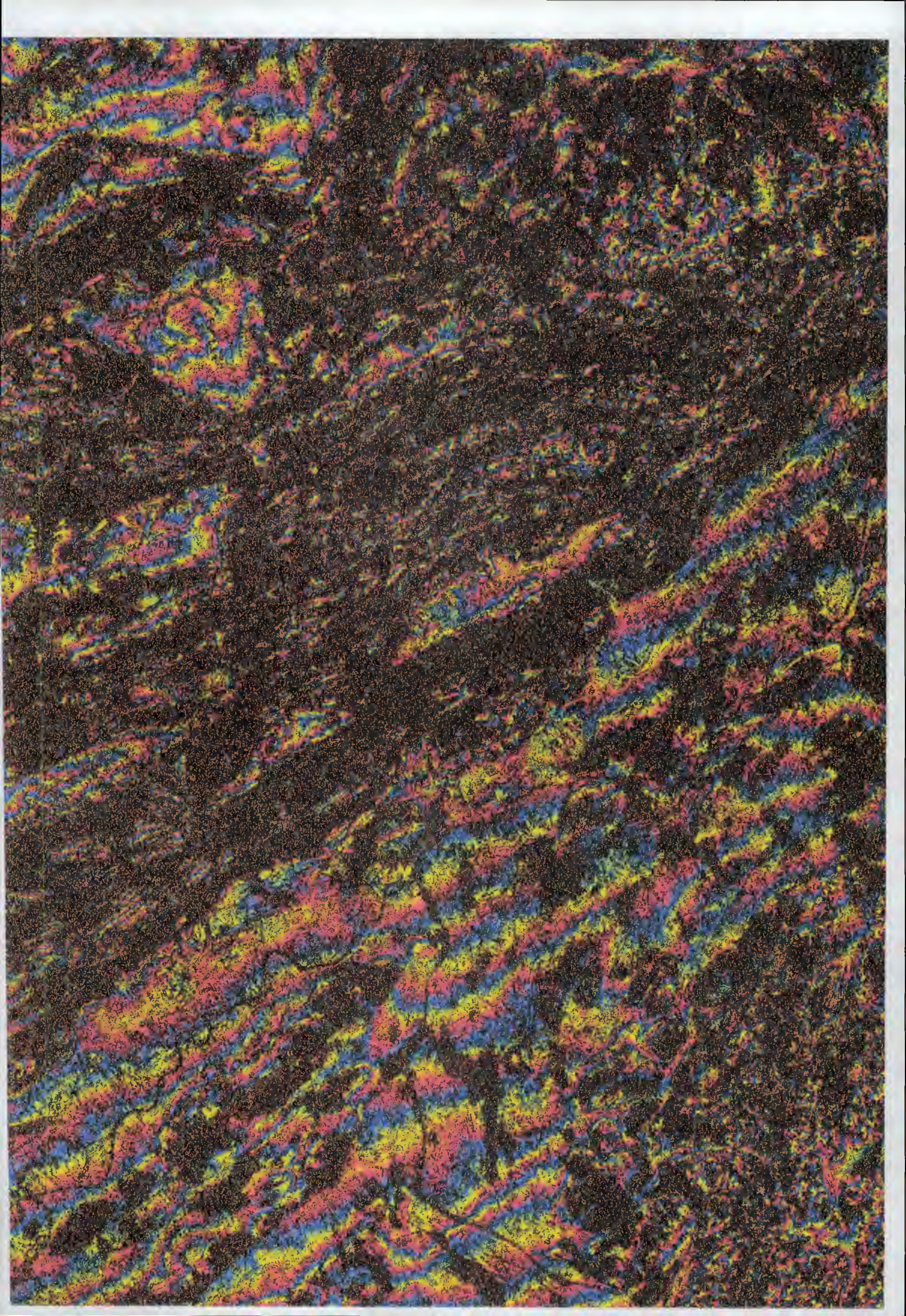


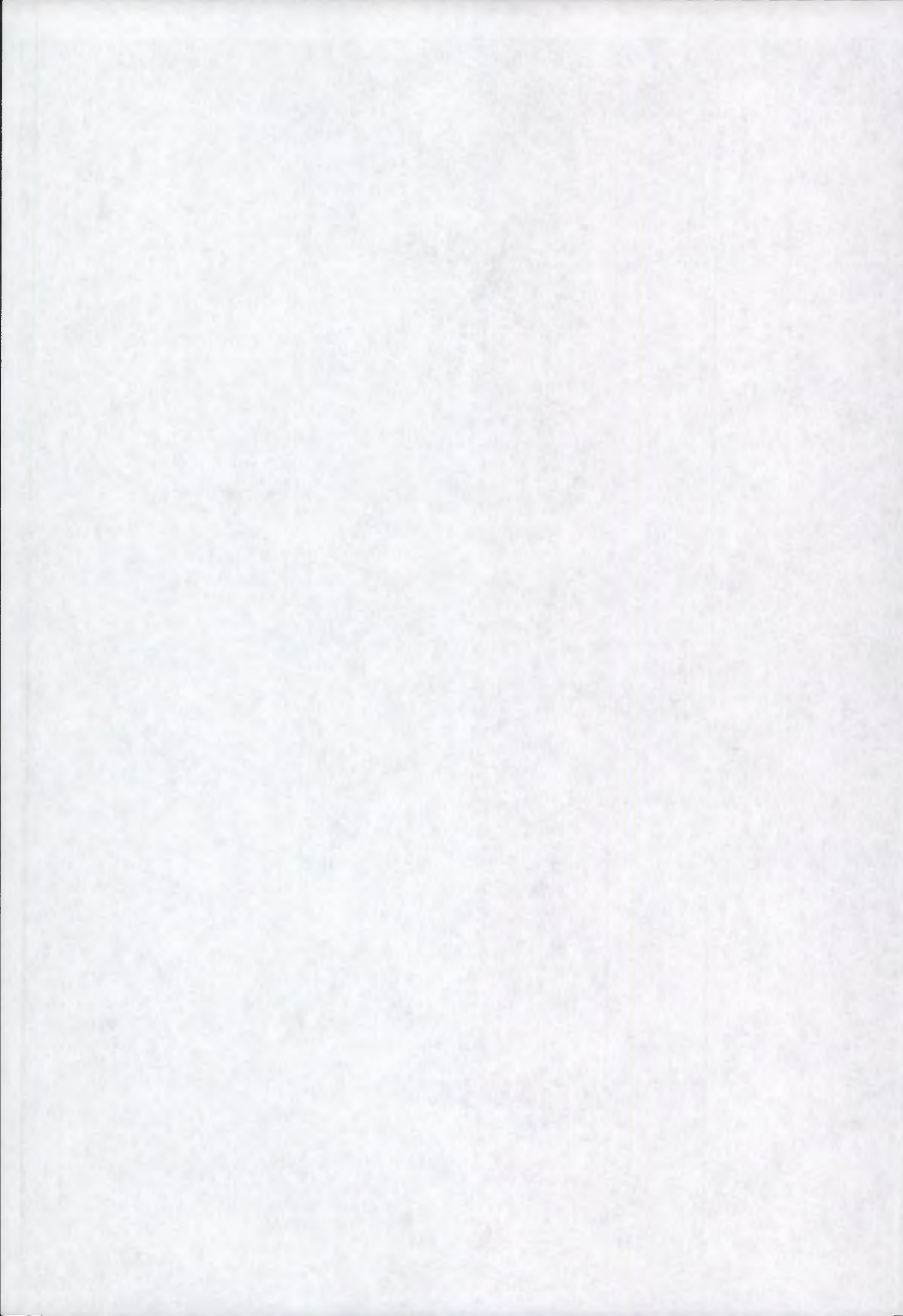


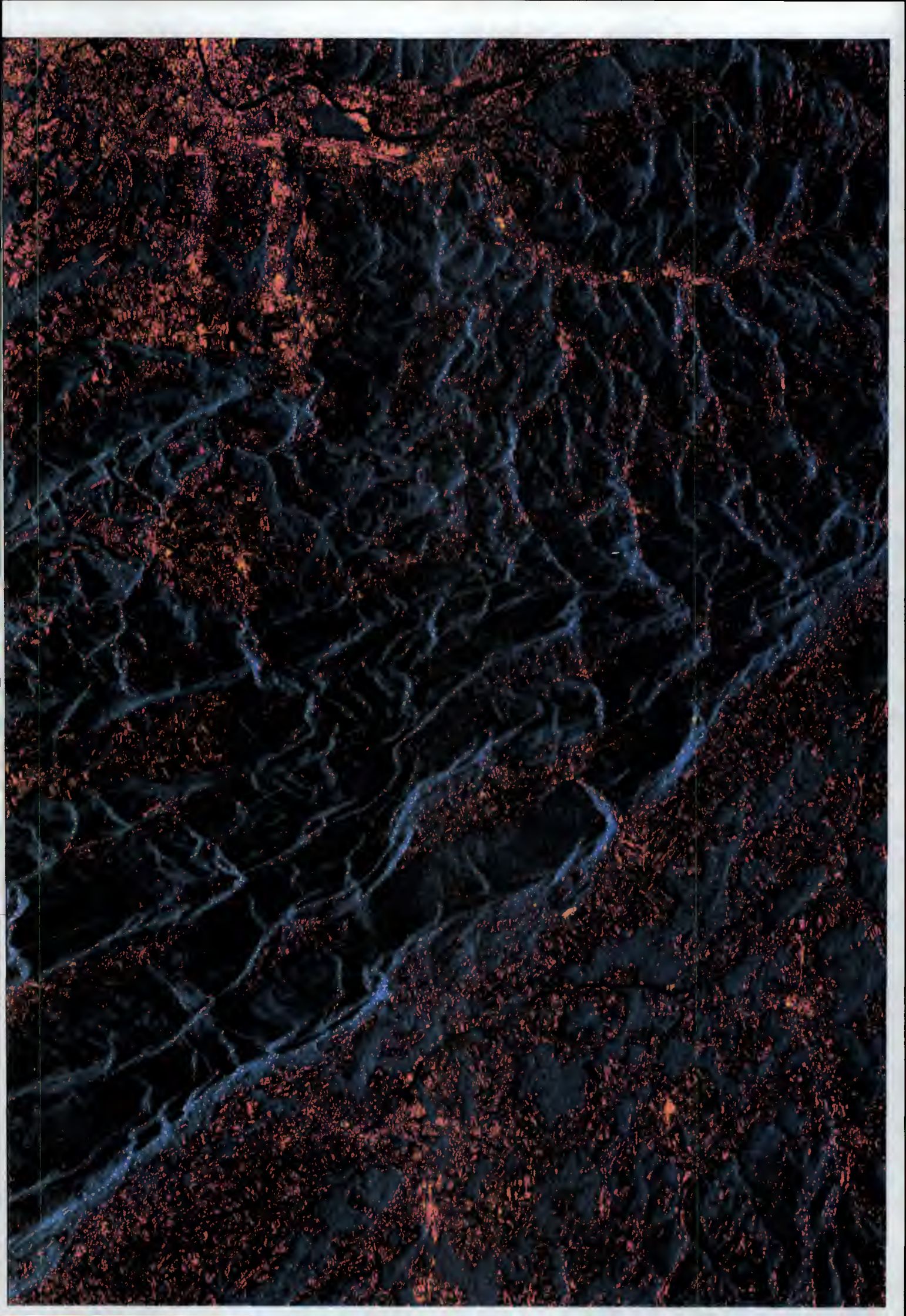


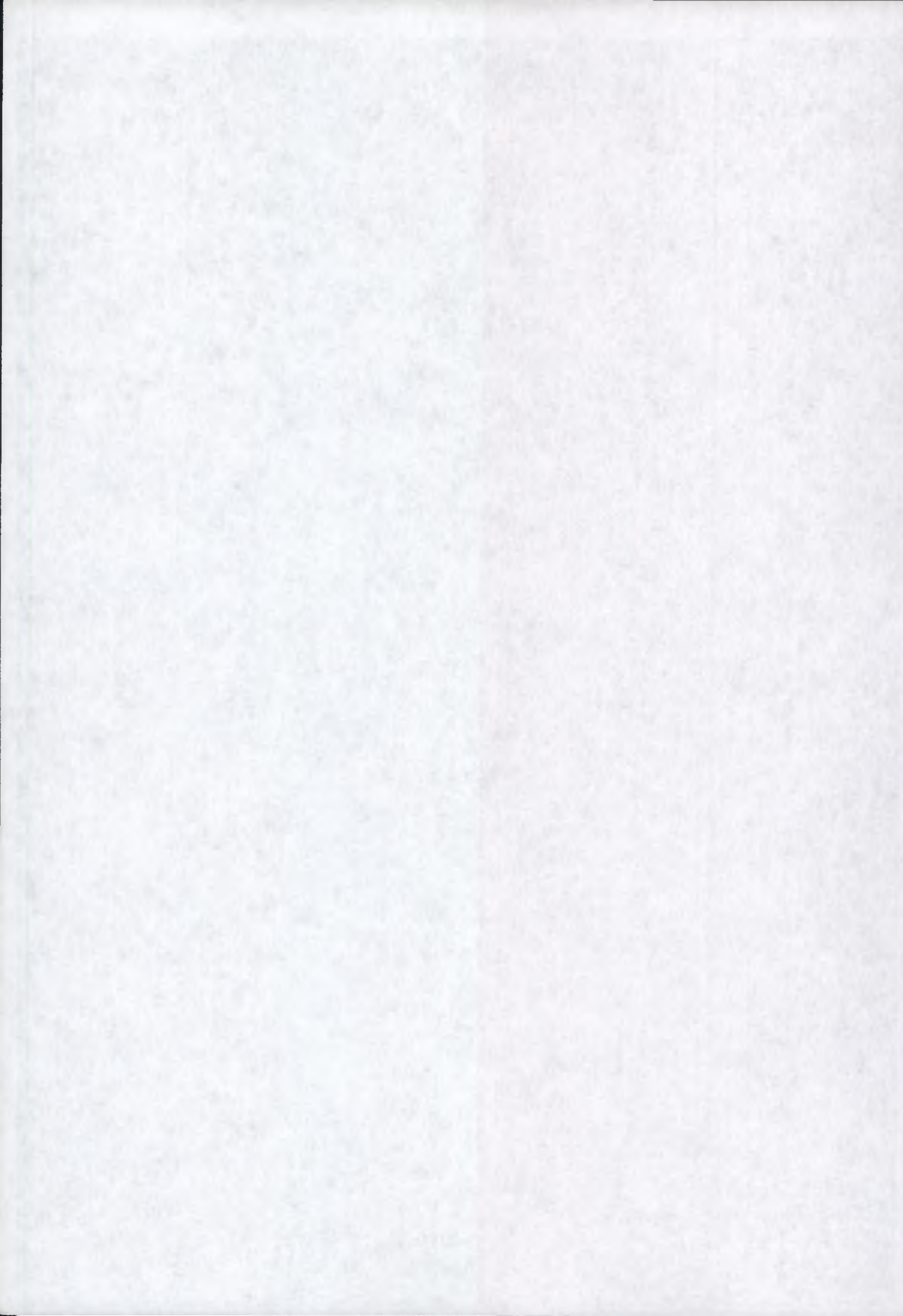












# Annex E

## **Geographical area**

Athabasca and Saskatchewan glaciers, Canada

## **Research institute**

CCRS, Canada

## **Application domain**

Ice motion / Glaciology

## **First results**

Two tandem pairs exhibiting high coherence ( $> 0.67$ ) were used to generate interferograms. These were then used to deduce ice motion velocities for the Athabasca and Saskatchewan. the results were checked against field measurements.. Velocity measurements from the interferograms assumed a plastic flow model for the glacier motion and flow vectors pointing down the direction of maximal slope., in turn determined from airborne interferometric SAR measurements.

Verification against field survey data indicated that measurements were accurate to within 2cm per day even for peak flow rates of the order of 40cm per day.



## Airborne and Spaceborne SAR Interferometry: Application to the Athabasca Glacier Area

P.W. Vachon, D. Geudtner, L. Gray, K. Mattar, M. Brugman<sup>1</sup>, I. Cumming<sup>2</sup>, J.-L. Valero<sup>2</sup>

Canada Centre for Remote Sensing, 588 Booth St., Ottawa, Ont. K1A 0Y7 CANADA  
Phone: (613) 998-9060 Fax: (613) 993-5022 E-mail: vachon@ccrs.emr.ca

<sup>1</sup>National Hydrological Research Institute, Saskatoon, Sask. S7N 3H5 CANADA

<sup>2</sup>Dept. of Electrical Engineering, University of British Columbia, Vancouver, B.C. V6T 1Z4 CANADA

**Abstract** – ERS tandem mode differential synthetic aperture radar (SAR) interferometry (InSAR) is used to measure the surface flow field of a mid-latitude alpine glacier. The interferometric imaging geometry was reconstructed using accurate orbit data and a digital elevation model (DEM) derived from the CCRS CV-580 cross-track InSAR. The flow field is favorably validated against historical and nearly coincident displacement measurements made using surveying techniques.

### INTRODUCTION

In this paper, InSAR measurements of the Athabasca and the nearby Saskatchewan and Dome Glaciers in the Canadian Rocky Mountains (N52.2° W117.25°) are considered. These typical mid-latitude alpine glaciers are tightly constrained by mountains, can move rather rapidly with significant vertical and horizontal velocity components, and may have significant summertime melt rates. It is important that long term monitoring of these glaciers be carried out in order to assess changes in glacier volume and mass transport rates. Such information is essential for validating and improving relevant hydrological models, and could have a role in assessing global climate change.

Differential InSAR offers the potential to provide the required monitoring and model validation capability and has already been studied in connection with polar ice sheets [1, 2]. We have considered three interferometry cases: first, CCRS CV-580 cross-track InSAR; second, ERS-1 interdisciplinary orbit repeat-pass InSAR with 35 days repeat cycle; and third, ERS-1/ERS-2 tandem mode repeat-pass InSAR with 1 day repeat cycle.

In the first case, two images with a known baseline are acquired simultaneously, allowing DEM generation from the interferogram phase [3]. In the second case, our experience has shown that the 35 day interval is too long to retain any useful scene coherence over the glaciers of interest. In the third case, we have found that useful interferograms (*i.e.* having significant scene coherence over the glaciers of interest) can be generated from the 1 day interval data, under certain weather conditions. In this case, the interferometric phase contains topographic as well as glacier displacement information.

### DATA AND RESULTS

A field program to the area from 23 to 26 August, 1995

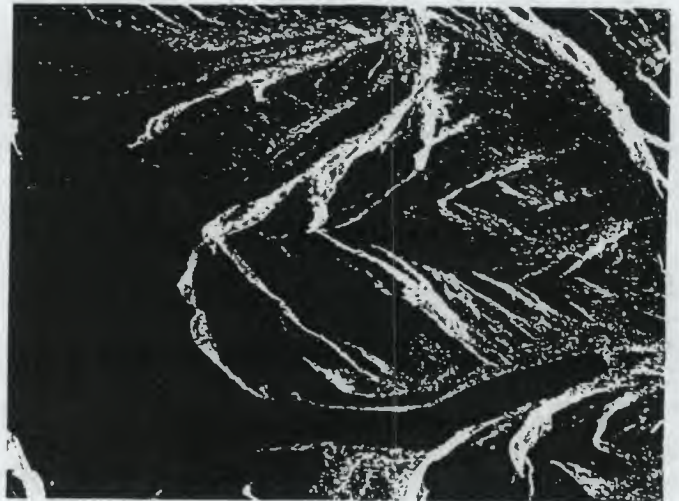


Figure 1: Interferogram magnitude, 24/25 Aug. 1995. Azimuth: bottom-to-top. Ground range: left-to-right. The scene covers 16-by-12 km.

included the installation of survey markers on Athabasca and Saskatchewan Glaciers. The marker positions were measured in Aug., Sept., and Dec. 1995. CV-580 cross-track InSAR data were collected in March and August, 1995 for reference DEM generation. Only ascending ERS passes were considered, because the glaciers of interest are well-aligned with the radar line-of-sight. The descending passes provide only limited coverage of the glaciers due to significant layover. We have considered passes from two different relative orbits (ROs) of the ERS-1/2 tandem mode phase G operations, with passes at 05:53 UTC (23:53 local time). The tandem mode passes considered so far are summarized in Table 1.

The interferometric processing was carried out as described in [4]. Fig. 1 is a representative interferogram magnitude image, while Figs. 2 and 3 are representative scene coherence maps for 24/25 Aug. 1995 and for 2/3 Nov. 1995. In each figure, Dome, Athabasca, and Saskatchewan Glaciers appear top-to-bottom, with the Columbia Ice Field to the left. The measured scene coherence  $\gamma$  on Athabasca Glacier is included in Table 1, along with temperature data measured by an automatic weather station located on the glacier. We require high scene coherence (say,  $\gamma > 0.25$ ) to warrant proceeding with differential interferogram generation. High scene coherence is



Figure 2: Scene coherence, 24/25 Aug. 1995.

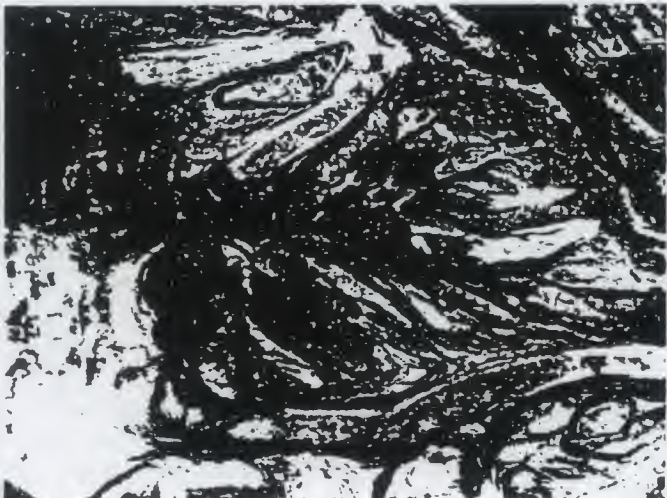


Figure 3: Scene coherence, 2/3 Nov. 1995.

usually associated with below freezing maximum temperatures, the absence of precipitation, and no blowing snow during the data collection interval.

The glacier flow field was derived from the ERS tandem mode image pairs having high scene coherence over the glaciers. The measured interferometric phase due to topography was removed using the DEM derived from the airborne SAR data. This was accomplished by using accurate ERS orbit data and an algorithm to reconstruct the ERS imaging geometry [5] and to map the phase derived from the DEM into the slant-range, azimuth coordinate system. The actual interferogram was multiplied by the complex conjugate of the synthetic interferogram, leaving the differential phase due to glacier motion. The differential phase was unwrapped using a variant of the cut-line method [6] controlled by a mask made from the scene coherence and layover maps, and was mapped back into UTM coordinates. In Fig. 4, we show the unwrapped differential phase for 21/22

Table 1: Summary of data and conditions.

dates 1995	RO	$B_n$ [m]	$\gamma$	$T_{max}$ [° C]	precip. [mm]
8/9 Aug.	220	55	0.22	+7	7
24/25 Aug.	449	78	0.17	+9	5
28/29 Sep.	449	248	0.21	+5	< 1
17/18 Oct.	220	203	0.36	-1	0
2/3 Nov.	449	94	0.77	-7	0
21/22 Nov.	220	17	0.67	-1	0
7/8 Dec.	449	205	0.28	-10	0



Figure 4: Unwrapped differential phase, 21/22 Nov. 1995.

Nov. 1995.

If we ignore any residual phase due to uncorrected topography over the glacier, which is well-justified for the cases with small baseline  $B_n$ , we can interpret the residual phase as relating to the surface displacement field of the glacier over a 24 hour period. The residual fringes are not related to atmospheric heterogeneities since the differential phase was consistent for the high coherence cases examined so far.

The surface displacement field is measured as projected along the radar line-of-sight. We have only one displacement component to work with, so we must make an assumption in order to derive the 3-dimensional surface flow field. In our case, we have assumed a plastic flow model and that the flow vectors point downslope, in the direction of maximum basal slope. This assumption is suitable near the centreline of the glacier, but may be unsatisfactory near the glacier's margins. The downslope direction was determined from the airborne SAR DEM, as shown in Fig. 5. In Fig. 6, we show a validation of the measured displacement along the centreline of Saskatchewan Glacier. Two separate InSAR-measured glacier flow fields, based on tandem mode pairs collected 19 days apart, are compared with the *in situ* measured point velocities derived from the historical [7]

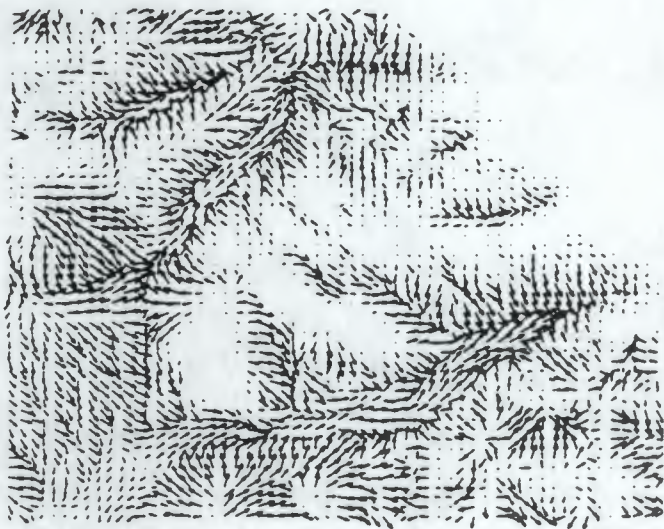


Figure 5: Airborne InSAR DEM flow directions. The arrow length is proportional to the surface slope.

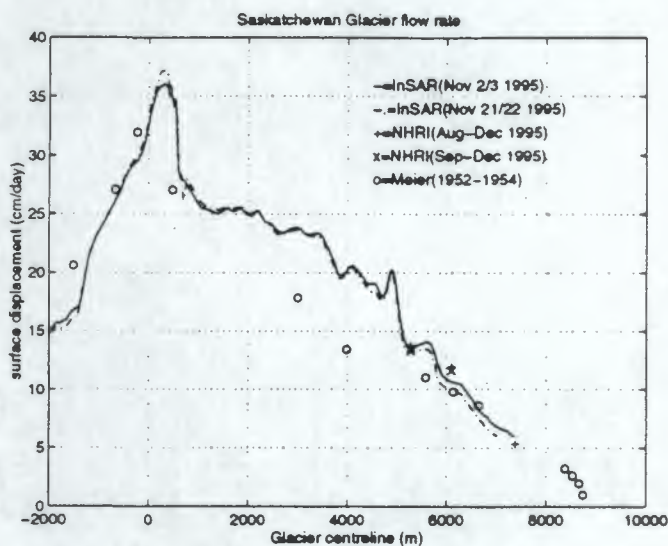


Figure 6: Displacement field validation.

and more recent point displacement measurements. The agreement between subsequent tandem mode image pairs is excellent and is consistent with both sets of surveying measurements.

### CONCLUSIONS

It has been shown that spaceborne SAR interferometric image pairs collected with a 24 hour interval may be used to measure the surface displacement field of a typical mid-latitude alpine glacier. This result was validated against historical flow field measurements and more recent surveying measurements coincident with the image pair acquisition time frame. We measured peak flow rates close to 40 cm/day on the Saskatchewan Glacier and fine scale velocity structure with a repeatability on

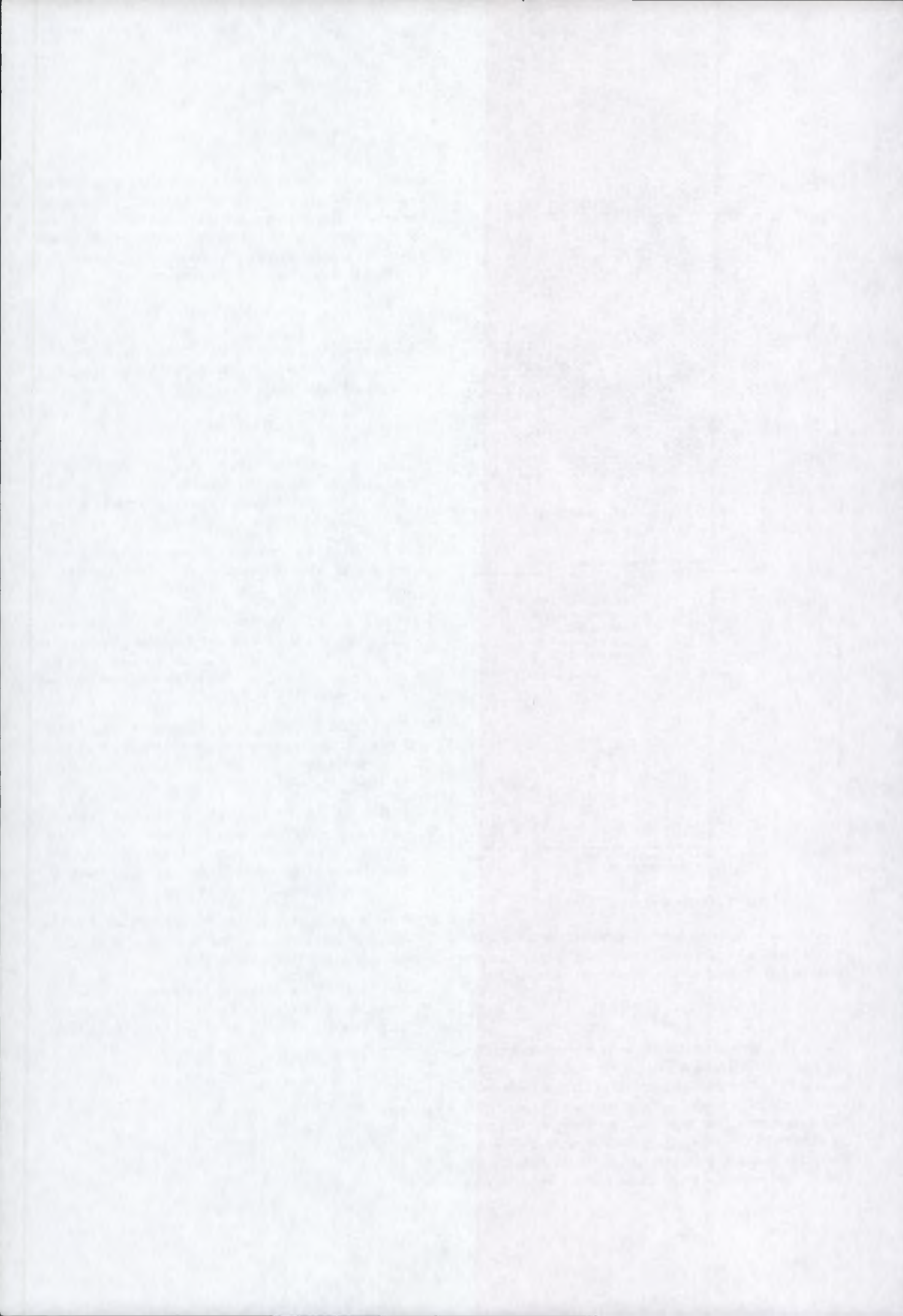
the order of 1 cm/day over a 19 day interval, suggesting that the measured small scale velocity structure is real. The principal limitation of this technique at our site was the loss of scene coherence, even over the 24 hour interval between subsequent passes. The technique appears to work best during winter when the potential of daytime melting is minimized.

### ACKNOWLEDGMENTS

We thank ESA for providing the ERS data, and in particular Steve Coulson (ESA/ESRIN) for ensuring correct scheduling of our tandem mode data.

### REFERENCES

- [1] R.M. Goldstein, H. Englehardt, B. Kamb, and R.M. Frollich. Satellite radar interferometry for monitoring ice sheet motion: Application to an Antarctic ice stream. *Science*, 262:1525-1530, 1993.
- [2] R. Kwok and M.A. Fahnestock. Ice sheet motion and topography from radar interferometry. *IEEE Trans. Geoscience Rem. Sens.*, 34(1):189-200, 1996.
- [3] A.L. Gray, K.E. Mattar, and M.W.A. van der Kooij. Cross-track and along-track airborne interferometric SAR at CCRS. In *Proc. 17th Canadian Symposium on Remote Sensing, 13-15 June 1995, Saskatoon, Saskatchewan, Canada*, pages 232-237, 1995.
- [4] P.W. Vachon, D. Geudtner, A.L. Gray, and R. Touzi. ERS-1 synthetic aperture radar repeat-pass interferometry studies: Implications for RADARSAT. *Can. J. Rem. Sens.*, 21(4):441-454, 1995.
- [5] D. Geudtner and M. Schwäbisch. An algorithm for precise reconstruction of InSAR imaging geometry: Application to "flat earth" phase removal, phase-to-height conversion, and geocoding of InSAR-derived DEMs. In *Proc. EUSAR'96, Königswinter, Germany, 1996*. In press.
- [6] R.M. Goldstein, H.A. Zebker, and C.L. Werner. Satellite radar interferometry: Two-dimensional phase unwrapping. *Radio Science*, 23(4):713-720, 1988.
- [7] M.F. Meier. Mode of flow of Saskatchewan Glacier Alberta, Canada. Professional Paper 351, 1960. U.S. Geological Survey, U.S. Government Printing Office, Washington, D.C.



# **Annex F**

## **Geographical area**

Vindeln, Sweden

## **Research institute**

Chalmers University of Technology, Sweden

## **Application domain**

Forestry

## **First results**

Based on a combined coherence and radiometry image produced from a tandem dataset, various land types could be classified by a visual interpretation. The land types identified were:

- marsh and bog land
- agricultural land
- forest areas

Coherence was too low for the production of a Digital Elevation Model (DEM) or to further characterise the forest areas. The data on which the analysis was based were acquired during the summer period. It is expected that the characterisation of forest areas should be better for winter data.



# Chalmers University of Technology

Department of Radio and Space Science  
Remote Sensing Group  
S-412 96 Göteborg, Sweden  
Prof. Jan Askne  
Telephone +46 31 7721843 Fax +46 31 164513  
<http://www.rss.chalmers.se>



Göteborg 1996-04-30

## Report on ERS-1/2 Tandem Demonstration

by Jan Askne, Patrik Dammert, and Gary Smith

**Abstract:** Only six pairs of ERS-1/2 images have been obtained from a forest area in northern Sweden. Of the six pairs only two ERS-1/2 summer pairs have had good coherence and been analysed. The coherence is slightly lower than from ERS-1 winter pairs. For applications related to forested areas, including slope and DEM production, it is important to have a short interval between the images. This makes tandem missions important while the 35 day repeat cycle envisaged for ENVISAT is too long.

### IMAGES AVAILABLE FROM THE HÖKMARK AREA IN NORTHERN SWEDEN

A large number of images have been acquired with the ERS-1/2 system but we have so far only obtained four image pairs, see Table 1, which makes an evaluation rather limited.

Table 1

Date	Technical conditions	Meteorological conditions	Coherence properties etc.
May 23/24	Estimated difference in Doppler centroid of 0.26.	Rain before image on 23rd, and between images	Unusual in that the backscatter from the fields is greater than from forest (in both images). Coherence too low to be useful for interferometry
June 27/28	Normal baseline of 48 m.	No rain before images for about 10 days. Wind speeds moderate on both days (6 and 7 m/s). Relative humidity increased from 39% to 64% over the day between images.	
August 1/2	Normal baseline of 15 m	No rain before images for 5 days. Very similar weather conditions (dry haze) on both days. Light winds (4 and 5 m/s respectively).	
November 14/15	Normal baseline of 1295 m		Baseline too long to be useful for interferometry

## ASPECTS ON INTERFEROMETRIC SAR PROCESSING

ERS-2's onboard SAR system was designed to be a copy of ERS-1's system, and there are only a few differences between the two systems. First, the yaw and pitch of the ERS-2 SAR antenna are slightly different than the ones for ERS-1. Second, the amplification is lower and the noise floor is higher (-24.3 dB compared to -25 dB for SLC products) in ERS-2 than in ERS-1.

The yaw and pitch differences is most noticeable when looking at the Doppler centroids of two images covering the same area, one from ERS-1 and one from ERS-2. We actually noted a 0.26 Doppler centroid difference (in fractions of sampling frequency) for the 23-24 May 1995 pair. Different Doppler centroids will have an impact on the measured coherence in interferograms, see Figure 1 below. For ERS-1 image pairs this was never a problem, since the highest noted difference in our images was approximately 0.02, which gives a negligible decrease in interferometric coherence.

For ERS-2 this poses a problem. The two images have sampled slightly different parts of the ground reflectivity spectrum in azimuth direction. Here we note the resemblance to the wavenumber shift in range direction and the solution is known (Gatelli et al., 1994). A band-pass filter with characteristics derived from the two Doppler centroids and known azimuth bandwidths will filter out the non-common parts of the ground reflectivity spectrum in the two images. The azimuthal band-pass filtering is also easier to carry out since it does not include the local topographic slopes for determining filter properties. Another way of doing the correction is to correct after the measurement is done using Figure 1 and underlying formulas.

In Table 2 examples of measured coherence after azimuthal bandpass filtering are given. Measurements are derived from the 27-28 June 1995 ERS-1/2 interferogram over the Hökmark area north in Sweden (for more information about this area, see (Hagberg et al., 1995)). Doppler centroids differed by 0.16 (in fractions of sampling frequency) which according to theory gives a 9% drop in coherence. The azimuthal bandpass filtering should therefore give a 10% rise in coherence measurements. Differences between theory and measurements can depend on mainly two things. First, the coherence measurement is only an estimate of the true coherence of the area. Second, the coherence estimation method has a bias which affects low coherence measurements.

Table 2. Measurements from the interferogram 27-28 June 1995.

Measurement areas	Bandpass filtered coherence	Actual improvement
Open field 1	0.78	6 %
Open field 2	0.69	7 %
Clear cut 1	0.69	6 %
Clear cut 2	0.73	6 %
Forest 1	0.36	8 %
Forest 2	0.32	8 %

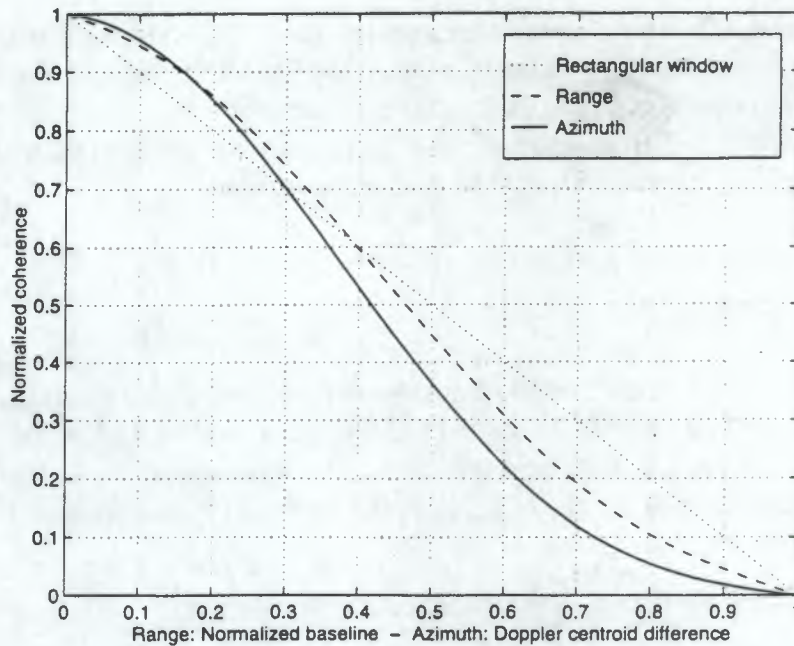


Figure 1. Systematic coherence effects due to data windowing in range and azimuth direction. In range the window is a Hamming window with  $\beta=0.167$  and in azimuth it is a Hamming window with  $\beta=0.167$  in combination with the antenna pattern. The value 1 on the horizontal axes equals maximum baseline in range direction (approx. 1200 meters) and totally different Doppler centroids in azimuth direction (a spectral analysis will give the same value for the Doppler centroids in this case due to aliasing while the antennas are pointing in totally different directions).

Since the noise floor is slightly higher in ERS-2 than in ERS-1, the coherence will be slightly decreased. The interferometric coherence can be expressed as, cf. (Askne et al., submitted)

$$\gamma = \gamma_{processor} \cdot \gamma_{noise} \cdot \gamma_{slanrange} \cdot \gamma_{azimuth} \cdot \gamma_{temporal} \cdot \gamma_{volume}$$

The slant range and azimuth coherence factors can be filtered out by the wavenumber shift filtering (Gatelli et al., 1994), a good processor will set the processor coherence factor to unity, the temporal and volume coherence factors are always present and the noise coherence factor is dependent on thermal noise in the receivers onboard the satellites. For ERS-1, the noise coherence factor was

$$\gamma_{noise} = \frac{1}{1 + \text{SNR}^{-1}}$$

However, since there is two different signal-to-noise (SNR) ratios for the ERS-1/2 interferograms, the formula has to be slightly revised as

$$\gamma_{noise} = \frac{1}{\sqrt{1 + (\text{SNR}_{ERS-1})^{-1}} \cdot \sqrt{1 + (\text{SNR}_{ERS-2})^{-1}}}$$

As long as the backscatter in the images are rather high (above -8 dB) the effect on coherence is small, but coherence measurements from ERS-1 repeat passes and ERS-1/2 passes should be checked in this respect.

The interferometry was performed on SLC images using the ISAR toolbox. This includes wavenumber shift filtering, but no filtering in azimuth (see below for discussion.)

Only two images were processed successfully, June 27/28 and August 1/2. For the production of coherence images, slope estimation and spatial averaging was performed. The coherence estimation window was 5x25 pixels (range and azimuth) in both images. The slopes were estimated with a FFT in a window of size 5x15 pixel for the June pair, and 5x25 for the August pair. Note that this affects the bias in the images.

From the images we estimate the coherence with a certain bias

$$\gamma_{est} = f(\gamma)$$

The effect of the coherence estimation and the involved estimation of the local slopes by means of an FFT-analysis is illustrated in Figure 2. The coherence estimation is limited by the number of pixels of the same land type. From the summer scenes August 1/2 we have an estimated coherence of the sea of  $0.267 \pm 0.001$  which is then corresponding to a true coherence of zero.

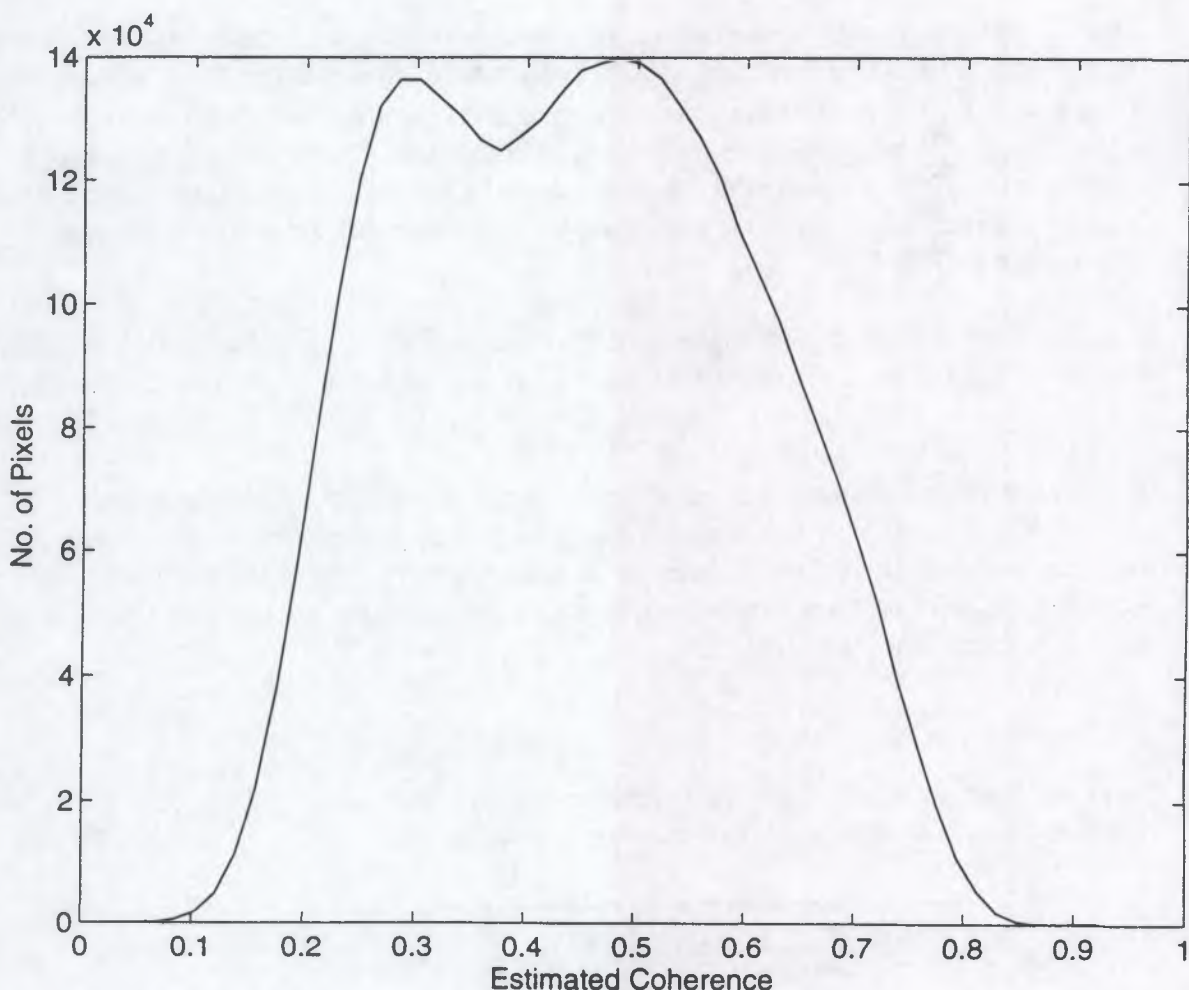


Figure 2. Illustrating histogram for the estimated coherence for the image pair from August 1/2. The low coherence peak is associated with lakes, the sea, and the forest areas, while the higher values are associated with open fields, clearcuts and bogs. The bias in the estimation process is showing up in the cut of off low values in the histogram.

## RESULTS

### *Measured coherence in images*

The coherence for forest, open fields, and old clear cuts was determined in two ERS-1/2 pairs of SLC-images.

Date	Comments
June 27/28	Coherence image appears very similar to ERS-1 winter images. Coherence of fields generally lower than 3 day repeat cycle in winter; clear-cuts more variable; for forest no discernible difference, in spite of the shorter time interval between images.
August 1/2	Short baseline, stable weather conditions with less wind than June 27/28 image pair, suggest that the coherence should be better for this pair. No significant difference for forest, clearcuts have higher coherence than in June. Fields have lower coherence in August than in June, possibly due to vegetation covering them. (as yet, no field inventory has been made for this area). At present, this is the only interferogram processed where the fields have a generally lower coherence than clearcut areas <sup>1</sup> , although the difference between fields and clearcuts appears to decrease with shorter time intervals between the images of the pair (see Figure 2).

The coherence for the ERS-1/2 1 day interval pairs is compared to the coherence obtained using ERS-1 image pairs from the 3-day repeat orbit in 1994 and the result is illustrated in Figure 3 below for increasing time interval and with increasing baseline for each time interval. In Figure 4 is illustrated the difference between coherence of fields and clear-cuts and how this difference is increasing on average with increasing time intervals between images. This result will be further analysed but indicate different temporal decay processes and that the identification of (old) clearcuts is easier with a somewhat long time interval during winter.

Table 3

Index Number	Time interval	Date of first image	Date of second image	Normal baseline /m
1	1	95-08-01	95-08-02	15
2	1	95-06-27	95-06-28	48
3	3	94-03-14	94-03-17	8
4	3	94-03-08	94-03-11	21
5	3	94-03-11	94-03-14	21
6	3	94-02-15	94-02-18	30
7	3	94-02-24	94-02-27	203
8	6	94-03-08	94-03-14	1
9	6	94-03-17	94-03-23	175
10	9	94-03-08	94-03-17	9
11	9	94-02-06	94-02-15	62
12	9	94-02-27	94-03-08	89
13	9	94-03-14	94-03-23	183
14	12	94-03-11	94-03-23	206
15	12	94-02-06	94-02-18	268
16	15	94-03-08	94-03-23	185

<sup>1</sup>With the exception of images with low coherence for all classes e.g. image pair index number 12 in Figure 3 and Table 3.

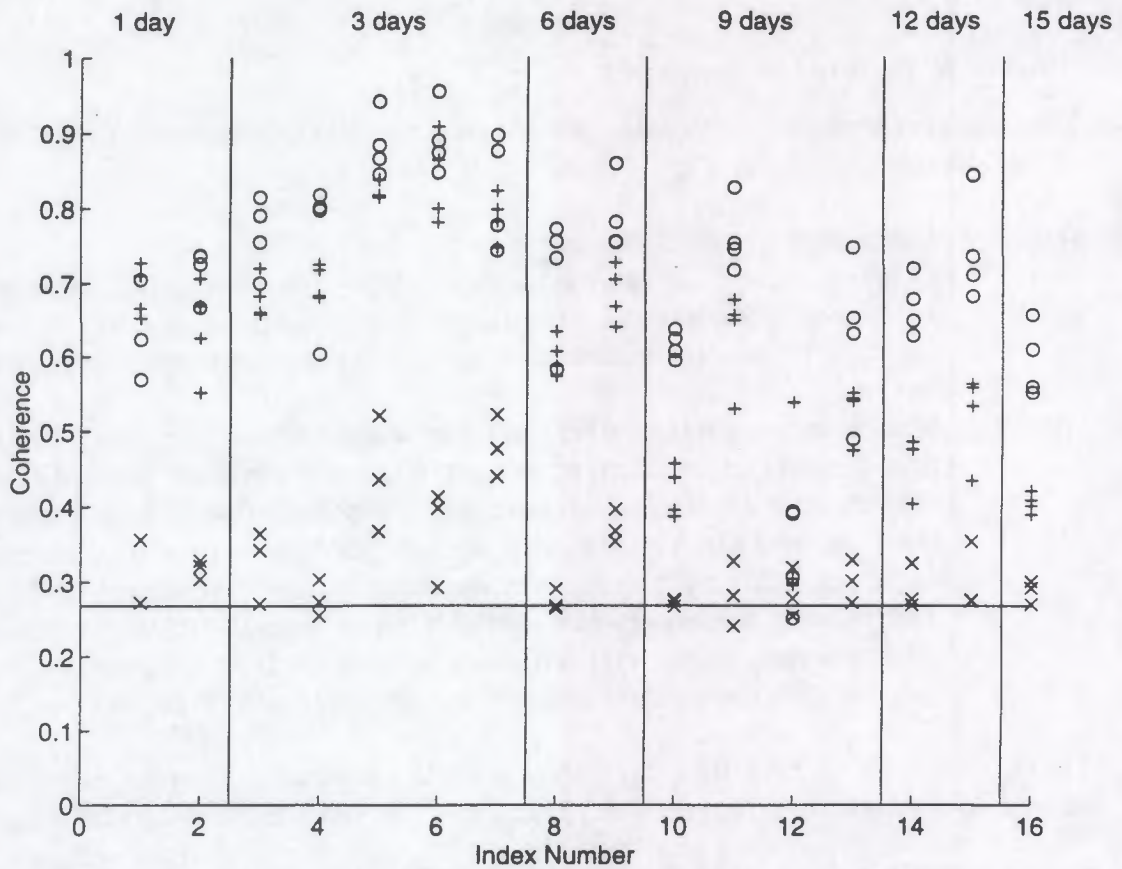


Figure 3: Estimated coherence for different type of areas in image pairs (characterised by an index number as given in Table 1 below). x-Measurements over forested areas; +-Measurements over clear-cut areas (cleared before 1988), o- Measurements over fields. Corrections for azimuth ambiguity not included. Straight line at 0.267 indicates the estimated coherence of the sea (true coherence zero).

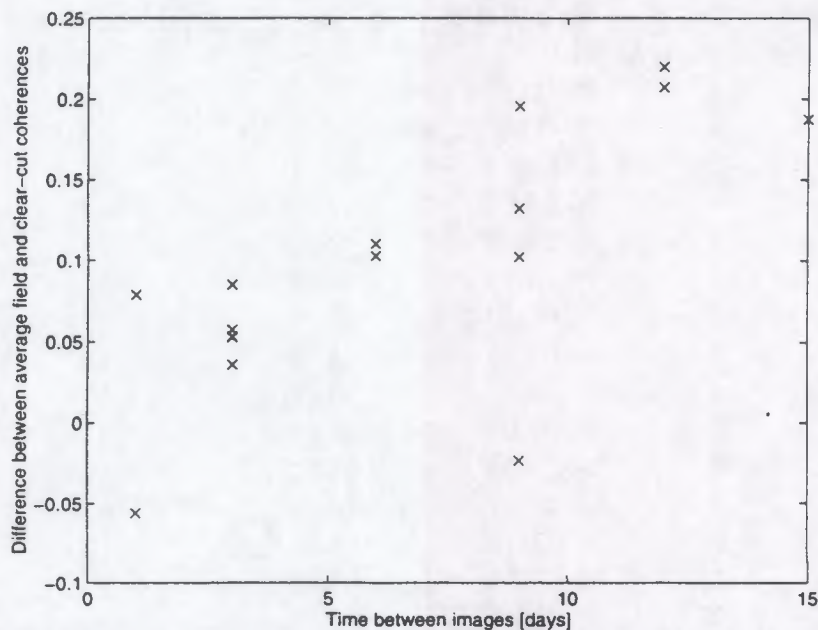


Figure 4 Indicating how the difference between coherence of fields and clear-cuts increases on average with increasing time intervals between images. The point with a negative difference at a time interval of 9 days corresponds to the image with index number 12 in Figure 3 and Table 3. This is indicative of the fact that this interferogram had low coherence over most of the area measured, possibly due to a storm between the dates of image acquisition.

The measurements were made over the largest areas possible, whilst still being certain of measuring only one class, and not including edge effects due to boundaries, roads, lakes, etc. In general this corresponded to roughly square areas with side about 100m. For the lower coherence values the accuracy in the estimated coherence values is about  $\pm 0.05$ . This means that many of the coherence values from forested areas are only upper limits with the estimation method used. This will be improved in the future by using a DEM for local slope estimation.

We have earlier concluded (Ulander et al., 1993; Hagberg et al., 1995) that a baseline of the order of 150 - 400 m is best for estimation of tree height while results using shorter baselines are corrupted by phase noise. In this data set we only have five pairs with such baselines while the rest has shorter baselines as prescribed by the conditions for the commissioning phase of ERS-2. We hope to be able in the future to study more pairs with baselines in the middle range.

### ***Interferometric SAR colour image of Hökmark August 1995***

The image in Figure 4 is produced using the SAR images from 1 August (ERS-1), 2 August (ERS-2). The colours correspond to coherence of interferogram (red), intensity of ERS-1 image (green) and intensity difference between the two SAR images.

#### **Image properties**

- Red channel: Directly related to the coherence of the interferogram, although a histogram stretch has been applied to improve the contrast. This is possible because the bias limits the lowest values of coherence measured, and a number of decorrelation effects produce a practical upper bound of less than unity.
- Green channel: Related to the backscattered intensity, but is uncalibrated. The intensity displayed is related to an appropriately scaled version of the square of the amplitude of the SLC value.
- Blue channel: Related to the difference between the backscattered intensities in the two images. The actual value is produced by taking the difference between uncalibrated, scaled, squared amplitude of pixel values. Note that the same scaling was applied to both images, and they display different mean values. This difference could be due to changes in the scene backscattering, or due to systematic differences. Systematic differences that are constant over the image area will not show up in the colour image as it only shows variations in intensity difference relative to other areas within the image.

#### **Area**

The image shows an area approximately 7 km square just to the North of Hökmark (64°30'N, 21°15'E) in northern Sweden. The area is mainly covered by boreal forest, with a number of marsh/bog areas, small lakes and some areas of deciduous trees (mainly birch). The image has not been geometrically rectified and is thus in the SAR imaging co-ordinates, with pixel sizes

of 7.9 m in range (approximately East-West), and 19.8 m (averaged by a factor five compared to raw image data) in azimuth (North-South).

### *Interpretation*

The magenta area slightly North of the centre of the image shows the fields around the village of Övre Bäck. These have high coherence, and low intensity so their appearance is dominated by the red and blue channels. Other field systems can be seen around Hökmark (central on the southern edge of the image), and Vallen in the South-West corner.

Similar in colour, but slightly lighter are the clear-cut and boggy areas. This is probably due to low vegetation cover over all three surfaces. The clear-cuts however appear a lighter colour than fields, with bogs coming out mainly white indicative of large intensity changes and high backscatter combined with high coherence.

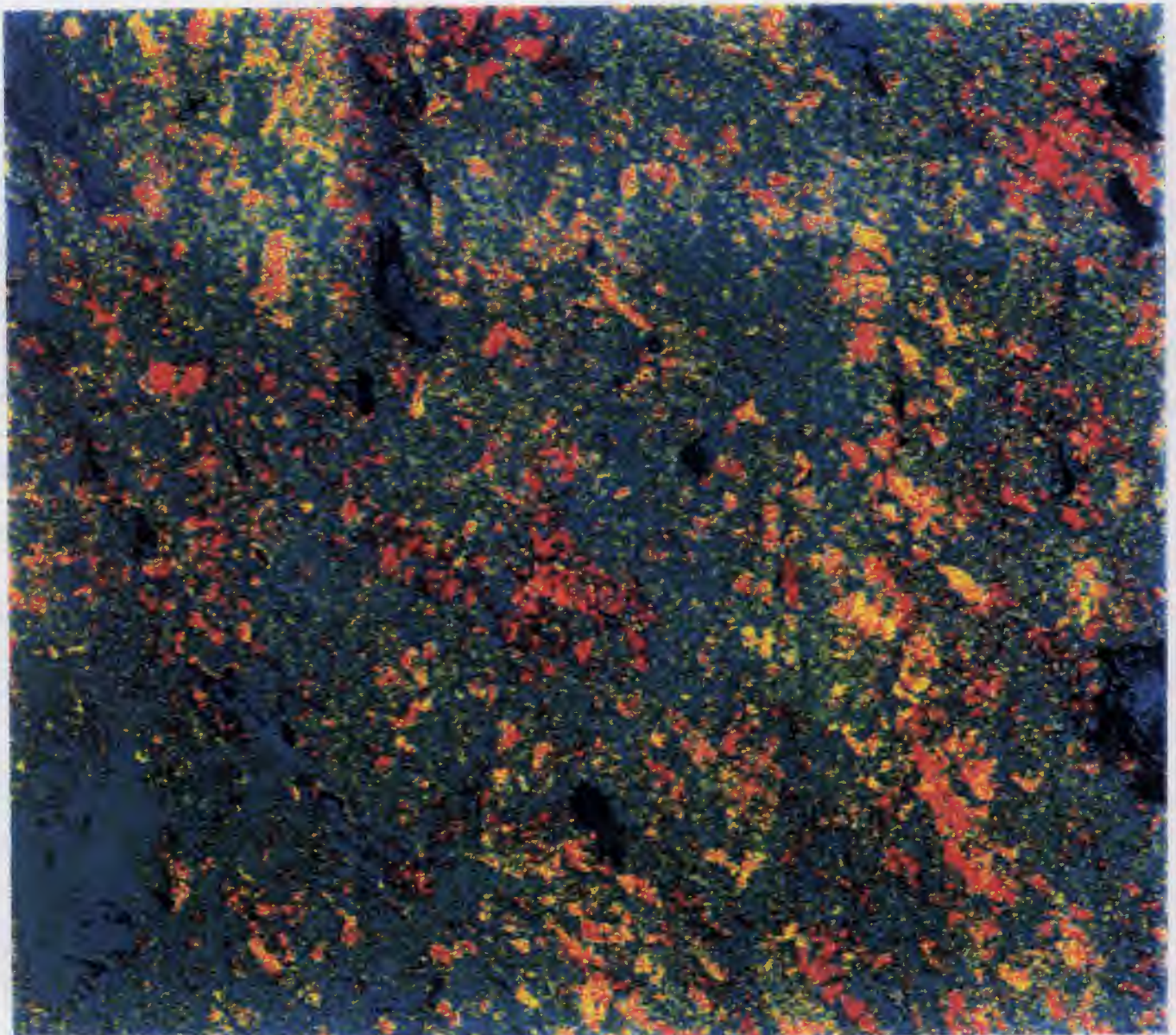


Figure 4 produced using the SAR images from 1 August (ERS-1), 2 August (ERS-2). The colours correspond to coherence of interferogram (red), intensity of ERS-1 image (green) and intensity difference between the two SAR images.

Lakes in the image appear blue (low coherence and backscatter, relatively large variation in backscatter), whilst the sea area (Gulf of Bothnia) in the North-East corner appears a more green colour, due to greater backscattering here. This can also be seen in larger lakes, and is probably enhanced backscatter due to wind effects.

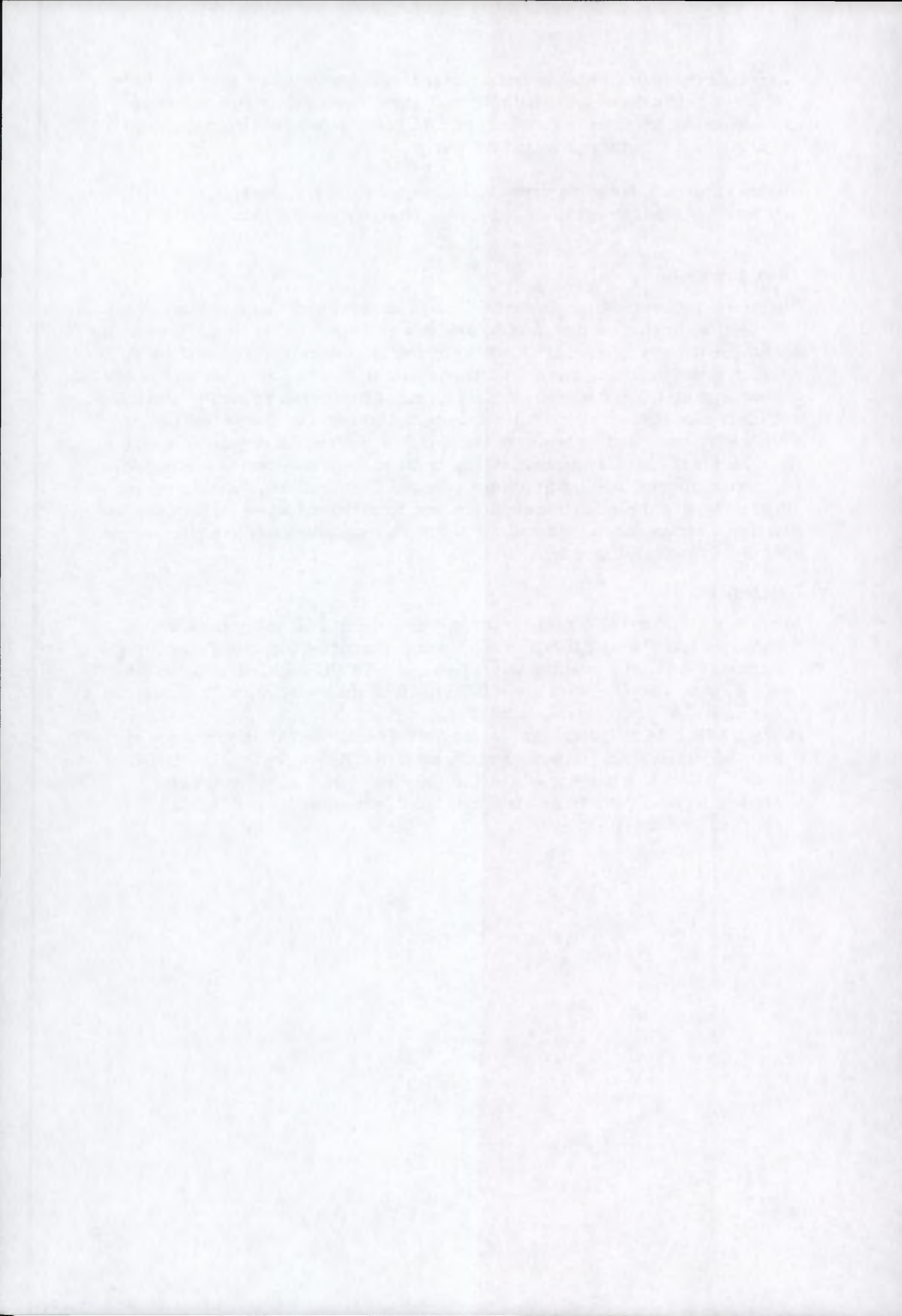
The remainder of the image is a bluish green colour, indicating low coherence, reasonably high backscatter and change in backscatter. These areas correspond to forested areas in the image.

#### FINAL COMMENTS

The observed coherence values for forested areas in northern Sweden are low. Many times we find values not much above the bias in the coherence estimation. This means that if we are to characterise forest by means of interferometry or if we are to determine slopes and digital elevation models by interferometric SAR from forested areas, we would like to have the best coherence possible. This is normally obtained for short time intervals between the acquisitions and that favours the tandem mission. However the highest values so far have been obtained with the same system and during winter conditions. It would therefore be valuable to study image pairs from the tandem mission for such conditions (so far only from summer period). For land classification using coherence, cf. (Askne and Hagberg, 1993), it is useful to have different values for the typical land areas of interest. From Figure 3 we see a tendency to have an increased separation between open fields and old clear cuts with a time interval of the order of 12 days indicating different decay processes.

#### REFERENCES

- Askne, J., et al., submitted: C-band repeat-pass interferometric SAR observations of forest
- Askne, J. and J. O. Hagberg, 1993, Potential of interferometric SAR for classification of land surfaces. *IGARSS'93, Symposium held in Tokyo, on 1993*, (IEEE 93CH3294-6), pp 985-987
- Gatelli, F., et al., 1994: The wavenumber shift in SAR interferometry, *IEEE Transactions on Geoscience and Remote Sensing* 32: 855-865.
- Hagberg, J. O., L. M. H. Ulander and J. Askne, 1995: Repeat-Pass SAR Interferometry over Forested Terrain, *IEEE Transactions on Geoscience and Remote Sensing* 33: 331-240.
- Ulander, L. M. H., J. O. Hagberg and J. Askne, 1993, ERS-1 SAR Interferometry over Forested Terrain. *Proceedings of the Second ERS-1 Symposium, Symposium held in Hamburg, on 1993*, pp 475-480



# Annex G

## **Geographical area**

Mount Etna, Sicily, Italy

## **Research institute**

CNES, France

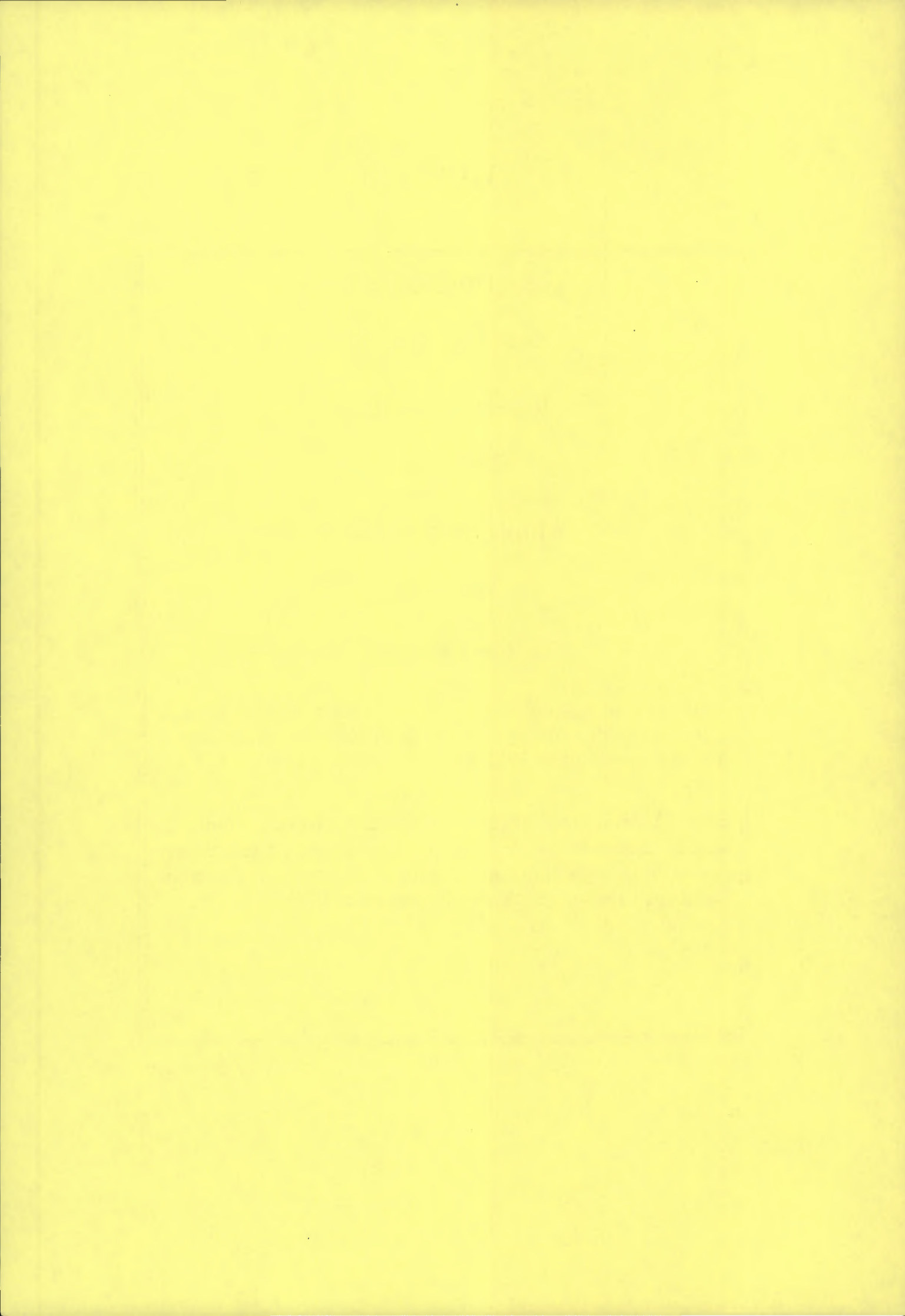
## **Application domain**

Volcanology

## **First results**

Previous results with ERS-1 35 day repeat data showed a deflation of Etna of the order of 14cm over a 1 year period during the eruption of 1992/93.

ERS Tandem Differential interferograms (corresponding to surface motion on the centimeter scale) indicate a re-inflation due to the growth of magma chambers. This work is currently being evaluated by geophysicists to quantify the effect.



**PRELIMINARY RESULTS OF  
TANDEM DATA ANALYSIS AT CNES**

D. Massonnet  
Radar Processing Department

To the attention of Gordon Campbell, ESRIN

Tandem data from ERS-1/ERS-1 were received by CNES on several sites since the launch of ERS-2. The sites are:

ICELAND : frame 2295, track 238

ETNA : frame 747, track 131 (descending); frame 2781, track 265 (ascending)

VESUVIUS : frame 801 and 819, track 129 (descending); frame 2835 and 2853, track 222 (ascending)

MAASTRICHT : opportunistic demonstration of tandem DEM capabilities which we conducted with ISTAR.

We had more opportunities of tandem operations with two sites:

HAUT SASSANDRA : frame 153, track 216. The site is part of a DEM project managed by J.P. Muller from UCL. We processed a pair of tandem images supposedly located on equatorial forest, with excellent results. The experimental conditions must still be ascertained before any claim of success on such a difficult target (see attached example).

WESTERN US; where 400000 sq. km. will be covered with up to ten passes, which represents more than 300 scenes. However, no ERS2 passes have been received yet.

All these sites are, in general, part of a investigation program devoted at various applications:

**In Iceland**, detection of continent drift at the rift location. The observables are the rifting process itself and the associated activity of magmatic chambers located along the rupture zone.

**In Sicily (Etna)**, we monitor the deformation of the volcano with ascending as well as descending passes. ERS1 and ERS2 scenes acquired after the launch of ERS2 contributed to our study in showing that the volcano inflated again. We follow this evolution with geophysicists.

**In Italy (Vesuvius)**, we monitor the volcano and the adjacent phlegrean fields.

**In Maastricht**, we experimented end to end DEM computation with ISTAR.

**In Africa** (Haut Sassandra), we experiment how tandem data could reach a level of coherence sufficient for DEM applications on the equatorial forests. Our previous attempts on Papua-New Guinea and French Guyana had been very partial successes or failures.

**In western US**, we want to characterize the local oscillators of ERS1 and ERS2 while keeping an opportunistic eye to this very active area, with earthquakes to the south and volcanoes to the north.

The results of the introduction of ERS-2 data brought additional data to the study of these sites, and contributed to some progress in each of the sites. A first lesson is that ERS-2 data have been used exactly the same way as ERS-1 data and we have many examples of ERS-1/ERS-2 interferometry as well as ERS-2/ERS-2 interferometry. Our software deals indifferently with the data of both satellites without specific changes. This highlights the similarity of the data, which we will seek to check in a more detailed way once we obtain ERS-2 data on the western US site, where accurate local oscillator monitoring can be performed. We could not obtain firm confirmation of a clock shift between ERS-1 and ERS-2 because the typical fringe pattern associated with such a shift can easily be mistaken for an orbital shift. We have found the use of precise orbits rather disappointing as it seems to create more orbital artefact. An investigation is conducted to decide whether the problem comes from inadequate orbit interpolation on our side or from time-variable levels of correction in the precise orbit, which would result in unacceptable level of difference when two precise orbits are included in the interferometric process.

In the sites we studied, which are characterized by relatively slow deformation, the use of tandem data interferograms is not very useful *per se*, and we see them as an error budget tool. The lessons we drew from interferometric tandem are not unexpected:

- the level of coherence is very satisfactory, and similar to what we obtain with 3-day data although, as with 3 day data, we do have examples of very poor results with one day delay (see attached example).

- the level of pollution by atmospheric propagation differences is similar to what we observe by ERS-1 interferometry. This indicates that the typical time of atmospheric change is much less than one day. Again, this is not a surprise. However, due to the high level of coherence and to the small sensitivity to topography resulting from a tighter orbital control, atmospheric artefacts appear very clearly in tandem interferograms. Interferometric tandem data are the

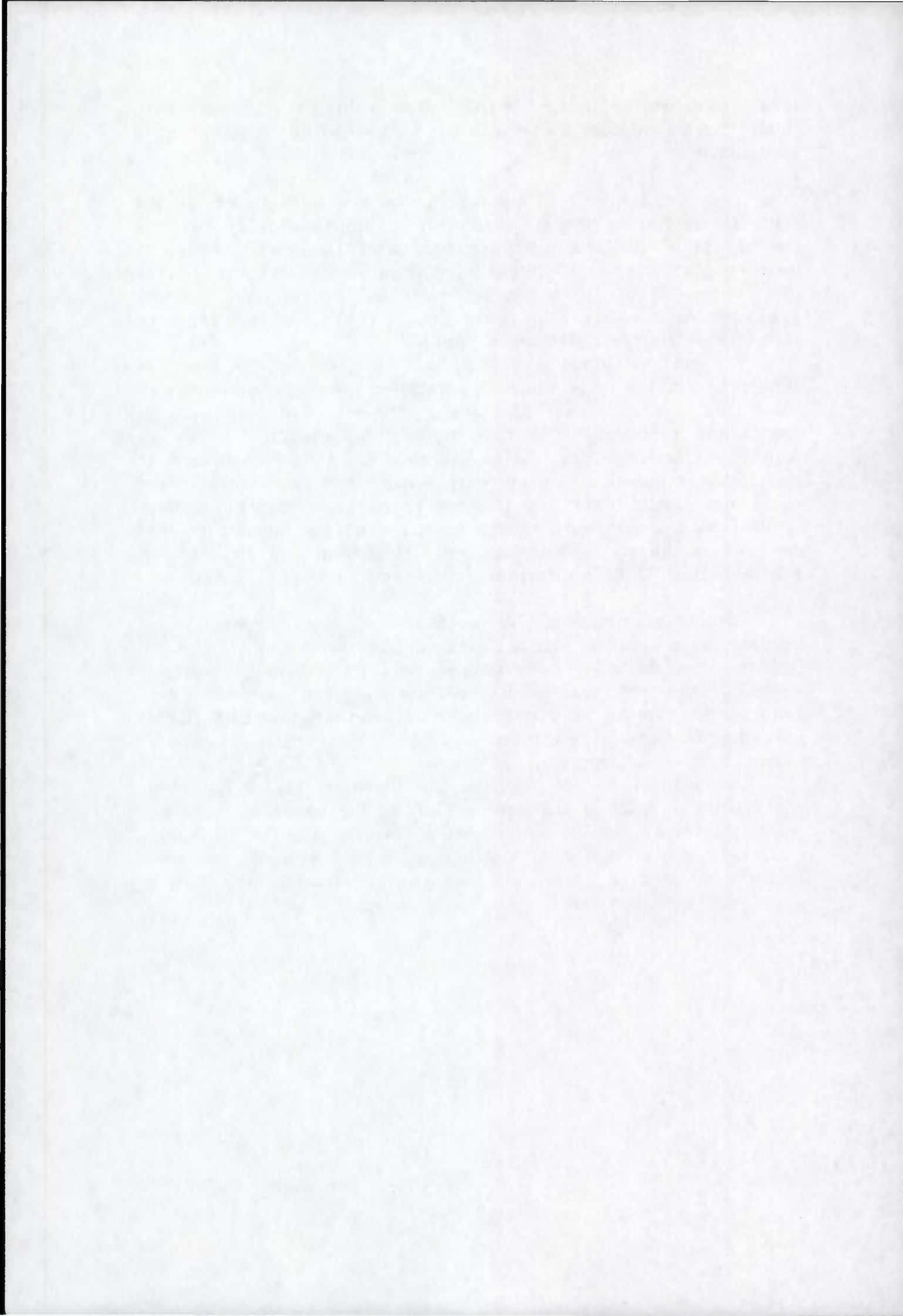
ideal tool for starting serious meteorological studies with interferometry, which would benefit to the whole interferometric community.

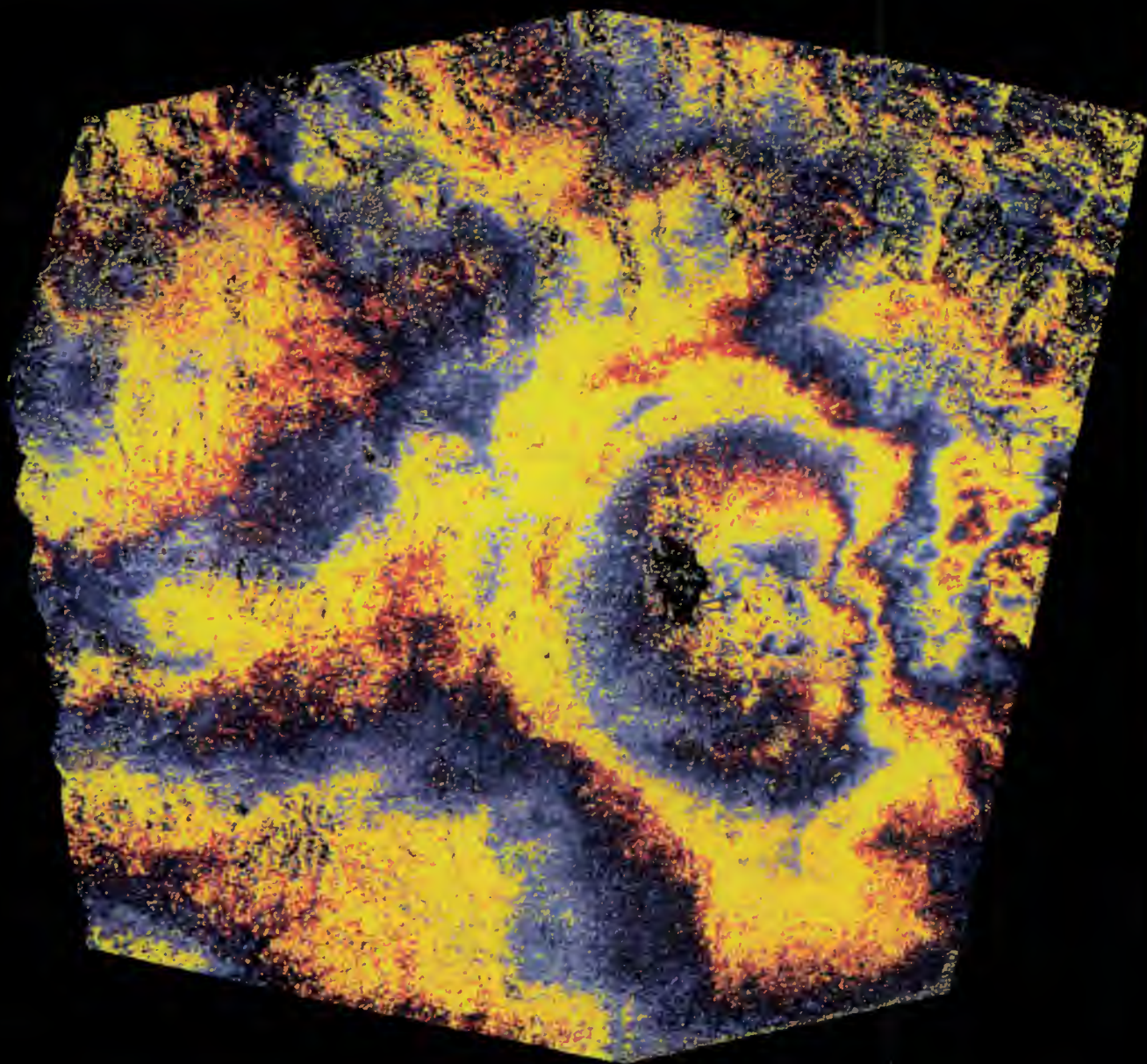
The availability of ERS-2 data has a mechanical effect on the statistics of interferometric pairing. It multiplies roughly by four the amount of available interferometric pairs. This increase benefits more to pairs with high altitude of ambiguity (the ones we are the most interested in) due to the tighter orbital control. Although not spectacular, **this increase is very beneficial to interferometric activity as a whole.**

Tandem operations increases, on the average, the level of coherence but does not make the transformation of interferograms into final products (DEM) easier (because of atmospheric propagation problems). The only foreseeable solution for dealing with atmospheric problems is to multiply the data acquisitions. If the tandem acquisitions are the only suitable for some areas in the world, one should make sure that enough pairs are secured in order to deal with atmospheric problems, and therefore make sure that the **tandem phase is long enough.** This point can be assessed only by actual DEM computation experiments in tropical countries.

Several examples on Mount Etna and Haut Sassandra are included. The work on Maastricht has already been sent to ESA. A DEM has been build, but not validated, by ISTAR. Typical cloud cell shapes can be observed on the raw interferogram, suggesting that atmospheric contribution could be evidenced in the ERS1/ERS2 interferogram if it is compared with an actual DEM or another, independent interferogram.

The example on Iceland illustrates the high rate of failure in this country, in case of snow cover (75% of the year). We have not yet tested the probability of success of tandem data in the winter time. In contrast, SAR interferometry in Iceland with data acquired in the summer time always achieves good coherence, even after a three year time difference.

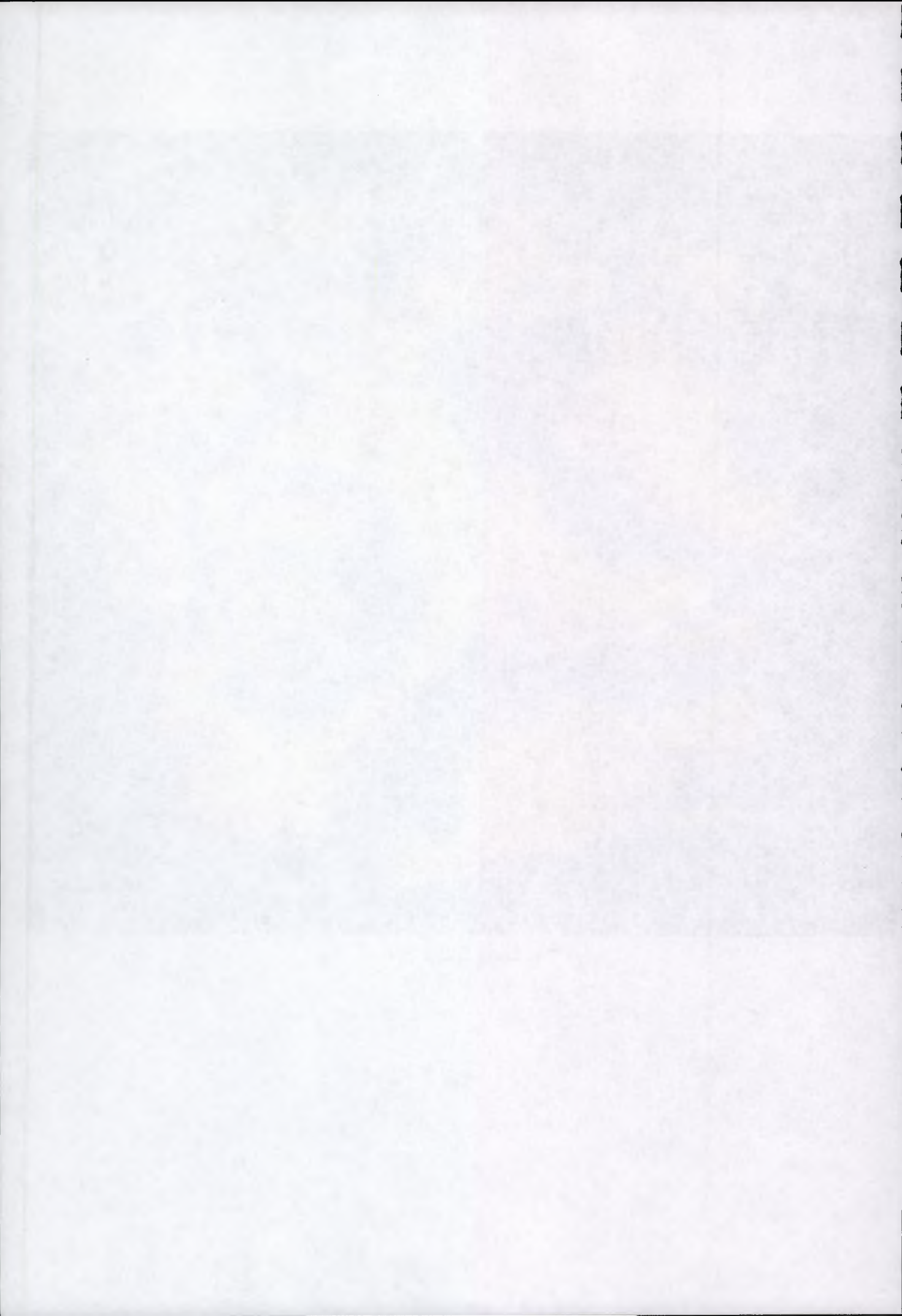


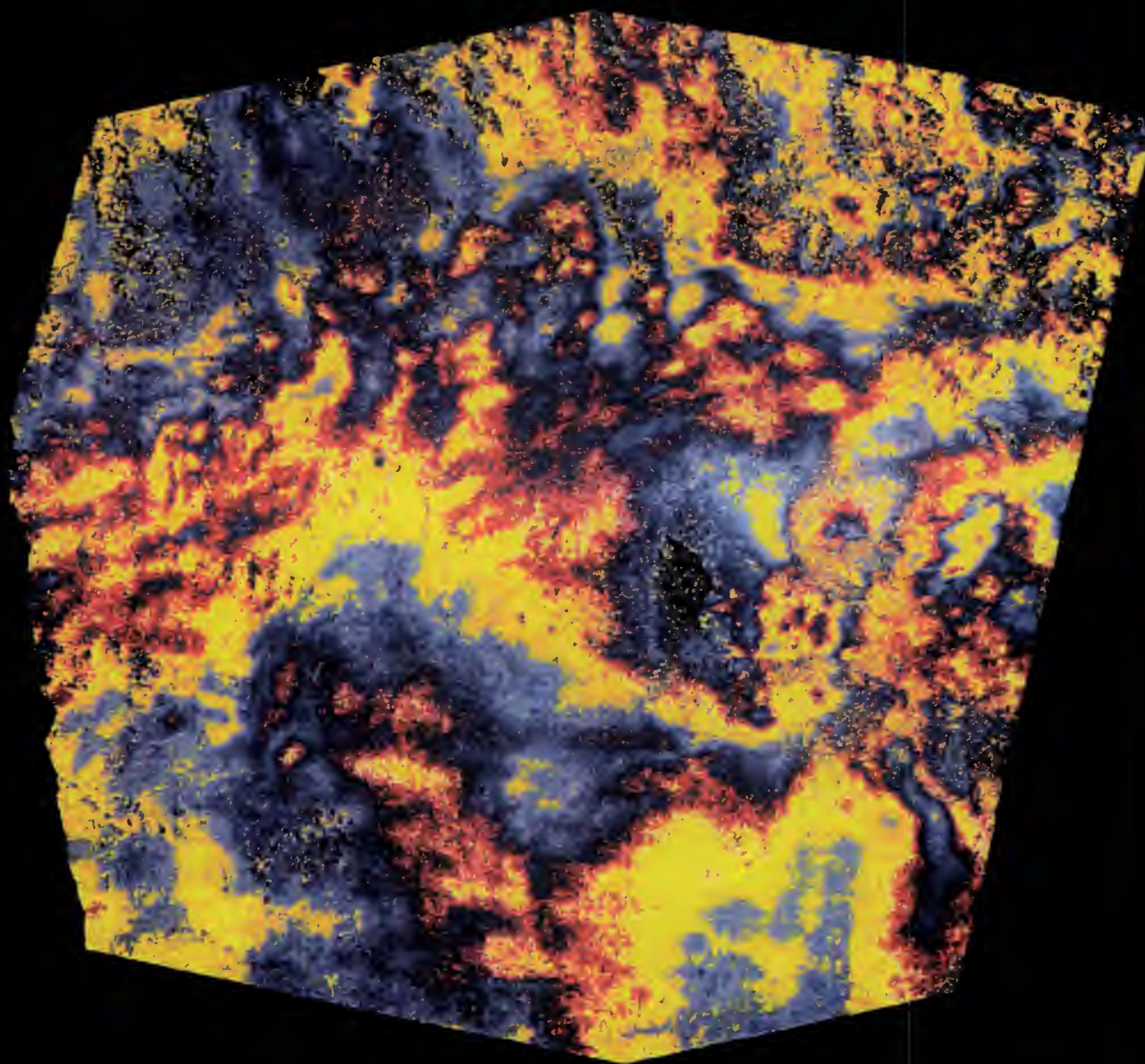


Tandem : 20658 - 985

Cnes - QTIS/PR

[ARNAUD]ETNA\_20658\_ETNA\_985\_NEW\_PRO.OCT - Propre

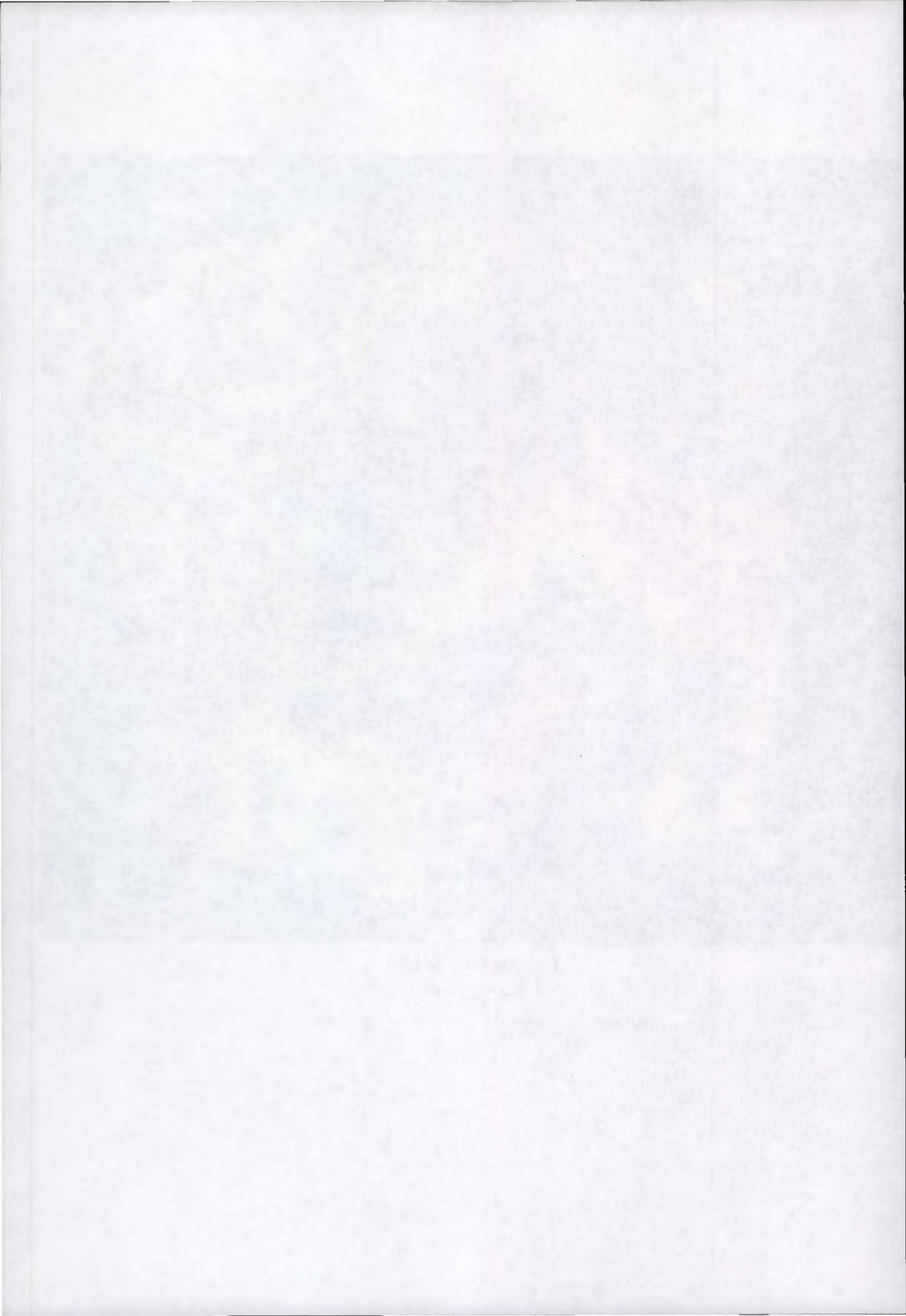


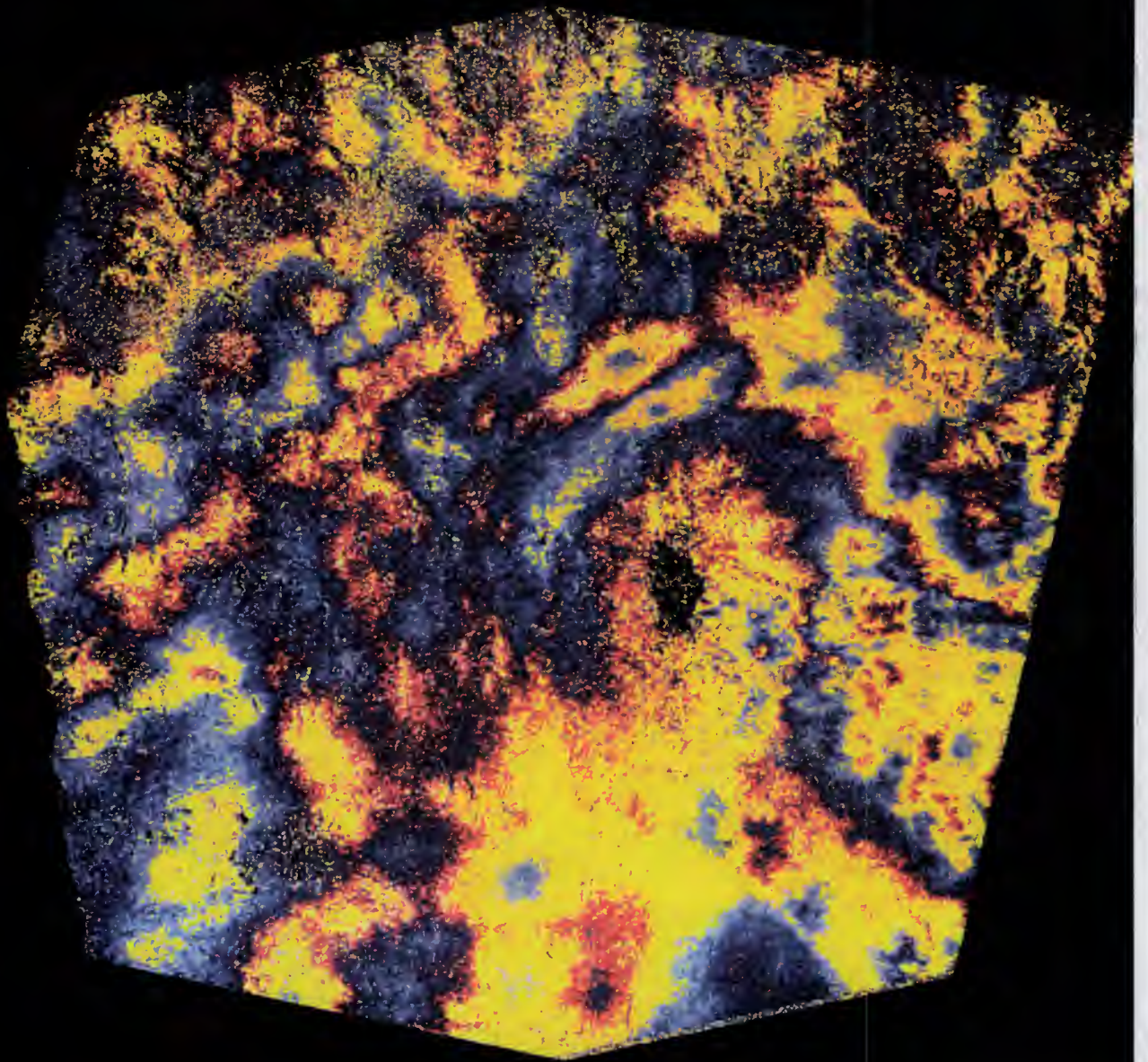


**Tandem : 21159-1486**

Cnes - QTIS/PR

Fichier S5SDKA200:[ARNAUD]ETNA\_21159\_ETNA\_1486\_I'HA\_OR.T.OCT;1

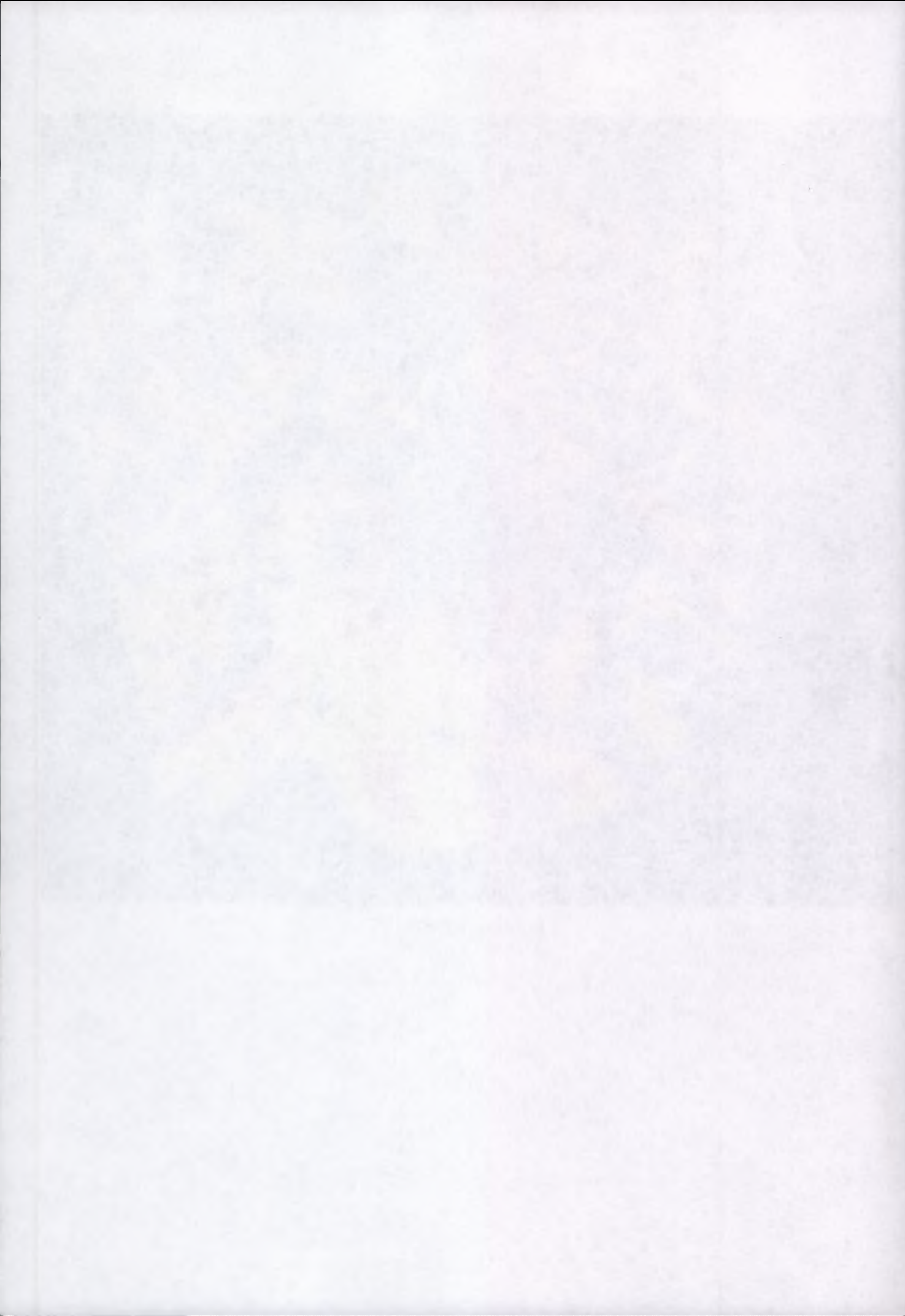


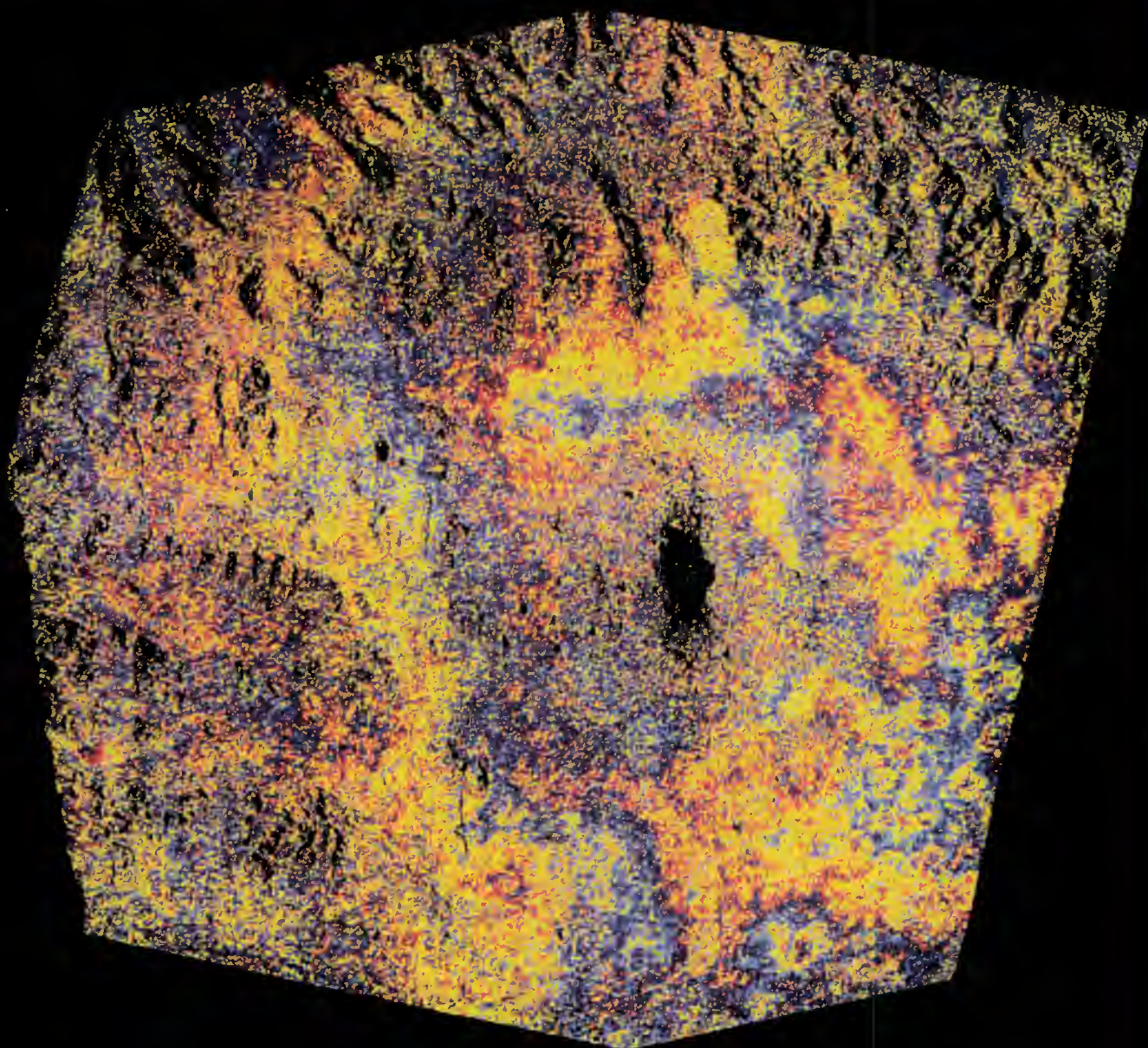


Tandem: 21660 - 1987

Cnes - QTIS/PR

Fichier S5SDKA200:[/RNAUD]ETNA\_21660\_ETNA\_1987\_PHA\_ORT.OCT;1

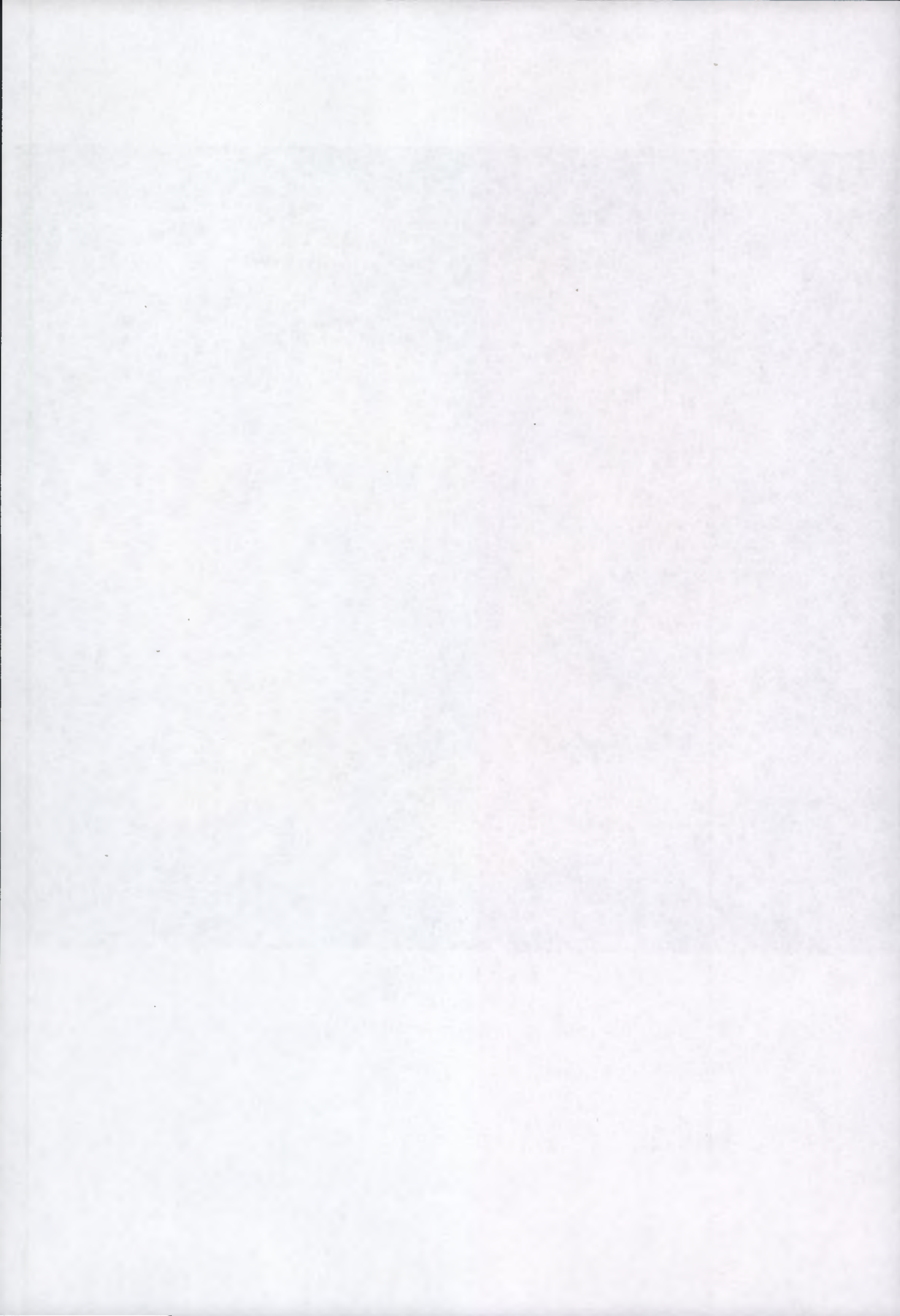


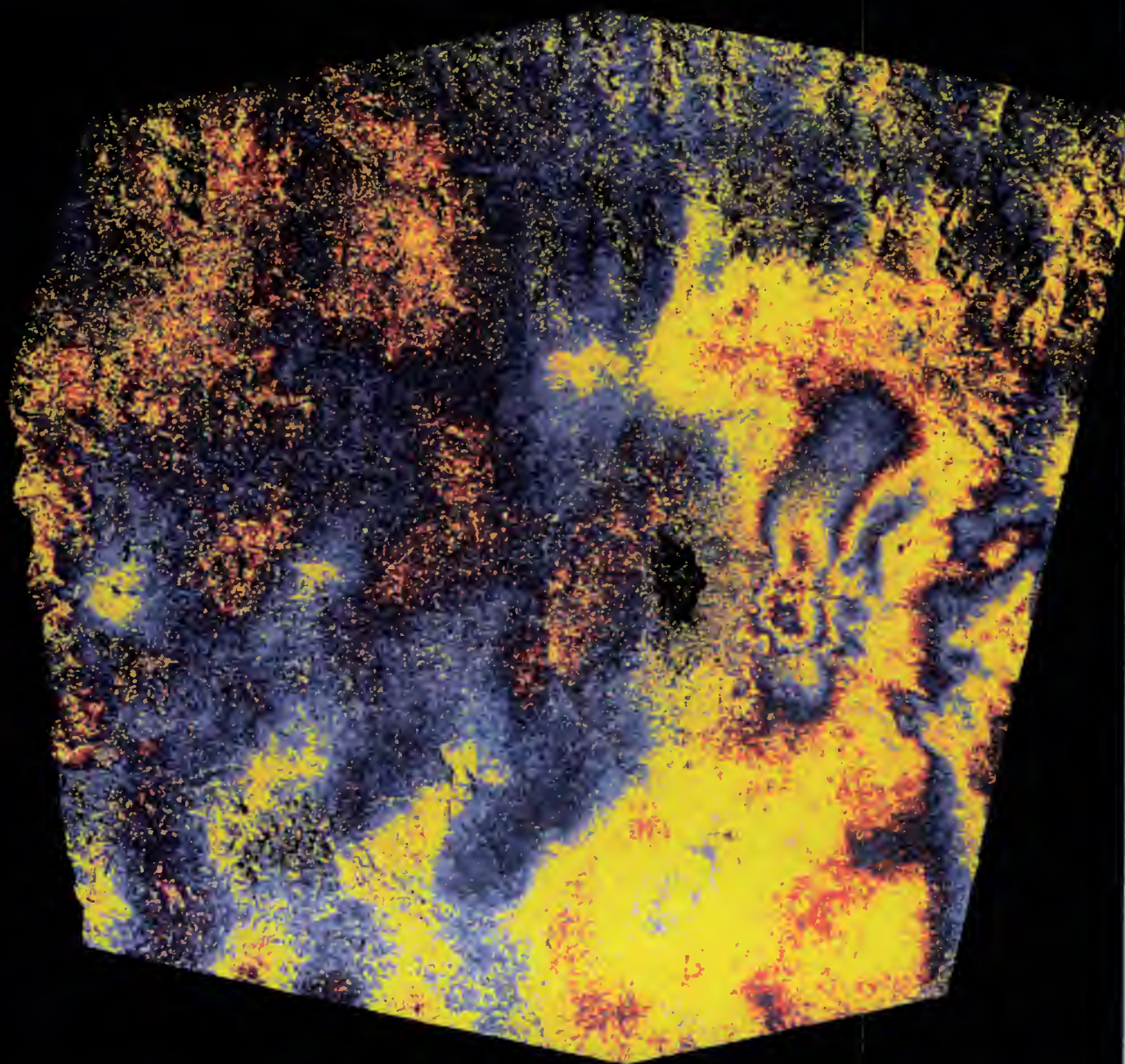


Tandem : 22161-2488

Cnes - QTIS/PR

Fichier S3SDK A2(X):[RADAR]ETNA\_22161\_ETNA\_2488\_PHA\_ORT.OCT;1

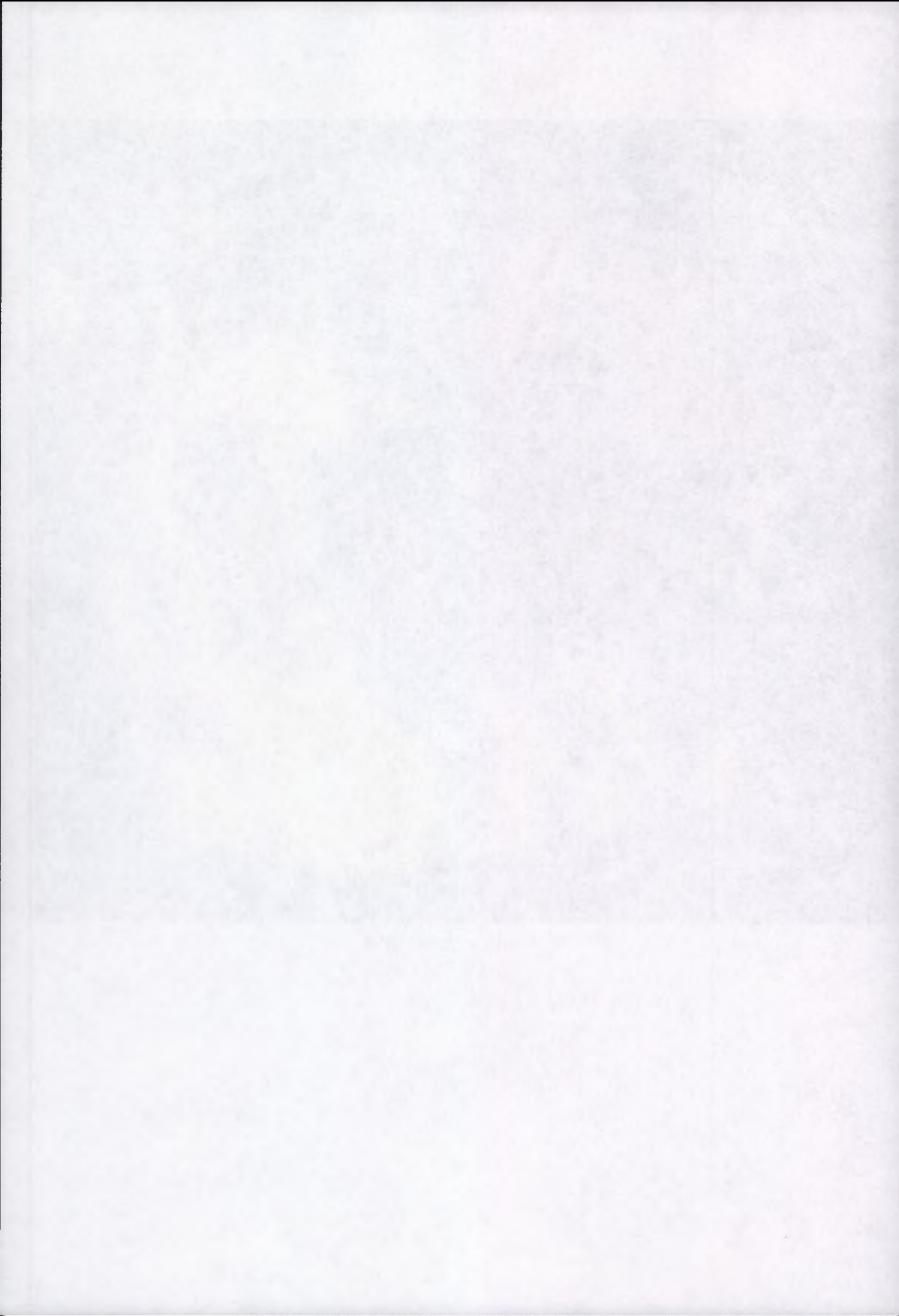


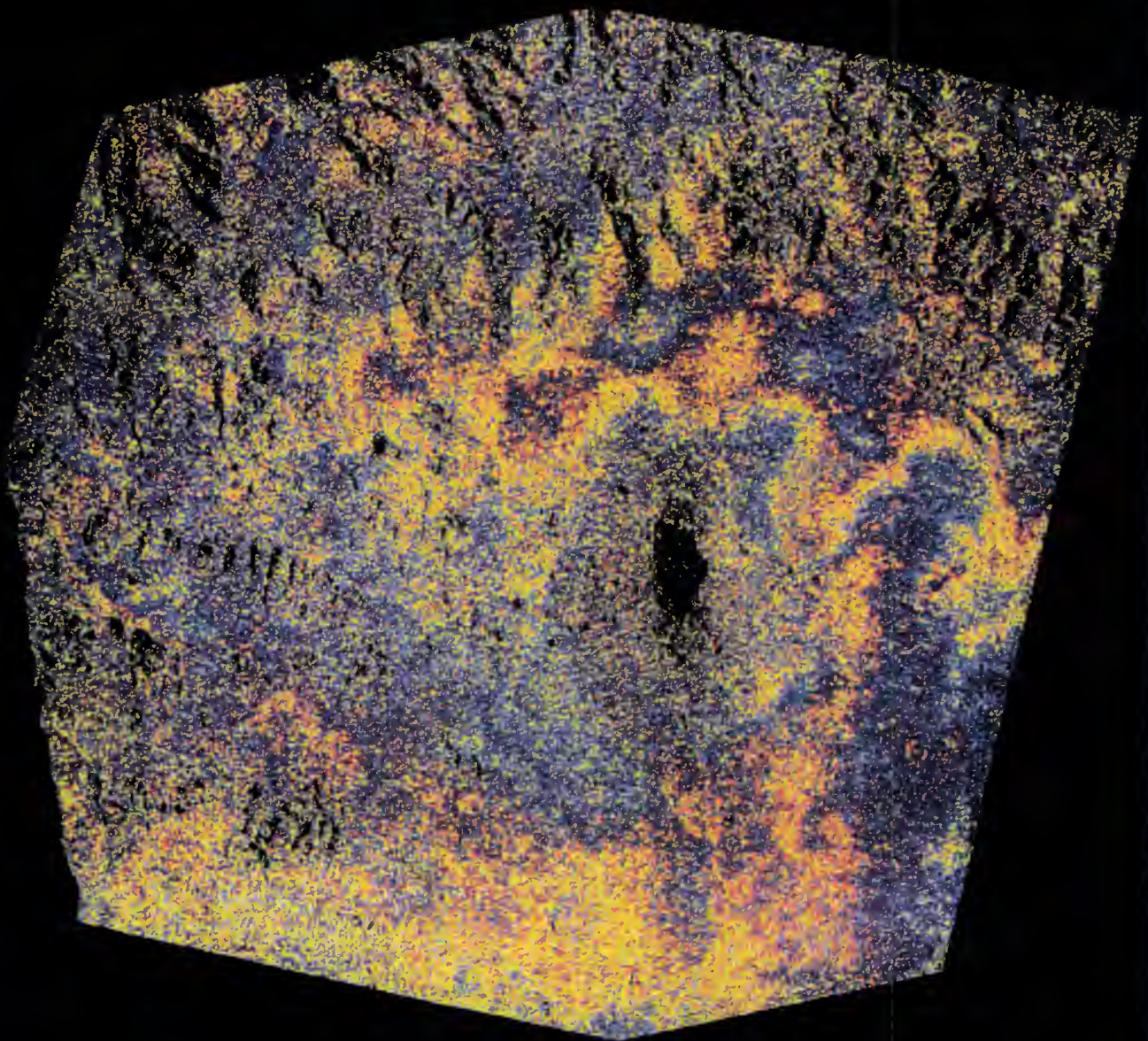


Tandem : 22662-2989

Cnes - QTIS/PR

Fichier S35DKA2(0):[RADAR]ETNA\_22662\_ETNA\_2989\_PHA\_ORT.OCT;1

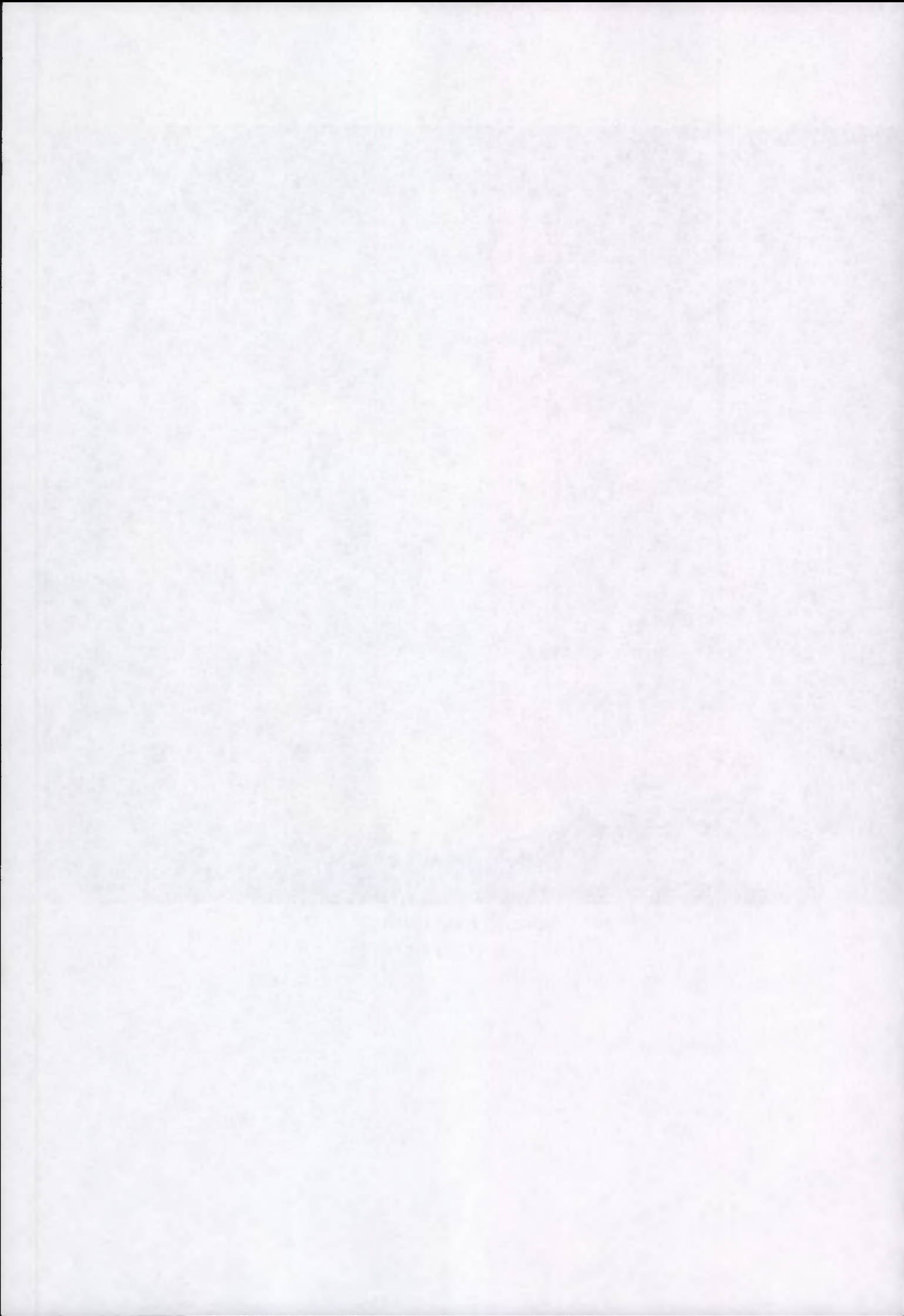




Tandem : 23163 - 3490

Cnes - QTIS/PR

Fichier S3SDKA200:[RADAR]ETNA\_23163\_ETNA\_3490\_PHA\_OCT.tif



# Annex H

## **Geographical area**

Haut Sassandra, Ivory Coast  
Vatnajokull ice cap, Iceland

## **Research institute**

CNES, France

## **Application domain**

DEM / Forestry / Ice Studies

## **First results**

ERS Tandem data for a tropical forest area were successfully processed to produce an interferogram. The accurate characterisation of the surface conditions for the area under study must be performed before any general conclusions regarding the viability of SAR Interferometry over tropical forests can be made.

ERS Tandem Interferogram showing almost total phase decorrelation for a rapidly changing snow covered area.

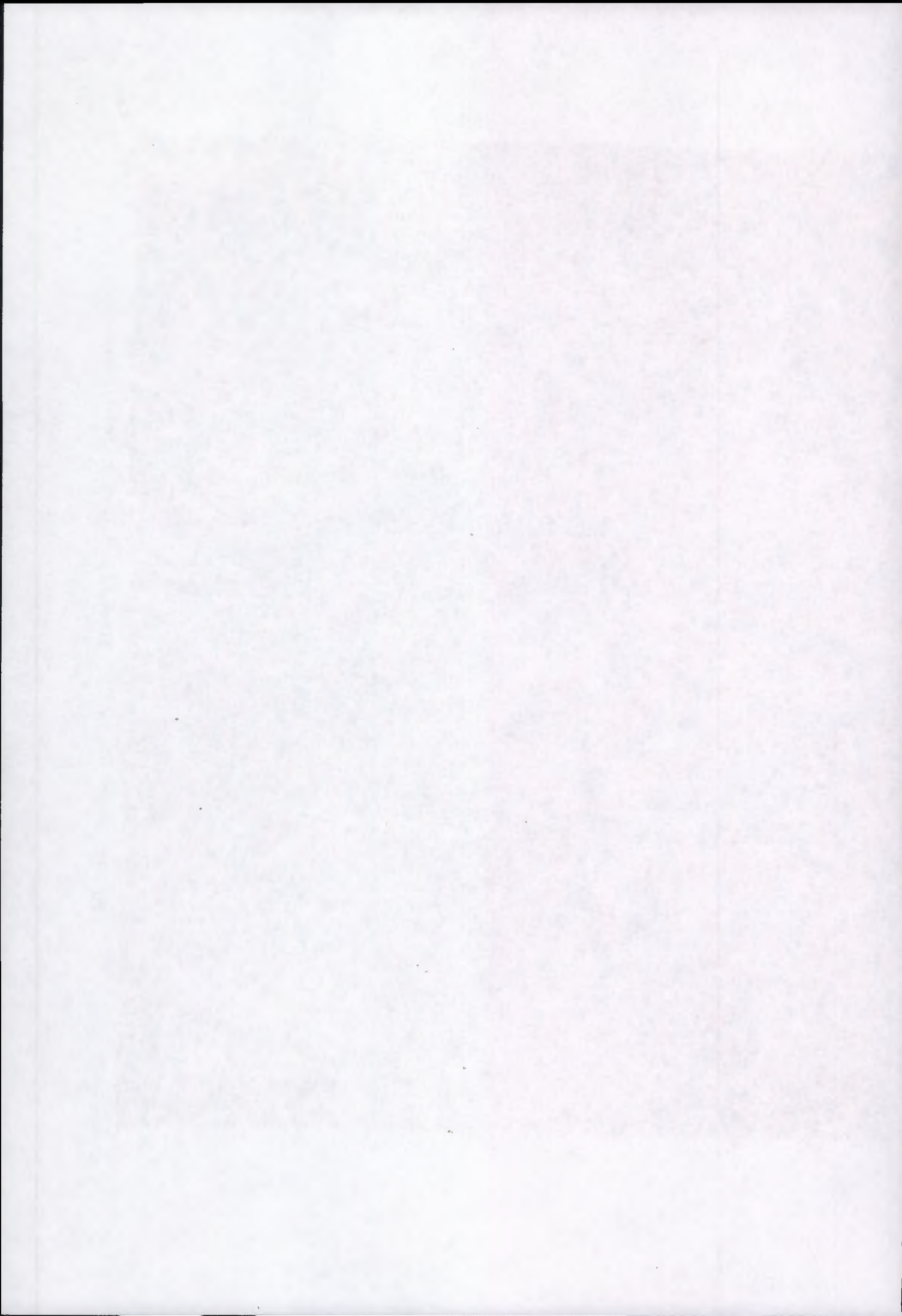


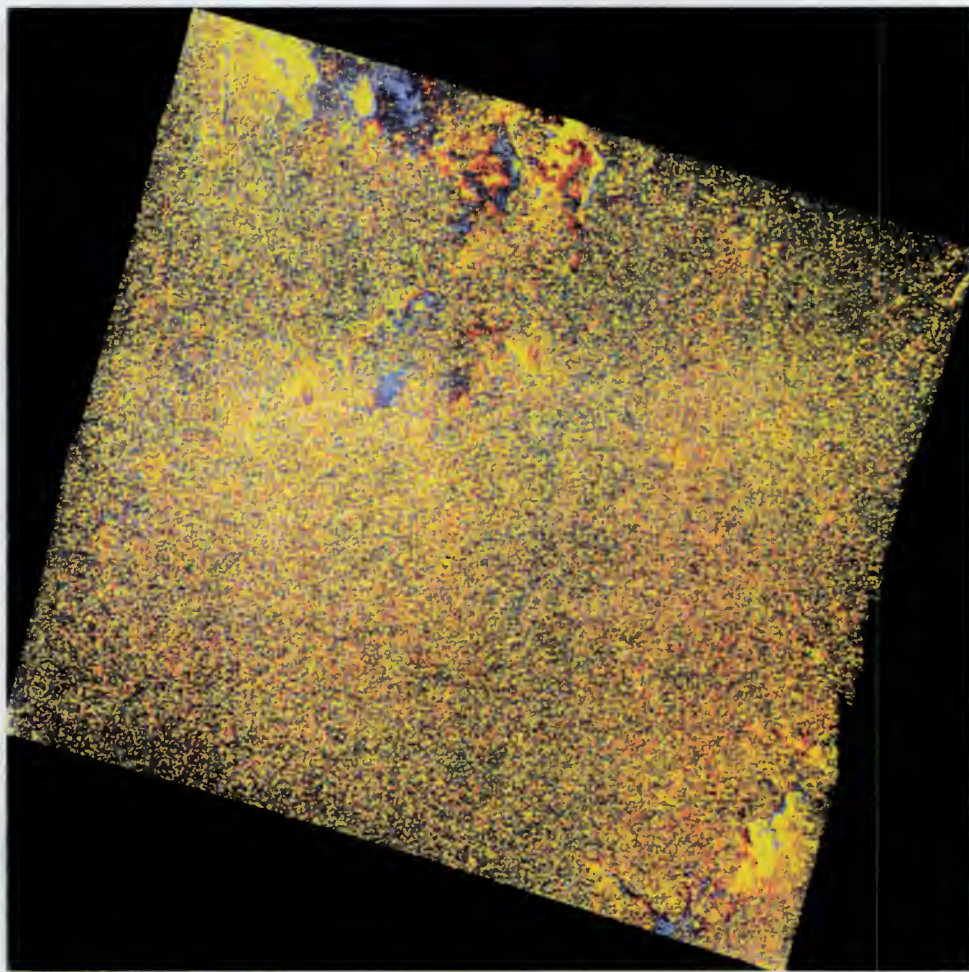


HAUT SASSANDRA (AFRIQUE) : étude de la forêt en Côte d'Ivoire

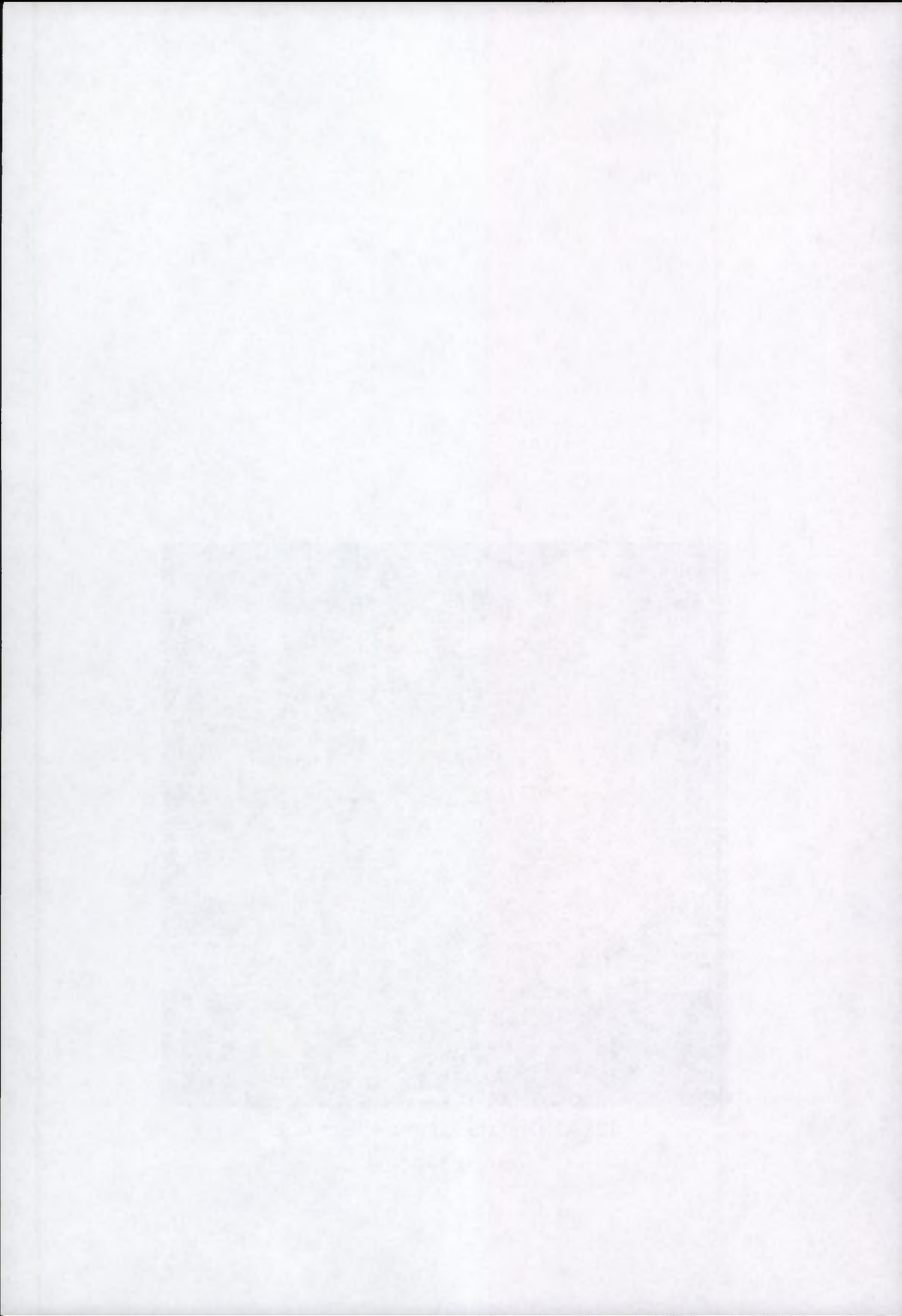
Cnes - QTIS/PR

Lignes 1248 à 2225, colonnes 826 à 2079 de S25DKB500 (RADAR.NADINEJHSASS\_PHA\_BR.OCT;1





ISLANDE ERS-2. Nouvelle chaine  
orbites 593-1094



# Annex I

## **Geographical area**

Maastricht, The Netherlands / Belgium Border

## **Research institute**

CNES, France

## **Application domain**

Digital Elevation Models (DEM)

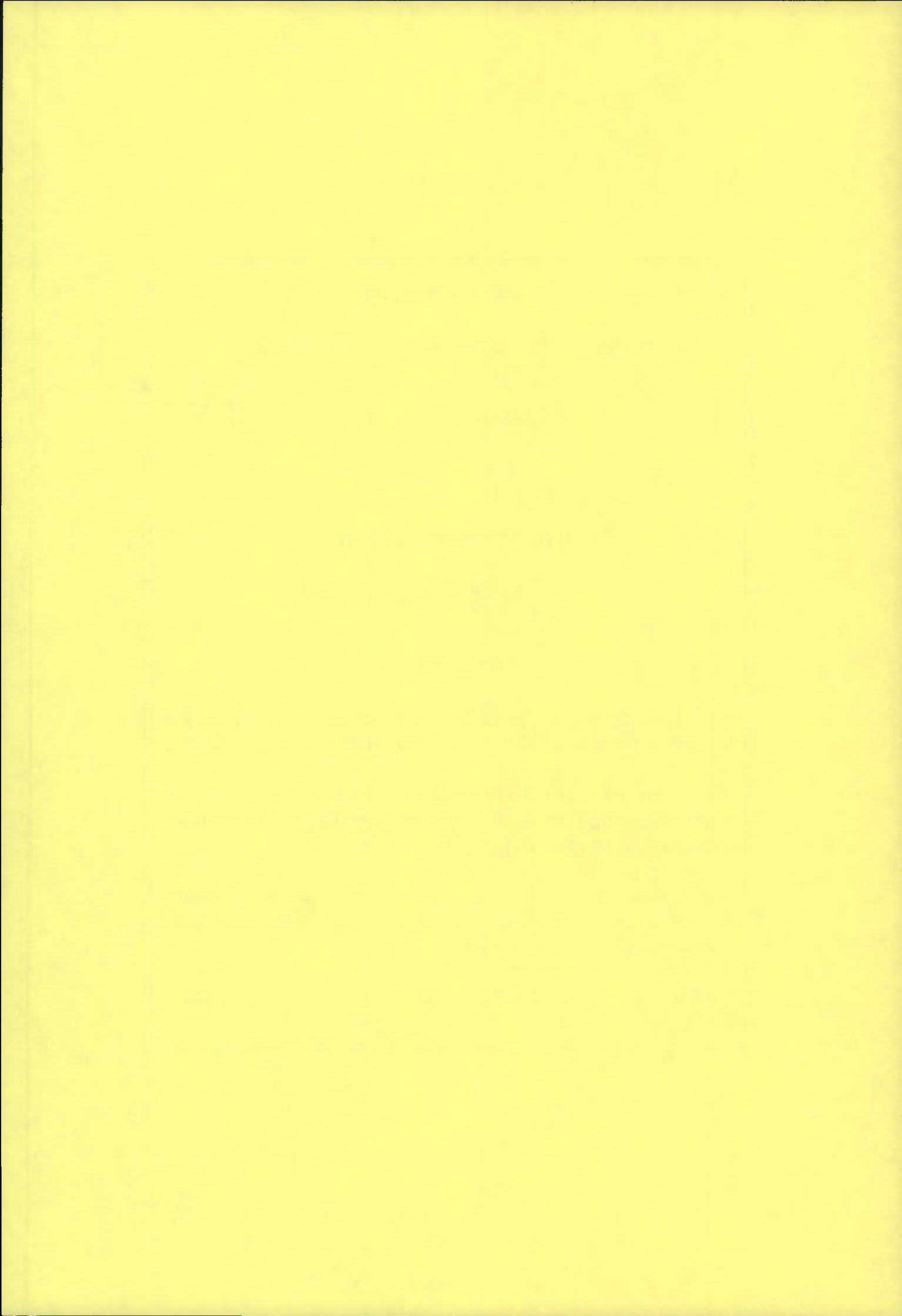
## **First results**

An Interferogram, a coherence image and a Digital Elevation Model for the area of Maastricht were successfully generated.

The coherence image shows large areas of high coherence and many interesting features not seen in the corresponding intensity images of ERS-1 or ERS-2.

The preliminary DEM is colour-coded (from low terrain height in green to hills in orange). It has not as yet been exhaustively compared with external data.

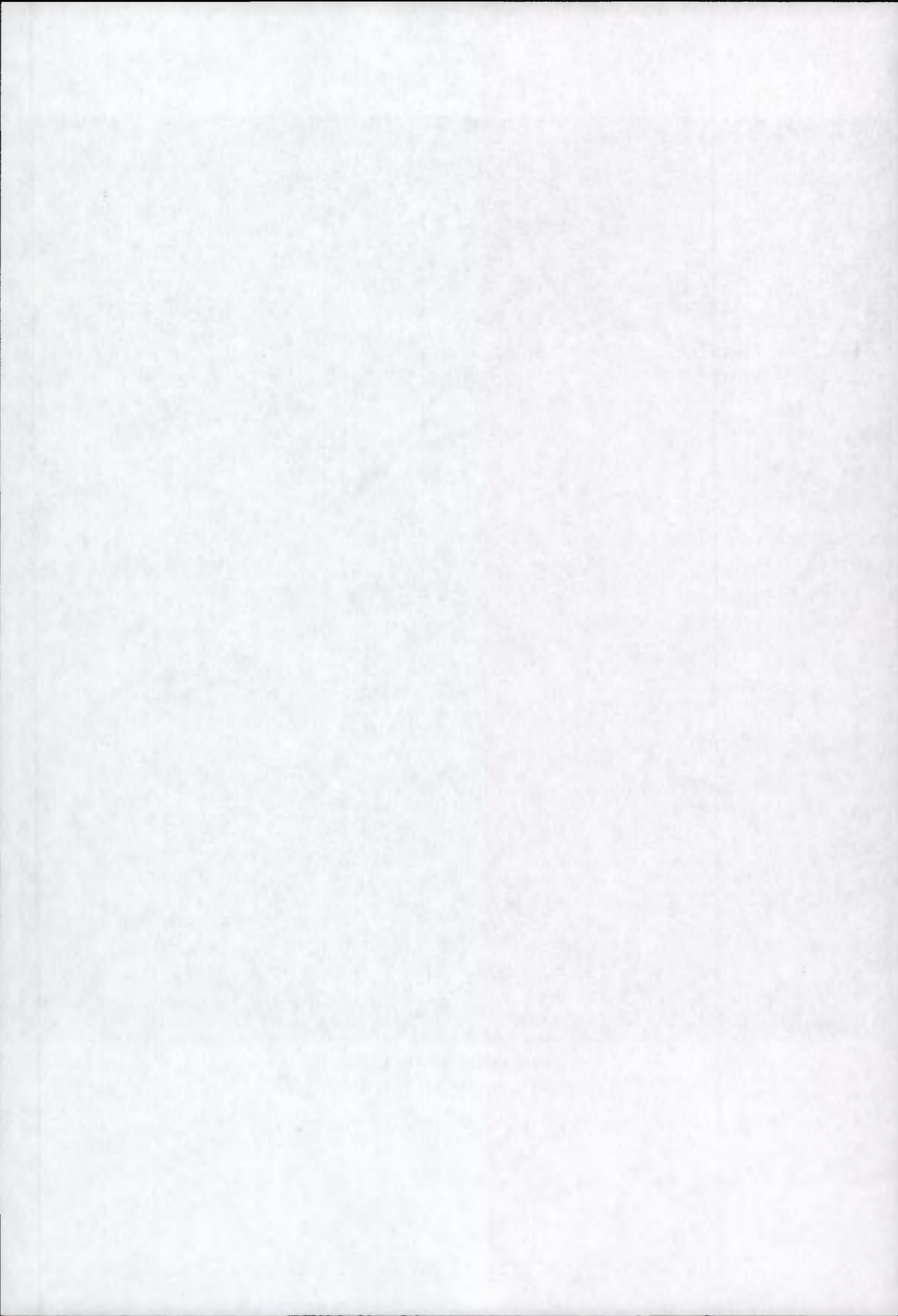
Final images are the ERS-2 intensity overlaid on to the Tandem DEM (full image & selected area).





**ERS1 SAR image - BELGIUM**  
ERS1 orbit 19907 (6 may 1995)

ERS1 data copyright ESA 1995, CNES processing

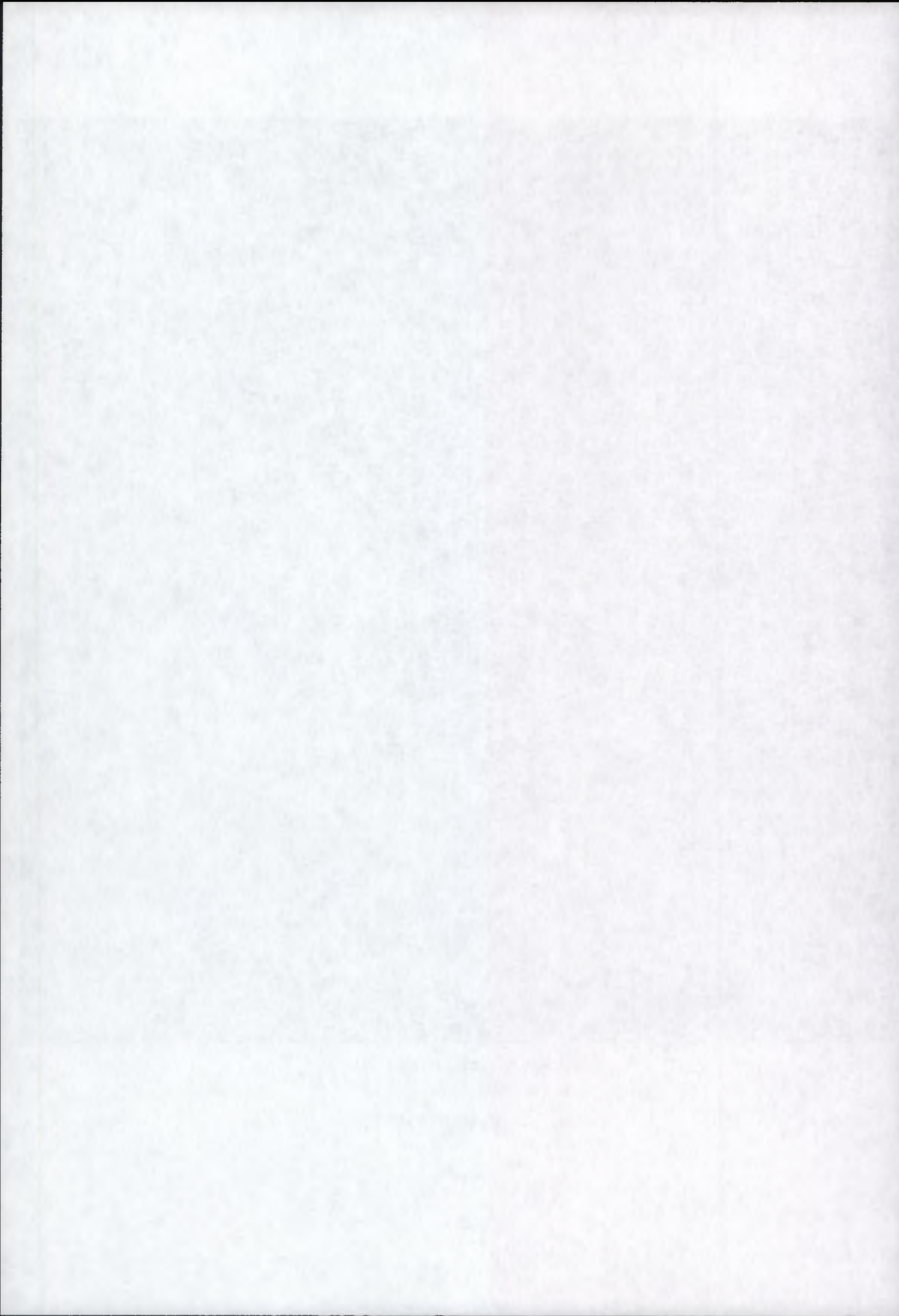




ERS2 SAR image - BELGIUM

ERS2 orbit 234 (7 may 1995)

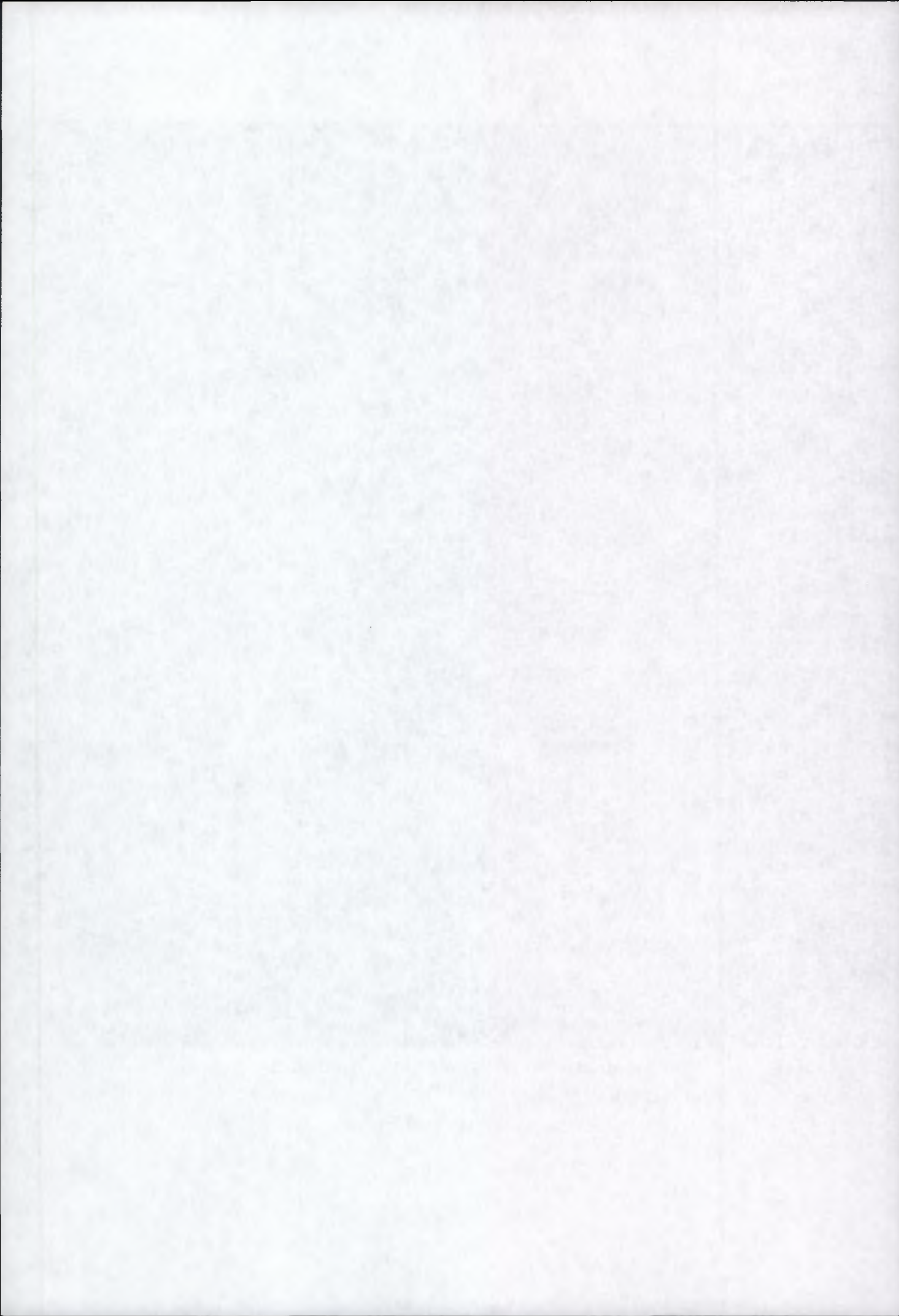
ERS2 data copyright ESA 1995, CNES processing

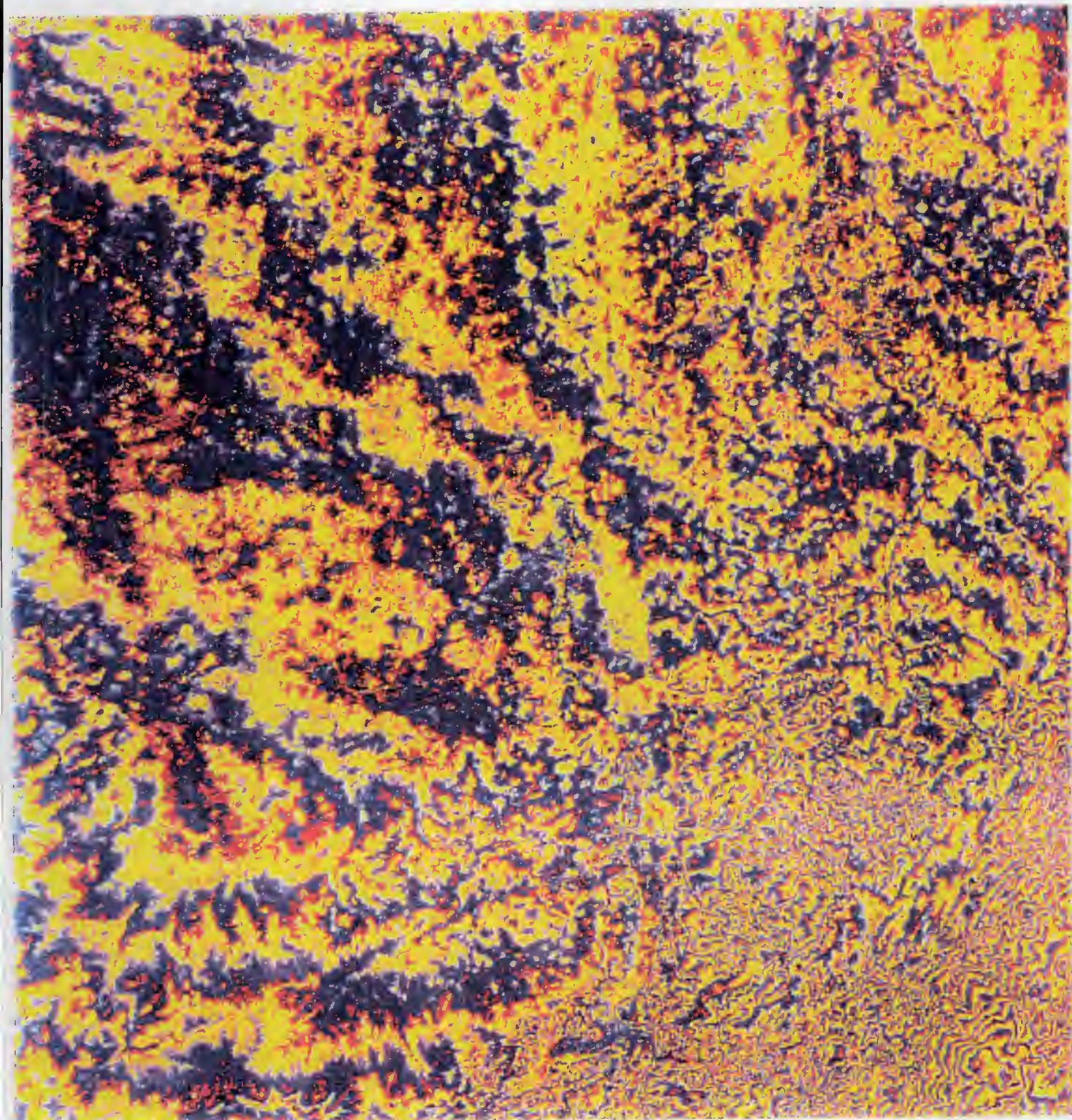




1 day ERS1/ERS2 TANDEM COHERENCE  
ERS1 orbit 19907 (6 may 1995) - ERS2 orbit 234 (7 may 1995)

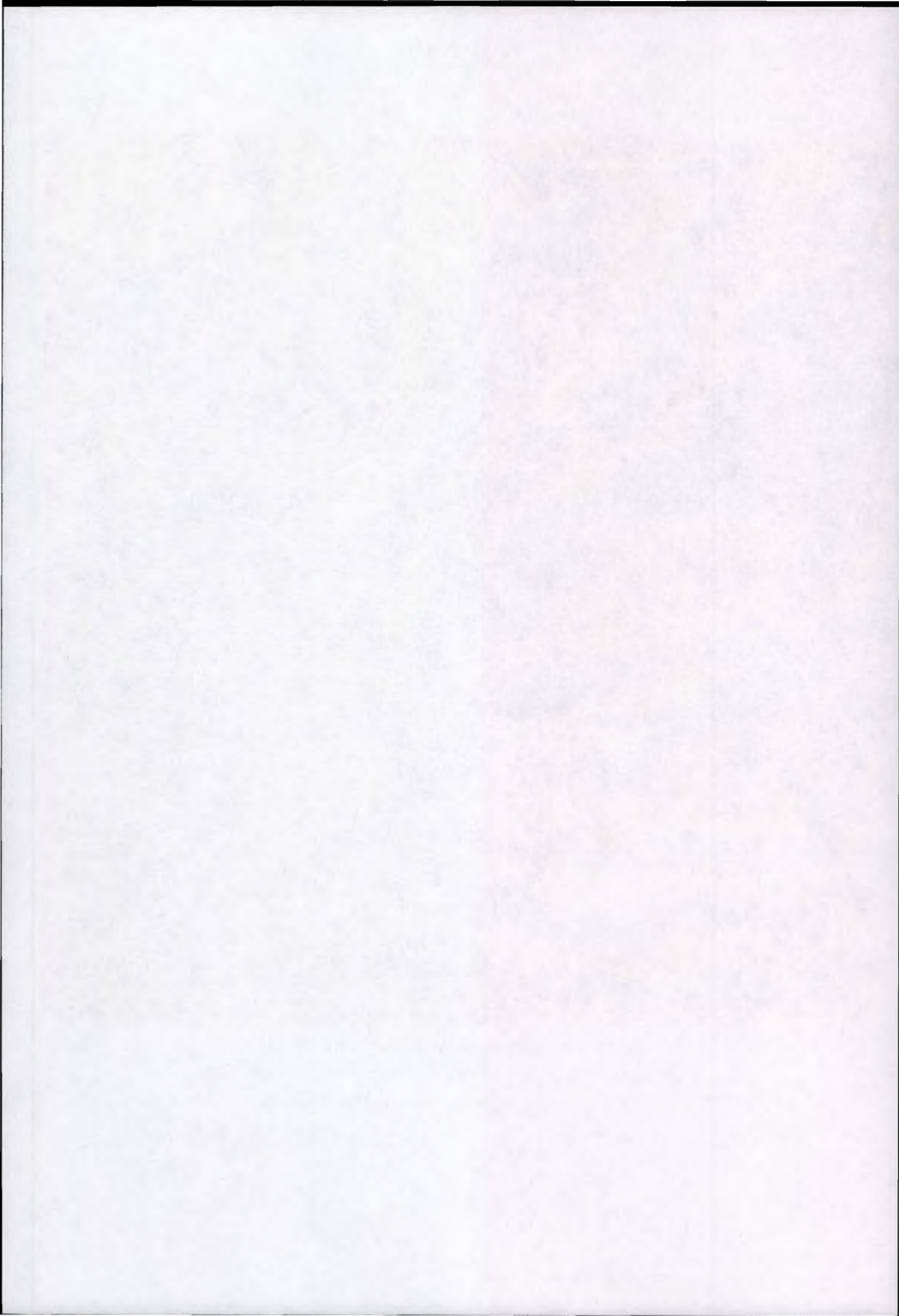
ERS1/2 data copyright ESA 1995, CNES processing

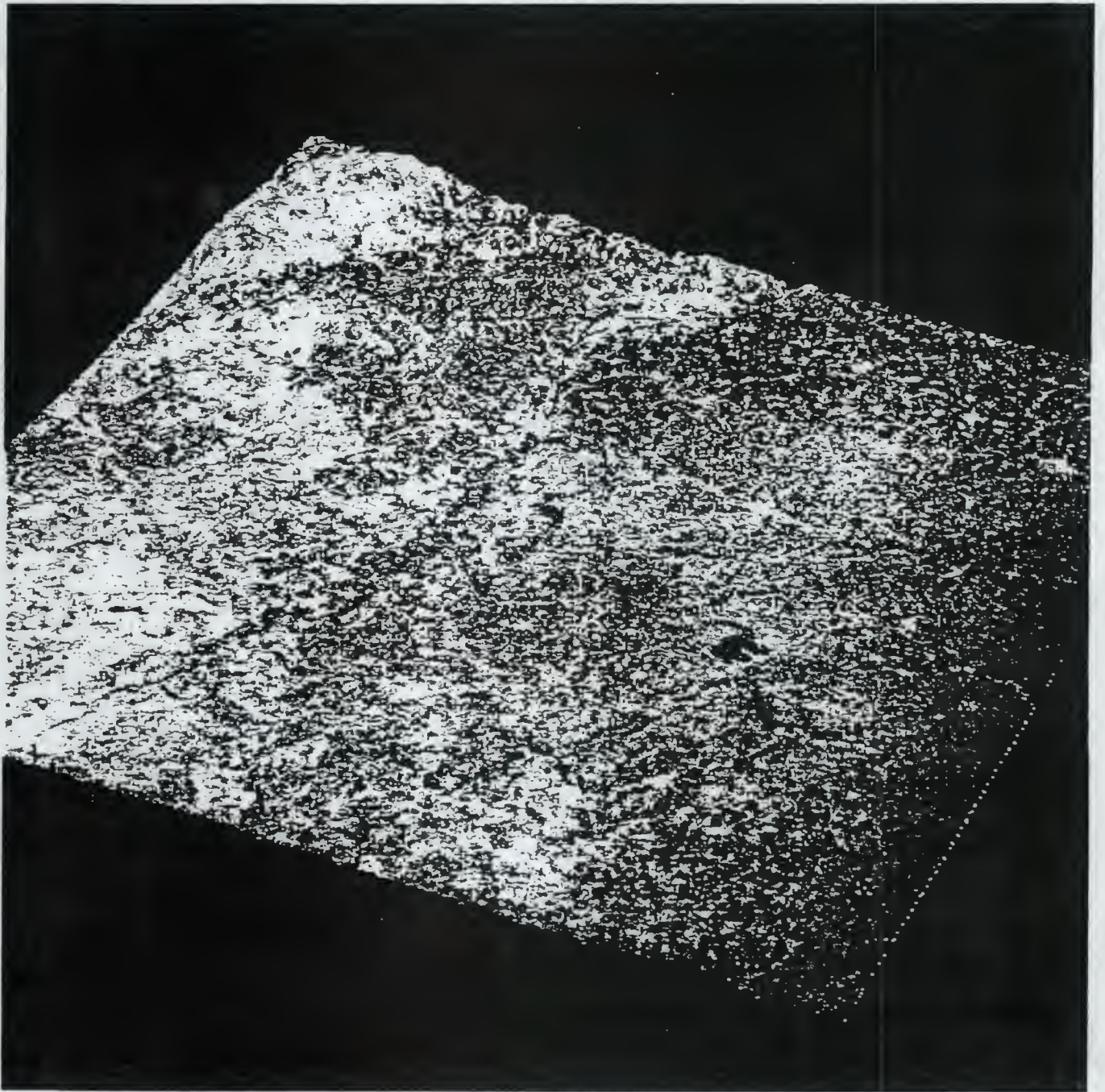


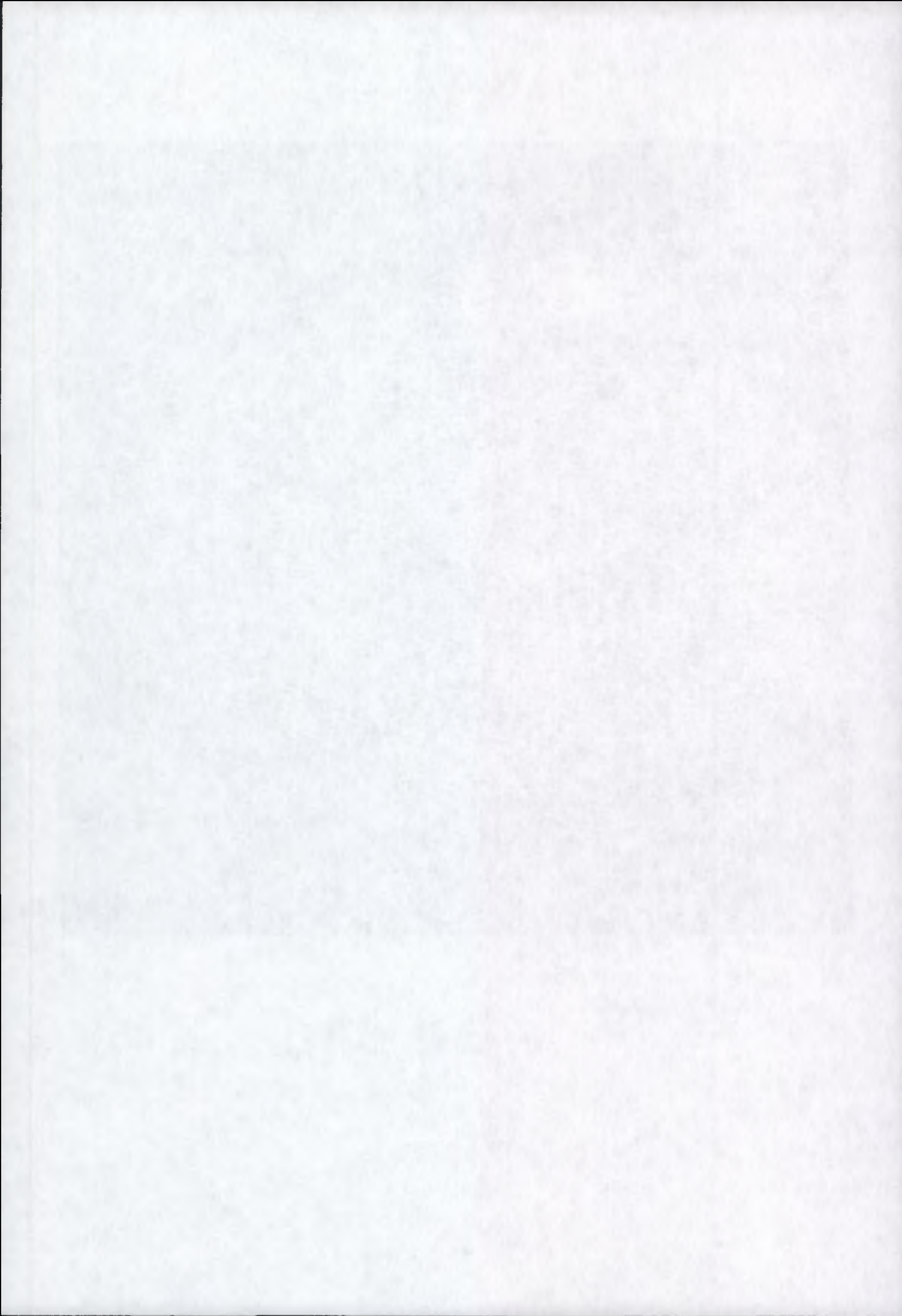


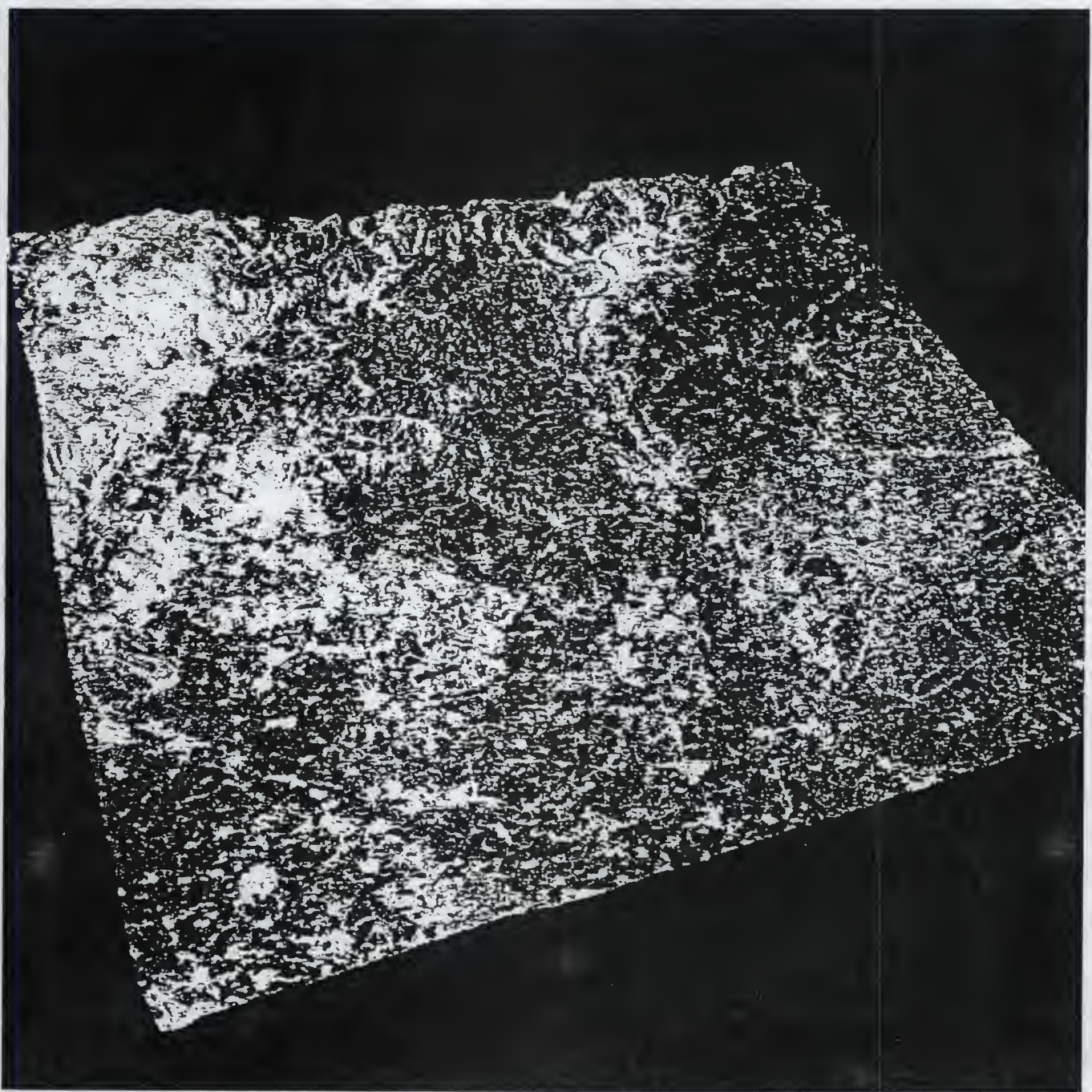
1 day ERS1/ERS2 TANDEM INTERFEROGRAM  
ERS1 orbit 19907 (6 may 1995) - ERS2 orbit 234 (7 may 1995)

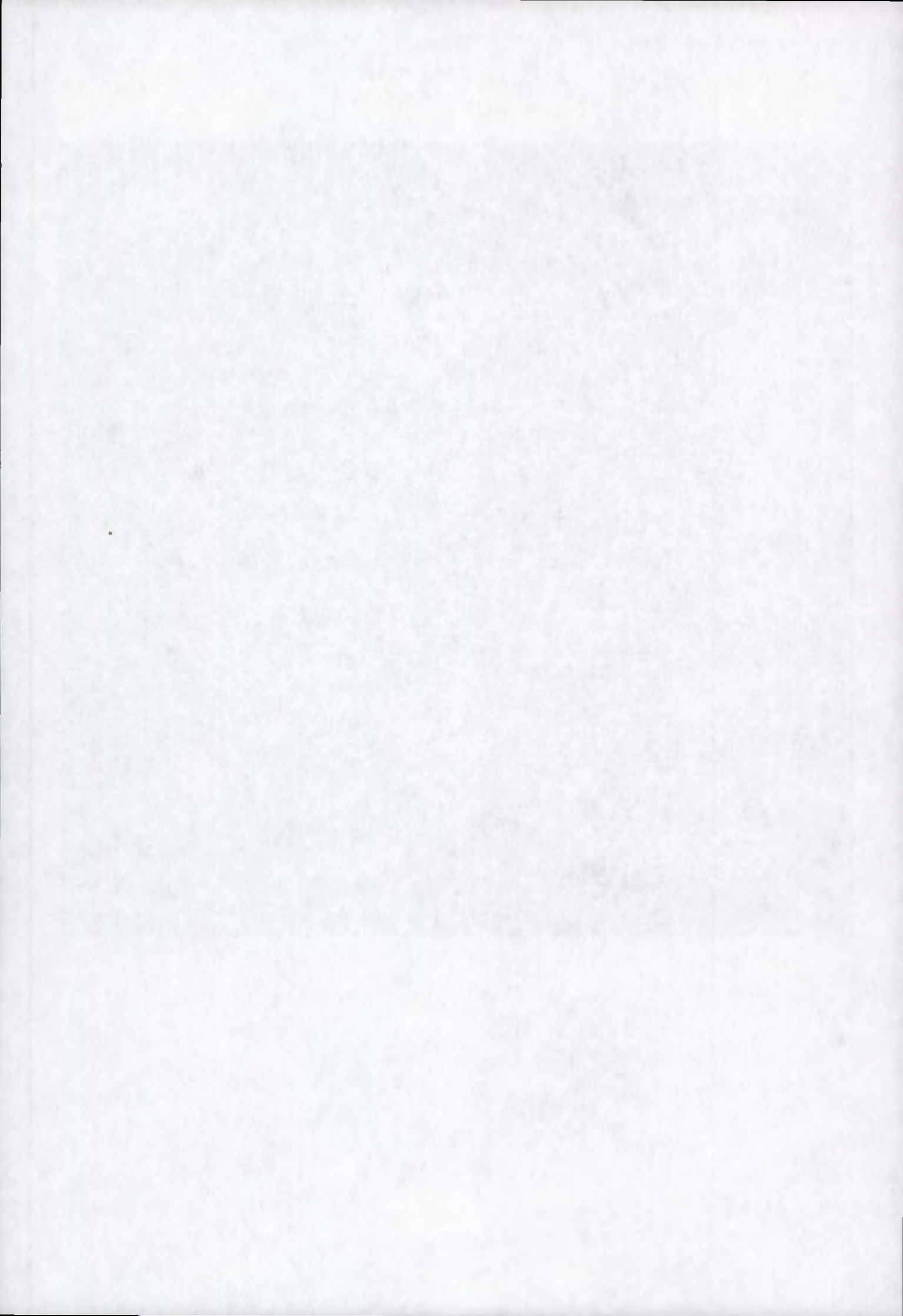
ERS1/2 data copyright ESA 1995, CHES processing











# Annex J

## **Geographical area**

Jacobshaven Glacier, Greenland

## **Research institute**

JPL, USA

## **Application domain**

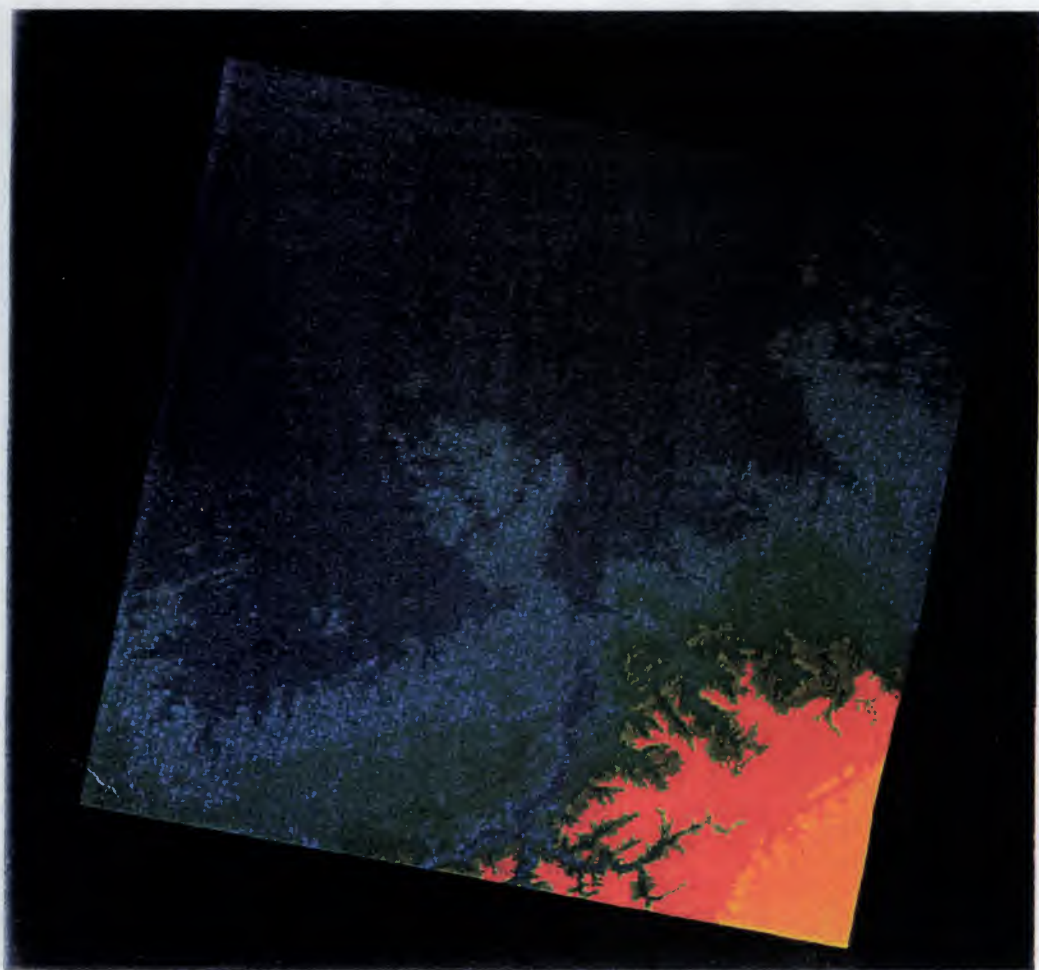
Ice motion / glaciology

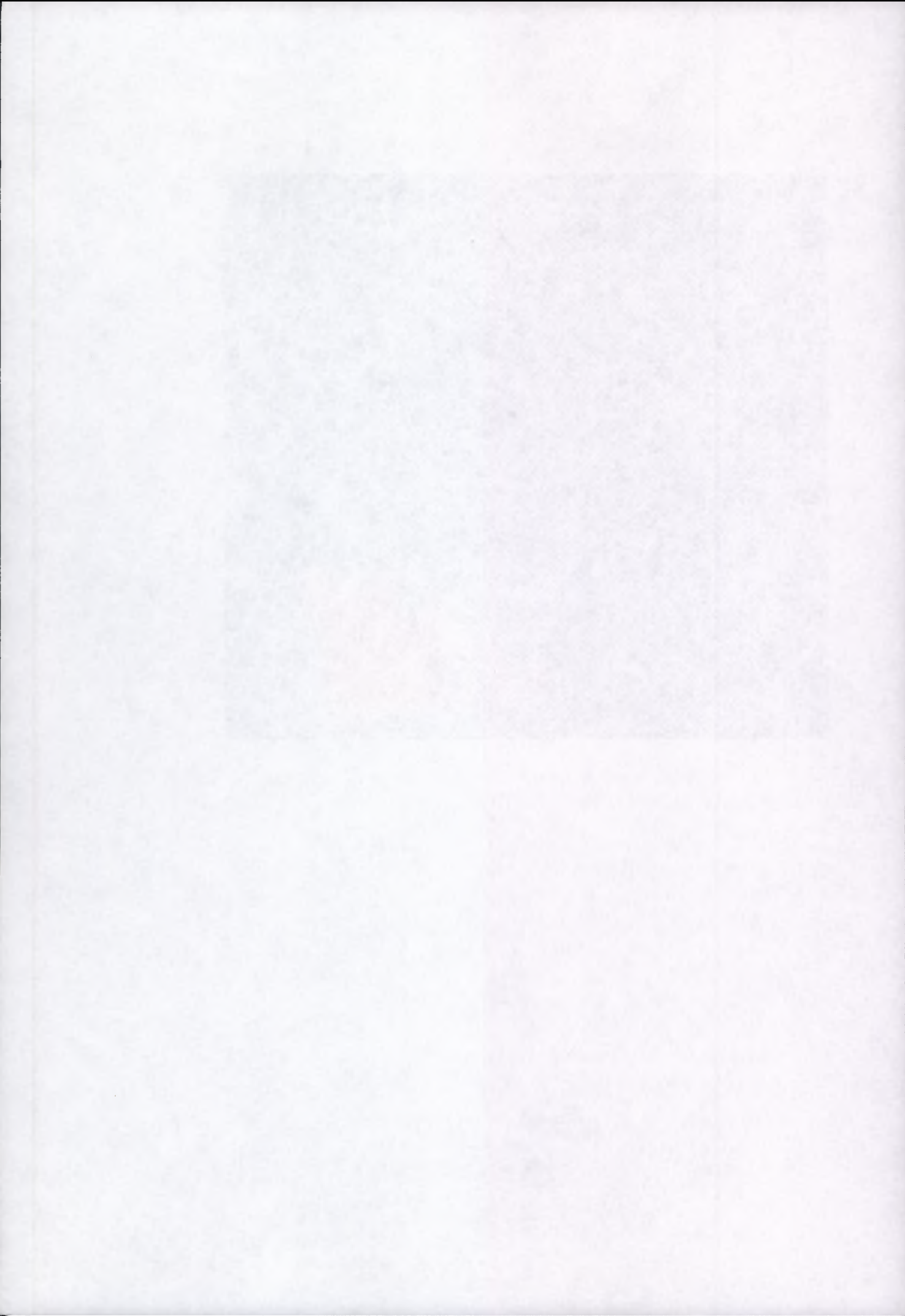
## **First results**

During summer, coherence on the Jacobshaven glacier was not sufficient for the generation of an interferogram.

With a winter dataset, interferometric fringes on the higher reaches of the Jacobshaven glacier are obtained. These fringes correspond to a combination of both topography and motion. Separation of the components is currently being performed with a further tandem dataset.







## **Early Tandem Interferometry Results**

R Goldstein, JPL

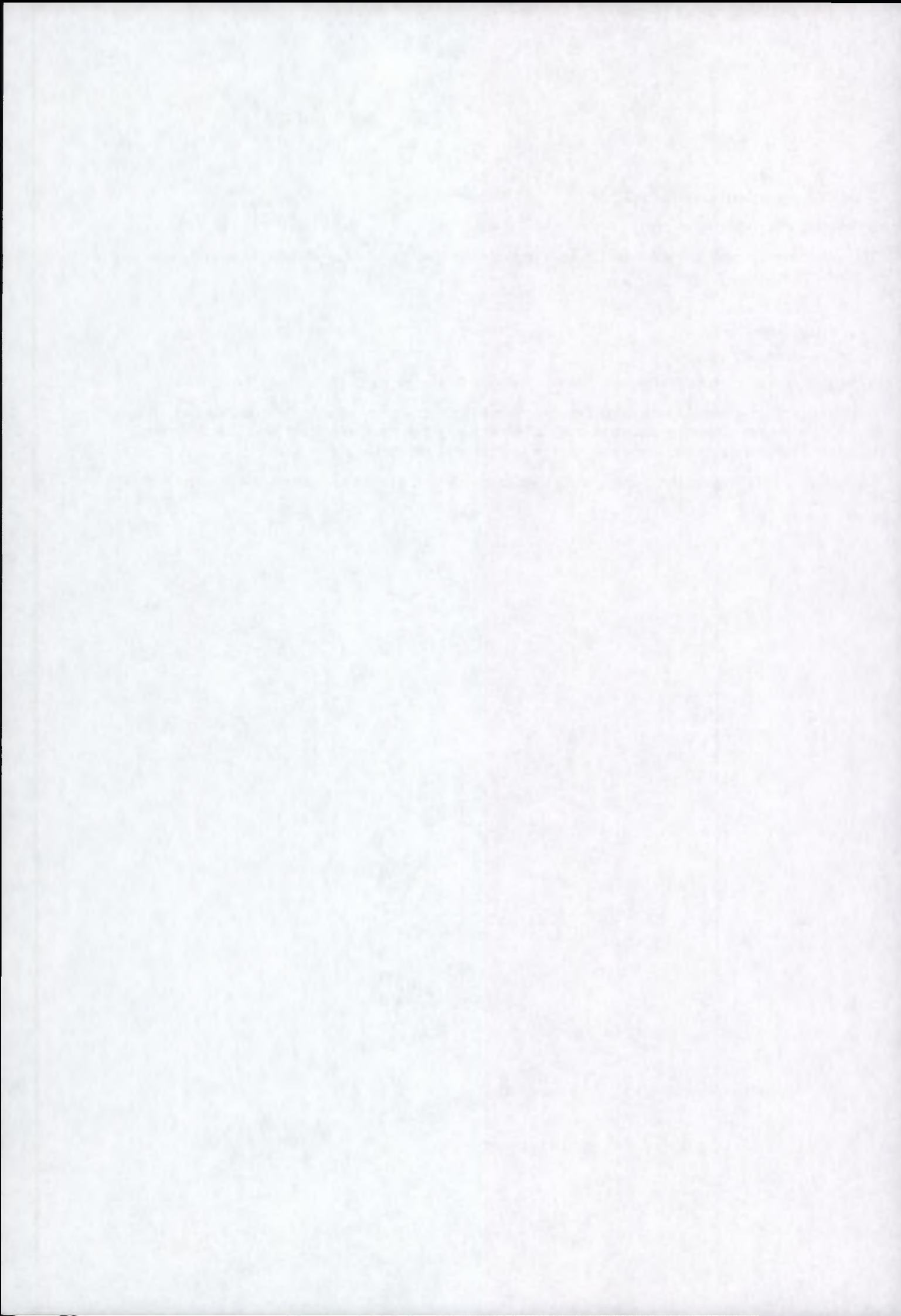
The raw signal samples of three sets of tandem data over the Jakobshavn Glacier in Greenland were processed. Data were acquired on the following dates:

- July 29 and 30
- September 2 and 3
- September 18 and 19

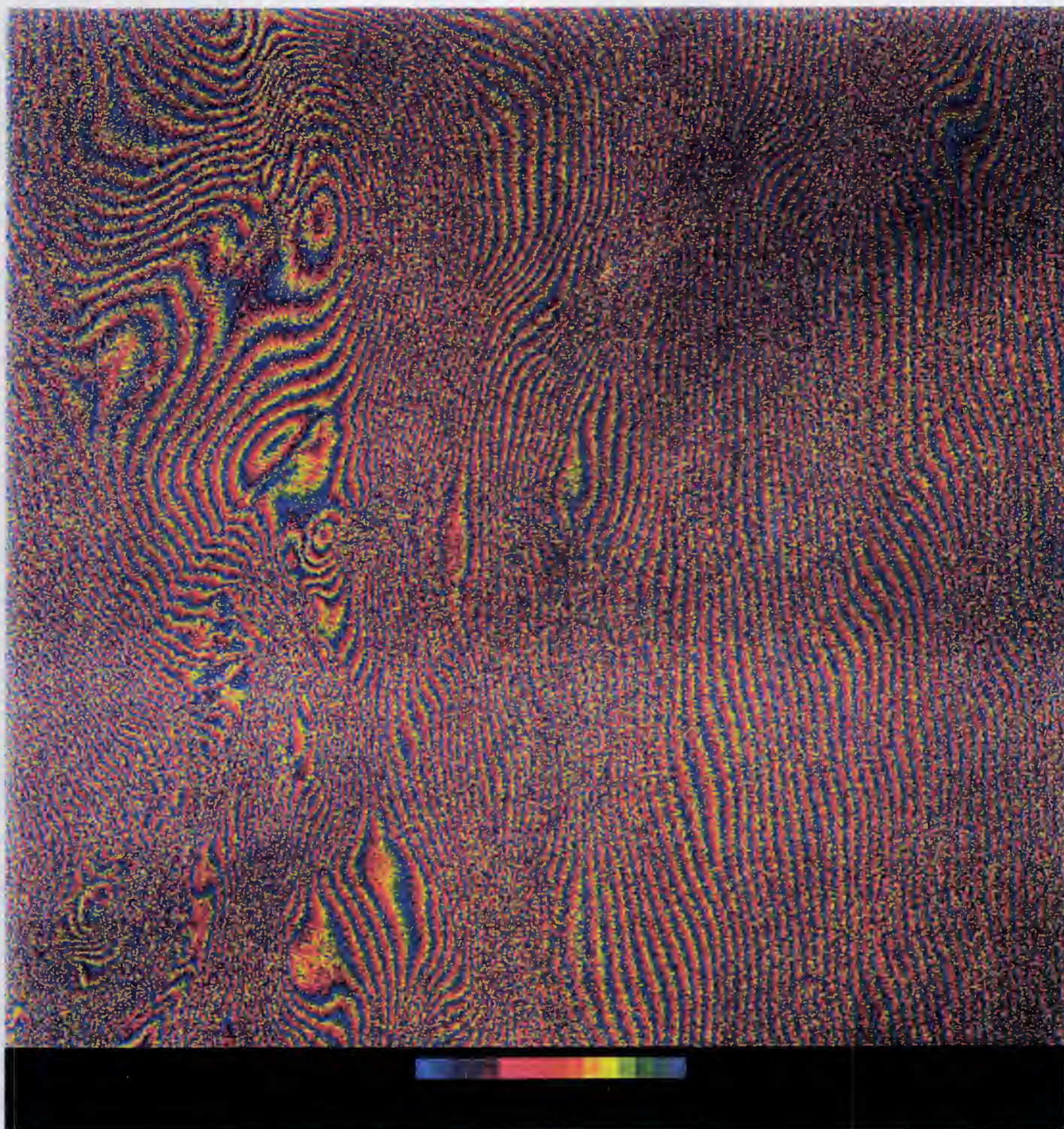
Although good fringes were observed over adjacent rocky areas, the fast moving glacier showed none.

In addition, a recent winter data set acquired December 16 and 17 has just been processed. These do show useful fringes on the higher reaches of the Jakobshavn Glacier as can be seen from the interferogram (figure 1) which has the radar brightness lightly superimposed. The second figure gives the radar magnitude only.

For separation of the fringes into topography and motion, another data set is required (which has now been received and is being processed).



**Figure 1. Interferogram over the Jakobshaven glacier**



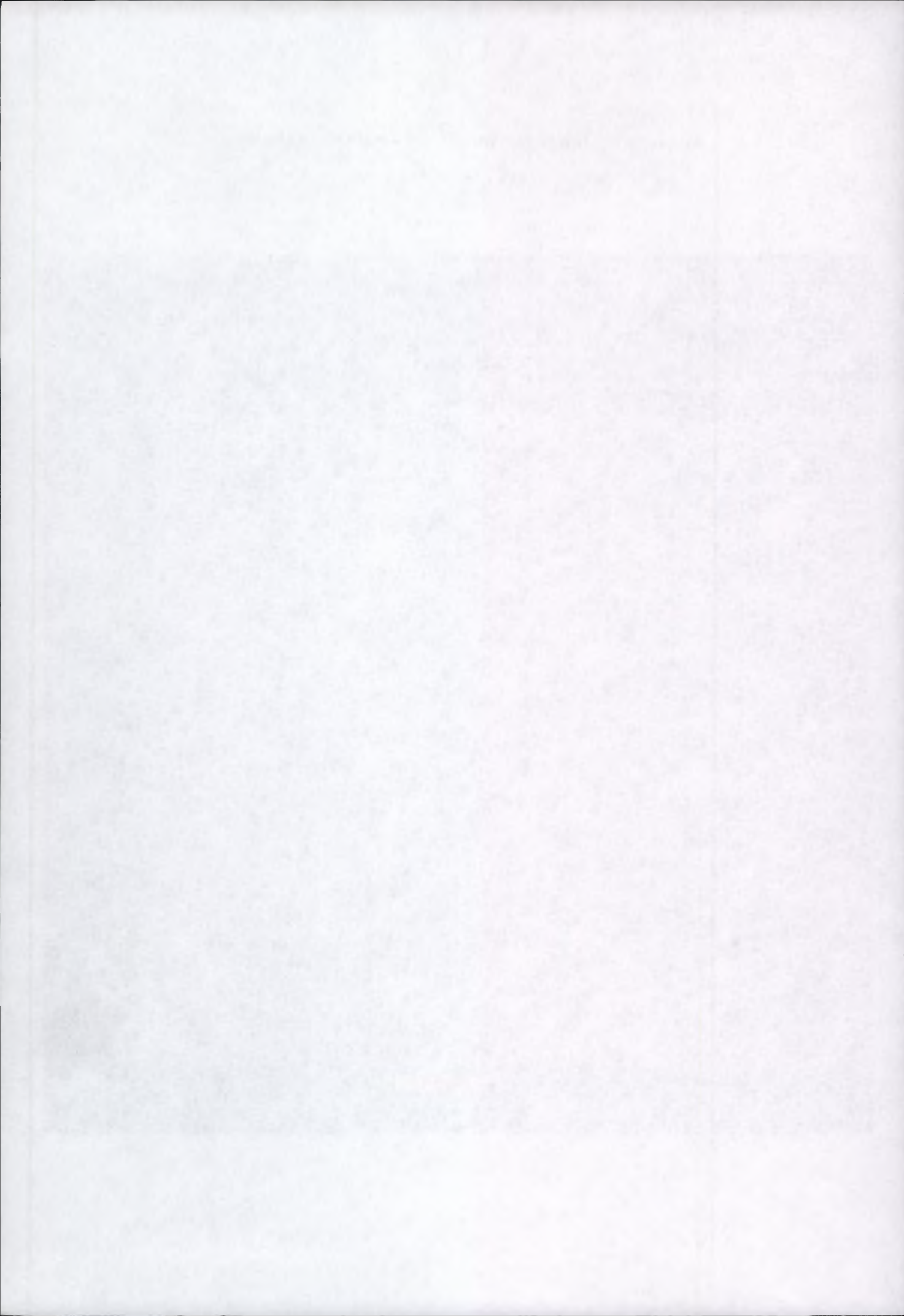


Figure 2. Radar magnitude





# Annex K

## Geographical area

Bern, Switzerland

Cairo, Egypt

Rabat, Morocco

## Research institute

Remote Sensing Laboratories, University of Zurich

## Application domain

Land use and DEMs

## First results

ERS-1 / ERS-2 Doppler spectra offset of 280 Hz observed.

A differential interferogram corresponding to the difference between ERS tandem height data and the Swiss DDHM25 height model was produced. After removal of small systematic phase trends (less than one fringe), the residual height error map is essentially flat.



# ERS-1/2 Tandem Mission

## FRINGE Report

to the

European Space Agency ESRIIN

C.P. 64

I-00044 Frascati, Italy

prepared by

Remote Sensing Laboratories RSL

Department of Geography

University of Zürich

Winterthurerstrasse 190

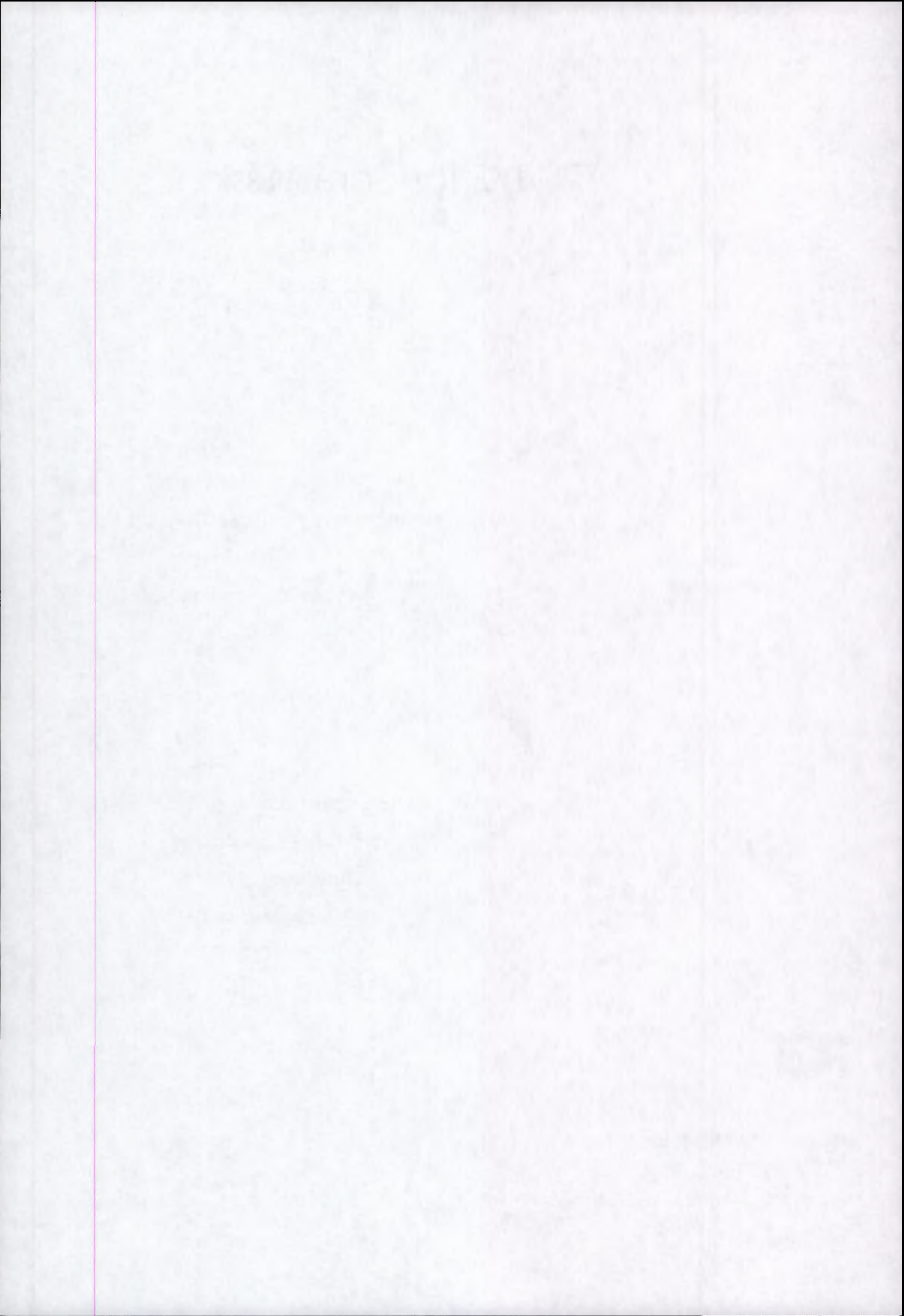
CH - 8057 Zürich

Switzerland

The logo for Remote Sensing Laboratories (RSL) consists of the letters 'RSL' in a bold, black, sans-serif font. The 'R' and 'S' are connected at the top, and the 'L' is positioned to the right of the 'S'.

*Document:* BriefReport-9604  
*Version:* 2.0

April 30, 1996



## 1 Introduction

This document describes the ERS tandem data processing at RSL to date. ESA-ESRIN SLC quarter scene data acquired over Bern, Switzerland, Cairo, Egypt, and Rabat, Morocco have been used to calculate interferograms and further value-added products. An earlier report from RSL (with extended analysis of sidelobe ambiguities and coherence-based thematic interpretation) was delivered to ESRIN in October, 1995.

## 2 Test Sites and Available Data

The tandem data available at RSL for this study are listed below. Overviews of both the geographic coverage and interferometric baselines are provided.

### 2.1 Bern, Switzerland

Multiple ERS Tandem data sets were delivered to RSL. Their coverage and the interferometric baselines relating them are described below.

#### 2.1.1 Geographic Coverage

For orientation purposes, Figure 1 illustrates the distribution of the individual quarter-scenes in the Bern area. The Single Look Complex (SLC) quarter scenes are labelled Q1-Q4. The processing at RSL has concentrated on the first quarter (Q1), with some limited processing devoted to Q2.

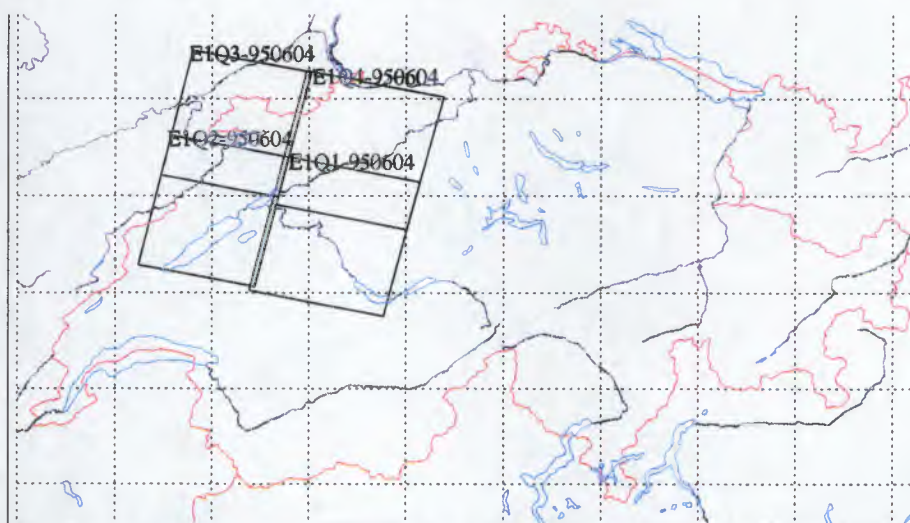
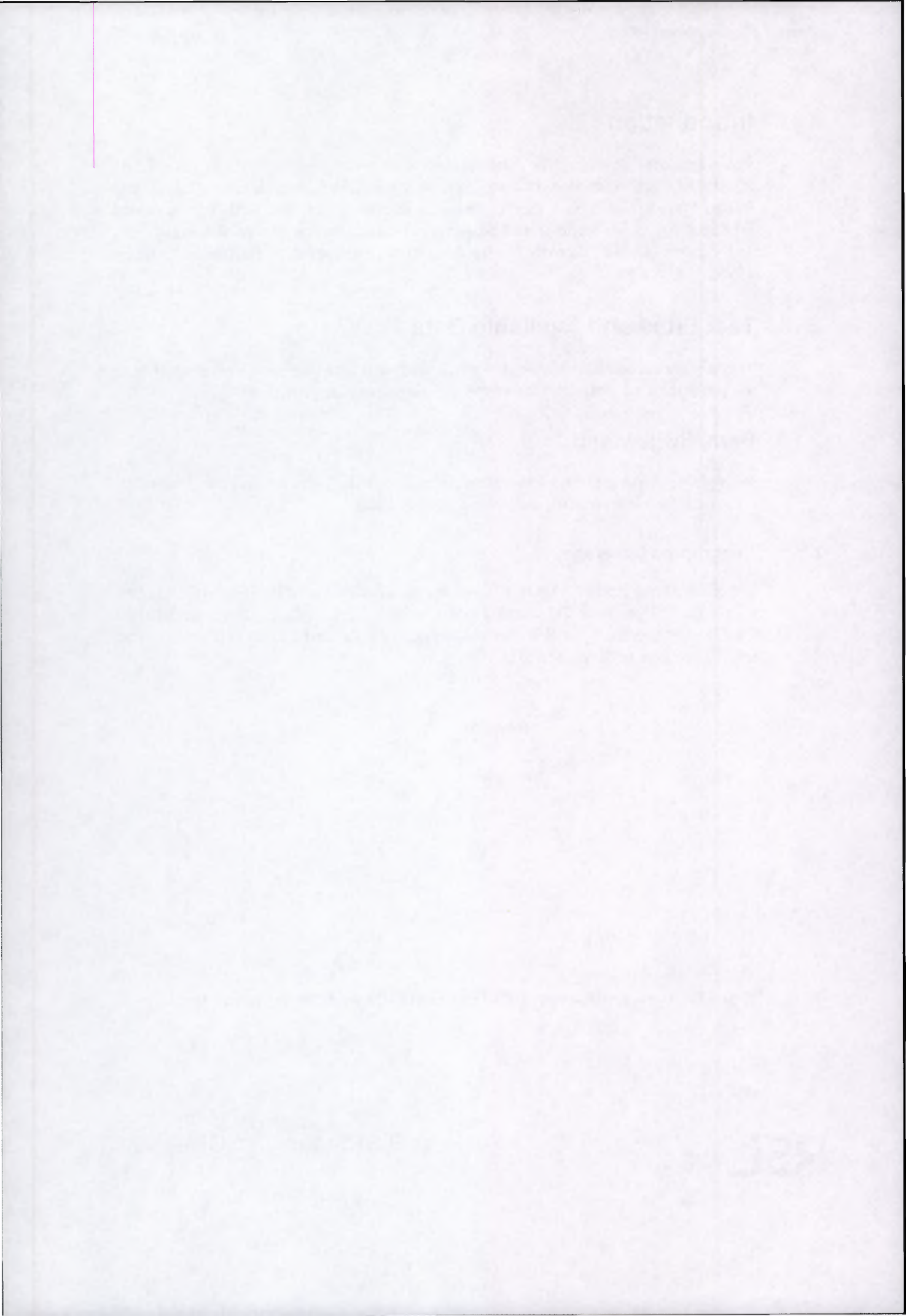


Figure 1: Bern, Switzerland - ERS Tandem SLC Quarter Scenes: June, 1995



## 2.1.2 Baselines

State vectors for each scene were read from the Verification Mode Processor (VMP) Specific Product Header (SPH). RSL Zürich InSAR Processor "ZIP" software was then used to calculate baselines for all scene combinations. State vectors from precise orbit (PRC) products were used when possible.

The baselines between the ERS tandem data are listed in Table 1. The 1-day repeat coverage provides a good variety of height sensitivities, interesting also for multi-baseline investigations.

Scene 1 Satellite, Orbit #, Date			Scene 2 Satellite, Orbit #, Date			$\Delta t$ [days]	$B_{\parallel}$ [m]	$B_{\perp}$ [m]
E1	20322	95.06.04	E2	649	95.06.05	1	-54	-118
E1	20823	95.07.09	E2	1150	95.07.10	1	-6	23
E1	21324	95.08.13	E2	1651	95.08.14	1	-24	-43
E1	22326	95.10.22	E2	2653	95.10.23	1	43	105
E1	22827	95.11.26	E2	3154	95.11.27	1	47	136
E1	23328	95.12.31	E2	3655	96.01.01	1	-78	-205
E1	24330	96.03.10	E2	4657	96.03.11	1	-23	-5

Table 1: Bern, Switzerland - ERS Tandem Baselines, June 1995 - March 1996

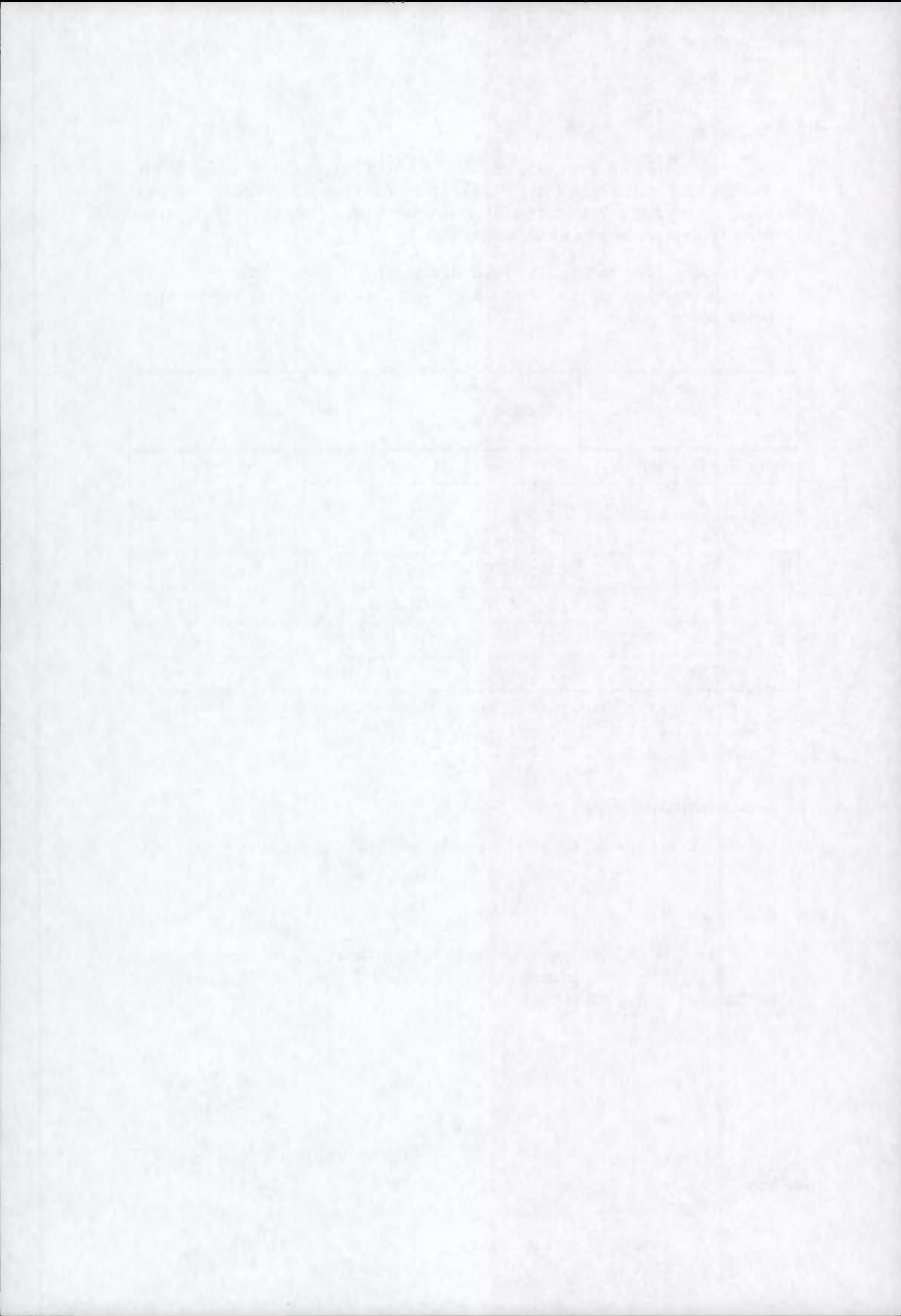
## 2.2 Cairo, Egypt

### 2.2.1 Geographic Coverage

For orientation purposes, the area covered by the ERS-1/2 Cairo scenes is shown in Figure 2.

### 2.2.2 Baseline

As for the Bern tandem pairs, the baseline between the two Cairo acquisitions was calculated. The baseline parameters are listed in Table 2. The relatively large baseline provides good height sensitivity.



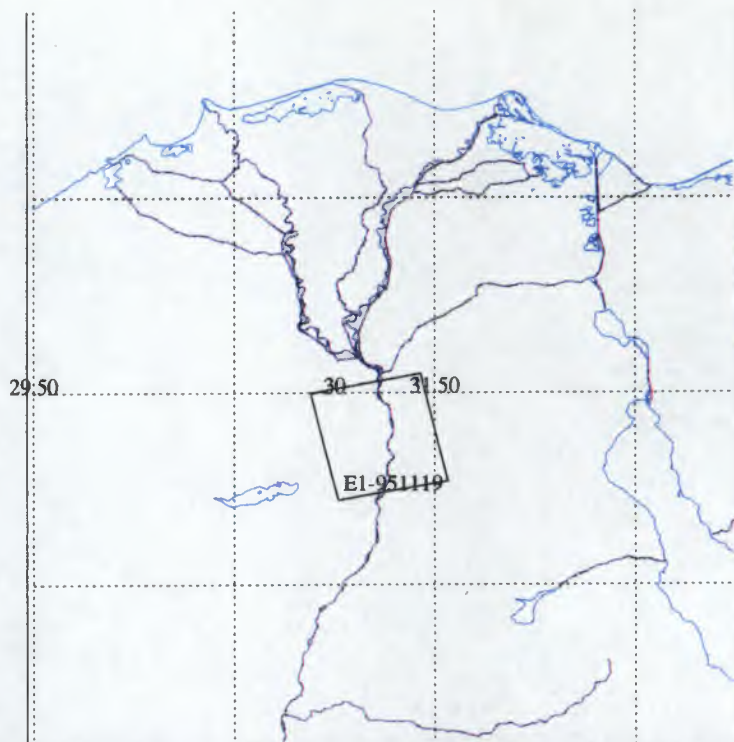


Figure 2: Cairo, Egypt - ERS Tandem SLC Quarter Scene: November, 1995

Scene 1 Satellite & Date		Scene 2 Satellite & Date		Time Difference [days]	$B_{\parallel}$ [m]	$B_{\perp}$ [m]
E1	95.11.19	E2	95.11.20	1	70	218

Table 2: Cairo, Egypt - ERS Tandem Baseline, November, 1995

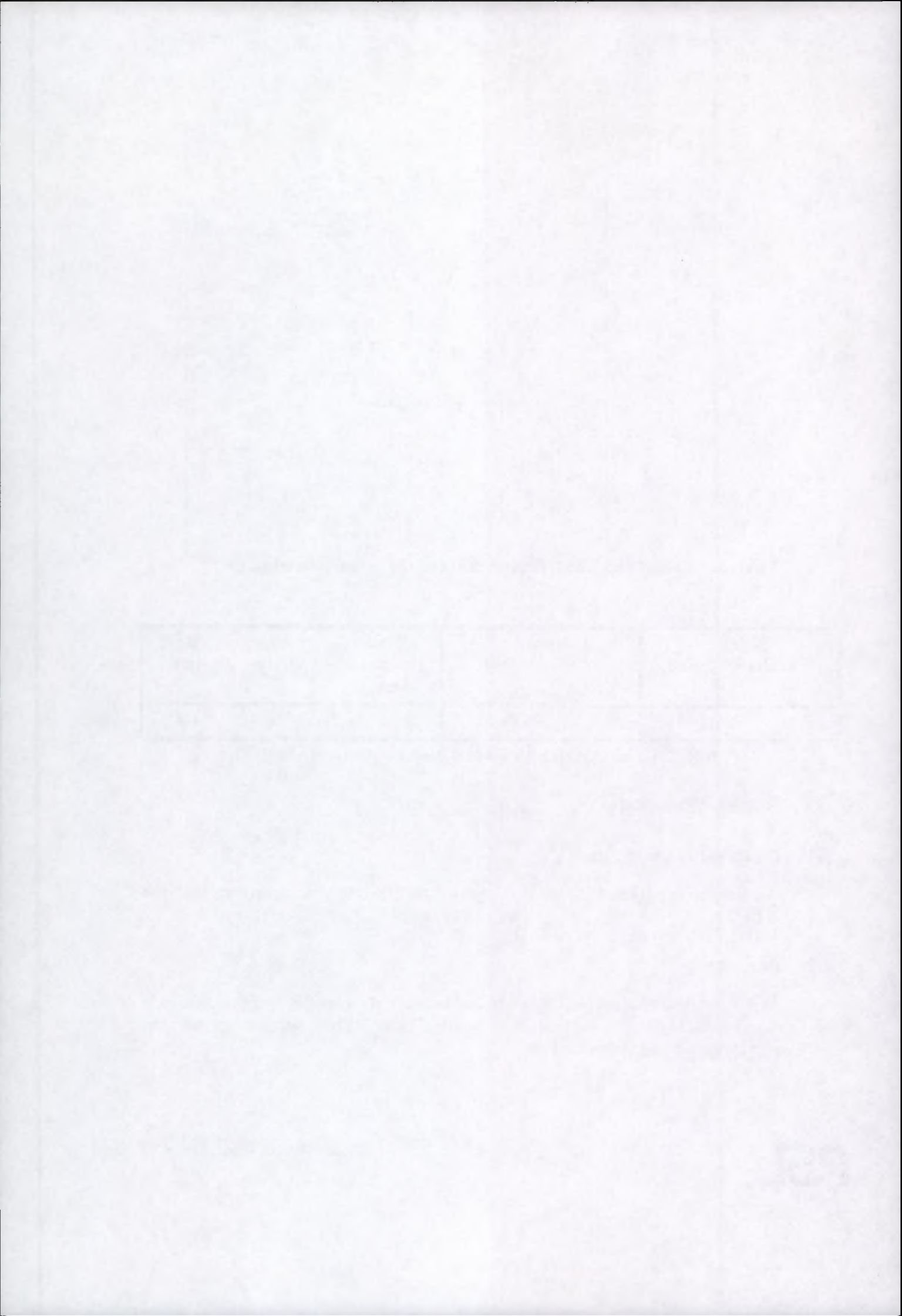
## 2.3 Rabat, Morocco

### 2.3.1 Geographic Coverage

For orientation purposes, the area covered by the ERS-1/2 Morocco scenes is shown in Figure 3.

### 2.3.2 Baseline

As for the Bern tandem pairs, the baseline between the two Rabat acquisitions was calculated. The baseline parameters are listed in Table 3. The relatively large baseline provides good height sensitivity.



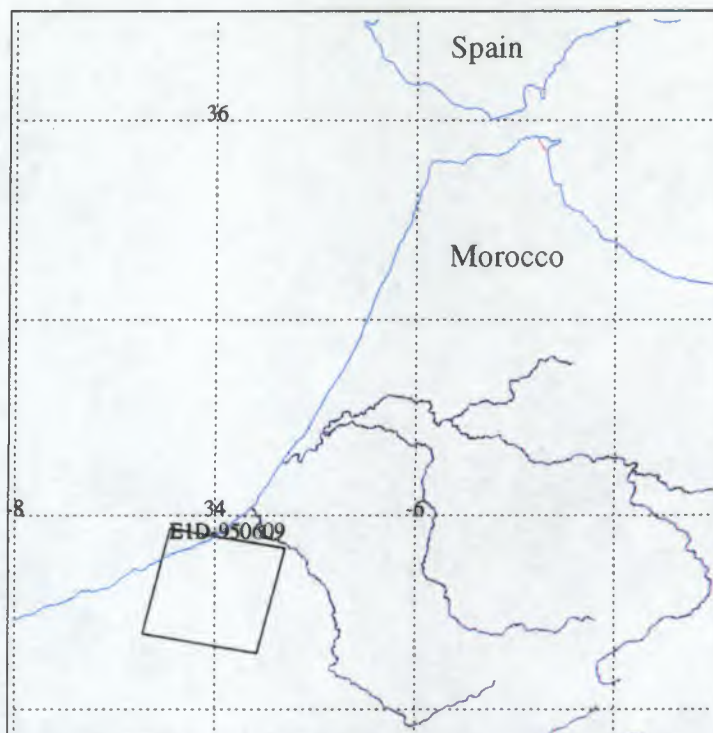


Figure 3: Rabat, Morocco - ERS Tandem SLC Quarter Scene: June, 1995

Scene 1 Satellite & Date		Scene 2 Satellite & Date		Time Difference [days]	$B_{\parallel}$ [m]	$B_{\perp}$ [m]
E1	95.06.09	E2	95.06.10	1	-70	-153

Table 3: Rabat, Morocco - ERS Tandem Baseline, June 1995

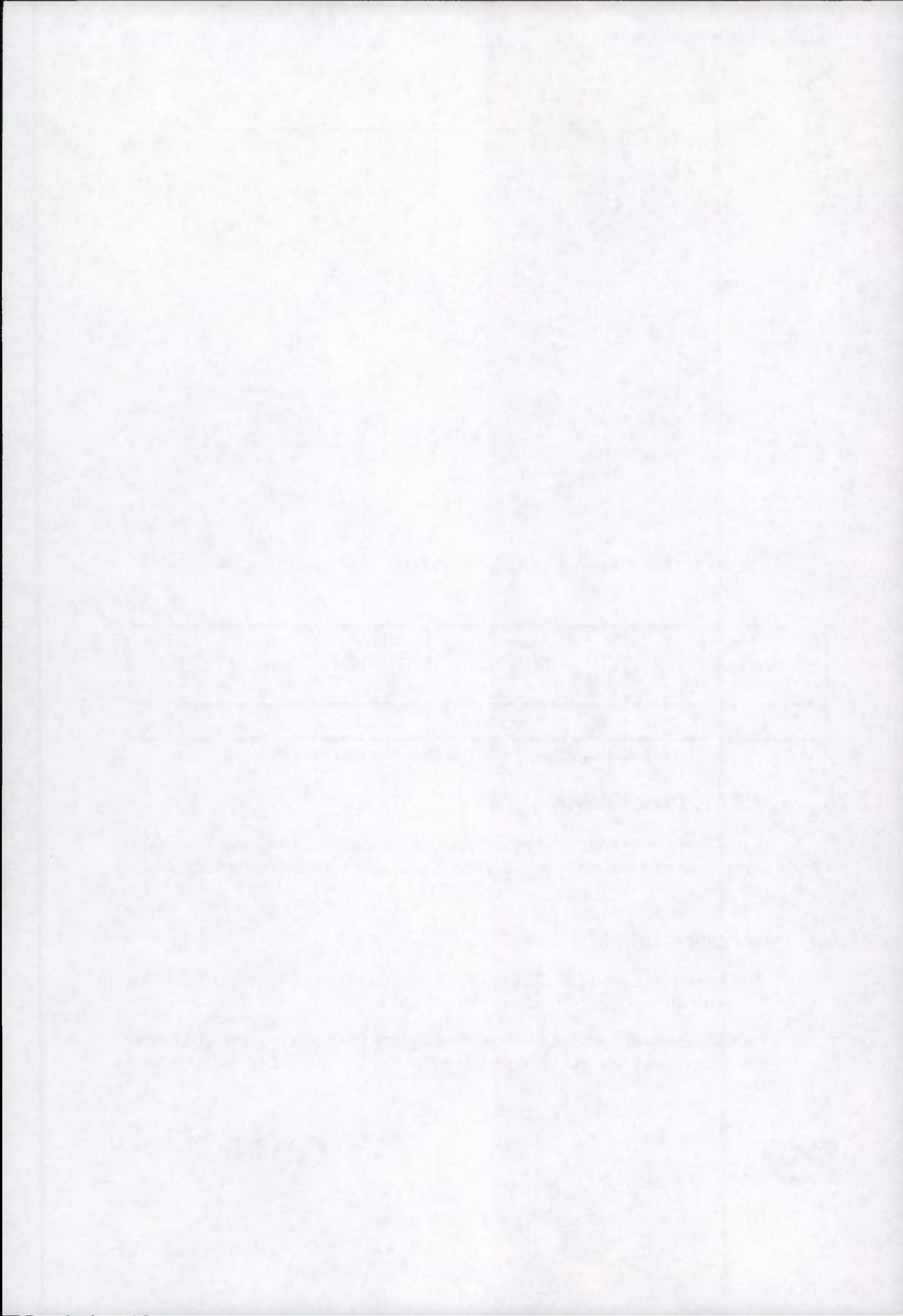
### 3 InSAR Processing

In the course of our interferometric processing, we discovered two anomalies: (a) a Doppler centroid shift between ERS-1 and ERS-2, and (b) azimuth sidelobe inconsistencies.

#### 3.1 Doppler Centroid

The Doppler centroids of ERS-1 and ERS-2 were found to significantly differ, with a mean difference of approximately 280 Hz.

The difference was observed between ERS-1/2 data from the first quarter (Q1) scene of the Bern data (June-August 1995) as well as the Egyptian and Moroccan tandem pairs.



Values read within the VMP-SPH header annotation generally agreed with centroids calculated through spectral summation. Figure 4 shows the Doppler spectra for the Bern Q1 data. The ERS-1 data behave consistently (note overlap), and the ERS-2 data are also consistent (with each other). However, the ERS-1 and ERS-2 centroid estimates clearly fall into two separate populations.

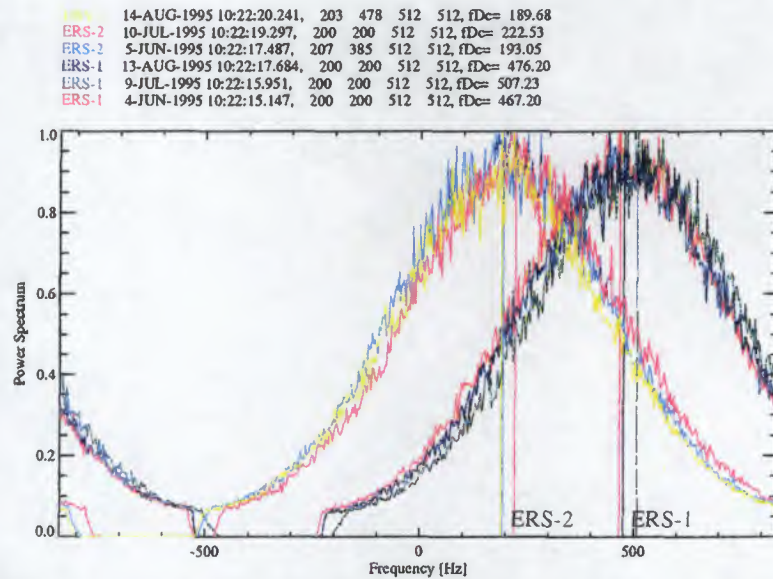


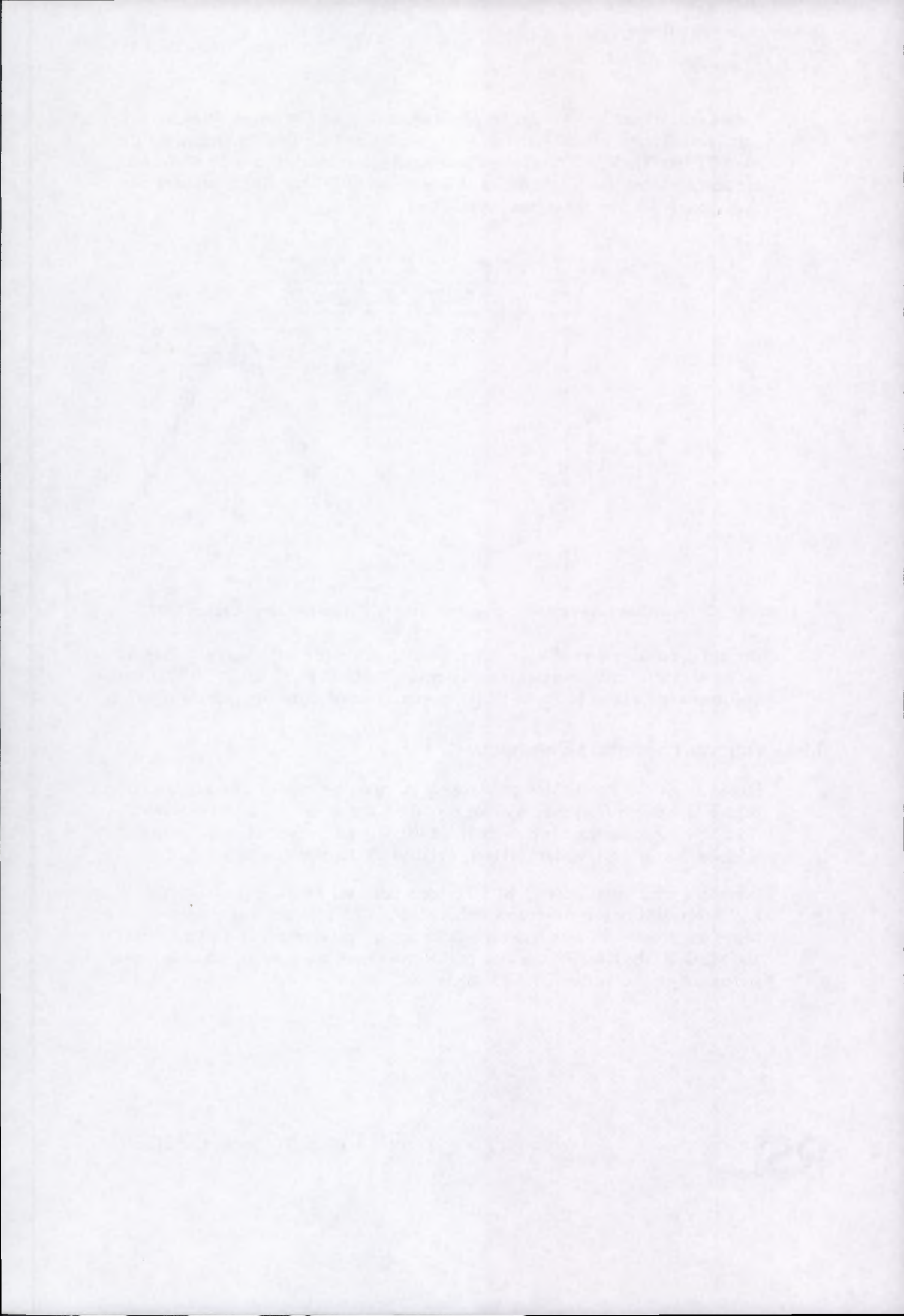
Figure 4: Bern, Switzerland - ERS-1/2 Doppler Centroid Estimates: June-August, 1995

Doppler spectra from the ERS-1 commissioning phase (Bern, November 1991), as well as the ERS-1 first ice phase (Bonn, Germany - March 14, 17, 20, 29, 1992) were also reviewed. In these cases, the ERS-1 spectra never exhibited any such shift.

### 3.2 Azimuth Sidelobe Behaviour

Inspection of the Rabat, Morocco imagery revealed anomalous azimuth sidelobe behaviour. Extracts from intensity images of the Rabat scenes are shown in Figure 5. Note how range sidelobe behaviour is similar in both images. However, azimuth sidelobes are (approximately) 5dB higher in the ERS-1 image than ERS-2.

Inspection of a multitemporal ERS-1 image provided by Juerg Lichtenegger of ESRIN revealed similar differences within a set of ERS-1 images. The multitemporal image was constructed with June'95 data feeding the red channel, May'95 the green, and March'95 the blue. Examination of Figure 6 shows that azimuth sidelobes were significantly higher in the March'95 acquisition.



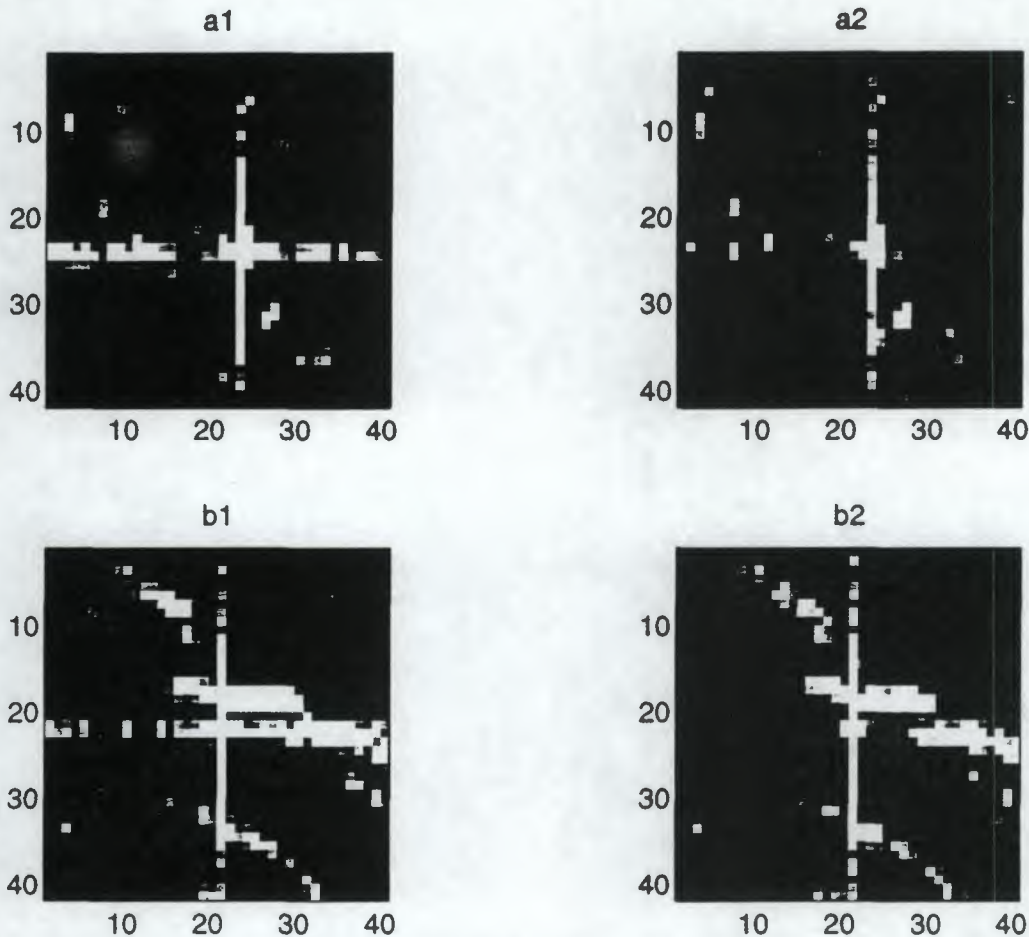
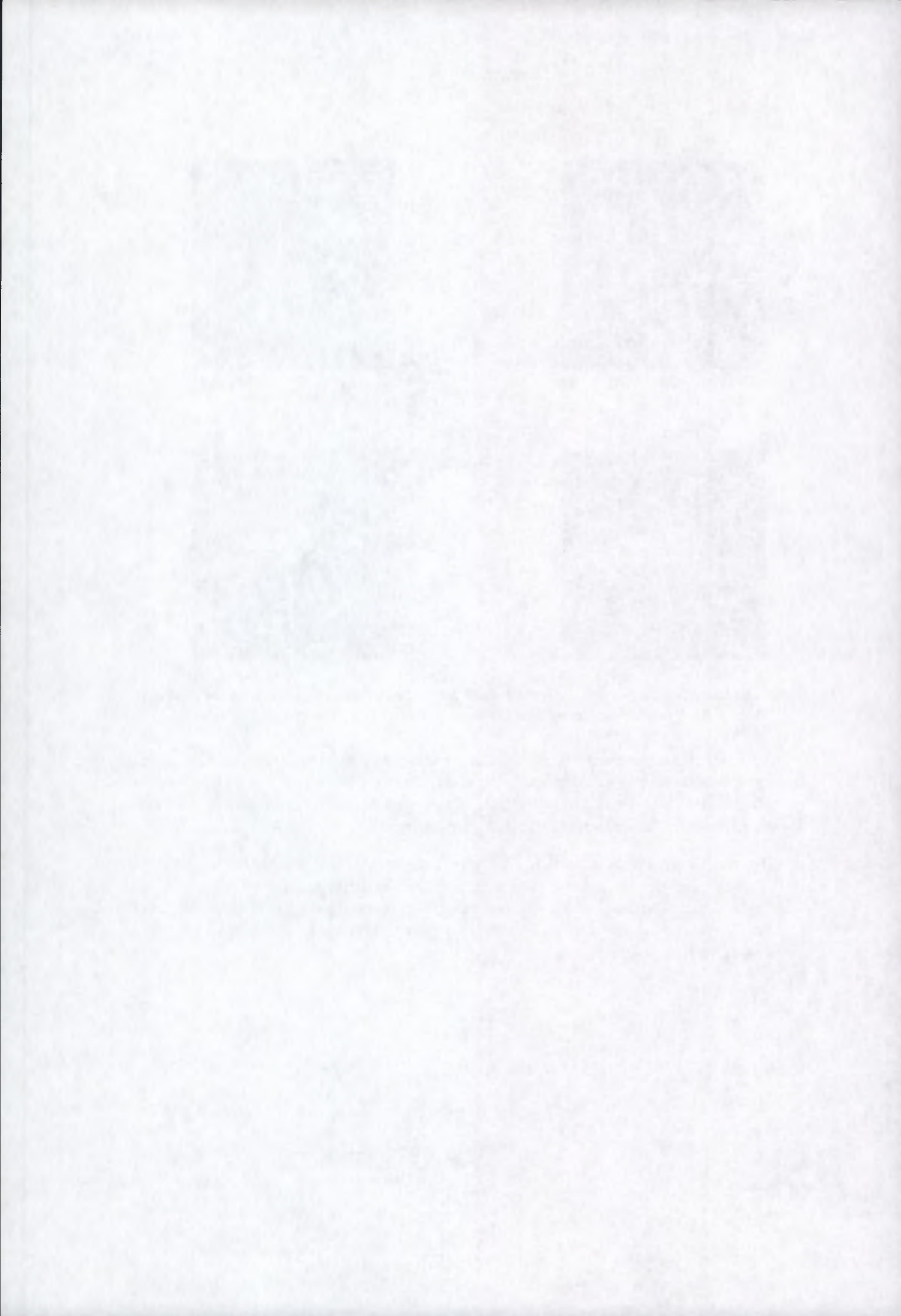


Figure 5: Rabat, Morocco - Inconsistent Azimuth Sidelobe Behaviour observed at two corner reflectors, Azimuth is horizontal, Range is vertical

We now believe that *quantization saturation* accounts for the inconsistency. In coastal regions with bright water returns, ERS 5-bit quantization can result in a large proportion of saturated returns. Other possible causes considered were: processing changes, and differences between ERS-1/ERS-2 gain settings.

The phenomenon, unfortunately, has *implications for interferometry*. In the *high sidelobe* case the local phase is determined by the main target, while in the *low sidelobe* case, the local phase derives from (non-homogenous) local scatterers, and the coherence is lost. Range sidelobes are also seen to reduce coherence in Figure 6, although not as severely.



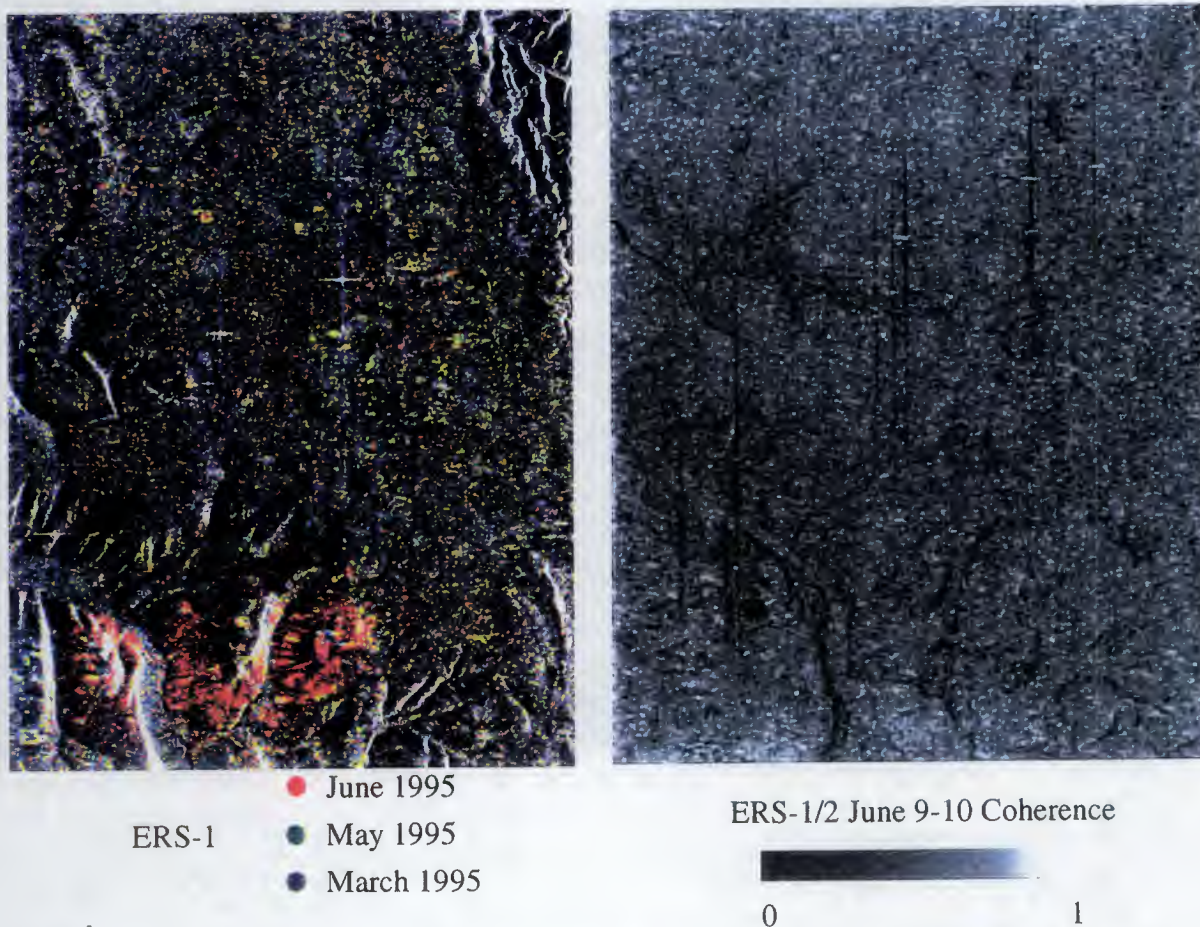
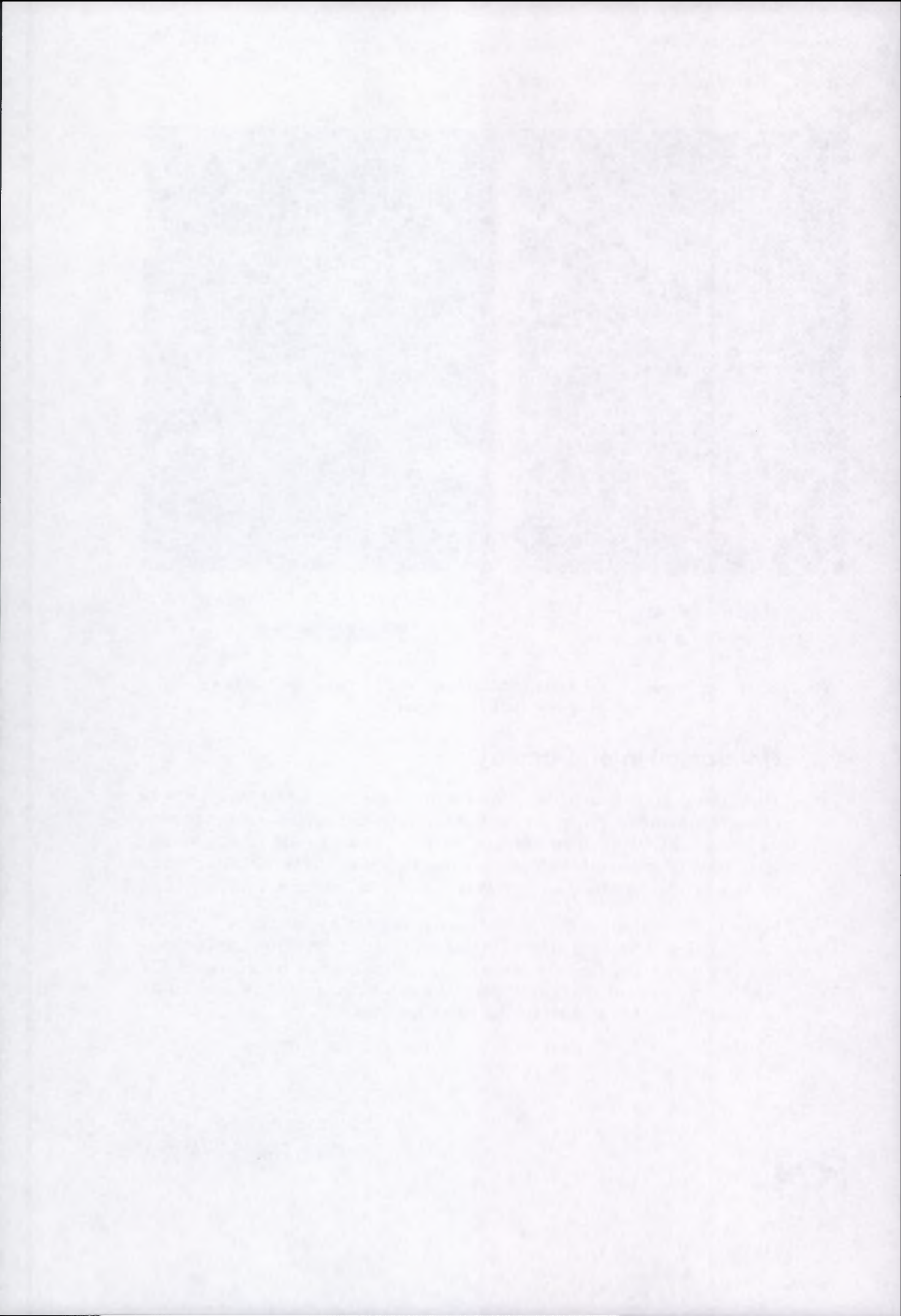


Figure 6: Rabat, Morocco - (a) PRI-based Multitemporal ERS-1, (b) Inconsistent Azimuth Sidelobes Destroy Coherence

#### 4 Differential Interferometry

The expected phase from a high resolution digital elevation model from the Swiss Federal Office of Topography was "subtracted" from ERS tandem interferograms to study the feasibility of differential interferometry studies. For the tandem mission, such "DEM subtraction" is more practical than the 3-pass "double difference" methodology, as the nearest third pass is always 35 days of decorrelation away.

Figure 7 shows a differential interferogram calculated by subtracting the Swiss "DHM25" height model from the October 1995 tandem interferogram. The small phase trend remaining (less than a fringe) was removed with a bilinear model. The resulting interferogram is nearly completely flat. Selected areas show a systematic phase shift (e.g. coherent forest stands, some urban areas).



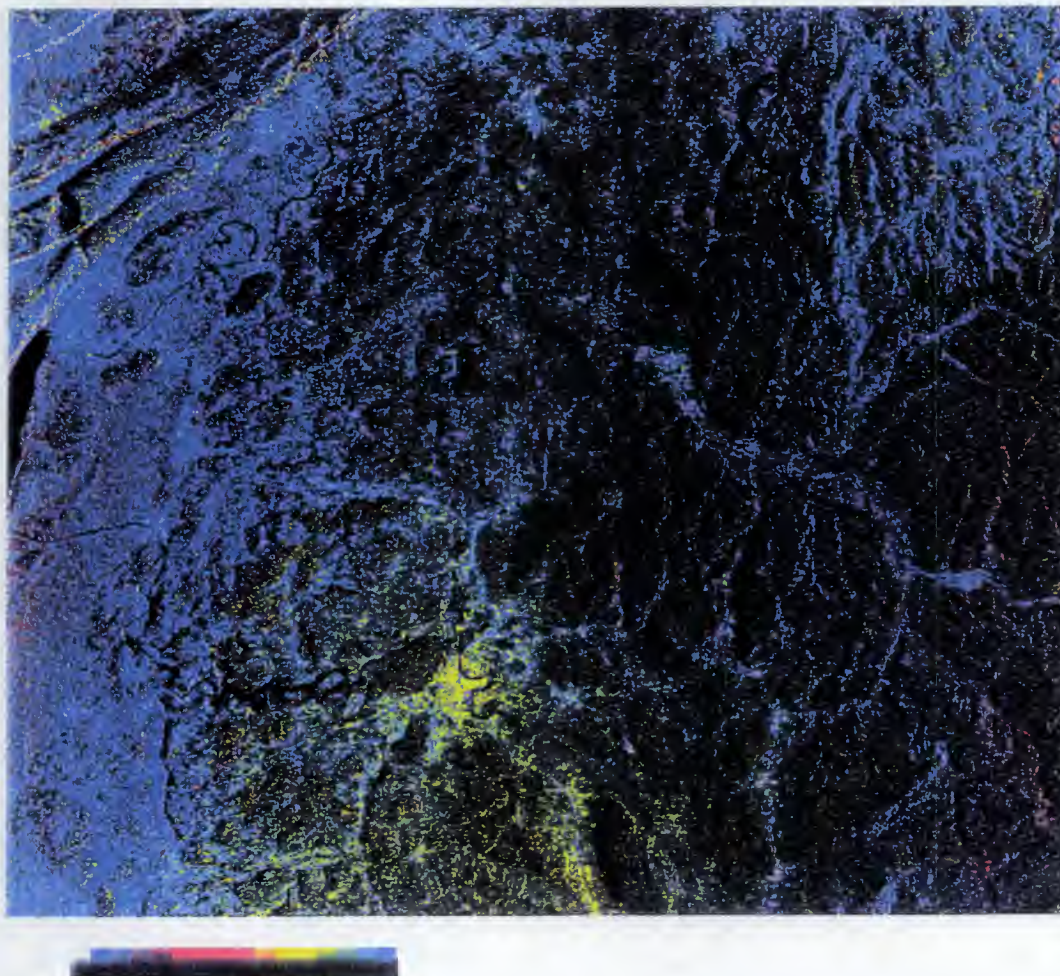
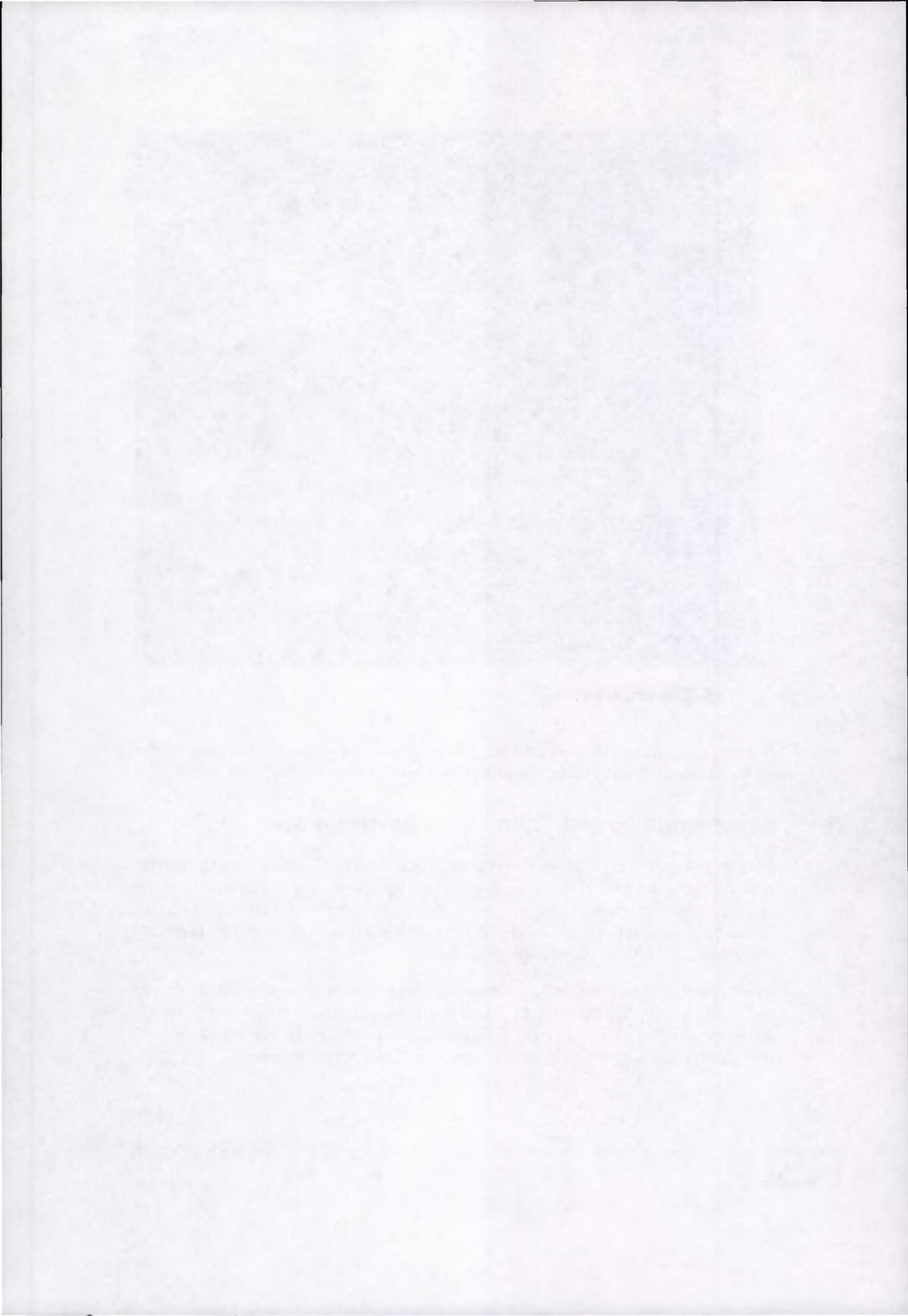


Figure 7: Bern, Switzerland - October 1995 Tandem interferogram flattened using Swiss Digital Height Model 25 (DHM25), courtesy Swiss Federal Office of Topography

## 5 Coherence-based Thematic Interpretation

For the first quarter (Q1) of the Bern tandem data (June 1995 - March 1996), interferometric signature visualization products were generated. The signatures were not always stable over time. However, given the proper weather conditions, landscape cover discrimination matches that obtained with previous data over the same area (November 1991 ERS-1 commissioning phase).

The tandem mission extends the potential coverage of such coherence-based interpretation. Potentially high-coherence pairs are provided for the first time not only over the limited repeat-orbits acquired during the ERS-1 commissioning and ice phases, but *systematically* over nine cycles of complete 35-day repeat coverage.



## 6 C-PAF / D-PAF / I-PAF SLC Product Comparison

SLC products from the C-PAF, D-PAF, and I-PAF were compared to validate the compatibility of their phase values. For the Bern and Cairo test sites, interferograms were formed using all combinations of the three data sets.

The final report will be delivered at ESRIN on May 10, 1996.

## 7 Ongoing Work

We began with investigation and validation of the ERS interferogram formation process in order to provide a firm foundation for further work. In addition to investigation of the anomalous azimuth sidelobes, and Doppler filtering during interferogram formation, the following topics are under continuing investigation. Updated results will be presented at the FRINGE'96 conference.

### 7.1 Coherence-based Thematic Interpretation

For the Bern test site, the measured coherence values will be compared to theoretical (expected) values for selected ground-cover types. This necessitates a transformation of the coherence images into a common geometry for comparison. The coherence time-series over a complete vegetation cycle will be used to construct a seasonal model for a set of land-cover types.

### 7.2 Generation of Height Models

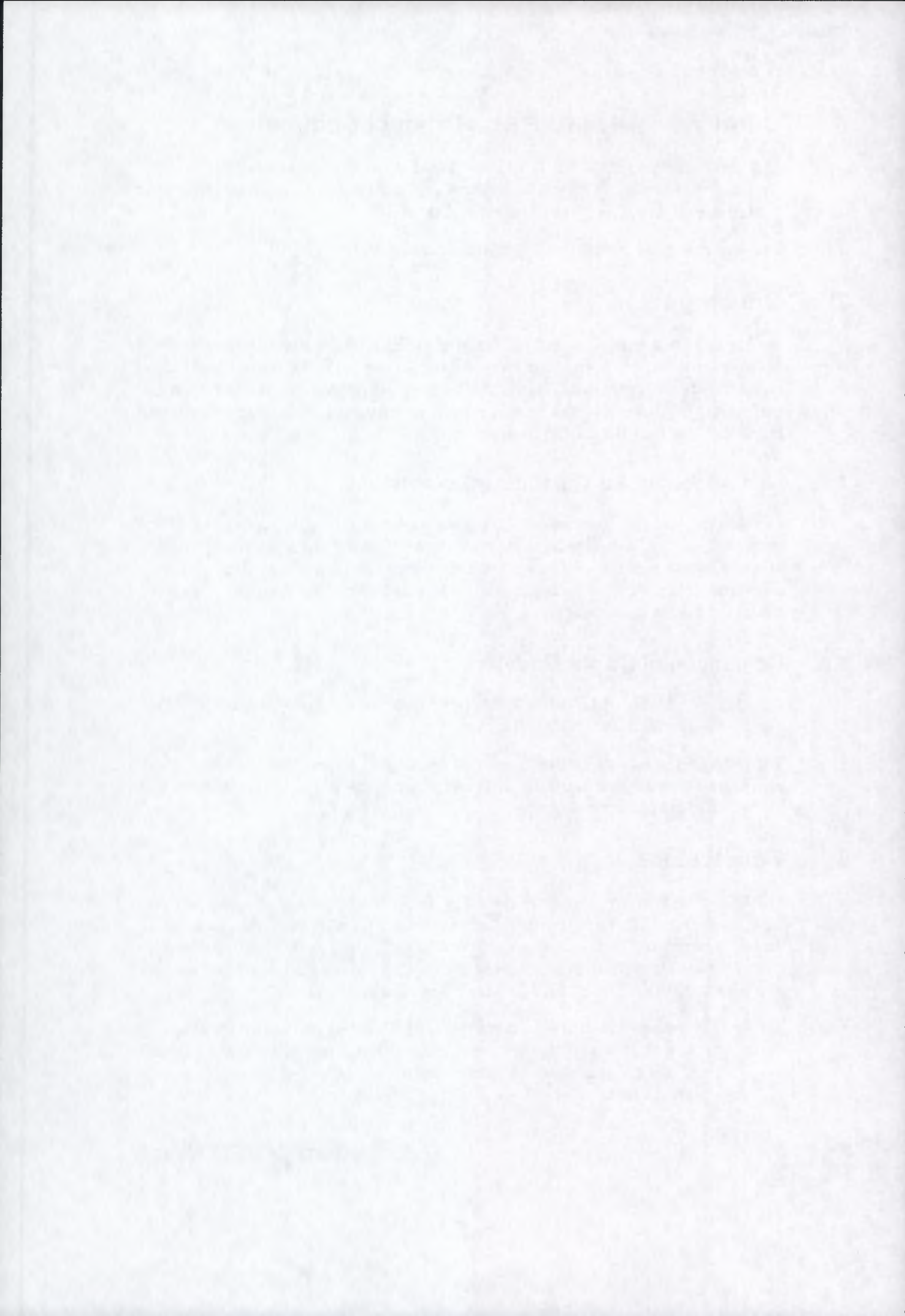
An adaptive notch filter is used to filter the flattened interferogram before phase unwrapping, and transformation to heights.

The low coherence obtained over vegetated areas limits the height accuracy obtainable from single-pair interferograms. The advantage of multiple baseline datasets will be studied to aid phase unwrapping.

## 8 Conclusions

The ERS-1 tandem mission vastly increases the store of potential spaceborne interferograms. Potential coverage is extended to the full ERS reception limits at unprecedentedly consistent high coherence. However, some land-cover types decorrelate within the one-day repeat; in these cases tandem data provides no significant qualitative advantage to the limited ERS-1 3-day repeat data available.

- For the generation of height models, the ERS geometry performs best in areas with only moderate slopes. Two-antenna interferometers (e.g. proposed third SIR-C mission) are favourable due to their lack of susceptibility to coherence loss.



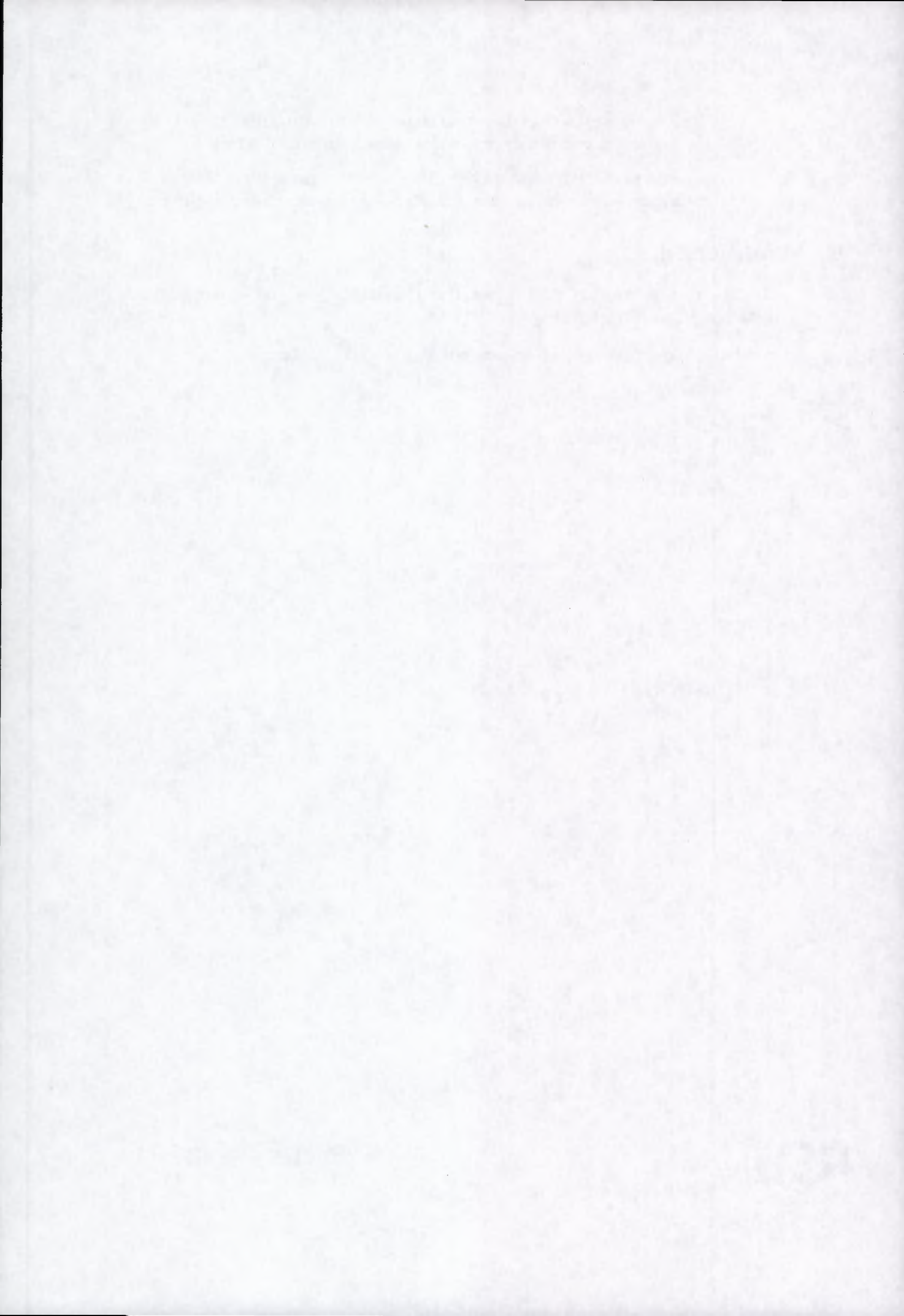
- The Doppler centroids of the two satellites were found to differ by some 300 Hz. The loss in coherence is removable through **azimuth filtering**.
- Anomalous azimuth sidelobes were discovered that can result in reduced coherence. We now believe this to be a coastal **raw data saturation** effect.

## 9 Authorship

This report was prepared by David Small, Paolo Pasquali, Oliver Stebler, Arnold Bar-mettler, and Daniel Nüesch of RSL.

In the case of questions, the authors may be contacted via e-mail at:

nuesch@geo.unizh.ch



# Annex L

## **Geographical area**

Vatnajokull ice cap, Iceland

## **Research institute**

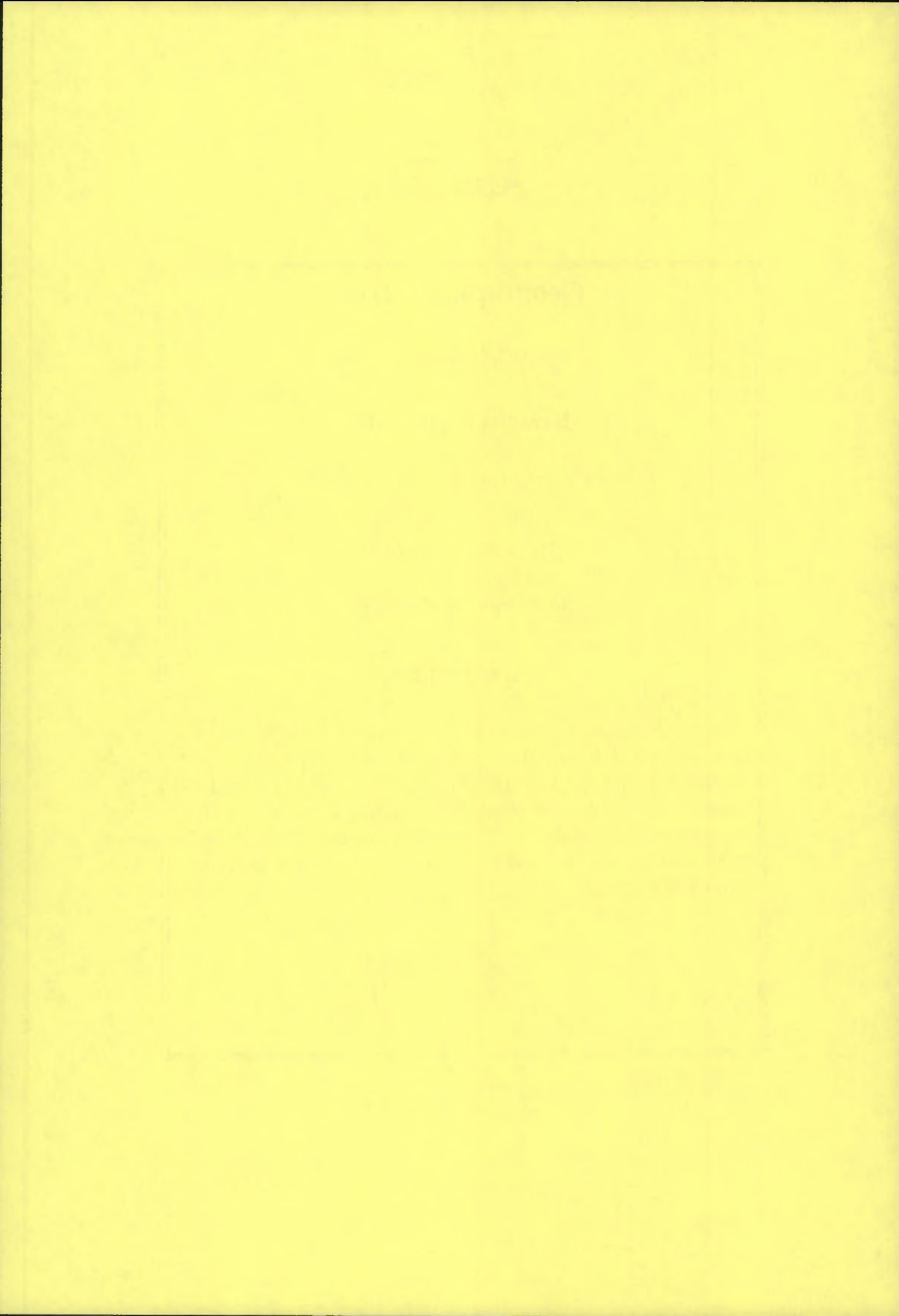
University College London, UK

## **Application domain**

Ice motion / glaciology

## **First results**

A considerable improvement in the coherence between tandem data and 35 data repeat data was observed. The data were acquired during the summer period so that even the tandem coherence was too low over ice covered regions, due to the occurrence of melting, to generate an interferogram. It was possible however, to generate fringes over non-ice areas for some tandem pairs.



## ERS-1/ERS-2 TANDEM INTERFEROMETRIC VALIDATION, VATNAJOKULL

Beverley Unwin, Dept. Space & Climate Physics, University College, London.  
Tel. 01483 274111  
Fax 01483 278312  
Elm bv@msl.ucl.ac.uk

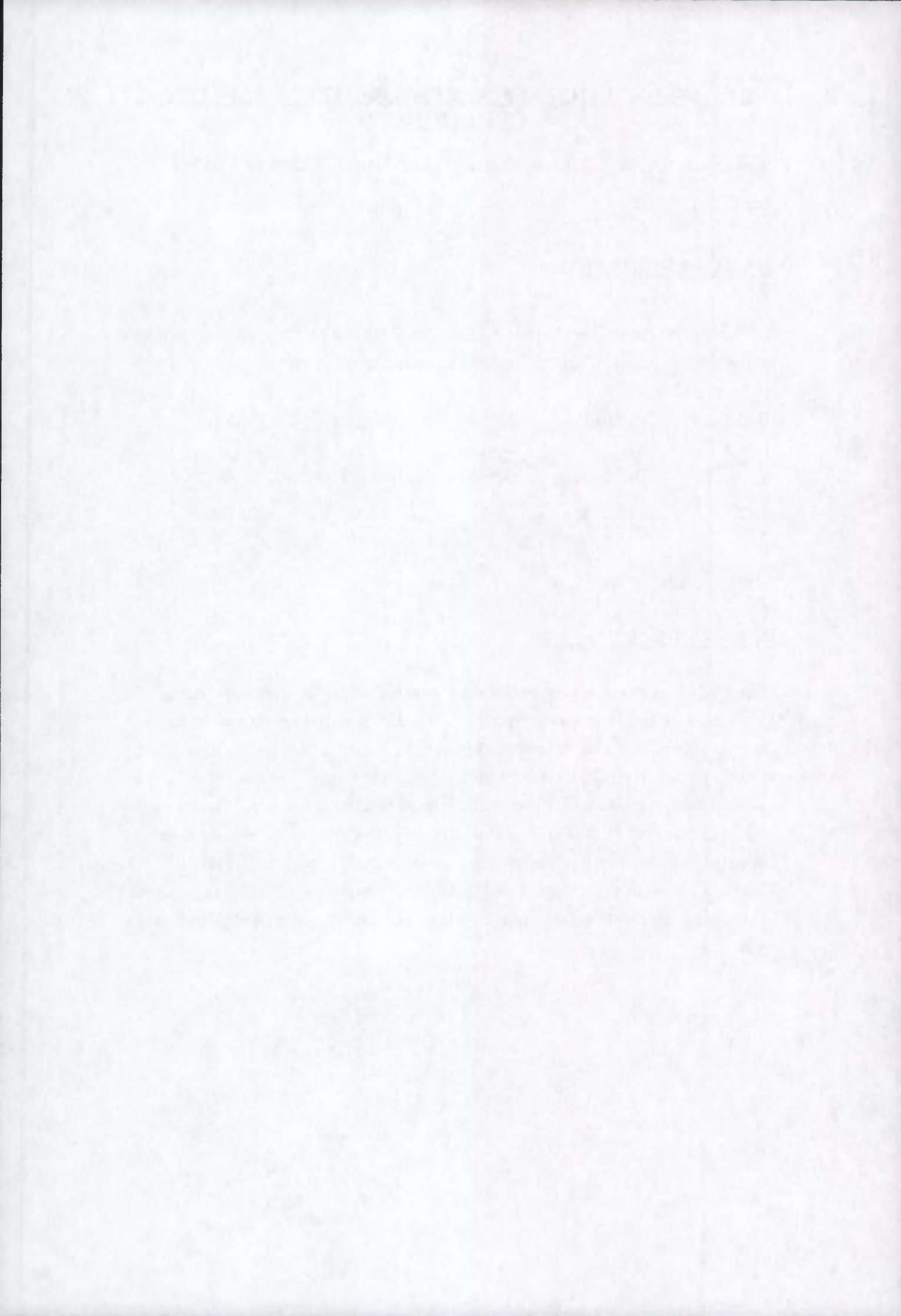
### DATA DESCRIPTION

The images received comprise two ERS-1/ERS-2 tandem pairs. They were acquired on descending passes. Their orbit and frame numbers are as follows :

<u>Ref. No.</u>	<u>Satellite</u>	<u>Orbit</u>	<u>Frame</u>	<u>Date</u>
1.	ERS-1	20266	2295	31 May 95
2.	ERS-2	00593	2295	01 Jun 95
3.	ERS-1	20767	2295	05 Jul 95
4.	ERS-2	01094	2295	06 Jul 95

### SCENE DESCRIPTION

Frame 2295 of the relevant orbits was acquired over the northern part of the Vatnajokull ice cap in Iceland. Figure 1 shows the amplitude component of image 3 (approx. 100km x100km). The darker, late azimuth portion is ice. The lighter, early azimuth portion represents volcanic rock. The highly ridged area in the north-east quadrant comprises basic and intermediate lavas of Pleistocene age. The smoother portion to the north-west of the image represents post-glacial lavas. The cone shaped feature in the centre of the top left quadrant is the Askja volcano (height 1053 m). There is a lake within its crater. The light coloured circular region in the upper centre of the image represents an inlier of Pleistocene rocks, entirely surrounded by younger lavas.



## COHERENCE IMAGES

Coherence images for the two tandem pairs are shown in Figure 2. The greyscale from black to white represents a coherence scale from 0 to 1. It can be seen that the coherence is very low over the ice. This is probably because the images were acquired in early summer when melting was occurring. The coherence over the outcropped rock is higher for the second tandem pair than it is for the first tandem pair. This may be due to a change in weather conditions.

Various features may be noted in the coherence image for the second tandem pair. The dark centre to the Askja volcano is the aforementioned lake. The dark feature to the east of the volcano is also a lake. The large river (Jökulsá á Fjöllum) that runs down the centre of the image to the northern edge of Vatnajökull may be clearly identified. The dark region around the volcano, and the two patches in the centre north, correspond to outcrops of hyaloclastite and pillow lava.

Coherence images for the two non-tandem pairs are shown in Figure 3. They are significantly darker than those of the tandem pairs, due to their 35-day repeat.

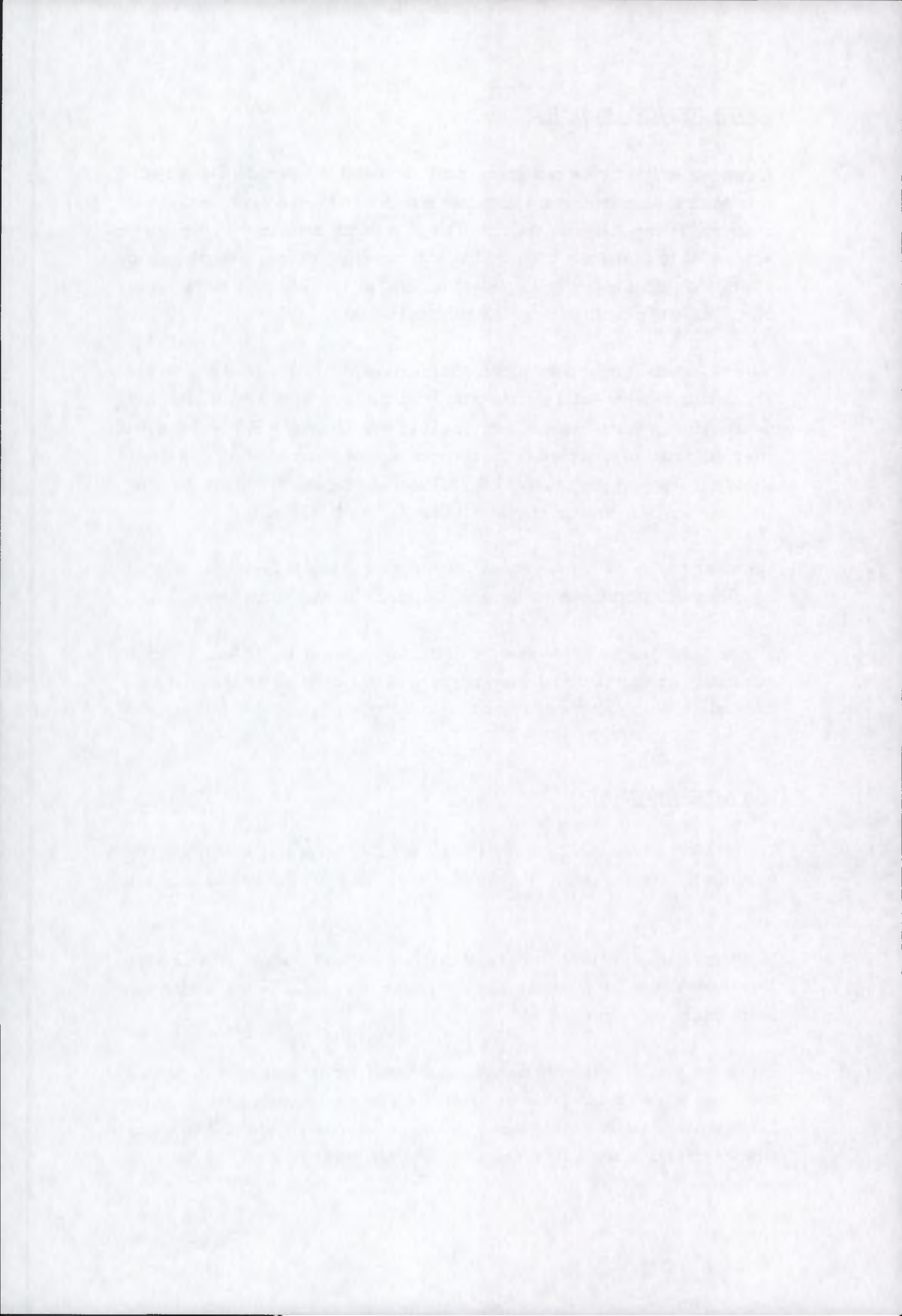
The coherence images are corrupted by dark, perpendicular lines. This feature is particularly apparent in the relatively bright coherence image of the second tandem pair, and presumably represents a processing problem.

## INTERFEROGRAMS

The baselines for the two tandem pairs (1/2 and 3/4) are of length 46m and 17m respectively. The baselines for the two non-tandem pairs (1/3 and 2/4) are 262m and 203m.

No fringes could be obtained over the Vatnajökull ice cap for any of the four pairs. This is due to the low coherence which is presumably caused by the melting that occurred between acquisitions.

The tandem pair 3/4, which had the highest coherence over the non-ice areas, was the only image pair for which extensive fringes could be obtained. Figure 4 shows the fringes formed from the northern half of the two early-azimuth image quadrants. The area represented is about 100km x 50km. No deramping or averaging has been



performed. It can be clearly seen that there is a sharp discontinuity in the spacing and orientation of the fringes at the join between quadrants. This is presumably a processing problem. None of the other three pairs produced sufficient fringes to allow a repeat of this phenomenon. Only very small fringe patches could be recovered from these remaining pairs, mainly in the central region at the top of the scene that appeared relatively bright on the coherence images.

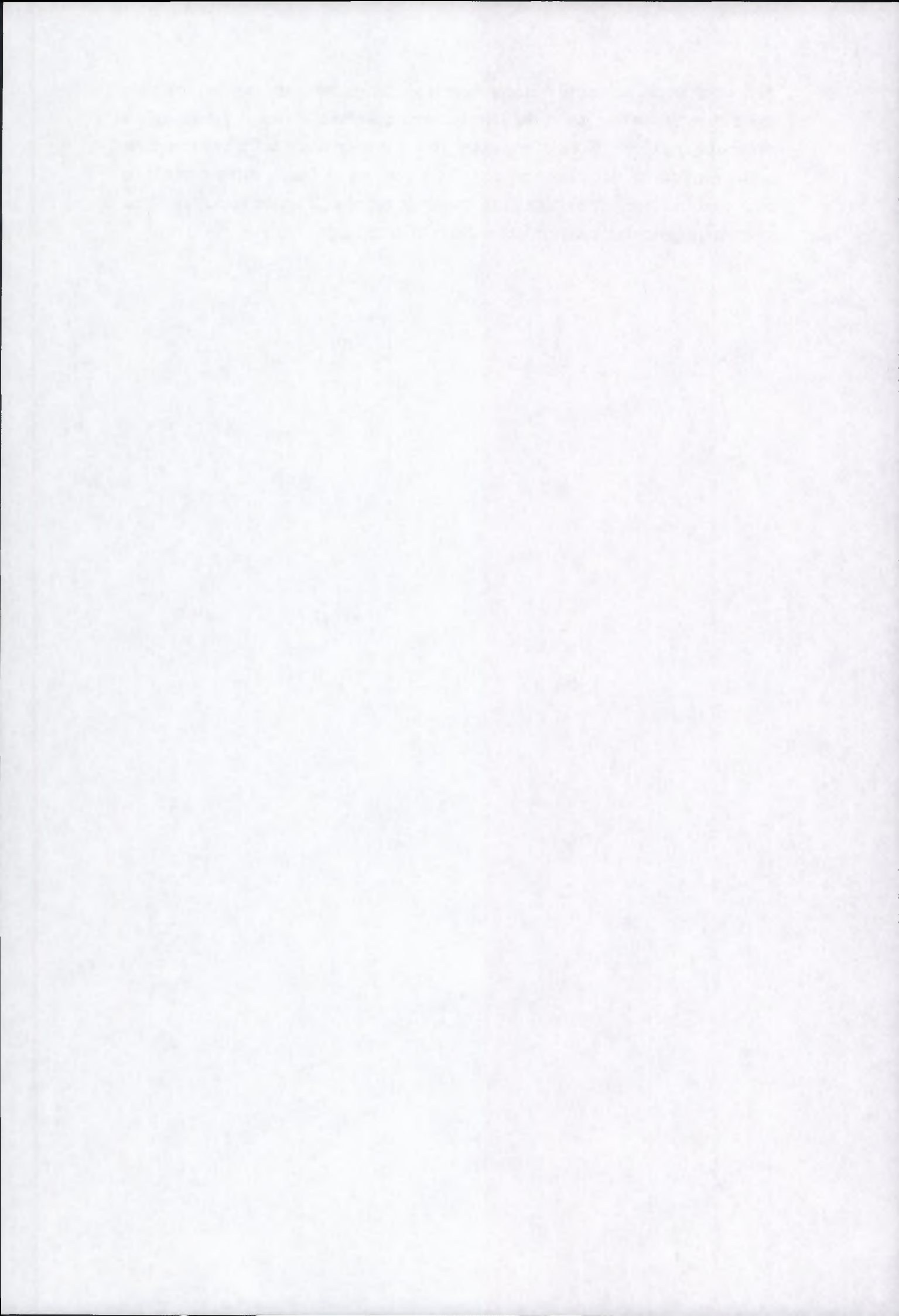


**Fig 1. ERS-1 SAR AMPLITUDE IMAGE  
ORBIT 20767, FRAME 2295  
DATE : 5 JULY 1995**



Dept. Space & Climate Physics

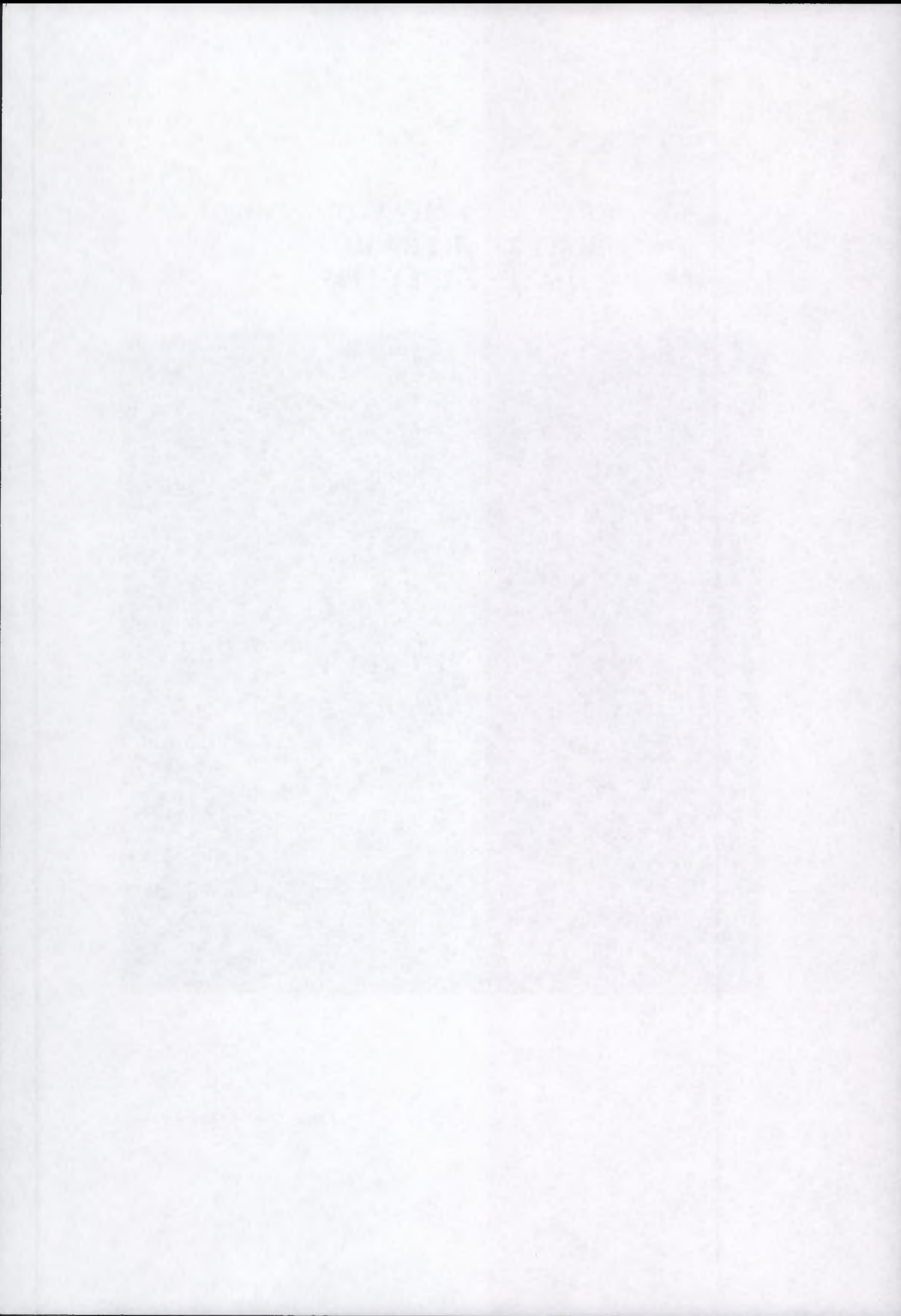


## Fig 2. TANDEM CORRELATION IMAGES



ERS-1 Orbit 20266, 31 May  
ERS-2 Orbit 00593, 01 June



ERS-1 Orbit 20767, 05 July  
ERS-2 Orbit 01094, 06 July



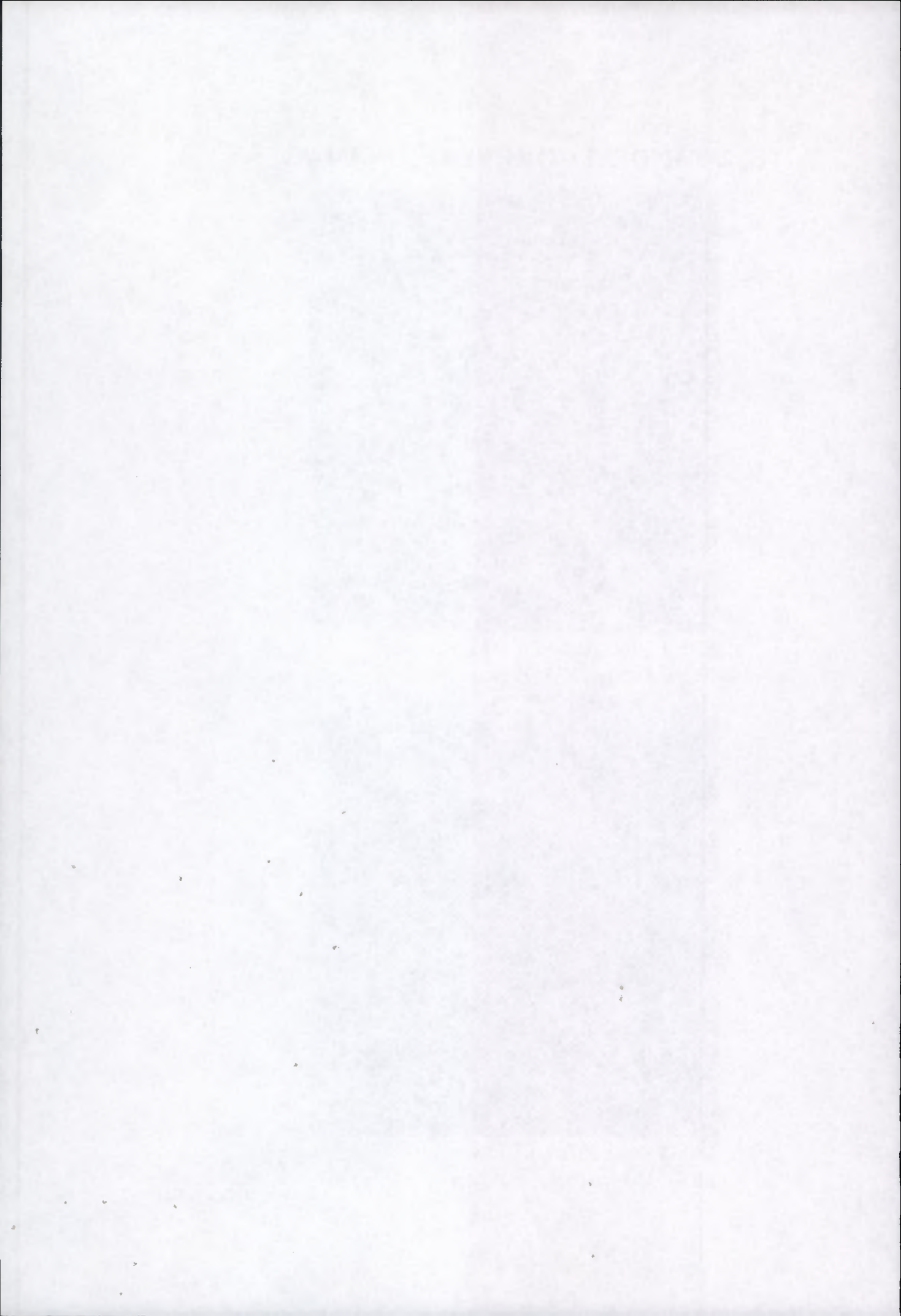


**Fig 3. NON-TANDEM CORRELATION IMAGES**

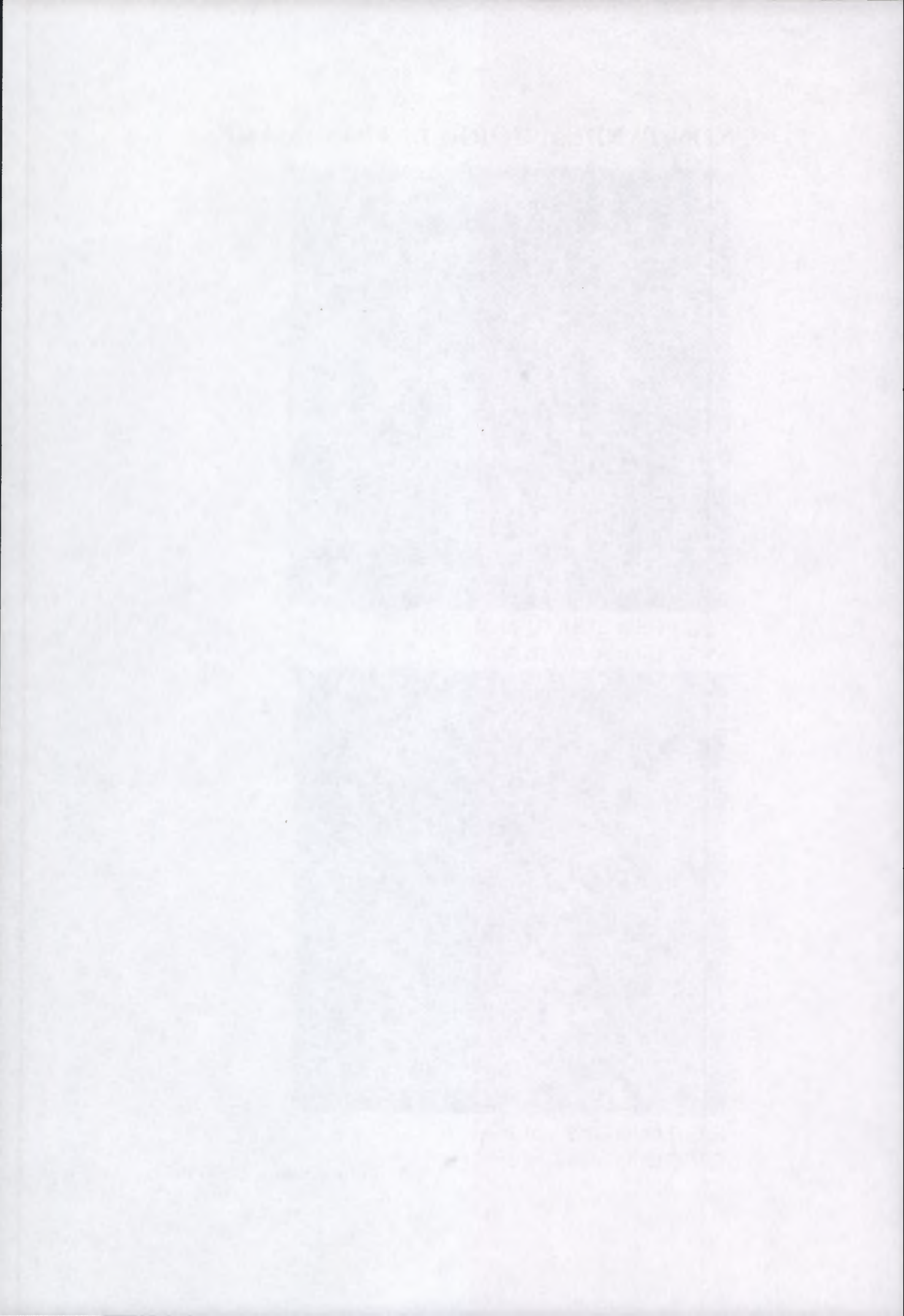


ERS-1 Orbit 20266, 31 May  
ERS-1 Orbit 20767, 05 July

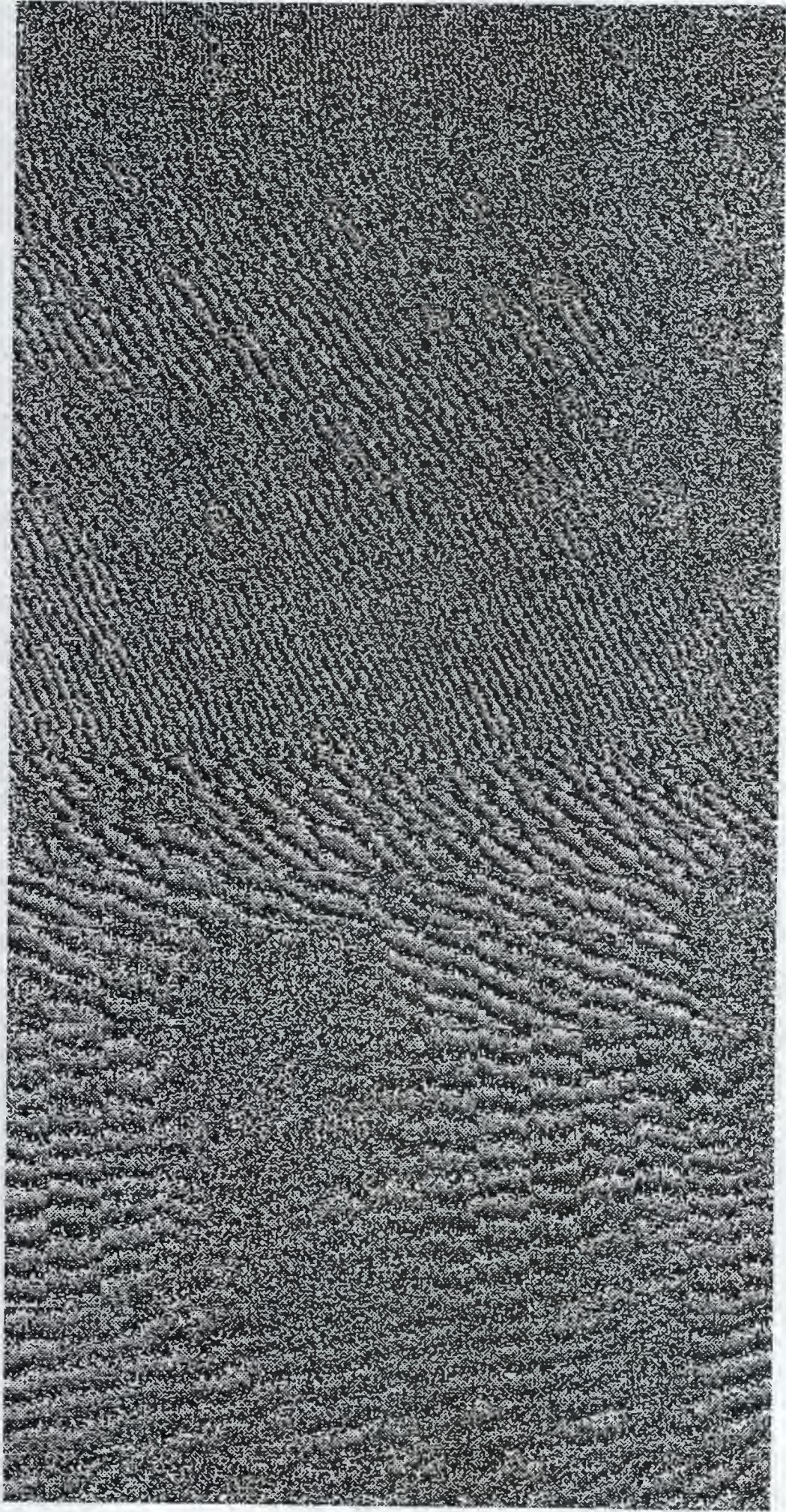


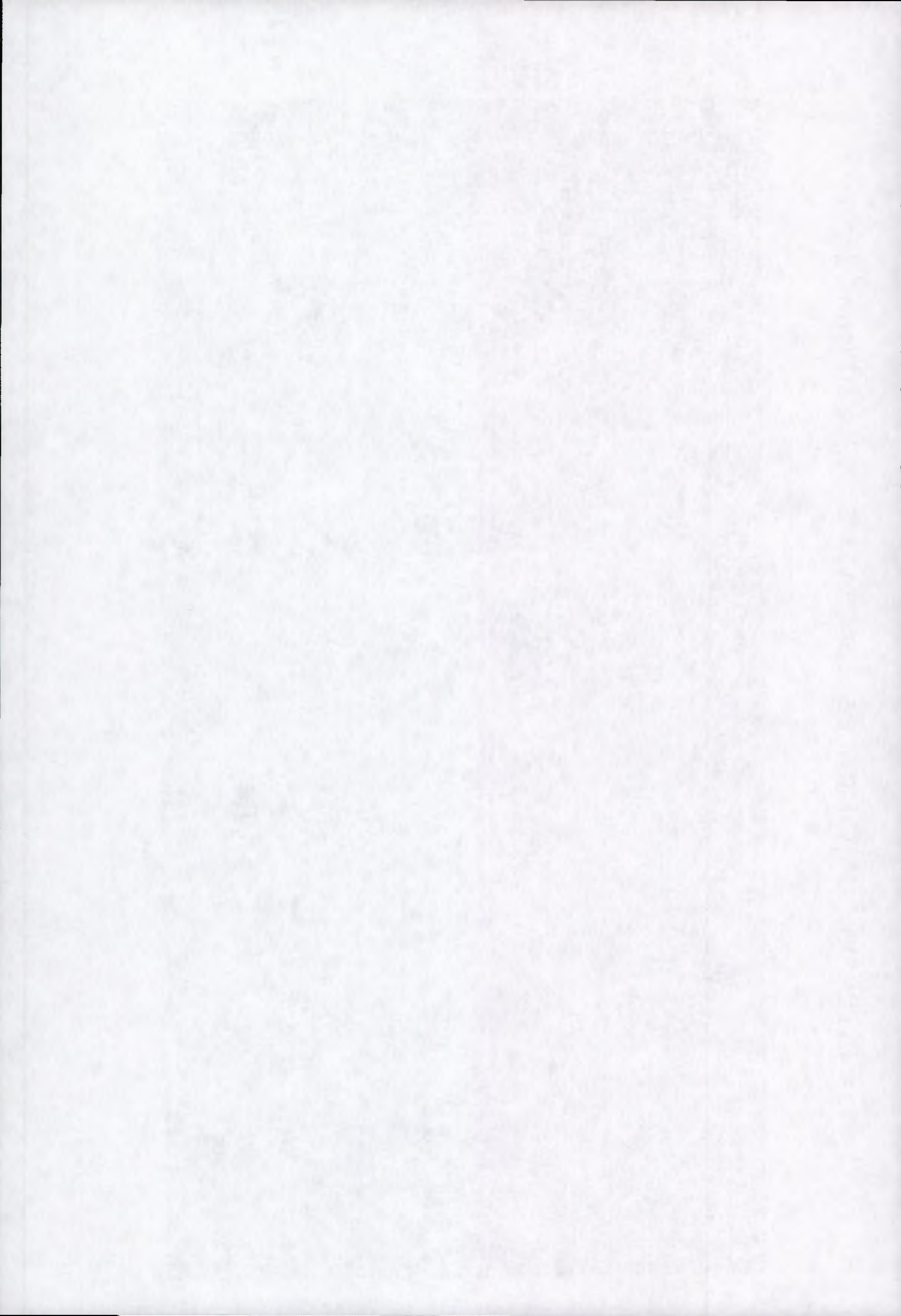
ERS-2 Orbit 00593, 01 June  
ERS-2 Orbit 01094, 06 July





**Fig 4. INTERFEROGRAM FOR PAIR 3/4, EARLY AZIMUTH QUADRANTS.**





# Annex M

## **Geographical area**

Bern, Switzerland

## **Research institute**

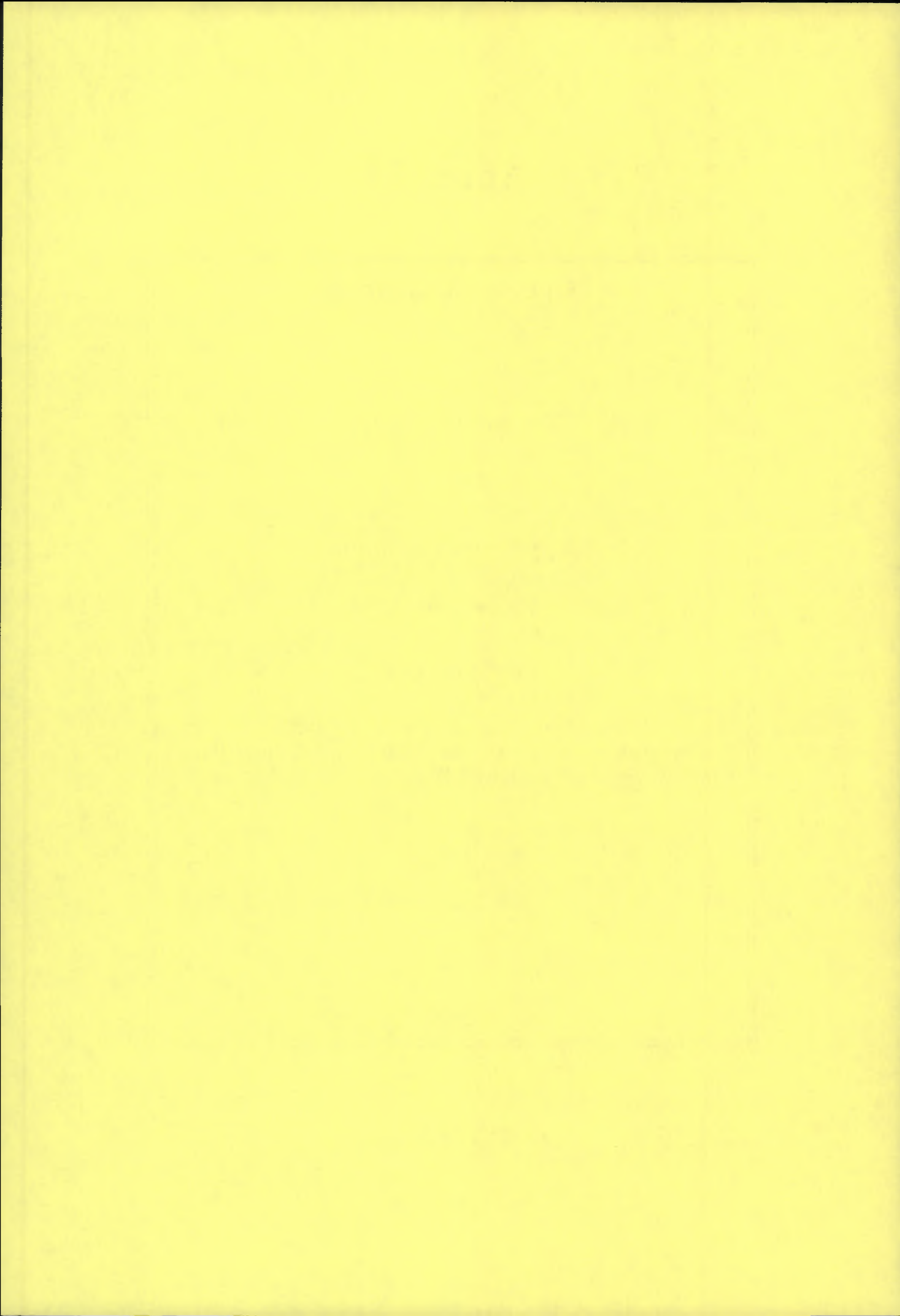
ESTEC

## **Application domain**

Digital Elevation Models

## **First results**

ERS Tandem Interferogram + Flat Earth removed  
Interferogram + Coherence Image + Un-Wrapped Phase Image  
combined with SAR Intensity + DEM.



the returned signal varies differently for each image from near to far range. This results in a beat frequency (a function of the baseline) which is clearly visible in the interferogram as a series of lines of constant phase running more or less parallel to the azimuth direction. By estimating this frequency, it can be eliminated leaving only phase difference information which is related to the height of the observed point on the ground. This process is termed "flat earth" removal as it involves removing the signal that would be present even if the scene were flat.

The same interferogram with "flat earth" removed is shown below:

[Image]

Interferogram of Bern Scene with "Flat Earth" Removed

### Slope Adaptive Filtering

The next step is to perform some filtering. This is necessary to reduce the amount of phase noise which is always present in SAR images. However, if a uniform filter mask is used across the image, it is likely that valuable information will be lost on steep slopes. It is for this reason that the filter mask size is adapted depending on the slope. The slope can be determined by looking at the rate of change of phase. The filtered interferogram is shown here:

[Image]

Filtered Interferogram

### Coherence

In the interferograms shown above there were areas which are devoid of fringes such as the Thunersee. This is because the returned signals are not coherent from water since it is constantly moving. Forested areas also have low coherence as do areas of radar overlay. The coherence can therefore be a very useful parameter in the process of phase unwrapping and so a map of the coherence is generated:

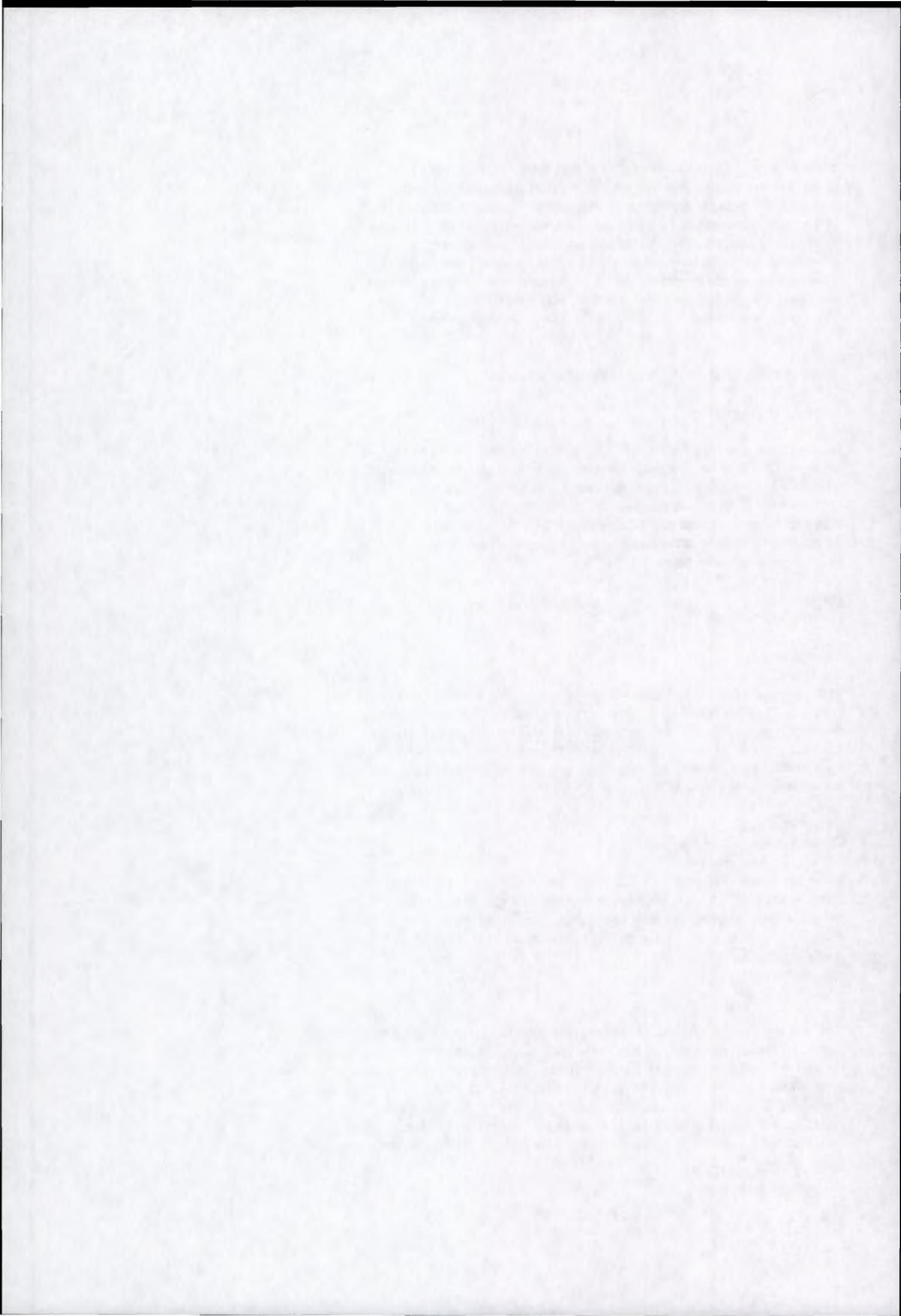
[Image]

Coherence Image of Bern Scene

In the coherence image the local coherence from 0 to 1 is represented by a colour scale of light blue to bright yellow. Areas of high coherence such as built up areas appear orange/yellow such as Bern in the centre. The intensity image has been used to modify the brightness which is why the lake appears black.

### Phase Unwrapping

The next step is to unwrap the filtered phase image. This is done by adding  $2\pi$  to the phase every time a fringe line is crossed. A fringe line is defined to be the point at which the phase jumps from  $+\pi$  to  $-\pi$ . In areas of very low coherence (such as the lake) it is not possible to see any fringe lines and so this area cannot be unwrapped directly although it can be assumed that it is flat so the phase at the edge should always be the same. Other areas of low coherence cause greater problems such as mountain



## ERS-1/2 Tandem Interferometry

### Digital Elevation Model Generation

Two scenes over Bern (CH) were used to prove the technique of SAR Interferometry for Digital Elevation Model (DEM) Generation during the SAR commissioning phase of ERS-2 carried out in the Microwave Instrumentation section (XRI) of ESTEC.

The two scenes used are the first quadrant of the ERS-1 image from 9 July 1995 and the equivalent from ERS-2 from 10 July 1996. A 20-look (2 in range and 10 in azimuth) image of each is shown below:

[Image]

ERS-1 Intensity image - 9 July 1996

[Image]

ERS-2 Intensity image - 10 July 1996

Bern is quite easily visible as the high backscatter area in the centre of the image with the double bow in the river flowing through it. The large lake in the bottom right of the image is the Thunersee with the town of Thun situated at the top of the lake.

[Image]

### Image Registration

The first step to producing a DEM of the scene is to register the two images to one another. In this case, the ERS-1 image was taken as the reference. By visual location of similar features in each image an estimation of the pixel offset in range and azimuth could be made. Using this rough offset it is then possible by calculation of the local coherence to come up with much more accurate points of reference. First a matrix of these points is generated (24 in range x 32 in azimuth) and from this a transformation matrix is created. The ERS-2 image is then resampled according to the transformation matrix to produce the registered image.

### Interferogram Generation

Once the images have been registered, it is possible to produce the phase difference image or interferogram. This is done by multiplying the complex pixel values of the ERS-1 image by the complex conjugate pixel values of the registered ERS-2 image.

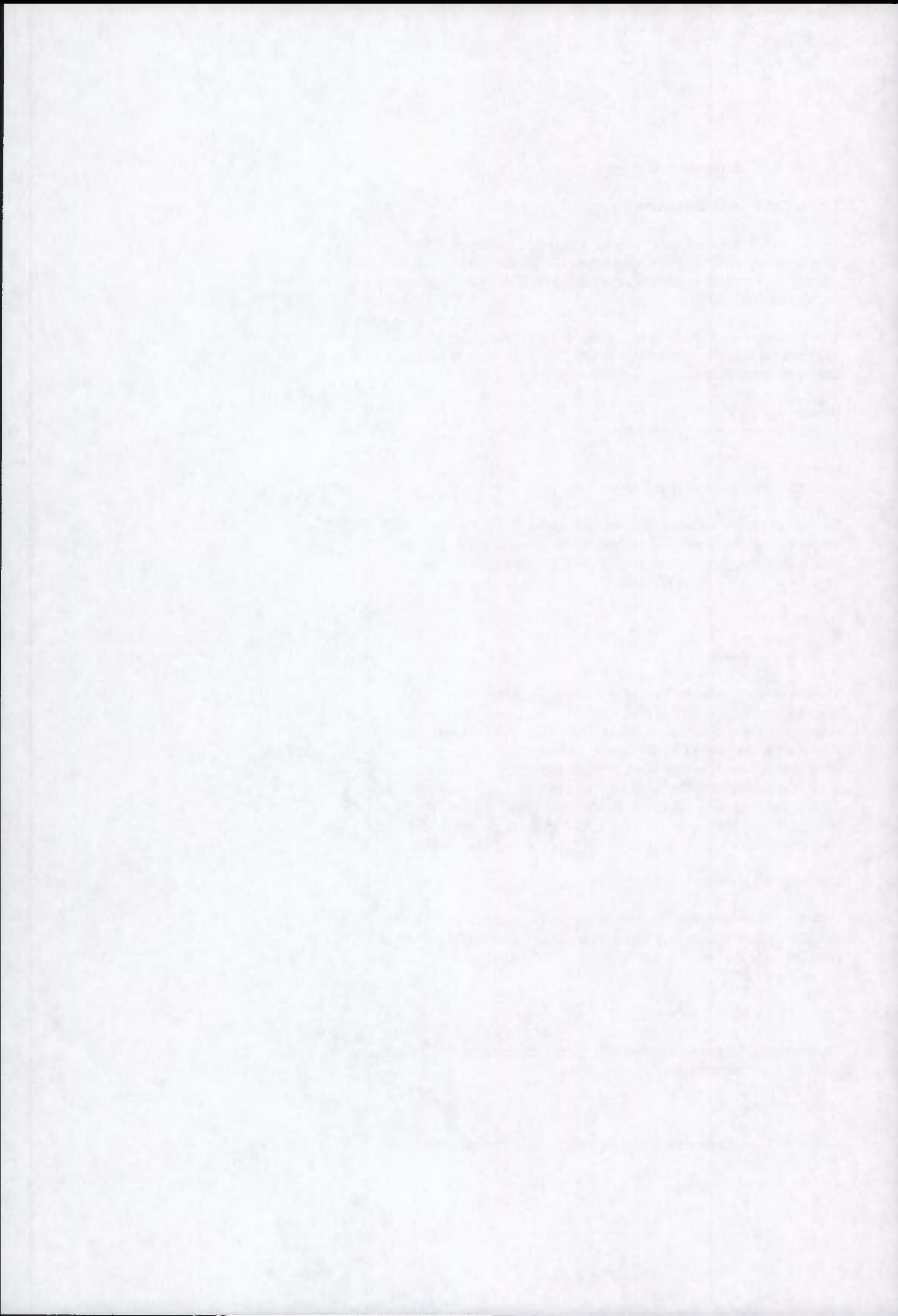
[Image]

Interferogram of the Bern scene

The interferogram shows the phase difference between the two images from  $-\pi$  to  $+\pi$  represented as a change in colour.

### "Flat Earth" Removal

Due to the baseline separating the two instruments in space, the phase of



slopes facing the radar. Here overlay occurs and it is possible that several fringe lines run together so that more than  $2\pi$  must be added to the phase when crossing these regions. Areas where fringe lines run together can be detected by locating the so-called Goldstein residues (four adjacent pixels whose sum is greater than  $2\pi$  or less than  $-2\pi$ ). By linking up the positive and the negative residues a cut mask can be created, the idea being that the phase unwrapping process does not cross these lines. The coherence map can be used here to guide the route between residues which the cut mask should make. This results in the unwrapped phase difference image:

[Image]

Unwrapped Phase Image (colour) + Intensity

Phase to Height

From this point it is a matter of geometry to convert the phases into heights. This can be determined from the baseline but in order to get a good estimate of the baseline some ground control points are needed. These were taken as a very rough estimate from an atlas using the tops of mountains (very poor choice but nothing else was available). The three points were Gurten (857m), Bantiger (947m) and Belp (895m).

[Image]

The (slant) height image then looks like this:

[Image]

Slant Height Image - Colour: Height 1 cycle = 200m - Brightness: Intensity

Geolocation

Using these slant range heights, it is now possible to construct a geolocated image of the scene. This means that "holes" will open up due to radar shadowing. Other black areas indicate lakes, rivers etc.

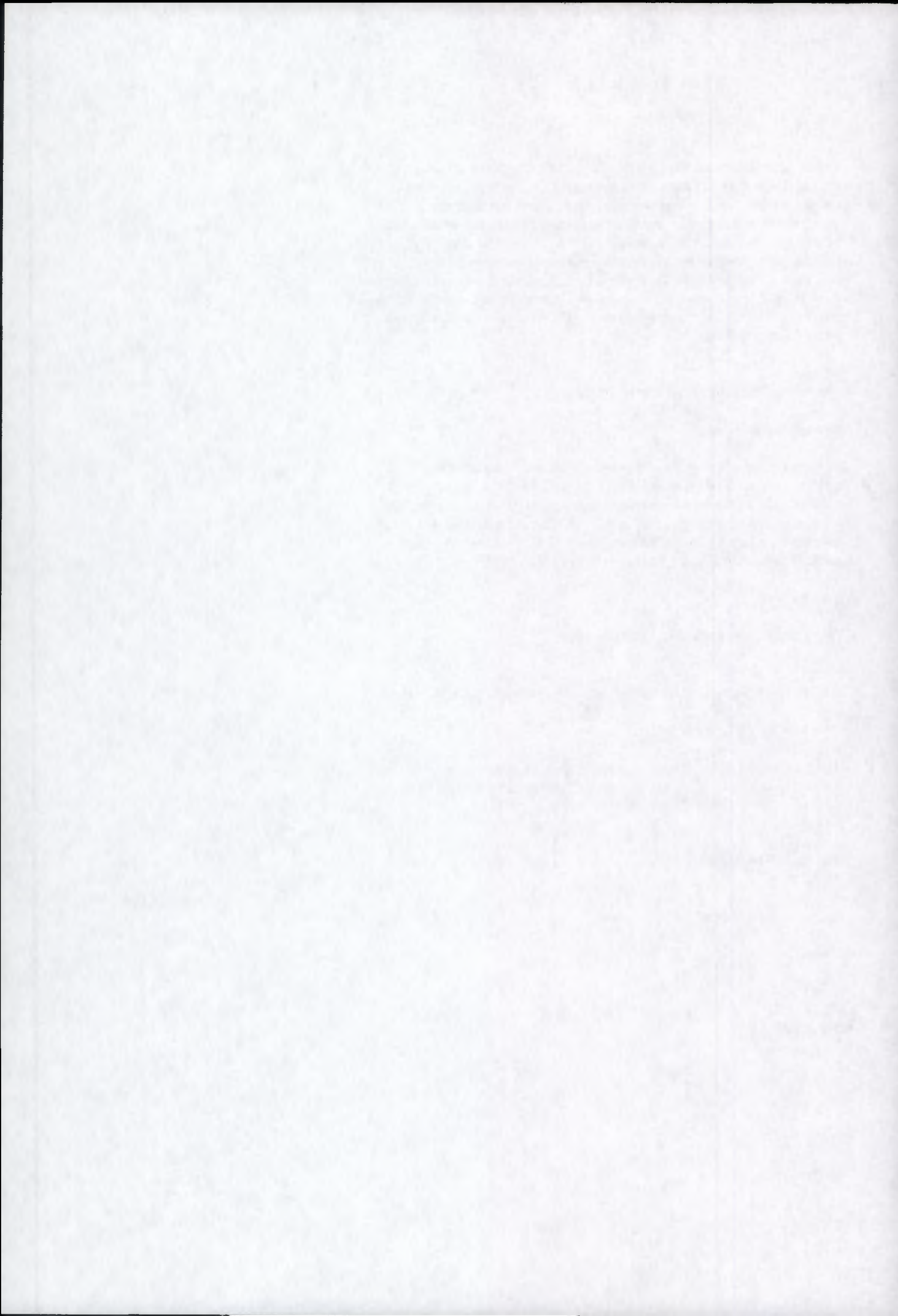
[Image]

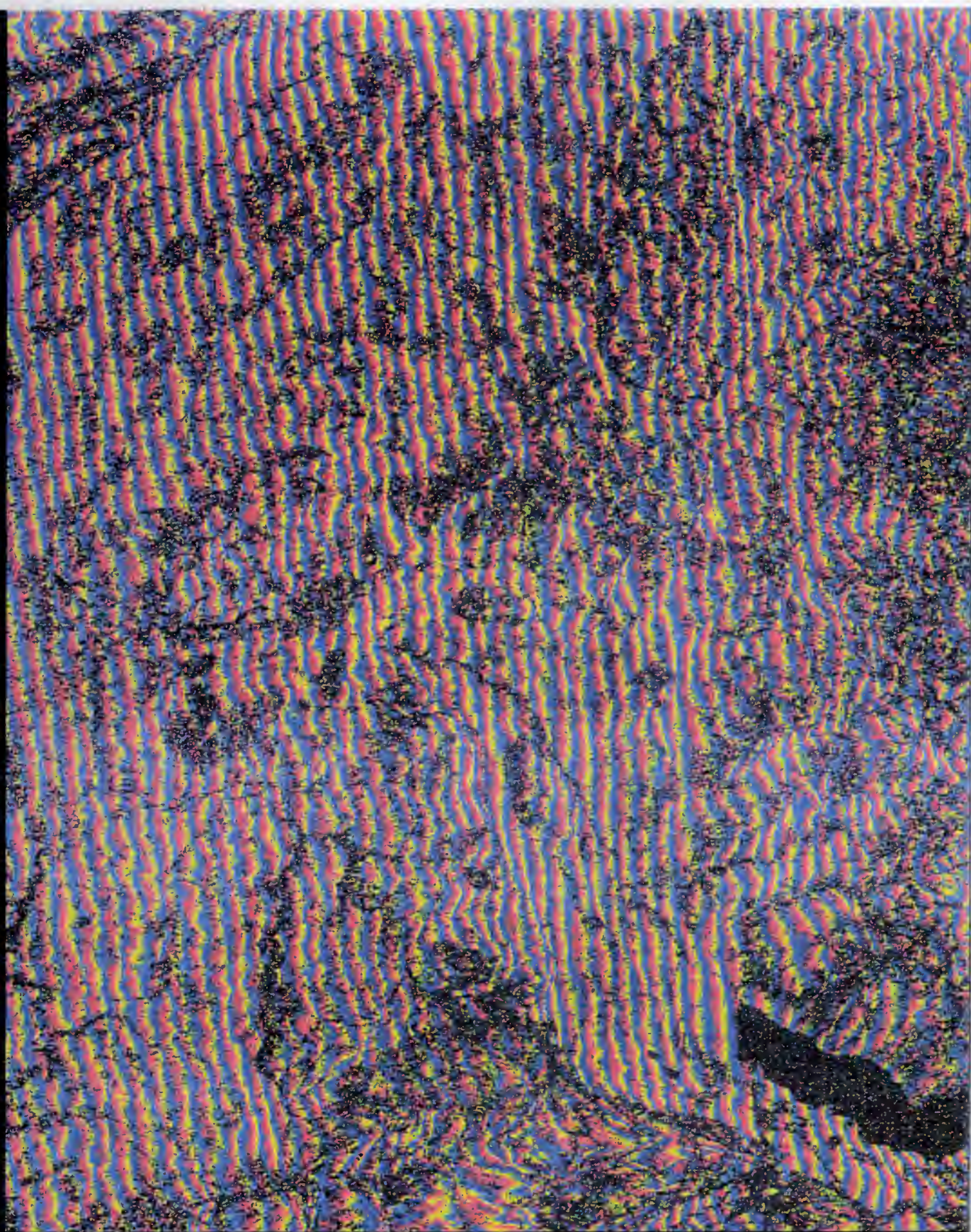
Geolocated Height Image - Colour: Height, 1 Cycle = 200m - Brightness: Intensity

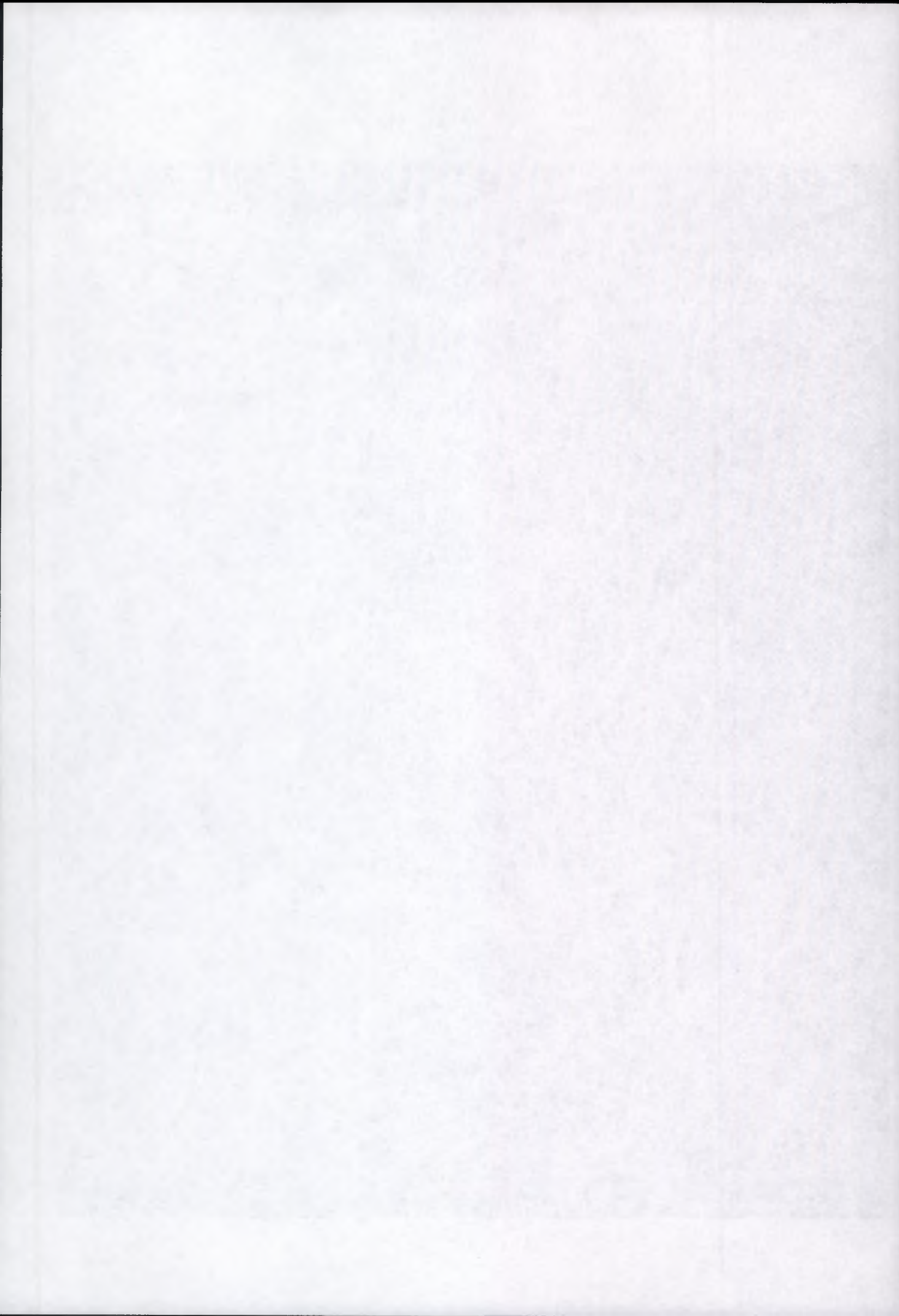
3D Projection of Scene

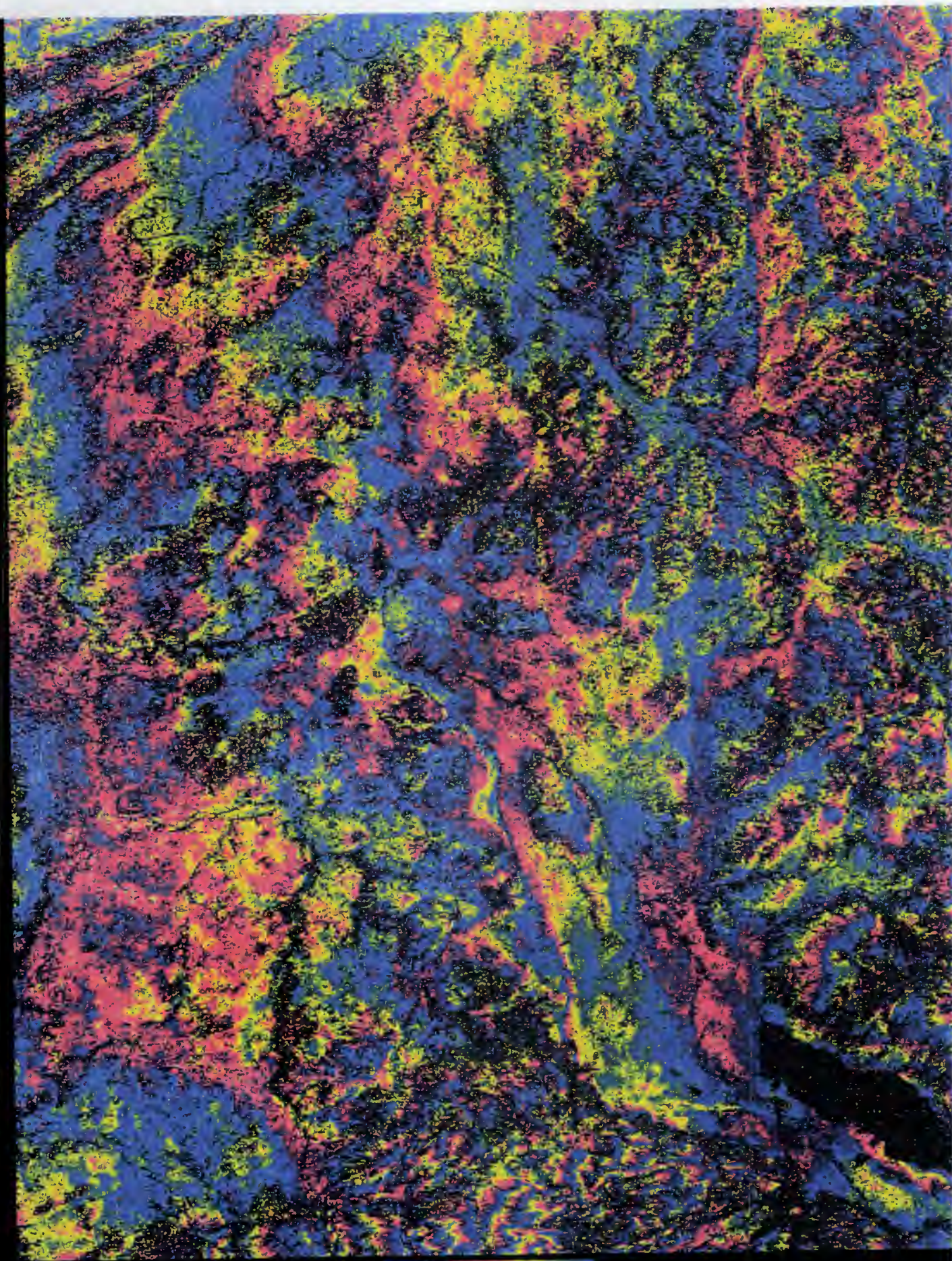
[Image]

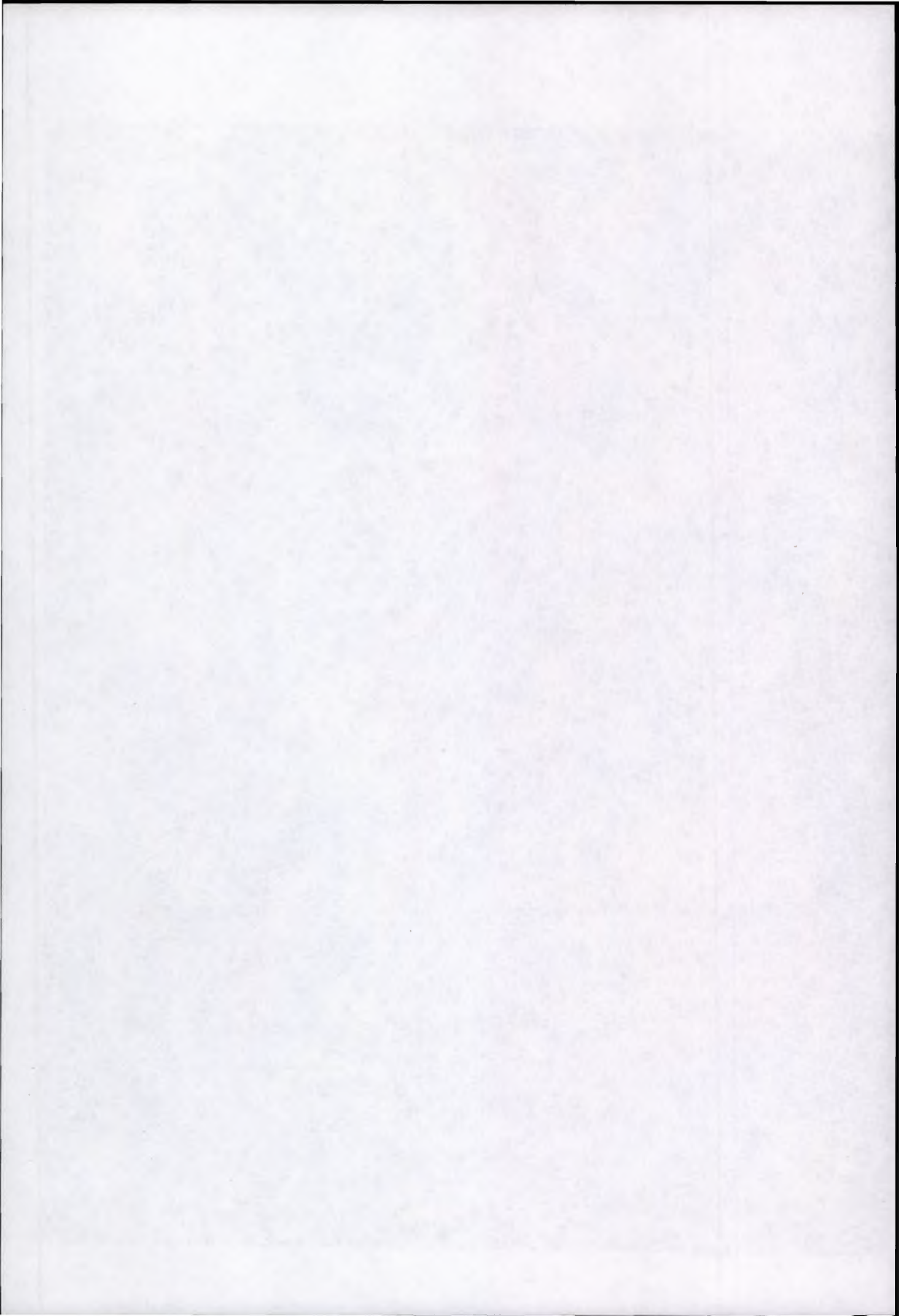
Chris Buck  
ESTEC XRI  
cbuck@iee.org

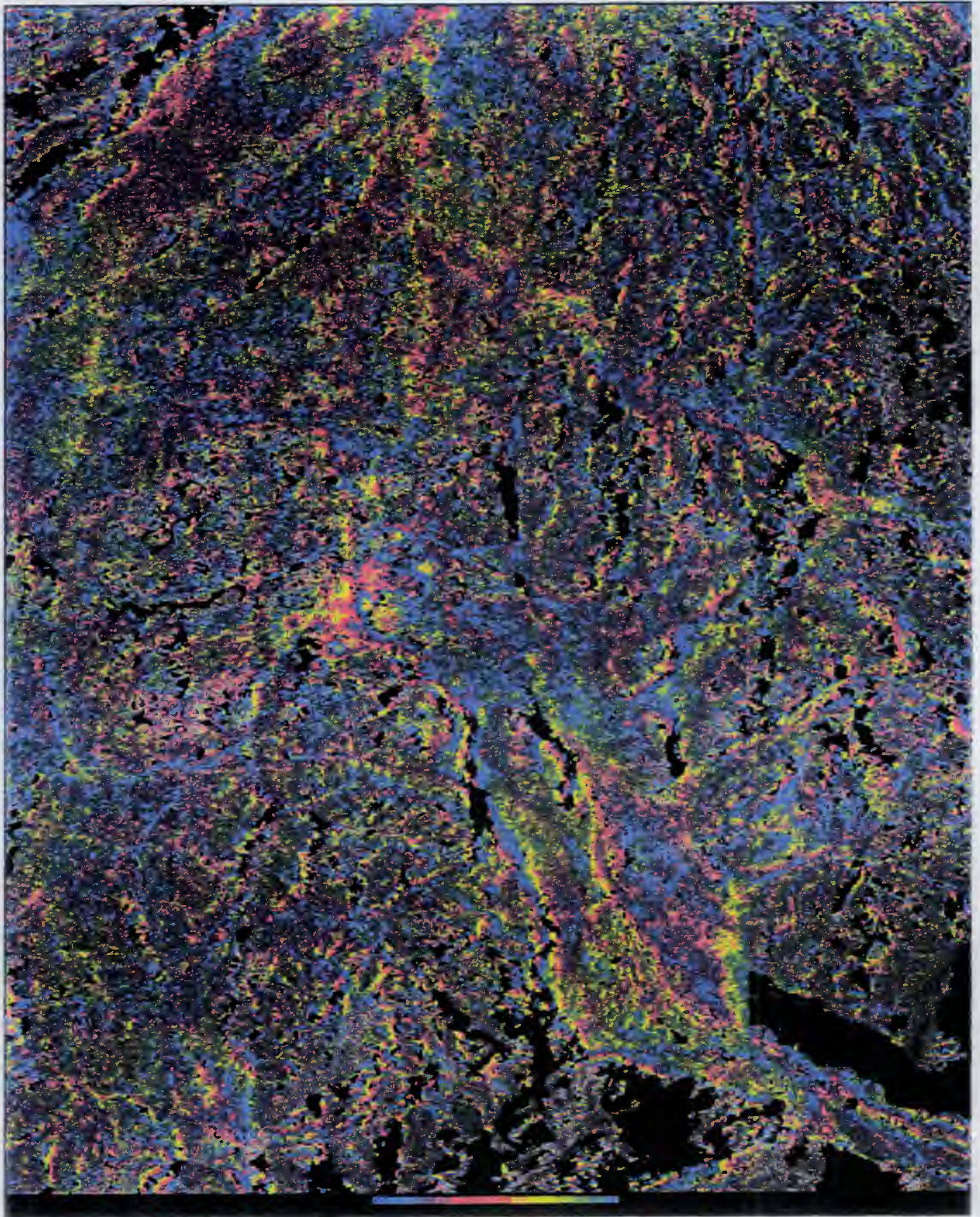


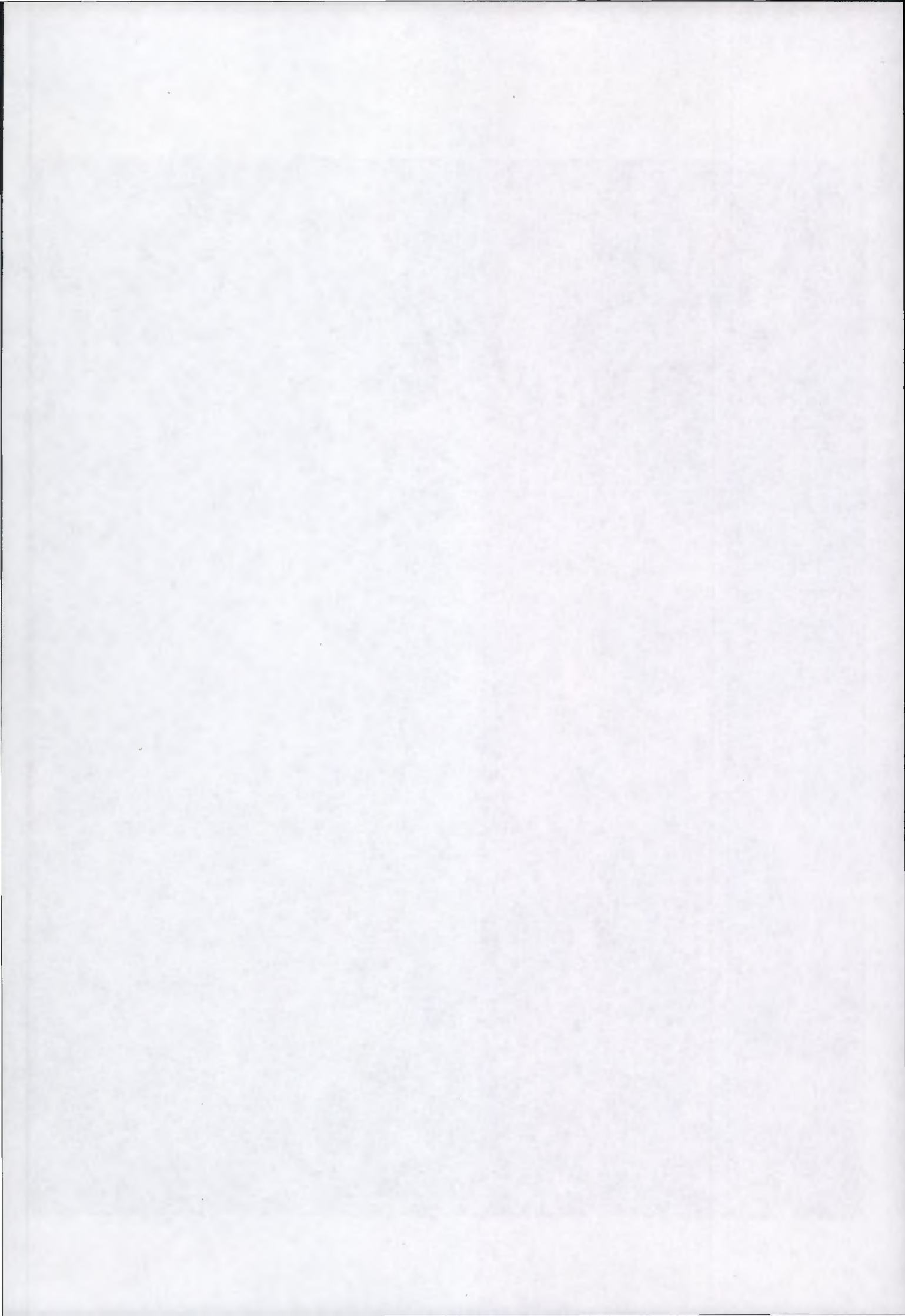


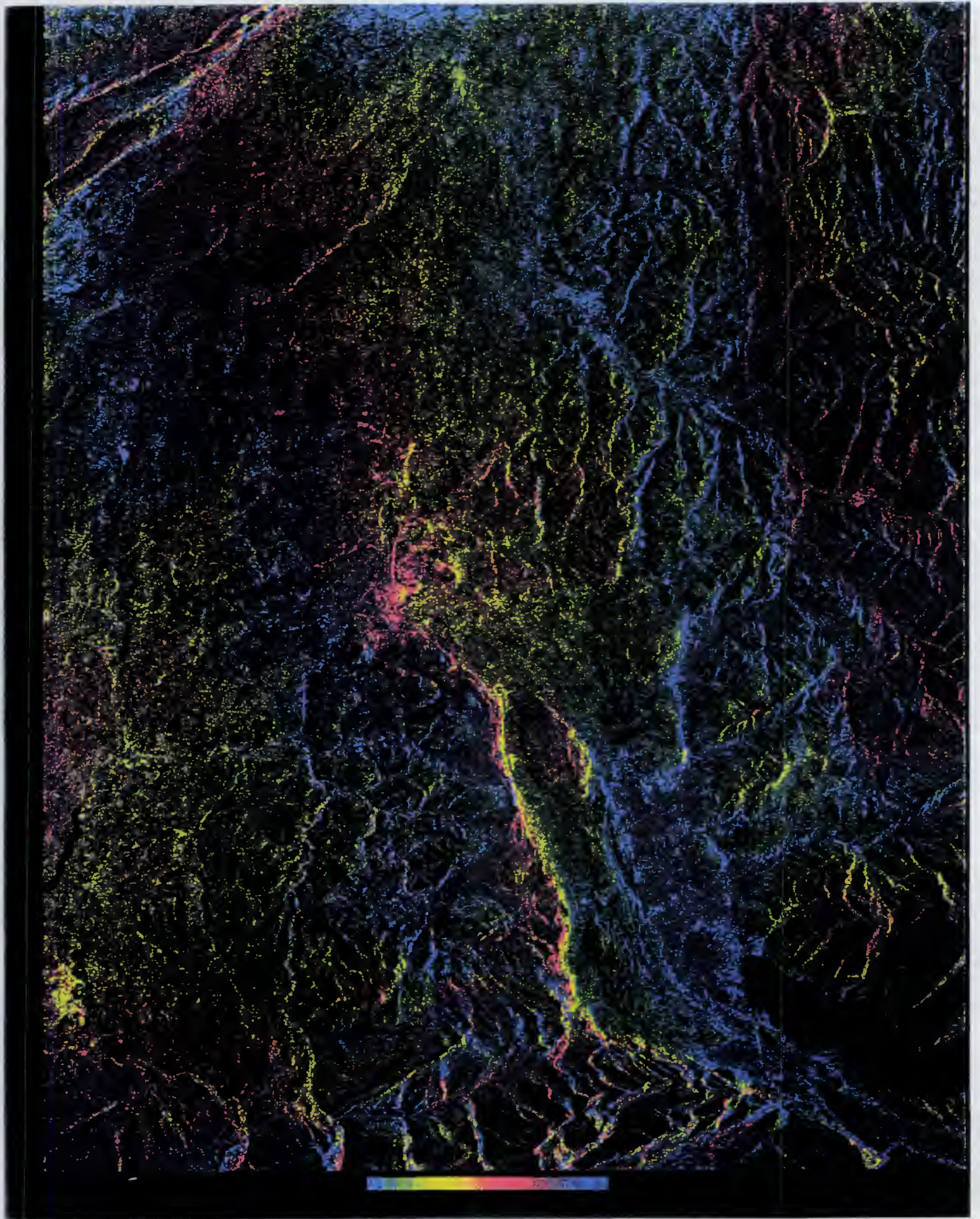


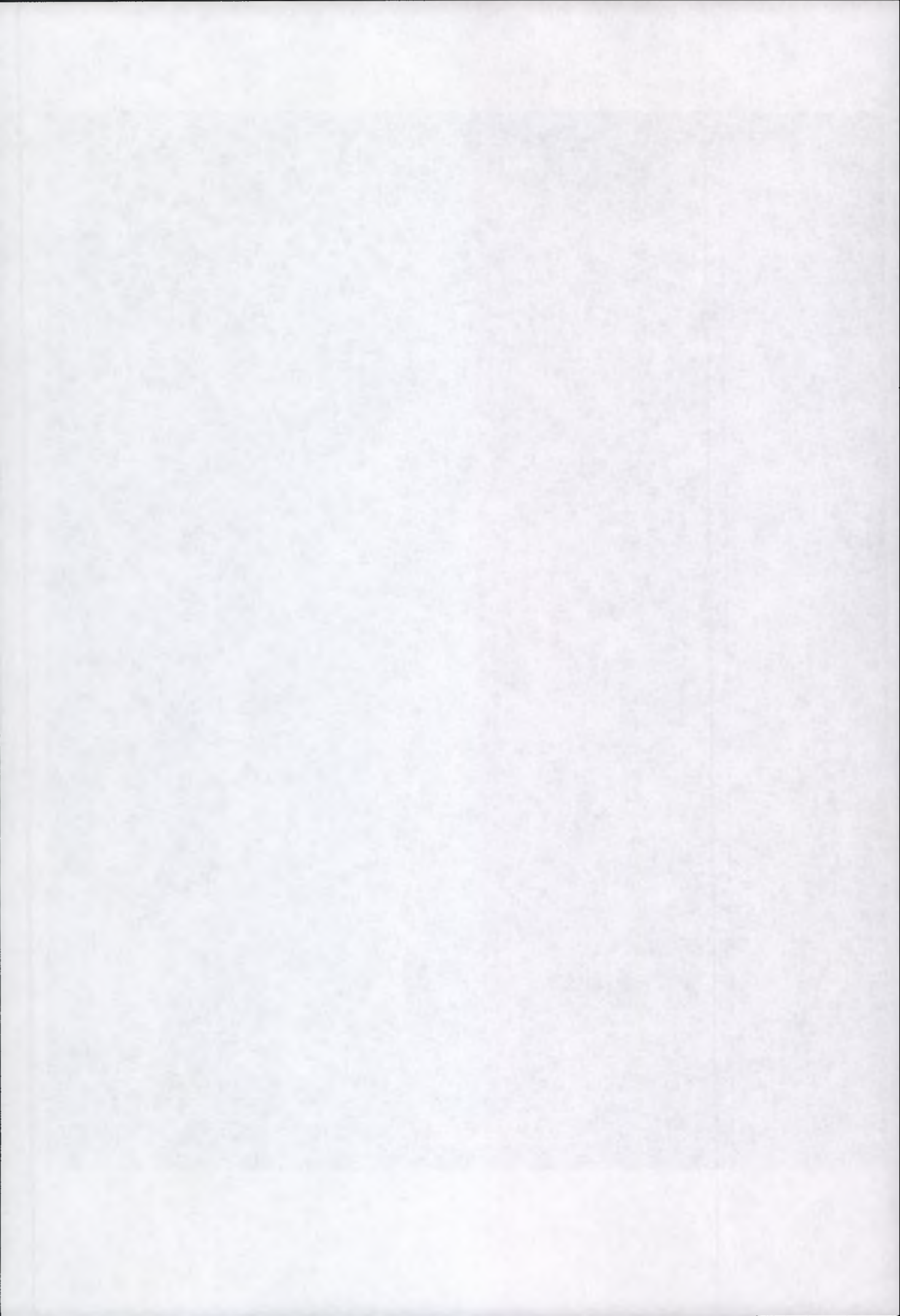


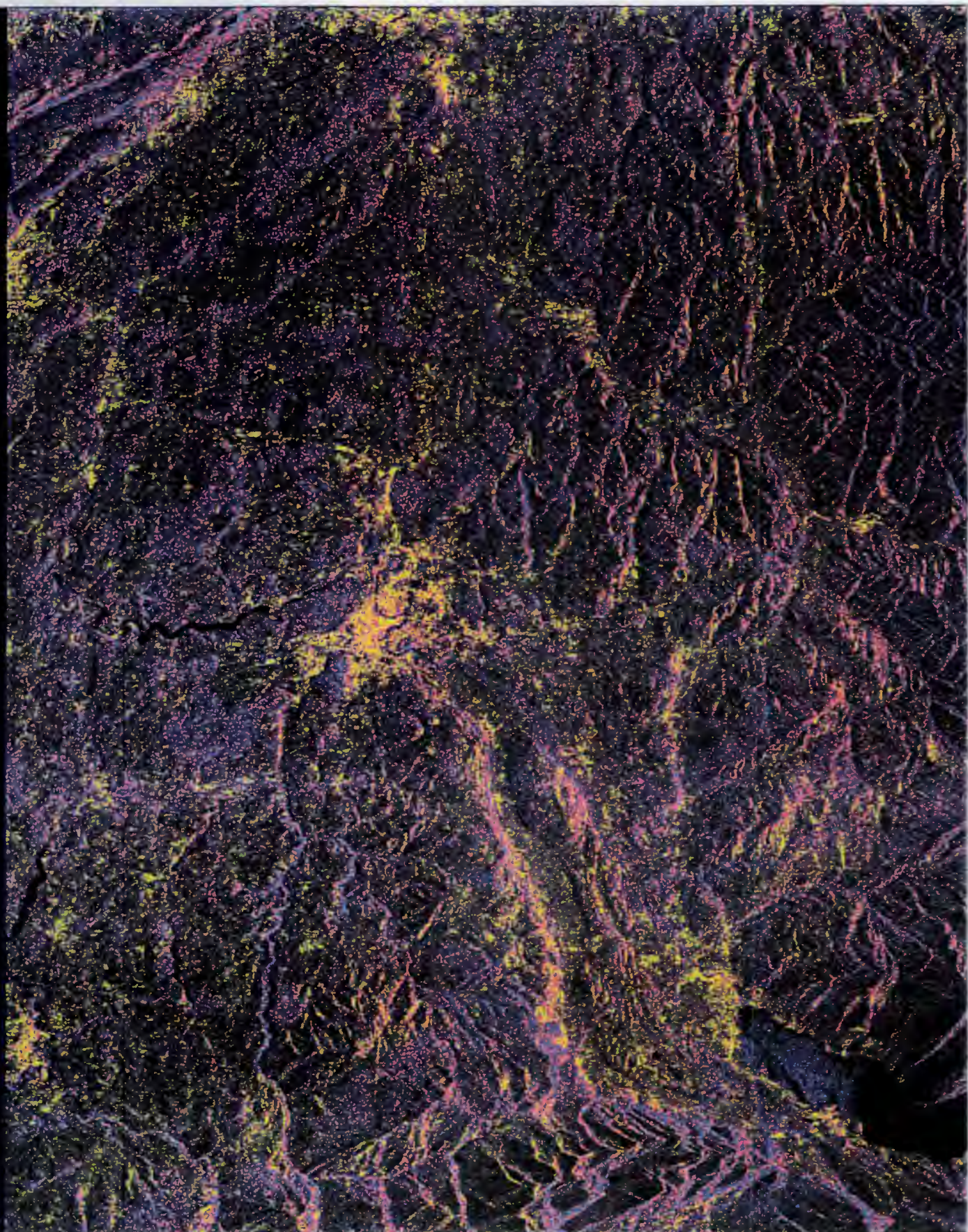


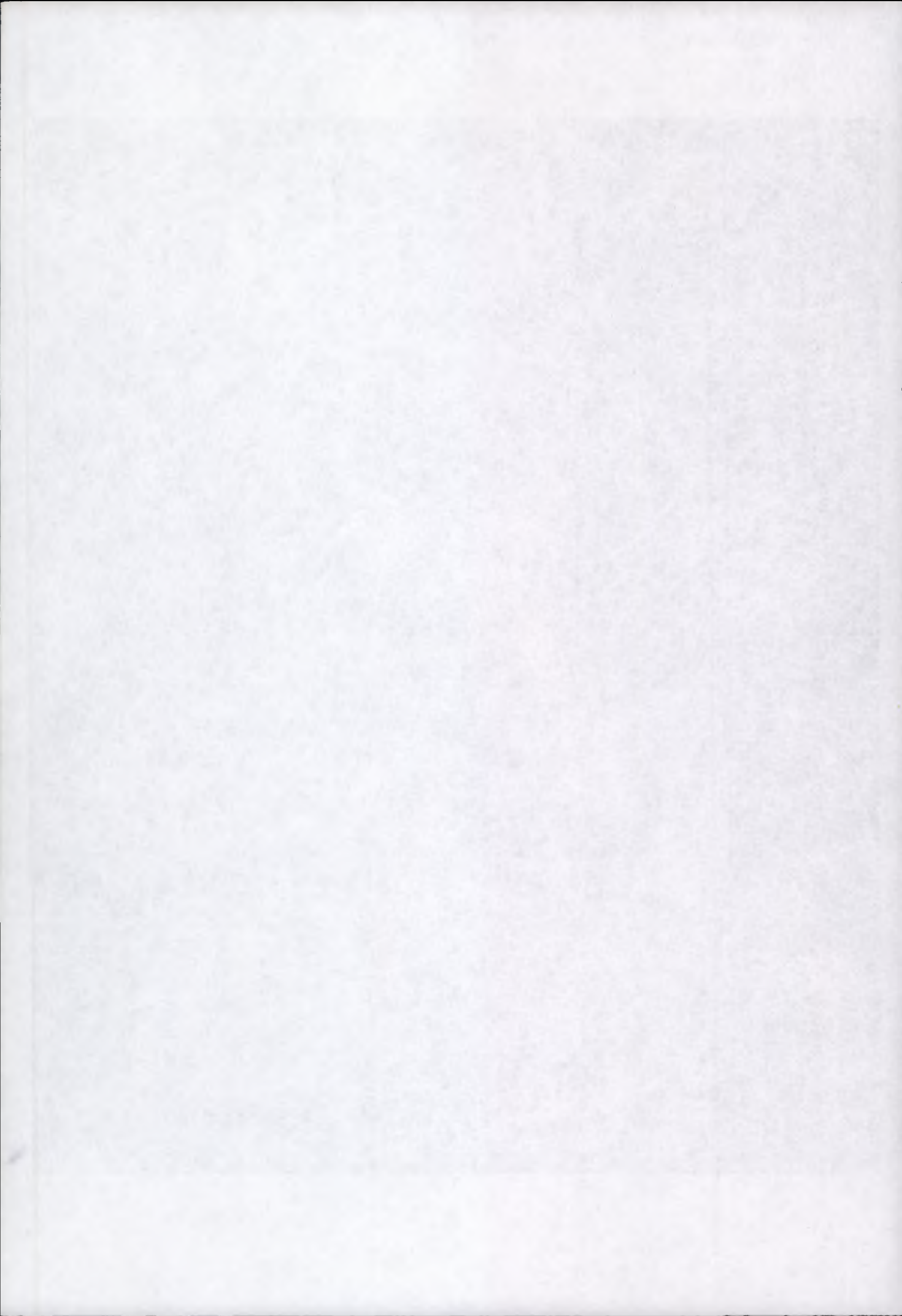




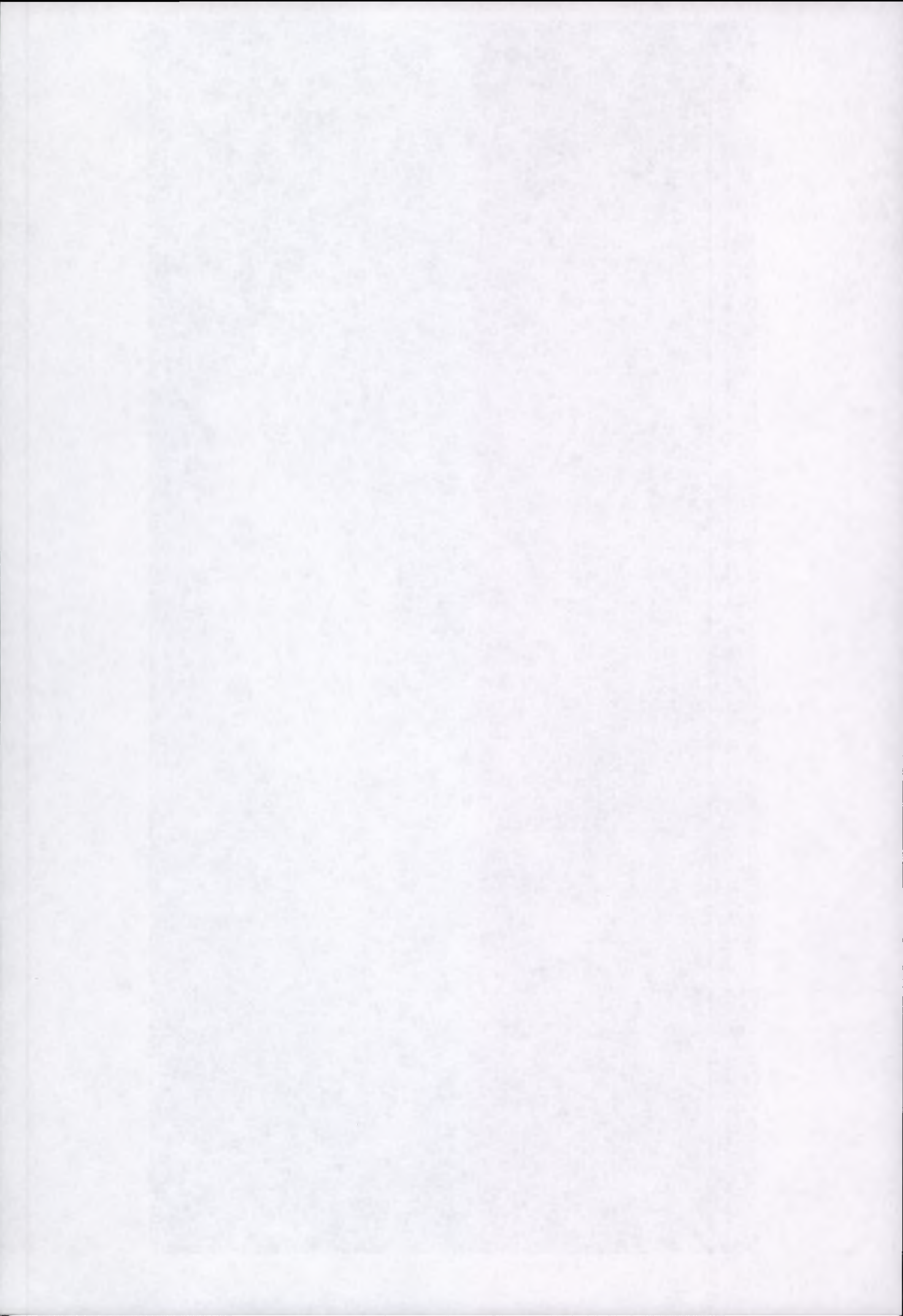












# Annex N

## **Geographical area**

Ukraine

## **Research institute**

Institute for Navigational Studies, Stuttgart, Germany

## **Application domain**

Digital Elevation Models

## **First results**

ERS-1 Intensity Image, Tandem Coherence Image & Tandem relative phase image.

Note the generally high values of coherence and several interesting isolated areas of low coherence indicating rapid change (not identifiable from single Intensity image).

Several fine scale topographic structures are visible in the relative phase image which are of potential interest to hydrological studies of the area.



**Results achieved with ERS-Tandem Data of the UKRAINE- area (Lat: 65.46 Lon: 73.28):**

Fig. 1: shows the Intensity image acquired by ERS-1  
date: 27.11.1995 Orbit: 22839 Frame: 2277

Fig. 2: shows the coherence image of the following ERS-1 / ERS-2 Tandem pair  
ERS-1: date: 27.11.1995 Orbit: 22839 Frame: 2277  
ERS-2: date: 28.11.1995 Orbit: 3166 Frame: 2277  
Baseline: 81 m

Fig. 3: shows the relative phase image of the following ERS-1 / ERS-2 Tandem pair  
ERS-1: date: 27.11.1995 Orbit: 22839 Frame: 2277  
ERS-2: date: 28.11.1995 Orbit: 3166 Frame: 2277  
Baseline: 81 m 2 Pi-Elevation: 140 m

